

Atmospheric Escape Processes and Planetary Atmospheric Evolution

Guillaume Gronoff¹, Phil Arras², Suleiman M Baraka³, Jared M Bell⁴, Gaël Cessateur⁵, Ofer Cohen⁶, Shannon M. Curry⁷, Jeremy J Drake⁶, Meredith K Elrod⁸, Justin T. Erwin⁹, Katherine Garcia-Sage⁸, Cecilia garraffo¹⁰, Alex Gloer⁴, Nicholas Gray Heavens¹¹, Kylie Lovato¹¹, Romain Maggiolo¹², Christopher D. Parkinson¹³, Cyril L. Simon Wedlund¹⁴, Daniel R Weimer¹⁵, and William B. Moore¹¹

¹Nasa LaRC

²University of Virginia

³Al-Aqsa University

⁴NASA/GSFC

⁵Belgian Institute for Space Aeronomy (IASB-BIRA)

⁶Harvard-Smithsonian Center for Astrophysics

⁷UC Berkeley

⁸NASA Goddard Space Flight Center

⁹University of Arizona

¹⁰Harvard-Smithsonian Center for Astrophysics,

¹¹Hampton University

¹²Belgian royal Institute for Space Aeronomy (IASB-BIRA)

¹³University of Michigan-Ann Arbor

¹⁴Space Research Institute

¹⁵Virginia Tech

November 24, 2022

Abstract

The habitability of the surface of any planet is determined by a complex evolution of its interior, surface, and atmosphere. The electromagnetic and particle radiation of stars drive thermal, chemical and physical alteration of planetary atmospheres, including escape. Many known extrasolar planets experience vastly different stellar environments than those in our Solar system: it is crucial to understand the broad range of processes that lead to atmospheric escape and evolution under a wide range of conditions if we are to assess the habitability of worlds around other stars. One problem encountered between the planetary and the astrophysics communities is a lack of common language for describing escape processes. Each community has customary approximations that may be questioned by the other, such as the hypothesis of H-dominated thermosphere for astrophysicists, or the Sun-like nature of the stars for planetary scientists. Since exoplanets are becoming one of the main targets for the detection of life, a common set of definitions and hypotheses are required. We review the different escape mechanisms proposed for the evolution of planetary and exoplanetary atmospheres. We propose a common definition for the different escape mechanisms, and we show the important parameters to take into account when evaluating the escape at a planet in time. We show that the paradigm of the magnetic field as an atmospheric shield should be changed and that recent work on the history of Xenon in Earth's atmosphere gives an elegant explanation to its enrichment in heavier isotopes: the so-called Xenon paradox.

Atmospheric Escape Processes and Planetary Atmospheric Evolution

G. Gronoff^{1,2}, P. Arras³, S. Baraka⁴, J. M. Bell⁵, G. Cessateur⁶, O. Cohen⁷, S. M. Curry¹¹, J.J. Drake⁸, M. Elrod⁵, J. Erwin⁶, K. Garcia-Sage⁵, C. Garraffo⁸, A. Glocer⁵, N.G. Heavens^{9,10}, K. Lovato⁹, R. Maggiolo⁶, C. D. Parkinson¹⁰, C. Simon Wedlund¹², D. R. Weimer^{4,13}, W.B. Moore^{4,9}

¹Science directorate, Chemistry and Dynamics branch, NASA Langley Research Center, 21 Langley Blvd.,

Mail Stop 401B Hampton, Virginia 23681-2199 USA

²Science Systems and Application Inc. Hampton, Virginia, USA

³Department of Astronomy, University of Virginia, P.O. Box 400325, Charlottesville, VA 22904, USA

⁴National Institute of Aerospace, Hampton, Virginia, USA.

⁵Heliophysics Division, NASA Goddard Space Flight Center, 8800 Greenbelt Rd, Greenbelt, MD 20771,

USA

⁶The Royal Belgian Institute for Space Aeronomy (BIRA-IASB), Avenue Circulaire 3, 1180 Brussels,

Belgium

⁷Lowell Center for Space Science and Technology, University of Massachusetts Lowell, 600 Suffolk St.,

Lowell, MA 01854, USA

⁸Harvard-Smithsonian Center for Astrophysics, 60 Garden St. Cambridge, MA 02138, USA.

⁹Department of Atmospheric and Planetary Sciences, Hampton University, 154 William R. Harvey Way,

Hampton, Virginia 23668 USA

¹⁰Space Science Institute, 4765 Walnut St, Suite B, Boulder, Colorado, USA

¹¹Space Sciences Laboratory, University of California, Berkeley, 7 Gauss Way, Berkeley, CA 94720, USA.

¹²Space Research Institute (IWF), Schmiedlstraße 6, 8042 Graz, Austria

¹³Center for Space Science and Engineering Research, Virginia Tech, Blacksburg, Virginia, USA.

Key Points:

- The different escape processes at planets and exoplanets are reviewed along with their mathematical formulation.
- The major parameters for each escape processes are described. Some escape processes currently negligible in the Solar system may be the major source at exoplanets, or for the early Solar system.
- A magnetic field should not be a priori considered as a protection for the atmosphere.

Corresponding author: Guillaume Gronoff, Guillaume.P.Gronoff@nasa.gov

Abstract

The habitability of the surface of any planet is determined by a complex evolution of its interior, surface, and atmosphere. The electromagnetic and particle radiation of stars drive thermal, chemical and physical alteration of planetary atmospheres, including escape. Many known extrasolar planets experience vastly different stellar environments than those in our Solar system: it is crucial to understand the broad range of processes that lead to atmospheric escape and evolution under a wide range of conditions if we are to assess the habitability of worlds around other stars.

One problem encountered between the planetary and the astrophysics communities is a lack of common language for describing escape processes. Each community has customary approximations that may be questioned by the other, such as the hypothesis of H-dominated thermosphere for astrophysicists, or the Sun-like nature of the stars for planetary scientists. Since exoplanets are becoming one of the main targets for the detection of life, a common set of definitions and hypotheses are required.

We review the different escape mechanisms proposed for the evolution of planetary and exoplanetary atmospheres. We propose a common definition for the different escape mechanisms, and we show the important parameters to take into account when evaluating the escape at a planet in time. We show that the paradigm of the magnetic field as an atmospheric shield should be changed and that recent work on the history of Xenon in Earth’s atmosphere gives an elegant explanation to its enrichment in heavier isotopes: the so-called Xenon paradox.

Plain Language Summary

In addition to having the right surface temperature, a planet needs an atmosphere to keep surface liquid water stable. Although many planets have been found that may lie in the right temperature range, the existence of an atmosphere is not guaranteed. In particular, for planets that are kept warm by being close to dim stars, there are a number of ways that the star may remove a planetary atmosphere. These atmospheric escape processes depend on the behavior of the star as well as the nature of the planet, including the presence of a planetary magnetic field. Under certain conditions, a magnetic field can protect a planet’s atmosphere from the loss due to the direct impact of the stellar wind; but it may actually enhance total atmospheric loss by connecting to the highly variable magnetic field of the stellar wind. These enhancements happen especially for planets close to dim stars. We review the complete range of atmospheric loss processes driven by interaction between a planet and a star to aid in the identification of planets that are both the correct temperature for liquid water and that have a chance of maintaining an atmosphere over long periods of time.

1 Introduction

The discovery of rocky exoplanets at distances from their host stars that might allow stable surface liquid water has led to a blossoming of studies of the habitability of such objects (Anglada-Escudé et al., 2016; Gillon et al., 2017; Zechmeister et al., 2019). While the ultimate objective of this work is the discovery of life on an exoplanet, detailed investigations of such planets may also shed light on the evolution –both past and future– of the planets in our own Solar system (Arney & Kane, 2018), in particular, how they came to be, remain, and/or ceased to be habitable for life as we know it (Moore et al., 2017; Editors of *Nature Astronomy*, 2017; Tasker et al., 2017).

The usual definition of the “habitable-zone” (HZ) (Kasting et al., 1988; Ramirez, 2018; Lammer et al., 2009, and references therein), is where a planet like the Earth would be able to maintain liquid water at its surface, however it says nothing about whether

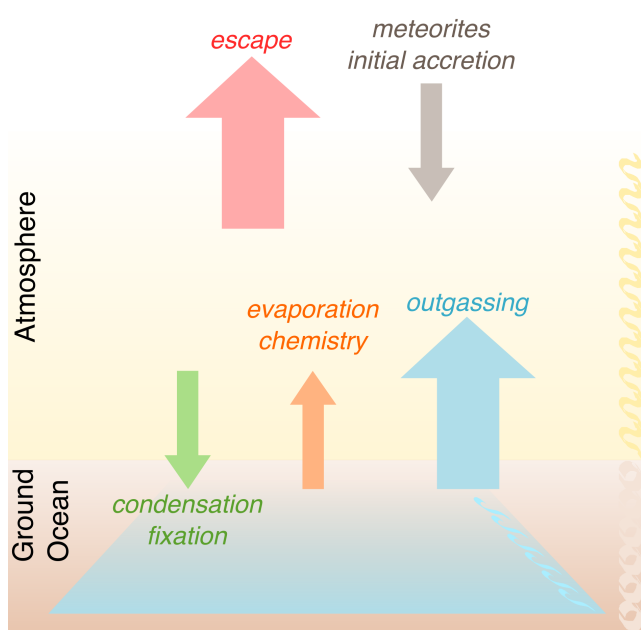


Figure 1. The processes leading to the creation and the destruction of an atmosphere. A stable balance between these processes is required for a habitable atmosphere.

81 the planet actually has any liquid water, or the necessary atmospheric pressure to sta-
 82 bilize the liquid state. This definition fails to take into account the necessary pathways
 83 to habitability: a planet forming in the habitable zone of a star will have to accrete volatiles
 84 from the protostellar nebula to be able to have an atmosphere and liquid water, and it
 85 will also have to keep them, which is not necessarily the case for the previously mentioned
 86 exoplanets –even if we suppose they have a strong intrinsic magnetic field– (Airapetian
 87 et al., 2017; Garcia-Sage et al., 2017; Howard et al., 2018). The concept of the HZ is there-
 88 fore distressingly incomplete, which led to the concept of Space Weather Affected Hab-
 89 itable Zone (Airapetian et al., 2017) .

90 One of the best examples of the problems with this definition comes from our un-
 91 derstanding of the early Earth: the so-called “Faint Young Sun” (FYS) paradox. 4 to
 92 3 Gyr ago, the Sun was fainter by about 30% (Claire et al., 2012), and our models pre-
 93 dict that surface water should have been frozen, and therefore that Earth was not in the
 94 HZ. There is however considerable evidence for an active hydrological cycle and excep-
 95 tionally warm and/or clement temperatures at that period (Mojzsis et al., 2001; Knauth
 96 & Lowe, 2003; Kasting & Ono, 2006; Lammer et al., 2009). The typical solution to the
 97 FYS paradox has been to propose that the Earth’s early atmosphere had a higher con-
 98 centration of greenhouse gases such as CO_2 , CH_4 , NH_3 , N_2O , etc., in a perhaps thicker
 99 atmosphere than now (Sagan & Mullen, 1972; Walker et al., 1981; A. A. Pavlov et al.,
 100 2000; Airapetian et al., 2016). Greenhouse gas levels have overall implications for geo-
 101 logical activity, cloud/aerosol formation, and atmospheric chemistry and escape that can
 102 preclude their existence, stability, or positive contribution to habitability altogether (Kuhn
 103 & Atreya, 1979; A. A. Pavlov et al., 2000; Trainer et al., 2006). Several hypotheses re-
 104 main concerning the nature of the Early Earth’s atmosphere; a major problem lies with
 105 the uncertainties on the nitrogen cycle in the past, and on the actual ground pressure
 106 that recent studies suggest being closer to 0.5 bar (Som et al., 2016; Zerkle & Mikhail,
 107 2017; Laneuville et al., 2018). For a simple example of the complexity to extend research
 108 to exoplanets, consider recent work by Airapetian et al. (2016), which suggests that the

109 higher solar activity has led to chemical reactions creating N_2O , a very efficient green-
 110 house gas in the Early Earth’s troposphere.

111 Another uncertainty comes from the magnetic activity of the host star, responsi-
 112 ble for the space-weather conditions of close-in planets, and expected to be much stronger
 113 for lower mass stars such as the Trappist–1 system star and M dwarfs in general. Since
 114 those stars could remain as active as the young Sun throughout their lifetime (Airapetian
 115 et al., 2019), it is theoretically possible that some of the planets orbiting them are cur-
 116 rently subject to a N_2O greenhouse effect while at the same time being out of the stan-
 117 dard HZ.

118 In order to produce a more useful concept of habitability, we must contend with
 119 all the processes that lead to the habitability of a planet, and how the different variables
 120 (such as the type of star, the rotation rate of the planet, etc.) affect it. The formation
 121 of a planetary atmosphere is a balance between the amount of volatiles brought during
 122 the accretion phase, and subsequently outgassed, and the subsequent escape or fixing
 123 of volatiles as the planet evolves. (Lammer et al., 2009, Figure 1).

124 Atmospheric escape is often overlooked in this type of analysis or only approximated
 125 by an energy-limited hydrodynamic escape. Modeling based on this approximation led
 126 a fraction of the community to conclude that Pluto’s atmosphere was greatly outgassing
 127 until the observations of New Horizons measured an escape rate four orders of magni-
 128 tude lower than predicted (Zhu et al., 2014; Gladstone et al., 2016). This leads to ma-
 129 jor questions concerning atmospheric escape that need to be solved.

130 1.1 The Outstanding Questions of Atmosphere Escape

131 Several major questions about the evolution of planetary atmospheres have been
 132 asked (Ehlmann et al., 2016), such as: “are [their] mass[es] and composition[s] sustain-
 133 able?”, “how do [they] evolve with time?”. Recent studies of atmospheric escape have
 134 led to the following major questions, specific to escape, that are being answered through
 135 experimental studies (e.g. satellites such as Venus Express -VEX-, Mars Express -MEX-
 136 , Rosetta, Mars Atmosphere and Volatile and Evolution mission -MAVEN-, etc.), and
 137 theoretical work.

- 138 **1. What is the current escape rate of planetary atmospheres, how does it**
 139 **vary with forcing parameters?** Measurements by different spacecraft enable
 140 estimates of the flux of ions and neutrals escaping a planet. However, limitations
 141 in temporal and spatial resolution render some observations very difficult; e.g., the
 142 ion plume of Mars was inferred from MEX observations, but only MAVEN could
 143 fully observe and characterize it. (Liemohn et al., 2014; Dong et al., 2015); iono-
 144 spheric outflow at Earth is observed, but the fraction of ions coming back, and the
 145 variation of outflow with latitude, magnetic local time, and solar and geomagnetic
 146 activity, is difficult to address accurately (Strangeway et al., 2000).
- 147 **2. What was the escape rate in the past? How did it vary with the vary-**
 148 **ing forcing parameters and the varying atmospheres of planets?** The iso-
 149 topic composition of an atmosphere hints at changes in its composition, and can
 150 be used to evaluate the total atmospheric loss. However, if some major param-
 151 eters of the composition have changed, extrapolating the current atmosphere to
 152 the past can be problematic. The Earth’s atmosphere is an emblematic example
 153 of an atmosphere that has greatly changed, with the appearance of oxygen in large
 154 quantities after about 2.5 Gyr ago (D. Catling, 2014). Observations of Sun-like
 155 stars in different stages of their evolution suggest that the Sun had more sunspots
 156 and flares in the past, which, undoubtedly, changed the escape conditions of the
 157 planets in the Solar system (Lammer et al., 2009).

- 158 **3. How will escape and other atmospheric evolutionary processes shape**
 159 **the future of the planetary atmospheres we observe today** For example,
 160 what will the habitability of the Earth and Mars be in a billion years? Variation
 161 of the Earth's magnetic field may affect escape rates, and dramatically change the
 162 atmosphere of the Earth. At Mars, the atmospheric photochemistry may lead to
 163 H₂O escape with the oxidation of the crust if O is not escaping enough (Lammer,
 164 Selsis, et al., 2003). Recent modeling shows that CO₂⁺ dissociative recombination
 165 is also an efficient loss channel (Lee et al., 2015). The adsorption of CO₂ into the
 166 crust (Takasumi & Eiichi, 2002; Zent & Quinn, 1995; Hu et al., 2015; Mansfield
 167 et al., 2017) implies that future change in Mars' obliquity will increase the out-
 168 gassing and therefore the surface atmospheric pressure of the planet. But what
 169 will happen if no more H₂O compensates for the escape? Is it possible for all re-
 170 maining Martian H₂O to escape? How much CO₂ could escape?
- 171 **4. Does a magnetic field protect an atmosphere from escaping?** Polar iono-
 172 spheric outflow is an efficient process to accelerate ions to escape speed. Since it
 173 is driven by the energy of the solar wind, funneled by the magnetic field, the stronger
 174 the magnetic field, the more energy is available for ionospheric outflow. In that
 175 sense, a planet with a magnetic field could be more sensitive to escape (Gunell et
 176 al., 2018). However, the returning component of the polar outflow is increasing,
 177 and therefore the net escape should be addressed in different conditions; there are
 178 many questions regarding how this component may evolve, and it may be so that
 179 it prevents an effective escape altogether. Do the similar escape rates measured
 180 at Earth, Venus, and Mars (Gunell et al., 2018) mean that there is no effective shield-
 181 ing, or is the comparison between these planets flawed because the upper atmo-
 182 sphere composition, and therefore the exospheric temperature are extremely dif-
 183 ferent? Is it just a coincidence that both the Earth and Titan are able to sustain
 184 a nitrogen atmosphere despite relatively large exospheric temperatures (more pre-
 185 cisely low λ_{ex} parameter, see Section 2.1.2) while being immersed in a magneto-
 186 sphere? Is the question of the magnetic field protection actually the relevant one?
- 187 **5. What is the escape rate from exoplanets; can we test our models against**
 188 **exoplanetary observations?** Some observed exoplanets are in hydrodynamic
 189 escape (Ehrenreich et al., 2015). It is possible to observe more extreme regimes
 190 for exoplanets than for planets in the Solar system; therefore the models devel-
 191 oped for the current Solar system conditions are likely to be inadequate for ex-
 192 oplanets. One of the main advantages of these tests is to be able to validate the
 193 conditions likely encountered in the early Solar system. One example of such a
 194 process that is believed to be more important in the past is sputtering, but how
 195 could we detect its efficiency at exoplanets?

196 1.2 Analytical Approach

197 The Solar system has a large variety of planetary bodies, with very different at-
 198 mospheres, including Mars with a thin CO₂-rich atmosphere, Venus with a thick CO₂-
 199 rich atmosphere (both of those presenting evidence of substantial escape), or Earth with
 200 a N₂/O₂ atmosphere. The difference between these planets is, in a large part, determined
 201 by how they are losing their atmospheres. Several missions, such as MAVEN, MEX, and
 202 VEX have been giving insights on the evolution of planetary atmospheres through their
 203 escape to space, and have led to a better understanding of which important processes
 204 are active to date, and maybe in the past. In addition, work on comets, such as 67P with
 205 Rosetta, highlight some of the fundamental processes that lead to escape in slightly dif-
 206 ferent regimes (D. Brain et al., 2016). Unfortunately, these results cannot be simply ex-
 207 trapolated to exoplanets, since they may be subject to very different conditions.

208 To that extent, it is necessary to know: (1) what the possible mechanisms by which
 209 planets lose their atmosphere into space are, (2) how these mechanisms behave with dif-

210 ferent conditions, (3) how they produce different observables, and (4) what our current
 211 understanding of these mechanisms is. Ultimately, one would like to:

- 212 • Determine what the escape processes are: review all the processes that have been
 213 suggested in the literature, review what their suggested rates were, and, since def-
 214 initions may vary between authors, decide for a standard definition.
- 215 • Determine what the key parameters are for each escape process, i.e. what vari-
 216 ations will be of importance, and how these parameters couple with each other.
- 217 • Determine the unknown parameters that need to be addressed to answer the ques-
 218 tions of section 1.1.
- 219 • Determine the observable for each escape process, and determine how to disen-
 220 tangle the observations of escape in different solar/stellar conditions to determine
 221 the relative importance of each processes.

222 This is why, in the present paper, we start by reviewing the different escape pro-
 223 cesses and their limitations (Section 2), what the major parameters that we need to know
 224 to calculate these escape processes and know their importance are (Section 3), before look-
 225 ing at how they influence the Solar system planets (Section 4) and some exoplanets (Sec-
 226 tion 5) in time. We will finally look at which measurements and models are needed to
 227 better understand the escape processes at planets and exoplanets (Section 6) before con-
 228 cluding.

229 2 The Escape Processes

230 The escape processes are usually separated into two parts: the thermal and non-
 231 thermal processes. The thermal processes are dependent on the temperature of the up-
 232 per atmosphere, usually controlled by the host star’s Extreme and X Ultraviolet (EUV-
 233 XUV) flux. The non-thermal processes are the result of more complex interactions, such
 234 as plasma interactions. Some non-thermal processes (such as sputtering) have a consis-
 235 tent nomenclature in the literature whereas others (such as ion outflow) have variable
 236 definitions depending on the authors. In Table 1, we summarize these escape processes
 237 and in Table 2 their main parameters. Those escape processes are sketched on Figure 2,
 238 and an evaluation of the current escape rates can be found on Table 3.

239 Non-thermal escape processes can be separated into Photochemical loss (Section
 240 2.2), Ion loss (Section 2.3), Ionospheric outflow (Section 2.4), and Other losses (Section
 241 2.5). Moreover, in order to compute the total loss of an atmosphere into space, it is nec-
 242 essary to take into account the problem of the ion return (Section 2.6). It is important
 243 to note that, while we are separating these processes, they do influence each other, and
 244 sometimes one leads to the other. For example, an ionospheric outflow process at Venus
 245 can produce fast particles involved in ion pickup and sputtering (J. Luhmann et al., 2008).

246 2.1 Thermal Escape

247 Thermal escape is one of the most important escape processes (Chassefière & Leblanc,
 248 2004; Selsis, 2006). It takes place in two regimes, Jeans escape and hydrodynamic es-
 249 cape, with a transition regime that is the subject of recent studies (e.g. D. F. Strobel
 250 (2008b); Volkov, Johnson, et al. (2011); Volkov, Tucker, et al. (2011); Erkaev et al. (2015)).
 251 Most of the observed isotopic fractionation in planetary atmospheres is interpreted as
 252 originating from thermal escape because of its energy efficiency at escaping large amount
 253 of gases.

Table 1. The escape processes

Process	Origin	Key parameters
Jeans escape	Temperature accelerate particle above the escape velocity	Temperature, gravity, T_c : λ_{ex} parameter > 2.5
Hydrodynamic escape	Thermal acceleration in a fluid way	Temperature, gravity, T_c : λ_{ex} parameter < 2.5
Photochemical/Ion recombination	Ion recombination releasing kinetic energy	Low gravity, molecular ion, requires ionosphere densities
Photochemical/Dissociations (photon, etc)	Molecular photodissociation release kinetic energy	Requires thermosphere densities, low gravity
Ion Pickup	Solar wind picks up ions from ionosphere	Requires compressed/no magnetosphere
Ion Sputtering	Accelerated ions from the ionosphere translate their kinetic energy	Requires compressed/no magnetosphere, B , U_{sw}
Charge exchange/trapped	Fast ion trapped in magnetosphere becomes ENA through charge exchange	Requires magnetosphere, ion density and temperature, neutral densities
Charge exchange/solar wind	Solar wind ion becomes ENA that can access thermosphere and increases heating	Requires large coronae, U_{sw} , N_{sw}
Charge exchange/particle precipitation,	Particle precipitating in thermosphere becomes ENA and translate kinetic energy	Requires precipitation fluxes, cross sections
Ionospheric outflow (often called polar wind in magnetized planets)	creation of ion upward wind through ambipolar diffusion	requires fields, ionosphere
Other ion escape	Plasma instabilities leading to ions going upwards and being picked by the solar wind	Requires fields, ion density and temperature

Table 2. Escape at Planets, parameters compiled from Hinson et al. (2017); L. A. Young et al. (2018); Johnson et al. (2013b)

Planet	Jeans λ_{ex} parameter	T_e (K)	T_c (K)	g (m/s ²)	R (km)	H_{exo} (km)	B (Gauss-R ³)	Average Solar EUV (W/m ²)	Solar Wind Pressure (nPa)	Q_c (W)
Mercury	2.2	500	725	3.70	2439.7		0.002	9082.7	13.8-21.0	7.31×10^{10}
Venus	22.3	290	4307	8.87	6051.8	15.9		2601.3	1.0-12.0	2.64×10^{12}
Earth	9.4-5.0	800-1600	5020	9.80	6378.1	8.5	0.306	1361.0	1.0-6.0	3.51×10^{12}
Moon	0.8	226	400	1.62	1738.1			1361.0	1.0-6.0	1.03×10^{10}
Mars	6.3-5.0	240-300	1014	3.71	3396.2	11.1	4.30	586.2	0.1-1.1	1.68×10^{11}
Jupiter	311-218	700-1000	145000	24.79	71492	27.0	0.215	50.26	0.05-0.10	5.92×10^{15}
Saturn	157-98	500-800	52200	10.44	60268	59.5		14.82	0.01-0.09	1.06×10^{15}
Titan	2.3	180	280	1.35	2575			14.82	0.01-0.09	1.84×10^{10}
for CH ₄	37.3		4475							3.7×10^{11}
Uranus	34	800	18300	8.87	25559	27.7	0.228	3.69	0.001-0.02	1.14×10^{14}
Neptune	48	700	22250	11.15	24764	19.1-20.3	0.142	1.508		1.26×10^{14}
Pluto	15.1	68	408	0.62	1184	78		0.873	0.006	8.4×10^8
for CH ₄	8.5		384			59				1.6×10^{10}

Table 3. The Present Escape Values. Total escape, in s^{-1} , followed by the fluxes, in $cm^{-2}s^{-1}$. Both are reported in the literature. While fluxes show the magnitude at a given planet, highlighting the intensity, total escape highlights the overall aspect of escape; when comparing planet to planet, none are satisfying since comparing the total escape of a Mars with e.g. Venus hides the size effects. On the other hand, comparing the fluxes from Earth with e.g. Mars hides local effects like exospheric temperature. We decided to show both values. References: ¹ - Lammer et al. (2008) and references therein. ² - Tian et al. (2013) and references therein. ³ - Jakosky et al. (2018) and references therein. ⁴ - Gunell et al. (2018) and references therein. ⁵ - Inui et al. (2019) and references therein. ⁶ At Earth, the Jeans' flux for the solar max is basically the same flux as for charge exchange at the solar min because H escape is diffusion limited, see Section 2.3.2. NB: we considered the fluxes at the exobases, at Venus, a 200 km exobase has a surface of $4.9 \cdot 10^{18} \text{ cm}^2$; at Earth, for a 500 km exobase, $5.9 \cdot 10^{18} \text{ cm}^2$; at Mars, for a 200 km exobase, $1.6 \cdot 10^{18} \text{ cm}^2$.

Process	Venus	Earth	Mars
Jeans escape	$2.5 \times 10^{19} - 5.1^{(1)}$	$6 \times 10^{26} - 10^8$ (Solar Max) ^(2,6)	H: $1.6 \times 10^{26} - 1.1 \times 10^{27} - 10^8 - 6.9 \times 10^8$ ⁽³⁾
Charge exchange/trapped	H: $5 \times 10^{24} - 5 \times 10^{25} - 10^6 - 10^7$ ⁽²⁾	H: $6 \times 10^{26} - 10^8$ (Solar Min) ^(2,6)	$10^{22} - 10^{23} - 10^4 - 10^5$ ⁽²⁾
Ion pickup	H ⁺ : $10^{25} - 2 \times 10^6$ ⁽¹⁾ ; O ⁺ : $1.5 \times 10^{25} - 3 \times 10^6$ ⁽¹⁾ He ⁺ : $5 \times 10^{23} - 5 \times 10^{24} - 10^5 - 10^6$ ⁽²⁾	Small ⁽²⁾	O ⁺ : $10^{24} - 10^6$ ^(2,3) ; C ⁺ : $1.6 \times 10^{23} - 10^5$ ⁽²⁾
Sputtering	O: $5 \times 10^{23} - 5 \times 10^{24} - 10^5 - 10^6$ ⁽²⁾	Small ⁽²⁾	O: $3 \times 10^{24} - 1.8 \times 10^6$ ⁽³⁾
Photochemical escape	$3.8 \times 10^{25} - 7.7 \times 10^6$ ⁽¹⁾	Small ⁽²⁾	C: $10^{23} - 10^5$ (Solar Min) $10^{25} - 10^7$ (Solar Max) ⁽⁵⁾
Magnetized Ion Outflow (Polar wind)	N/A	H ⁺ : $8 \times 10^{25} - 1.3 \times 10^7$ ⁽⁴⁾ O ⁺ : $3 \times 10^{25} - 5 \times 10^6$ ⁽⁴⁾ O ⁺ : $6 \times 10^{24} - 1 \times 10^6$ ⁽²⁾	O: $5 \times 10^{25} - 3 \times 10^7$ ⁽³⁾ ; C: $10^{24} - 10^6$ ⁽²⁾ N/A (crustal escape included in outflow)
Unmagnetized Ion Outflow/K-H/Clouds	$5 \times 10^{24} - 1 \times 10^{25} - 1 \times 10^6 - 2 \times 10^6$ ⁽¹⁾		$10^{25} - 10^7$ ⁽⁵⁾

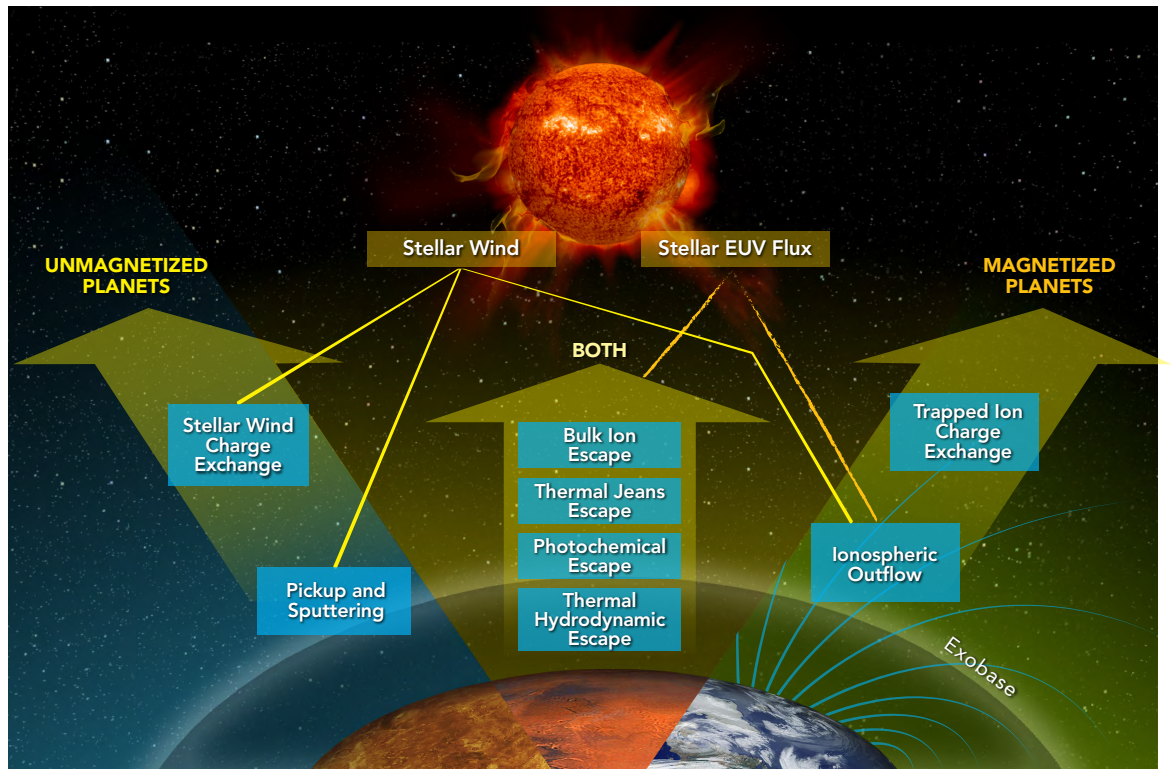


Figure 2. The main processes of atmospheric escape, along with their typical efficient altitudes domains (near the thermosphere/exobase or away from it) and their conditions of efficiency/occurrence (magnetic field).

254

2.1.1 Fundamental Theory

255

256

257

2.1.1.1 *Jeans regime* The neutral atmospheric constituents in the upper atmosphere are in local thermodynamic equilibrium (or close to it). Therefore, their distribution function can be approximated by a Maxwellian function (Mihalas & Mihalas, 1984):

$$\begin{aligned} f(\vec{x}, \vec{v}) &= N \left(\frac{m}{2\pi kT} \right)^{3/2} e^{-\frac{mv^2}{2kT}} \\ &= N \left(\frac{1}{u_i \sqrt{\pi}} \right)^3 e^{-v^2/u_i^2} \end{aligned} \quad (1)$$

258

where $u_i = \sqrt{\frac{2kT}{m_i}}$ is referred to as the thermal speed for the species i .

259

260

261

262

263

264

The exobase is quantitatively defined as the level where l_i , the mean free path of the i th constituent is equal to the scale height (H) (Hunten, 1973; Shizgal & Arkos, 1996). At the exobase, we consider that a molecule of the i th constituent going upwards at the escape velocity, $v_{esc} = \sqrt{2GM/r}$ will not impact another molecule, and therefore will escape. This approximation is the equivalent of considering an atmosphere collisionless above the exobase and fully collisional below (Fahr & Shizgal, 1983).

265

266

267

By integrating the vertical flux, $v_i \cos(\theta) \times f_i$, at the exobase, for the velocities greater than the escape velocity (v_{esc}), and neglecting the collisions above it, we retrieve the flux of escaping molecules.

$$\Phi_i(\text{escape}) = \int_0^{2\pi} \int_0^{\pi/2} \int_{v_{esc}}^{\infty} v_i \cos(\theta) f(v_i) v_i^2 \sin(\theta) dv_i d\theta d\Psi \quad (2)$$

268

Carrying out this integration gives:

$$\Phi_i(\text{escape}) = N_i \left(\frac{kT_e}{2\pi m_i} \right)^{1/2} \left(1 + \frac{m_i v_{esc}^2}{2kT_e} \right) e^{-\frac{m_i v_{esc}^2}{2kT_e}} \quad (3)$$

$$= N_i \left(\frac{u_i}{2\sqrt{\pi}} \right) \left(1 + \frac{v_{esc}^2}{u_i^2} \right) e^{-\frac{v_{esc}^2}{u_i^2}} \quad (4)$$

269

270

271

In Eqs. 3 and 4, it is important to use the values of v_{esc} and u_i at the exobase (using the temperature, T_{exo} , and radius r_{exo} at the exobase) to get a correct estimation of the escape flux.

272

273

274

275

It is common to introduce the non-dimensional *Jeans parameter* to express the escape flux, and we will see later that this parameter is very useful in understanding the thermal escape process. The Jeans parameter is the ratio of gravitational energy to thermal energy, expressed as $\lambda_{ex} = \frac{GMm_i/r}{kT} = \frac{v_{esc}^2}{u_i^2}$. Using this, the escape flux becomes:

$$\Phi_i(\text{escape}) = N_i \left(\frac{u_i}{2\sqrt{\pi}} \right) (1 + \lambda_{ex}) e^{-\lambda_{ex}} \quad (5)$$

276

277

278

279

280

281

282

283

Eq. 2 assumes that we can approximate the distribution at the exobase by a Maxwellian despite the fact that molecules faster than v_{esc} are removed. When the escape rate is high enough, a non-Maxwellian correction must be applied to consider that the high-energy tail of the Maxwellian is depleted, following J. W. Chamberlain and Smith (1971). This correction lowers the escape rate by about 25%. However, this correction is based on the assumption of an isothermal atmosphere below the exobase and has been evaluated for H and He escape within a O or CO₂ rich background atmosphere, i.e. the thermosphere of the Earth and Mars/Venus etc.

284 A more realistic simulation, performed by Merryfield and Shizgal (1994), that con-
 285 sidered the effect of increasing temperature with altitude, shows that the escape from
 286 the deeper layer should also be considered (i.e. it cannot be assumed that a Maxwellian
 287 is a good approximation of the atomic/molecular distribution at the exobase). In that
 288 case, the correction is an increase of the order of 30%. Therefore, for extremely precise
 289 determination of escape, it is important to solve the Boltzmann equation; one of the most
 290 used techniques is the Direct Simulation Monte Carlo (DSMC) method (Volkov, John-
 291 son, et al., 2011; Tucker & Johnson, 2009), whose results show that the source of escap-
 292 ing particles is distributed over a wide altitude range above and below the exobase.

293 Overall, equation (4) is a good approximation for the thermal escape when the at-
 294 mosphere is strongly gravitationally bound to the planet, and this formula is valid for
 295 all the constituents independently. Ideally this equation would be evaluated at or near
 296 the nominal exobase, but can be applied far below the exobase assuming no addition heat-
 297 ing if a correction factor is applied (Volkov, 2015; R. Johnson et al., 2016).

298 It is important to note that while the Jeans parameter is the main parameter of
 299 thermal escape, the location of the exobase is extremely important. In the case of Ti-
 300 tan or a possible early Moon atmosphere (Aleinov et al., 2019) the altitude of the exobase
 301 is non-negligible compared to the radius of the planet, and while the flux per unit sur-
 302 face is small, it can become the most important source of loss when taking the whole exobase
 303 surface into account.

304 *2.1.1.2 Hydrodynamic regime* In cases where the internal energy of individual
 305 gas molecules approaches the kinetic energy required for escape ($\lambda_{ex} \approx 1$), the gas will
 306 begin to escape as a flow of continuous fluid (Hunten, 1973; Gross, 1972; Watson et al.,
 307 1981).

308 Qualitatively, the fundamental distinctions between the Jeans and hydrodynamic
 309 regimes can be viewed in two helpful and complementary ways. First, the Jeans regime
 310 is “collisionless” (Shizgal & Arkos, 1996): it is one where collisions between molecules
 311 define an exobase as a surface (or at least a narrow region). The atmosphere is not only
 312 retained by the gravitational pull on individual molecules but also by the effective force
 313 of collision with other atmospheric molecules. In the “collisional” hydrodynamic regime,
 314 the molecules are so energetic that collisions are insufficient to restrict escape. Indeed,
 315 the escaping flow of lighter gases (the ones that are most likely to be escaping) is capa-
 316 ble of exerting an effective force and dragging heavier gas molecules such as water and
 317 the noble gases (Pepin, 1991; Zahnle & Kasting, 1986). And furthermore, hydrodynamic
 318 escape can take place far below the exobase.

319 Second, the distinction between Jeans and hydrodynamic escape is analogous to
 320 that between evaporation at temperatures below the boiling point and boiling. In this
 321 analogy, the exobase is like the surface of the evaporating fluid, the force of gravity is
 322 like the atmospheric pressure, and the effective pressure of other molecules is like the ef-
 323 fective pressure of other molecules in the liquid. Quantitatively, hydrodynamic escape
 324 is approached by numerical solution of an appropriate system of inviscid fluid dynam-
 325 ical equations (Watson et al., 1981; Tian & Toon, 2005). For instance, the one-dimensional
 326 time-dependent inviscid equations for a single constituent, thermally conductive atmo-
 327 sphere in spherical geometry is given by Tian and Toon (2005) as:

$$\frac{\partial(\rho r^2)}{\partial t} + \frac{\partial(\rho v r^2)}{\partial r} = 0 \quad (6)$$

$$\frac{\partial(\rho v r^2)}{\partial t} + \frac{\partial(\rho v^2 r^2 + p r^2)}{\partial r} = -\rho G M + 2 p r, \quad (7)$$

$$\frac{\partial(E r^2)}{\partial t} + \frac{\partial[(E + p) v r^2]}{\partial r} = -\rho v G M + q r^2 + \frac{\partial \kappa r^2 \frac{\partial T}{\partial r}}{\partial r} \quad (8)$$

328 where $E = \rho(v^2/2 + e)$ (the equation for the total energy density), $e = p/[\rho(\gamma -$
 329 $1)]$ (the definition of the internal energy), and $p = \rho RT$ (the ideal gas law). Here, ρ is
 330 the density of the gas, p is the pressure, γ is the polytropic index of the gas, R is the uni-
 331 versal gas constant, κ is the thermal conductivity, and q is the volume heating rate. Thus,
 332 Eq. 6 is the continuity equation, Eq. 7 is the momentum conservation equation, and Eq.
 333 8 is the energy conservation equation.

334 If energy conservation is neglected and the temperature is held constant, steady
 335 state solutions to the above system are possible. It is convenient in that case to rewrite
 336 p and GM such that:

$$p = \rho v_0^2 \quad (9)$$

$$GM = 2r_0 v_0^2, \quad (10)$$

337 where v_0 is the sound speed and r_0 is a critical radius based on the relative gravitational
 338 potential energy and kinetic energy of a particle at the sound speed.

339 A single differential equation is then obtained:

$$\frac{1}{v} \frac{dv}{dr} \left(1 - \frac{v^2}{v_0^2} \right) = \frac{2r_0}{r^2} - \frac{2}{r} \quad (11)$$

340 Eq. 11 has an obvious critical point at $(\pm v_0, r_0)$ and thus various solutions to the
 341 differential equation can be derived by integrating from these two critical points to some
 342 other velocity and radius, assuming v_0 is constant. The example of interest here is the
 343 transonic outflow solution obtained by integrating Eq. 11 from the critical point to higher
 344 velocity, v , and radius, r .

$$\log \frac{v}{v_0} - \frac{1}{2} \left(\frac{v^2}{v_0^2} \right) + \frac{2r_0}{r} + 2 \log \frac{r}{r_0} = \frac{3}{2} \quad (12)$$

345 A good discussion of the various solutions and their significance can be found in
 346 Pierrehumbert (2010).

347 It is possible to derive a theoretical upper bound for hydrodynamic escape of a sin-
 348 gle constituent atmosphere at a given temperature and atmospheric level. This bound
 349 is given by Eq. 4 in the limit where $\lambda_{ex} \approx 0$ (Hunten, 1973):

$$\Phi_i(\text{escape}) = N \left(\frac{kT_e}{2\pi m} \right)^{1/2} \quad (13)$$

350 At this bound, escape takes the form of a one-dimensional outflow at the thermal
 351 velocity. In realistic models of atmospheres, however, hydrodynamic loss rates tend to
 352 be much lower than the theoretical limit for reasons to be discussed below. In addition,
 353 the use of an hydrodynamic escape approach is easily abused, especially when many as-
 354 sumptions have to be made on the nature of the atmosphere (such as the composition
 355 and the exospheric temperature). A solution to that problem is to estimate the **criti-
 356 cal heating rate** (Johnson et al., 2013b, 2013a, and Section 3.1.1).

357 *2.1.1.3 Fluid-Kinetic Models* Applying the Jeans equation requires that the tem-
 358 perature and density to be known near the exobase. As an alternative to the hydrody-
 359 namic model, one can still use the fluid equations 6 - 8 by utilizing the Jeans escape rate
 360 and energy escape rate as upper boundary conditions. This Fluid-Jeans model has been
 361 adapted to hot gas giants (Yelle, 2004), as well as to terrestrial planets like Earth (Tian
 362 et al., 2008). One advantage of these methods is the solution is valid up to the exobase,
 363 so that heating, photochemistry and diffusion can be included and their effects on the

364 escape rate investigated. Using this Fluid-Jeans model, Tucker et al. (2012) and Erwin
 365 et al. (2013) refined the escape rate using DSMC to get a Fluid-DSMC result. This ex-
 366 tends the Fluid-Jeans result to model the transition from the collisional to collisionless
 367 regimes, and demonstrates the breakdown in the fluid equations below the exobase. These
 368 models predict that escape rates at Titan and Pluto are roughly consistent with Jeans
 369 escape even with low gravity or with high-heating rates.

370 *2.1.1.4 Limiting factors to thermal escape* One limit arises from the impact of
 371 thermal escape on the energetics of the upper atmosphere. Removal of the escaping ma-
 372 terial either will cool the atmosphere around the exobase or lower the altitude of the exobase.
 373 Either way, some energy source will be necessary to maintain escape in a steady state.
 374 That energy source is whatever stellar EUV < 90 nm that can be absorbed near the exobase
 375 (this absorption threshold is set for H, as this is the main species evaluated in the con-
 376 text of energy limited escape, but is generally valid for upper atmospheric species) which
 377 results in one form of the energy-limited escape rate (Watson et al., 1981; Erkaev et al.,
 378 2007):

$$\Phi_i(\text{limited escape}) = \epsilon F_{\odot, EUV} \left(\frac{GMm}{r} \right)^{-1} \quad (14)$$

379 where ϵ is the EUV heating efficiency and $F_{\odot, EUV}$ is the solar (or stellar) EUV flux.

380 When fluxes of EUV are high, energy-limited escape is defined by the balance be-
 381 tween conductive heating of absorbed solar EUV from the exobase with adiabatic cool-
 382 ing of the thermosphere, as initially argued by Watson et al. (1981). Thus, at increas-
 383 ingly higher levels of EUV flux, the thermospheric temperature profile should evolve from
 384 one in which temperature increases monotonically to the exobase to one where peak tem-
 385 perature is significantly below the exobase. And after a certain point, the higher the in-
 386 coming solar flux, the lower the exobase temperature (Tian et al., 2008): a regime thought
 387 to have limited the thermal escape rate on the early Earth (the authors refer to hydro-
 388 dynamic escape as the regime where the adiabatic flow is important in the upper ther-
 389 mosphere, even though they are using Jeans escape to define the escape rate at the up-
 390 per boundary). Where increased EUV flux simultaneously reduces other cooling mech-
 391 anisms (such as IR emission from CO₂ on Mars (Tian, 2009)), the adiabatic cooling-driven
 392 energy limit to thermal escape is less relevant. Erwin et al. (2013) showed that Pluto's
 393 atmospheric escape is energy-limited even with the small EUV flux experienced at its
 394 orbit.

395 The final limit arises from the impact of thermal escape on the composition of the
 396 upper atmosphere. Escaping species typically cannot be supplied to the escaping region
 397 of the atmosphere at rates comparable to the various theoretical upper limits for either
 398 Jeans or hydrodynamic escape. Escape rates are then controlled by the flux of escap-
 399 ing species to the region of escape, a regime known as diffusion-limited escape because
 400 diffusion is the principal transport mechanism in the escape regions of the most famil-
 401 iar planetary atmospheres (Hunten, 1973; Kasting & Catling, 2003). Consider a trace
 402 gas of density n_i significantly lighter than the mean molecular mass of a planetary at-
 403 mosphere and present at the homopause, where eddy diffusion is too weak to mix the
 404 atmosphere thoroughly. The separate gases will unmix by molecular diffusion and seg-
 405 regate. Unmixing at the homopause sets the limiting diffusion rate, which is dependent
 406 on the mixing ratio at the homopause itself as well as the diffusion coefficient of the light
 407 trace gas in the heavier principal constituents ($b_{i, dom}$) (Hunten, 1973) (In the following
 408 equation the mass of the trace gas, is very small compared to the mass of the principal
 409 constituent, its number density is also very small, and we neglect thermal diffusion; we
 410 will explore diffusion limited escape more in Section 3.1.3; n is the number density of the
 411 main constituent).

$$\Phi_i(\text{escape}) = \left(\frac{b_{i,\text{dom}}}{H} \right) \frac{n_{i,\text{homopause}}}{n} \quad (15)$$

412 Note that the dependence of the diffusion rate at the homopause on the concen-
 413 tration of the light species at the homopause makes diffusion-limited transport also de-
 414 pendent on all barriers to transport of the light gas lower in the atmosphere such as an
 415 atmospheric cold trap. Escape of H at Earth is a perfect example of diffusion limited es-
 416 cape (Shizgal & Arkos, 1996).

417 Thus, thermal escape has three classes of rate limit: (1) an absolute one based on
 418 fluid dynamics at the exobase; (2) an energetic one based on the absorption of solar EUV
 419 near the exobase; and (3) a compositional one based on atmospheric vertical transport
 420 below the exobase.

421 **2.1.2 Key parameters**

422 The most important parameters controlling thermal escape are the atmospheric scale
 423 height in the thermosphere, H , which depends upon the exospheric temperature T_e (Sec-
 424 tion 3.3.2) and the mass of the atmospheric constituents, m_i .

425 The regime of thermal escape is governed by the dimensionless Jeans parameter
 426 $\lambda_{ex} = (GMm_i/r)/(kT)$ with r being taken either as the distance from the center of the
 427 planet to the surface, exobase, or the location of the molecule(s) in question. There is
 428 a critical value for λ_{ex} , below which there is a transition between between hydrodynamic
 429 and Jeans escape. Simply equating the internal energy and the escape velocity would
 430 suggest that the critical value of λ_{ex} is $\frac{1}{\gamma-1}$, with γ begin the heat capacity ratio, directly
 431 linked to the degree of freedom of the molecule/atom. This would correspond to 1.5 for
 432 ideal monoatomic gases and 2.5 for ideal diatomic gases. Thus, Selsis (2006) refers to
 433 a critical value of 1.5 for simplicity. Simulations by Erkaev et al. (2015) of an atmosphere
 434 dominated by H_2 show a transition in escape rates near $\lambda_{ex} = 2.5$, which implies that
 435 $\frac{1}{\gamma-1}$ is indeed a good estimate of λ_{ex} .

436 Following Selsis (2006), we can define a critical temperature T_c for which $\lambda_{ex} =$
 437 1.5 for the different planets, which is valid for a H atom.

438 At Titan, the eventual escape of material to space is determined by the combined
 439 effects of the deep atmosphere limiting flux and the effects of photochemical loss (for CH_4)
 440 or production (for H_2) above the homopause region (J. M. Bell et al., 2014). Each of the
 441 major species, N_2 , CH_4 , and H_2 possess separate critical points, but the nominal exobase
 442 is located near 1500 km, which is a significant fraction of the radius of Titan (2575 km).

443 Selsis (2006) gives a table of critical temperature, λ_{ex} (noted χ in that paper) and
 444 exospheric temperature for different objects in the Solar system. Table 2 is an update
 445 taking into account the recent data, e.g. from New Horizons.

446 In Johnson et al. (2013b, 2013a) a criterion for where the transition between Jeans
 447 escape and hydrodynamic escape should be considered, based on the heating rates, has
 448 been described.

449 **2.1.3 Questions and Important Points**

450 **2.1.3.1 How the transition between the thermal escape and the hydrodynamic es-**
 451 **cape is done?** Motivated by *Cassini* spacecraft data for Titan, and *New Horizons* data
 452 for Pluto, there has been renewed interest in the physical assumptions underlying plan-
 453 etary escape. Following Hunten (1982), it was assumed that if the binding parameter
 454 $\lambda_{ex} < 1$ near the exobase, an organized hydrodynamic flow would result, whereas if $\lambda_{ex} >$
 455 10 that collisionless Jeans escape would result. Intermediate models called *slow hydro-*

456 *dynamic escape* including transport effects such as thermal conduction were also devel-
 457 oped (Watson et al., 1981; Hunten & Watson, 1982; D. F. Strobel, 2008b) to bridge the
 458 intermediate values of λ_{ex} between the two limits. Recently, Volkov, Johnson, et al. (2011)
 459 used DSMC to model atom/molecule motions under gravity and collisions. It was as-
 460 sumed that heating occurred below the base of the simulation domain, so that particles
 461 enter the domain with a Maxwell-Boltzmann distribution at a prescribed temperature.
 462 Subsequent collisions between particles then transport heat upward effectively by a heat
 463 conduction flux (although the Fourier law may be inaccurate to describe this flux). The
 464 particle density at the base of the simulation domain was parameterized through the ra-
 465 tio of mean free path to the scale height (the Knudsen number), which is a measure of
 466 the frequency of collisions. The surprising result of the simulations presented in Volkov,
 467 Johnson, et al. (2011) was that a sharp transition occurs from the hydrodynamic to the
 468 Jeans escape limits, near $\lambda_{ex} \sim 2 - 3$ depending on the particle interaction law. Ana-
 469 lytic support of these results was given in Gruzinov (2011). For $\lambda_{ex} > 3$, the bulk fluid
 470 velocity never becomes supersonic, and the escape rate is near the Jeans escape rate. Hence,
 471 given the assumptions of that study, hydrodynamic outflow is limited to small values of
 472 the binding parameter. Early in the Cassini mission to the Saturn system, D. F. Stro-
 473 bel (2008b) posited that slow hydrodynamic escape could be occurring in the upper at-
 474 mosphere of Titan, due the moon’s low gravity and the extended nature of its atmosphere.
 475 Further still, the combined works of D. F. Strobel (2008b, 2012) and Yelle et al. (2008)
 476 went a step further and suggested that hydrodynamic escape was in fact the only mech-
 477 anism that could adequately reproduce the observations of methane. However, later in-
 478 vestigations by J. M. Bell et al. (2011) and later in J. M. Bell et al. (2014) demon-
 479 strated that, by self-consistently coupling dynamics, composition, and thermal structure calcu-
 480 lations, that the in-situ measurements of methane by the Ion-Neutral Mass Spectrom-
 481 eter (INMS) (J. H. Waite et al., 2004; Magee et al., 2009) could be explained with the
 482 atmosphere in a nearly diffusive state without the need for invoking slow hydrodynamic
 483 escape of methane.

484 Similar to the situation at Titan, the data obtained by the New Horizons flyby of
 485 Pluto and Charon was not consistent with a previously posited hydrodynamic escape mech-
 486 anism occurring at the dwarf planet Gladstone et al. (2015). Prior to this observation,
 487 Pluto was suggested to be the archetype for a planetary atmosphere in a state of hydro-
 488 dynamic escape. Instead, the DSMC simulation by Tucker and Johnson (2009); Tucker
 489 et al. (2012), which suggested that Pluto’s atmosphere could be simulated without in-
 490 voking hydrodynamic escape, seem to better match observations made by New Horizons.
 491 Thus, despite being posited as occurring at several bodies in the Solar system, there is
 492 no clear evidence for slow hydrodynamic escape occurring in our Solar system during the
 493 current epoch.

494 **2.1.4 Observables**

495 When observing escape in real time, thermal escape can be viewed as principally
 496 a function of the density of the escaping species and exospheric temperature (Eq. 4). A
 497 typical technique is to infer density and temperature from airglow emission, which is also
 498 a function of density and exospheric temperature (e.g. M. S. Chaffin et al. (2014)). In
 499 some cases, *in-situ* mass spectrometry of neutrals can enable better constraints on den-
 500 sity (e.g. Cui et al. (2008)), while satellite drag can add yet another constraint jointly
 501 dependent on bulk atmospheric density and temperature (e.g. Krauss et al. (2012)).

502 The central value of observing airglow emission for planets in the Solar system and
 503 the difficulty of obtaining additional constraints on escape from exoplanets strongly sug-
 504 gests that airglow emission will be the key observable for quantifying thermal escape at
 505 exoplanets, whether by Jeans or hydrodynamic escape. The expected observable for in-
 506 tense hydrodynamic escape is of a highly extended hydrogen corona containing relatively
 507 large amounts of heavier atoms rather than a rapid fall-off in the concentration of such

508 atoms beyond the exobase (Vidal-Madjar et al., 2003). Airglow, however, is extremely
 509 difficult to observe at exoplanets and can be affected by particle precipitation (Bernard
 510 et al., 2014). For small/rocky planets such as a Earth-like or a Mars-like exoplanet, a
 511 technique based on CO₂ or O₂ absorption due to stellar occultation in the near UV can
 512 be used, but is extremely challenging (Gronoff, Maggiolo, et al., 2014).

513 The main observable for thermal escape in a planet’s past is mass fractionation of
 514 the isotopic composition of the atmosphere from the stellar value. However, caution must
 515 be exercised. Isotopic composition can be affected by the outgassing of primordial ma-
 516 terials and low-temperature chemical reactions unrelated to escape (Pepin, 2006; E. C. Pope
 517 et al., 2012). Moreover, isotopic composition is strongly sensitive to Jeans escape but
 518 variably sensitive to hydrodynamic escape.

519 For Jeans escape, it can be inferred from Eq. 4 that the escape rate is proportional
 520 to $m_i^{-1/2}$ for small values of λ_{ex} and $m_i^{1/2}e^{-\lambda_{ex}}$ for large values of λ_{ex} . The former case
 521 would be hydrodynamic escape. So for Jeans escape, deuterium escapes at a rate less
 522 than atomic hydrogen.

523 In the case of hydrodynamic escape, the principal escaping species drags gases lighter
 524 than the “crossover mass” (m_c) (Hunten et al., 1987).

$$m_c = m_{esc} + \frac{kT\Phi_{esc}}{bgX_{esc}} \quad (16)$$

525 where $_{esc}$ refers to the principal escaping species, b is the binary diffusion coefficient (the
 526 diffusion coefficient in a 2-components gas), and X is the mole fraction. If the escape
 527 flux of the principal escaping species can be defined at a reference altitude Φ_{esc}° and is
 528 sufficiently small, then the escape flux of the trace species at the reference altitude Φ_{trace}°
 529 is:

$$\Phi_{trace}^{\circ} = \frac{X_{trace}}{X_{esc}} \Phi_{esc}^{\circ} \left[\frac{m_c - m_{trace}}{m_c - m_{esc}} \right] \quad (17)$$

530 (Hunten et al., 1987). It is in these slower hydrodynamic escape cases that significant
 531 fractionation is possible on geological timescales. Otherwise, the larger species are car-
 532 ried along with the flow. And everything scales with mole fraction.

$$\Phi_{trace}^{\circ} = \frac{X_{trace}}{X_{esc}} \Phi_{esc}^{\circ} \left[1 - \frac{bg^{\circ} X_{esc}}{kTF_{esc}^{\circ}} (m_{trace} - m_{esc}) \right] \quad (18)$$

533 (Hunten et al., 1987). In this case, fluxes are weakly dependent on mass at masses close
 534 to the mass of the principal escaping species but more strongly dependent on mass at
 535 masses much greater than that of the principal escaping species, resulting in minimal frac-
 536 tionation of low mass species but significant fractionation of high mass species (Hunten
 537 et al., 1987; Tian et al., 2013).

538 As noted in Pepin (1991); Shizgal and Arkos (1996); Pepin (2006), the uncertainty
 539 in the hydrodynamic escape parameters, notably with the EUV output of the Young Sun,
 540 the noble gas reservoirs, the volatile outgassing (etc.), are a problem to retrieve the whole
 541 history of a planetary atmosphere. In addition, other escape processes lead to isotopic
 542 fractionation.

543 2.2 Photochemical Escape

544 The dominant non-thermal loss processes vary for each planetary body. The rel-
 545 ative significance of each process depends on planetary mass, atmospheric composition,
 546 and distance from the sun. For instance, at Mars, the current dominant non-thermal loss
 547 processes are photochemical, while at Venus is it thought to be through ionospheric es-
 548 cape (Lammer et al., 2008).

549 The photochemical escape of a planetary atmosphere is a non-thermal loss process
 550 due to exothermic chemical reactions in the ionosphere that provide enough kinetic en-
 551 ergy for the escape of the neutral constituents. Photochemical escape often includes di-
 552 rect interactions of photons and photoelectrons with thermospheric and exospheric molecules,
 553 as well as chemical reactions of ions with neutrals and electrons. In the following, we will
 554 add the symbol * to neutral and ionized species to show that they have a non-negligible
 555 amount of kinetic energy. Such species are usually called “hot”; and for the neutral atoms,
 556 the term ENA, for Energetic Neutral Atom, is often used.

557 The general method of computation for the escape of a fast atom or ion can be found
 558 in Shematovich et al. (1994). The general transport equation for any species in the at-
 559 mosphere is:

$$\frac{\partial f}{\partial t} + \vec{v} \frac{\partial f}{\partial \vec{x}} + \frac{\vec{F}}{m} \frac{\partial f}{\partial \vec{v}} = Q + H_{h\nu} + J_{el} + J_q + J_{cx} \quad (19)$$

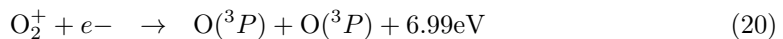
560 where Q represents the productions, $H_{h\nu}$ the spontaneous transition to another state
 561 –typically by light emission–, J_{el} the loss due to elastic scattering (and therefore momen-
 562 tum transfer) (Lilensten et al., 2013), and J_q the loss due to quenching. Note the ad-
 563 dition of an extra loss term, J_{cx} , for charge exchange. The transport equation should be
 564 taken into account for all the species, and they can be coupled when the loss of one species
 565 creates another one. An example of that situation is the coupled transport between H
 566 and H^+ , where a proton undergoing a charge exchange will become a fast H, that can
 567 be re-ionized later. This equation is also valid for the excited state species, such as $O(^1S)$
 568 and $O(^1D)$, that are notably responsible for the green line and the red line in aurorae
 569 (Gronoff, Simon Wedlund, Mertens, & Lillis, 2012; Gronoff, Simon Wedlund, Mertens,
 570 Barthélemy, et al., 2012).

571 In the following subsections, we review the main processes creating ENA/fast ions.
 572 Charge exchange is described in a later section. While the same equation should be solved
 573 to address atmospheric escape, approximations are often used for the coupled ion/ENA
 574 equations, angular diffusion, and upper atmospheric densities (Rahmati et al., 2018). These
 575 approximations are used for several reasons. One particularly problematic point in the
 576 simulations is the distance at which a particle is considered lost in space; some studies
 577 take a few planetary radii, other a few exospheric altitudes. Such approximations can
 578 create difficulties when comparing with observations (Baliukin et al., 2019).

579 **2.2.1 Ion recombination**

580 An exothermic ion recombination (or chemical reaction) can give enough kinetic
 581 energy to one of its products so that it can escape. Ion recombination is the most effec-
 582 tive channel to escape O in the present Martian atmosphere. It is, in general, an efficient
 583 way to heat up an atmosphere through non-thermal process. It is also a process lead-
 584 ing to the escape of heavier atoms from light planets or bodies. The process has been
 585 largely studied in the past (Shizgal & Arkos, 1996), and is being refined in support of
 586 the MEX and MAVEN missions (Cipriani et al., 2007; Yagi et al., 2012; Valeille et al.,
 587 2010; Zhao & Tian, 2015; Lillis et al., 2017).

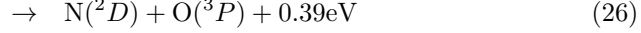
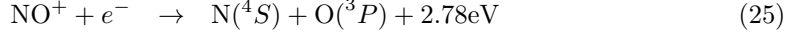
588 At Mars, the main photochemical escape process is the loss of oxygen through the
 589 reaction:



590 Recent studies by MAVEN were able to show the hot oxygen corona produced by
 591 these recombination reactions (Deighan et al., 2015). A study by Cravens et al. (2017)
 592 shows that, in the limits of the current solar conditions at Mars, a linear dependence of
 593 the escape rate to the EUV flux can be made.

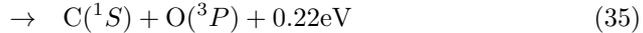
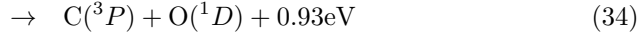
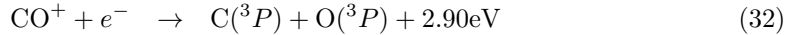
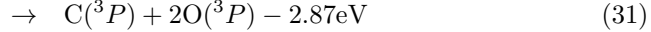
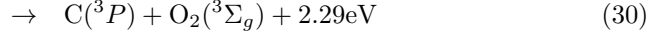
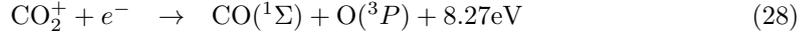
594 Another interesting reaction is $\text{N}_2^+ + e^- \rightarrow 2\text{N}^*$ which is efficient enough for the
 595 removal of ^{14}N but not ^{15}N at Mars, and could explain the isotopic fractionation (Shizgal
 596 & Arkos, 1996).

597 At Earth and Mars, we also have (Shizgal & Arkos, 1996; Gröller et al., 2014) (the
 598 channel with $\text{O}(^1\text{D})$ has branching ratio close to zero):



599 To compute the photochemical escape through these processes, it is first necessary
 600 to compute the ion density. This involves, first, computing the ion productions (via pho-
 601 toionization, secondary electron ionization, etc.); second, computing the resulting chem-
 602 istry and transport to get the ion densities; third, computing the hot atom production,
 603 using the densities and the reaction rate; fourth, compute the actual escape by comput-
 604 ing the transport of the hot atom. Such an escape should include collisions with other
 605 species; if the hot atom creation rate is important enough, it should be taken into ac-
 606 count that these collisions heat up the upper atmosphere, and therefore change its pro-
 607 file towards more escape.

608 Recent work at Mars shows that the CO_2^+ dissociative recombination is a non-negligible
 609 source of hot oxygen (Lee et al., 2015; Zhao & Tian, 2015). In the following, the first re-
 610 action is believed to have a branching ration between 96% and 100%:



611 Hot oxygen in a planetary thermosphere can also induce escape of lower mass species
 612 by sputtering (Shizgal, 1999).

613 **2.2.2 Photodissociation**

614 Another process leading to the creation of fast ions or atoms is the direct dissoci-
 615 ation by photon, electron, or proton impact.

616 In Shematovich et al. (1994) an example is given by the reaction $\text{O}_2 + h\nu \rightarrow \text{O}(^3\text{P}) + \text{O}(^3\text{P}, ^1\text{D}, ^1\text{S})$;
 617 the kinetic energy given to the products is the difference between the energy of the pho-
 618 ton and the binding energy (i.e. the threshold energy for the reaction). Similar processes

619 can be evaluated for N_2 , CO_2 , etc. Photodissociation reactions are seldom considered in
 620 evaluating escape rates since the production of fast enough particles to escape is small
 621 with respect to ion recombination processes. To properly evaluate these productions, it
 622 is necessary to have an accurate set of cross sections (see Section 3.2.4). In general, ther-
 623 mospheric codes consider that the kinetic energy given by these photodissociations ends
 624 up in heating, therefore one has to be careful to not count that loss of energy twice in
 625 their simulations.

626 **2.2.3 Di-cation dissociation**

627 The di-cation dissociation effect on planetary escape has been proposed by Lilensten
 628 et al. (2013). It is a non-thermal process that is based on the fact that the Coulom-
 629 bian dissociation of a molecular doubly charged ion may give enough energy to one or
 630 both of the ions to allow their escape.

631 The typical example for this process is $\text{CO}_2^{2+} \rightarrow \text{CO}^+ + \text{O}^+$, as described in Lilensten
 632 et al. (2013). Other processes such as $\text{N}_2^{2+} \rightarrow 2\text{N}^+$ (Gronoff et al., 2007), or $\text{O}_2^{2+} \rightarrow 2\text{O}^+$
 633 (Simon et al., 2005; Gronoff et al., 2007) can give sufficient energies for the ion to escape.
 634 To account for the flux of escaping particles through that process, it is necessary to com-
 635 pute the transport of the fast ions from where they are created to the exobase. Since it
 636 is ions that are escaping, they are not necessarily escaping even if they reach the exobase
 637 with sufficient energy: the presence of magnetic fields could prevent their escape, and
 638 return them into the atmosphere where they could create some additional heating (the
 639 Coulomb energy being in the range of several 10 eV, such ions could not efficiently sput-
 640 ter, except if they are further accelerated by the solar wind). A process not accounted
 641 for in the Lilensten et al. (2013) paper is the heating of the ionosphere and the creation
 642 of fast ENA through charge exchange of the fast ions with the atmosphere (a process sim-
 643 ilar to the one described in Chassefière (1996a)). On the contrary, ions with energy lower
 644 than escape energy could escape due to electromagnetic forces, as will be explained in
 645 Section 2.4 and 2.5.

646 The calculation of the dication escape in a non-magnetized atmosphere proceeds
 647 as follows: from $P_{i^{2+}}(z)$, the production rate of the specific dication i^{2+} in function of
 648 the altitude z , we compute its density $n_{i^{2+}} = P_{i^{2+}}(z)/L_{i^{2+}}(z)$ from the chemical loss
 649 processes L , neglecting the transport because of the small lifetime of the dication (for
 650 a detailed analysis of the production processes see e.g. Gronoff, Simon Wedlund, Mertens,
 651 and Lillis (2012); Gronoff, Simon Wedlund, Mertens, Barthélemy, et al. (2012)). From
 652 there, the standard transport equation of fast ion in the atmosphere can be used. The
 653 study of Lilensten et al. (2013) does not take into account the loss of energy of O^{+*} im-
 654 pacting atmospheric O, therefore overestimating the escape (the study considers impact
 655 on CO_2 , which has a smaller scale height). On the other hand it underestimates the es-
 656 cape rate by not doing a coupled equation transport and therefore not taking into ac-
 657 count the escape of O^* created by charge exchange of O^{+*} with other thermospheric species.

658 **2.2.4 Key parameters**

659 Modeling photochemical loss requires the cross section for ionization by the differ-
 660 ent processes (including elastic, inelastic, and charge exchange), and the chemical reac-
 661 tion rates for the density/recombination (including the branching ratio and the prod-
 662 ucts speed probabilities). The ionospheric electron temperature is overall extremely im-
 663 portant since the recombination cross section is likely to be extremely sensitive to it (Sakai
 664 et al., 2016). For the simulation of the ion/electron composition and temperature, it is
 665 necessary to perform a 3-D modeling of the ionosphere.

666 **2.2.5 Questions**

667 The evaluation of escape rates from photochemical reactions has mainly been done
 668 for Solar system planets, especially Mars and Venus. Once we consider exoplanets or the
 669 Young Solar system, questions remains about the efficiency of each processes. The ion
 670 recombination or the usually neglected processes such as particle impact dissociation could
 671 become more important when increase in XUV or precipitating particle flux occur. This
 672 question is difficult to answer since each process affects the state of the upper atmosphere
 673 and the efficiency of each other.

674 **2.2.6 Observables**

675 The recombination processes create ENA at very specific energies, typically in the
 676 5 eV range. Since collisions occurs, changing the spectral shape of the energy distribu-
 677 tion, the direct observation of these energies peaks is extremely challenging. Indirect tech-
 678 niques, based on modeling the hot oxygen corona are used. At Mars, a technique to ob-
 679 serve the product of photochemical reactions involved observing the hot oxygen geocorona
 680 (Deighan et al., 2015). As explained in Shizgal and Arkos (1996), photochemical escape
 681 can explain the fractionation of $^{14}\text{N}/^{15}\text{N}$ at Mars. A more recent work from Mandt et
 682 al. (2015) shows that non-thermal processes except photodissociation can explain the iso-
 683 topic enrichment. The work of Liang et al. (2007) shows that self-shielding effects can
 684 lead to an increase in heavier isotopes (here ^{15}N at Titan) escape from photodissocia-
 685 tion.

686 **2.3 Ion Loss**

687 The ion loss mechanisms begin with the interaction of the upper atmosphere and
 688 ionosphere with the solar wind. Neutral atoms can be ionized by solar UV, charge ex-
 689 change and electron impact, and can be scavenged by the solar wind. There are differ-
 690 ent processes and loss channels through which the planetary ions can escape to space,
 691 including pickup and sputtering, charge exchange, and outflow, which will have its ded-
 692 icated subsection. Ion escape is believed to be one of the major sources of atmospheric
 693 escape in the current Solar system and also at exoplanets around M-dwarfs (Garcia-Sage
 694 et al., 2017).

695 **2.3.1 Pickup and sputtering escape**

696 *2.3.1.1 Pick-up escape* Pick up ion loss is due to the ionization of neutral con-
 697 stituents in the exosphere and upper atmosphere that sense an electric field and can be
 698 “picked up” and swept away. In the presence of the magnetic field, at Earth for exam-
 699 ple, the polar wind drives pick up ion escape (T. E. Moore et al., 1997). At lower alti-
 700 tudes, this interaction can compress the magnetic field on the sunward side, forming a
 701 tail on the anti-sunward side. At high altitudes, the loss of H^+ , He^+ and O^+ can occur
 702 when thermal plasma originating from the polar regions in the ionosphere is accelerated
 703 into the magnetosphere and escapes downtail (Johnson et al., 2008). These processes will
 704 be detailed in Section 2.4 and 2.6.

705 At weakly magnetized planets, such as Mars and Venus, the lack of an intrinsic dipole
 706 magnetic field creates a scenario where the solar wind directly interacts with the upper
 707 atmosphere. In this situation, neutral constituents are ionized and picked up by the back-
 708 ground convection electric field that is driven by the solar wind, where $\vec{E}_{\text{SW}} = -\vec{U}_{\text{SW}} \times$
 709 \vec{B}_{SW} where \vec{E}_{SW} is the electric field induced on an ion by the solar wind (and there-
 710 fore that ion will be subject to a force $\vec{F} = q\vec{E}_{\text{SW}}$), \vec{U}_{SW} is the solar wind speed and
 711 \vec{B}_{SW} is the interplanetary magnetic field. The main channels for ionizing planetary neu-
 712 trals are photoionization, charge exchange and electron impact ionization. Curry et al.
 713 (2013) investigates these mechanisms as a function of solar zenith angle, bulk velocity

714 and plasma temperature, respectively, finding that the majority of pick-up ions are formed
 715 in the corona and sub-solar region of Mars. The origin of pickup ions plays a major role
 716 in their fate as escaping particles or precipitating particles (Fang et al., 2010). In the for-
 717 mer case, the pick-up ions can accelerate to twice the solar wind speed and their gyro-
 718 radii are on the order of a planetary radius, and are likely to escape. The maximum en-
 719 ergy of a picked-up ion is $E_{max} = 2mU_{SW}^2 \sin^2(\theta_B)$ where θ_B is the angle between the
 720 solar wind direction and the interplanetary magnetic field (Rahmati et al., 2015). In the
 721 case of precipitating ions, the pick up ions will collide with neutrals in the exobase or
 722 thermosphere and transfer enough energy and momentum to the neutral that they could
 723 be able to exceed the escape velocity; a process known as sputtering. Ion precipitation
 724 also impacts the atmosphere through heating. The sputtering process can also happen
 725 at Earth, inside the polar regions (Shematovich et al., 2006), but it is a small process
 726 there.

727 *2.3.1.2 Pick-up equations* If we consider n_{SW} as the solar wind density, n_O the
 728 density of oxygen where that solar wind is located, σ_{CX} the average charge exchange cross
 729 section between the solar wind and oxygen and $\sigma_{PI}(\lambda)$ the photoionization cross section,
 730 we have an ion production of $P_I = n_O(\int \sigma_{PI}(\lambda)\Phi_{EUV}(\lambda)d\lambda + \sigma_{CX}n_{SW}U_{SW})$ (and
 731 other ionization processes can be added such as electron impact) (Rahmati et al., 2015,
 732 2017), that production is balanced by the pick-up transport. If we consider $P_I(\vec{v})$ the
 733 production of ion at a speed defined by \vec{v} (so that $\int P_I(\vec{v})d\vec{v} = P_I$), e the charge of the
 734 ion and m its mass, then the velocity distribution function $f(\vec{x}, \vec{v})$ for the picked-up ions
 735 is governed by (Hartle et al., 2011):

$$\vec{E}_{SW} = -\vec{U}_{SW} \times \vec{B}_{SW} \quad (38)$$

$$\vec{v} \cdot \frac{\partial f}{\partial \vec{x}} + \frac{e}{m} (\vec{E}_{SW} + \vec{v} \times \vec{B}_{SW}) \cdot \frac{\partial f}{\partial \vec{v}} = P_I(\vec{v}) \quad (39)$$

$$\Phi(\vec{x}) = \int v f d\vec{v} \quad (40)$$

736 with e the ion charge. Several techniques can be used for solving Equation 39; the com-
 737 plexity arises from the solar wind piling up around the planet (or the comet (Coates, 2004),
 738 creating complex magnetic field geometries. Typically, it has been solved using test par-
 739 ticles (Monte Carlo simulations) in fields from MHD or self consistent hybrid codes, as
 740 by (Jarvinen & Kallio, 2014).

741 *2.3.1.3 Sputtering* The yield Y of sputtered neutrals is defined by the sputter-
 742 ing efficiency. This yield is the ratio of the number of escaping particles and the num-
 743 ber of incident particles, which varies inversely with the planet’s gravitational energy (Johnson,
 744 1994; Leblanc & Johnson, 2002; Johnson et al., 2008). Sputtering is dependent on the
 745 incident particles’ energy and angle of incidence, as well as the mass of the incident par-
 746 ticle. For lighter incident pickup ions, the direct scattering of planetary neutrals is known
 747 as “knock-on”, which dominates at low, grazing incidence angles. For heavier incident
 748 pickup ions, the additional momentum can create a cascade of collisions at high enough
 749 energies to cause a neutral to escape, where $Y \geq 1$ (Leblanc & Johnson, 2001; Johnson
 750 et al., 2008). This occurs for O^+ pickup ions at energies of \sim keV to \sim hundred keV. This
 751 is especially important when the pickup ion gyroradius is of the order of the planet ra-
 752 dius, as at weakly magnetized bodies such as Mars, Venus and Titan.

753 Sputtering is widely believed to be the dominant escape process at Mars and Venus
 754 during earlier epochs of our Sun, which has major implications for exoplanetary atmo-
 755 spheres. J. G. Luhmann et al. (1992) calculated the flux of precipitating pick-up ions and
 756 ENAs using a 1D exospheric model of the O density and a gas-dynamic model of the
 757 solar wind and found compared to pickup ion and photochemical escape, sputtering drove
 758 the highest rates of atmospheric erosion (see Figure 3). Other studies using MHD and
 759 hybrid models have found similar results (Chaufray et al., 2007; Wang et al., 2014). Sput-
 760 tering as a dominant driver of atmospheric escape is further supported by current iso-

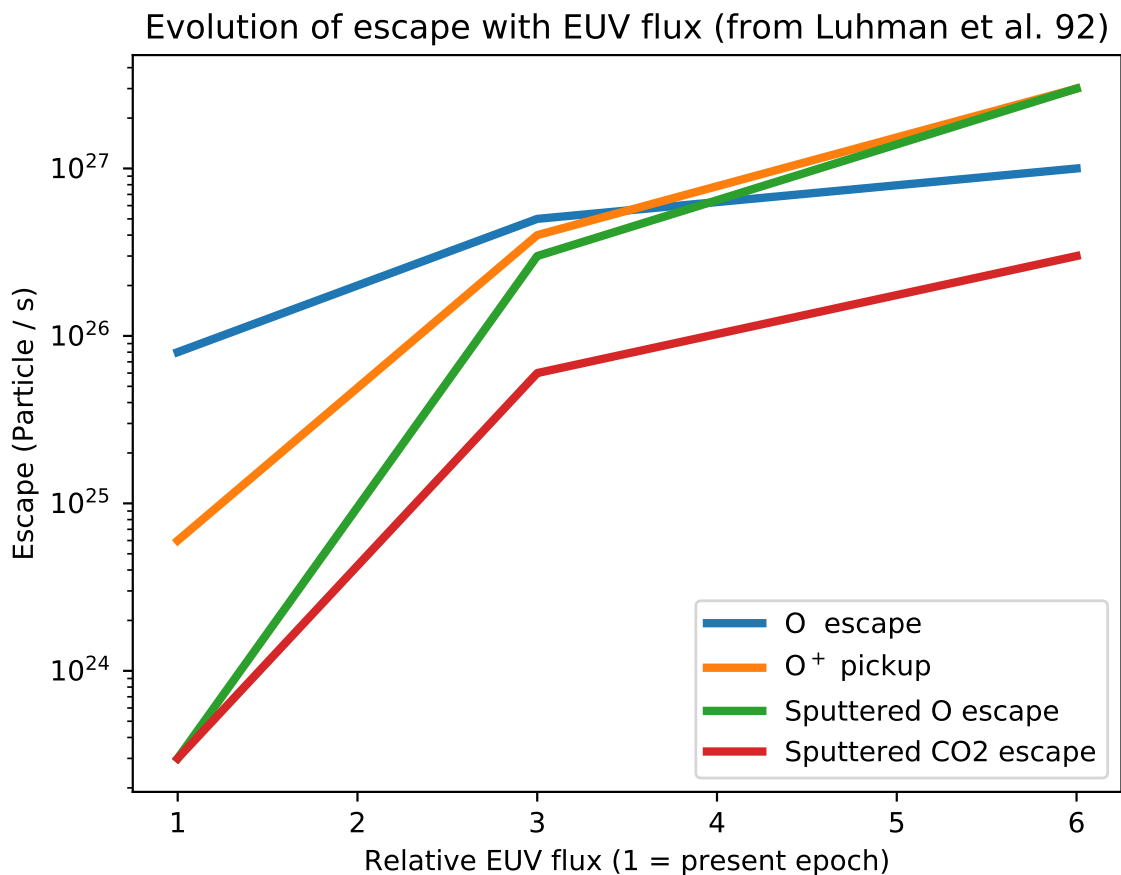


Figure 3. EUV dependence of the escape process at Mars. Simulations data from J. G. Luhmann et al. (1992)

761 tope ratios. Specifically, Ar is an important atmospheric tracer because once Ar is in the
 762 atmosphere, the only loss process is escape to space (as opposed to volcanic outgassing
 763 from the interior, impact delivery, and mixing with the crust), which limits the exchange
 764 pathways that become complicated for most planetary volatiles (Jakosky & Phillips, 2001).
 765 Thus, measurements of the present day atmosphere reflect the importance of these ex-
 766 changes over billions of years and emphasizes the need for understanding our own ter-
 767 restrial planets' atmospheric evolution as a ground truth for understanding exoplanetary
 768 atmospheres.

769 Unfortunately, sputtering is incredibly difficult to observe as the sputtered compo-
 770 nent at Mars is indiscernible from photochemically produced oxygen. Thus models have
 771 typically predicted what the sputtered component would be in a variety of scenarios. The
 772 passage of the Siding Spring comet close to Mars (Bodewits et al., 2015) created a high
 773 flux of O⁺ ions that impacted the atmosphere as predicted in (Gronoff, Rahmati, et al.,
 774 2014). Observations by the MAVEN Solar Energetic Particle instrument (SEP) and the
 775 Mars Odyssey-High Energy Neutron Detector (HEND) indicate an increase in the O⁺
 776 pickup during the passage; however, an increase in solar activity at the same time pre-
 777 vents a clear conclusion on whether or not it was due to the comet (Sánchez-Cano et al.,
 778 2018). Wang et al. (2016) computed the impact of these ions on the escape rate, and found

779 that up to 10 tons of atmosphere may have escaped while 1 ton of material was added.
 780 Another formulation of the escape by sputtering can be found in Shizgal (1999). In this
 781 paper, it is the sputtering by the hot oxygen of Venus that leads to the escape of H and
 782 D. The main difference with the usual pickup-sputtering process is the origin of the hot
 783 O, from the thermosphere itself, and therefore that the forcing by an external flux and
 784 the use of yield function cannot be applied. Shizgal (1999) developed a specific kinetic
 785 model for the escape.

786 *2.3.1.4 Sputtering equations* The rate of species n_j escaping an atmosphere from
 787 sputtering is given by $\frac{\partial n_j}{\partial t} \approx 2\pi R_{exo}^2 < \Phi_a Y_j >$ (Johnson, 1994) where Φ_a is the flux
 788 of the particle leading to the sputtering and Y_j the sputtering efficiency for that pecu-
 789 liar species. For sputtering by an incident particle A and a target species B, and of re-
 790 spective masses M_A and M_B i.e. a thermosphere whose main constituent is B, the yield
 791 can be computed as follows. First, for an incident particle of energy E_A , it is necessary
 792 to evaluate the elastic cross section $\sigma_d(E_A)$ which is related to the momentum transfer
 793 (or knock-on, elastic nuclear) stopping cross section $S_n(E_A)$ through:

$$\gamma = \frac{4M_A M_B}{(M_A + M_B)^2} \quad (41)$$

$$\sigma_d(E_A) = \frac{\gamma}{2} E_A S_n(E_A) \quad (42)$$

794 The overall yield is the result of single impact plus multiple impact momentum trans-
 795 fer at energy greater than the escape energy. It can be approximated by (Johnson, 1994;
 796 Johnson et al., 2000):

$$Y(\theta, E) \approx \frac{\alpha \beta S_n(E)}{2U_{es} \sigma_d(\bar{E}_{es}) \cos^p \theta} \quad (43)$$

$$\bar{E}_{es} \approx U_{es} \quad (44)$$

797 where θ is the incident angle, U_{es} is the gravitational binding energy at the exobase, \bar{E}_{es}
 798 is the average energy of the escaping particle. α , β , and p are constants depending upon
 799 the impact particles, see Johnson (1994) for some numerical values in the literature. The
 800 sputtering yield may be enhanced by the sputtered particles that are picked-up and ac-
 801 celerated towards the atmosphere (equation 2 in Johnson (1994)). If the efficiency of es-
 802 cape for a sputtered particle is Y_a and its ionization and return is p_i , then the effective
 803 yield is $Y_{eff} = Y / (1 - p_i (Y_a - 1))$.

804 *2.3.1.5 Other impact processes* The classical sputtering process involves the im-
 805 pact of an ion that has been accelerated by pick-up, i.e. a non-thermal processes out-
 806 side of the thermosphere. Gacesa et al. (2012) proposed a very similar mechanism where
 807 the impact of hot O from the Martian corona sputters light gases. Their computations
 808 suggest it is the main channel for HD and D₂ direct escape. To validate that approach,
 809 it is suggested to observe the emission of H₂ ro-vibrationally excited by the impact. ENA
 810 impact on the Martian atmosphere are also a source of escape, especially when they have
 811 been created by charge exchange from the solar wind (Lewkow & Kharchenko, 2014),
 812 which leads us to the other class of escape processes.

813 **2.3.2 Charge exchange of a magnetically trapped particle**

814 The basic idea of charge exchange escape is that a magnetically trapped energetic
 815 ion, such as H⁺, exchanges its charge and becomes an energetic neutral atom (ENA) that
 816 can escape or sputter (an ion trapped in a magnetic mirror may be prevented to reach
 817 the thermosphere and therefore to efficiently sputter) (Shizgal & Arkos, 1996). The tem-
 818 perature dependence is complex: at Earth it decreases with exospheric temperature for
 819 H (Shizgal & Arkos, 1996) so that the escaping flux from charge exchange plus Jeans es-
 820 cape is constant, reaching the diffusion-limited value.

821 A simple approach adopted by Yung et al. (1989) was to consider that the ion H^+
 822 had a Maxwellian distribution at the temperature T_{ion} . Having exchanged its charge,
 823 the energetic neutral atom could escape, and it would have the same energy as the ini-
 824 tial ion. The efficiency for an escaping charge-exchanged atom, with respect to the tem-
 825 perature of the initial ion is

$$\alpha_i(R) = B_{CX} \left[1 - \frac{v_{esc}^2}{u_j(R)^2} \right] e^{-\frac{v_{esc}^2}{u_j(R)^2}} \quad (45)$$

826 with $u_j(R) = \sqrt{2kT_{ion}(R)/m_i}$. Considering k_{i+-j} the charge exchange rate between
 827 the ionized species i and a neutral species j (rate that can vary with temperature), this
 828 gives the escape flux

$$\phi = \int_{R_{exo}}^{R_{pp}} \left(\frac{R}{R_{exo}} \right)^2 \alpha_i(R) \sum_j k_{i+-j} [i^+][j] dR. \quad (46)$$

829 The B_{CX} factor in the definition of α_i is an efficiency factor, that was taken identical
 830 to the one for thermal escape in the Yung et al. (1989) paper. The rest of the equation
 831 is similar to the thermal escape equation, except the $\frac{u_i}{2\sqrt{\pi}}$ factor (which was taken off
 832 for considering it is hidden in the charge exchange rate). The equation in Yung et al. (1989)
 833 paper has a negative sign that should be positive: using the equation with that nega-
 834 tive sign leads to negative escape fluxes. Using that equation, it happens that the charge
 835 exchange flux should increase with increasing exospheric temperature, which is not what
 836 is observed. It means that this simplified approach is not good enough for evaluating the
 837 charge exchange flux at Earth.

838 Shizgal and Lindenfeld (1982) developed a collisional model for computing the charge
 839 exchange induced escape. The main difference with the previous approach is that the
 840 efficiency of charge exchange with respect to the temperatures is taken into account fol-
 841 lowing Fitzpatrick and Shizgal (1975). It is shown that the charge exchange is, at Earth,
 842 the most efficient mechanism to remove H from the upper atmosphere during low solar
 843 activity (low exospheric temperature) while Jeans' escape is the main mechanism dur-
 844 ing high solar activity. It is important to remember here that H escape is diffusion lim-
 845 ited at Earth. In the following, A corresponds to the neutral atmosphere (O and H), \bar{n}
 846 to the average density (of A, O, and H^+) over the region of charge exchange and σ cor-
 847 responds to the energy independent hard sphere cross section, and $a = \frac{m_A}{m_O}$

$$\lambda_{CX} = \frac{m_H v_{esc}^2}{2kT_{ion}} \quad (47)$$

$$\hat{n} = \frac{\sigma_{H^+,A} \left[\frac{n_{H^+} \bar{n}_A}{\bar{n}_O} \right] \Gamma(a)}{\sigma_{H,O} [1+a]} \quad (48)$$

$$\tau_{CX} = \frac{T_{exo}}{T_{H^+}} - 1 \quad (49)$$

$$\begin{aligned} \Phi_{CX}(\text{escape}) &= \hat{n} \sqrt{\frac{2kT_{exo}}{\pi m_H}} \frac{e^{-\lambda_{CX}}}{\tau_{CX}} \\ &\times \left[(1 + \tau_{CX}) - \sqrt{1 + \tau_{CX}} e^{-\lambda_{CX} \tau_{CX}} \right] \end{aligned} \quad (50)$$

848 This equation is valid for the escape of H at Earth from charge exchange. It sup-
 849 poses that (1) the H^+ density varies slowly with altitude at the location where this pro-
 850 cess is the most efficient (from the exobase to 3000 km), (2) the only species interact-
 851 ing are H, O, and H^+ , and (3) the distributions are Maxwellian, with a fixed temper-
 852 ature in the altitude range.

853 At Earth, the charge exchange is the main mechanism to remove O^+ from the ring
 854 current (Daglis et al., 1999). The exchange creates ENA that can be imaged to study
 855 the ring current evolution.

856

2.3.3 Charge exchange with the solar wind

857

858

859

860

861

862

The charge exchange between the solar wind and the upper atmospheric species can enhance the escape rate through pick-up like processes: a species M exchanges its charge with, for example, a proton from the solar wind $H^{+*} + M \rightarrow H^* + M^+$. The solar wind proton becomes an ENA, and can create additional heating that increases the thermospheric temperature, and therefore escape (Chassefière, 1996a). The created ion can escape thanks to pickup by the magnetic field.

863

864

865

866

867

868

869

870

871

872

873

874

875

876

877

878

879

At comets, charge transfer reactions primarily involve solar wind ions, H^+ , He^{2+} but also multiply-charged minor species such as O^{6+} , Si^{10+} , or C^{5+} (Cravens, 1997; Bodewits, 2007; Simon Wedlund et al., 2016), with water molecules continuously outgassing upon sublimation from the nucleus. As the atmosphere of a comet is in expansion, charge-transfer reactions take place over a large region of space (of the order of several 10^6 km) and will have time to facilitate the absorption of the solar wind, converting fast ions into slow-moving ones. Charge transfer has recently been evidenced by the ESA/Rosetta ion spectrometers at comet 67P/Churyumov-Gerasimenko (67P), with the observation of H^- ions (Burch et al., 2015), and He^+ fast ions (Nilsson et al., 2015). The latter charge-exchanged ions, originating from solar wind He^{2+} ions (composing about 4% of the bulk of the undisturbed solar wind), were present throughout the mission from a heliocentric distance ranging from 3.4 to 2 AU (Simon Wedlund et al., 2016; Simon Wedlund, Behar, Kallio, et al., 2019; Simon Wedlund, Bodewits, et al., 2019; Simon Wedlund, Behar, Nilsson, et al., 2019). The net effect of the charge transfer of He^{2+} solar wind ions with the neutral atmosphere of the comet (composed of molecules M) is the production of ENAs following the typical sequence of electron capture reactions (double charge transfer, and stripping reactions are ignored here for simplicity):



880

881

882

This set of reactions is equivalent to coupled differential flux continuity equations which can be solved analytically for the simplified case or numerically (Simon Wedlund et al., 2016; Simon Wedlund, Bodewits, et al., 2019).

883

884

885

886

887

888

889

890

891

892

893

Similar equations can also be derived for the coupled (H^+, H) system. These processes lead to the almost total conversion of the solar wind into ENAs, potentially escaping or sputtering the nucleus, by the time the solar wind impinges within a few tens of kilometres from the comet's surface, in the case of a highly outgassing nucleus (perihelion conditions). This total conversion depends on many parameters: outgassing rate, heliocentric distance, solar wind density and speed (Simon Wedlund, Behar, Kallio, et al., 2019; Simon Wedlund, Bodewits, et al., 2019; Simon Wedlund, Behar, Nilsson, et al., 2019). The effect of minor solar wind species (multiply-charged heavy ions) can be seen in the production of X-rays through charge exchange emission with the cometary atmosphere (Cravens, 1997). The case of comets provides a unique opportunity to study charge-exchange processes within different and varying atmospheric environments.

894

895

896

The observation of escape from HD 209458 has been interpreted as increased by charge exchange processes between the solar wind and the hydrogen from the upper atmosphere of the planet (Holmström et al., 2008).

897

2.3.4 Charge exchange with a precipitating particle

898

899

900

901

902

903

Particles precipitating in the atmosphere of planets can give rise, through charge exchange with the ambient neutral atmosphere, to the local production of ENAs. This is particularly significant at Earth in the case of protons of solar wind origin, first accelerated in the magnetosphere and then precipitating down the magnetic field lines in the polar regions. When protons are neutralized in collisions with neutrals (mainly oxygen atoms above 200 km altitude, O_2 and N_2 below), a process referred to as *electron*

904 *capture*, the newly produced hydrogen ENAs, not being sensitive to the magnetic field,
 905 travel in straight trajectories, whose direction is related to the pitch angle distribution
 906 of the impinging protons, resulting in a horizontal spreading of the precipitating beam
 907 (see, for example, Rees (1989); Kozelov et al. (1994); Galand et al. (1997, 1998); Basu
 908 et al. (2001); Simon et al. (2007)). Hydrogen ENAs, keeping most of the kinetic energy
 909 of the incoming proton, can in turn be ionized (*electron stripping*). Due to magnetic mir-
 910 roring and angular re-distributions stemming from collisions between the energetic species
 911 and the atmosphere, downwelling (or precipitating) and upwelling (or backscattered) ions
 912 and ENAs will coexist at any given altitude above the *E*-region peak of the initial pro-
 913 ton energy deposition (for a 10 keV initial proton peak will occur at 120 km altitude at
 914 Earth). The energy and angular degradation of a (H⁺,H) beam in the atmosphere is usu-
 915 ally formalized as a coupled system of two non-linear Boltzmann transport equations (Galand
 916 et al., 1997, 1998), including angular re-distributions due to the non-uniformity of the
 917 magnetic field and to collisions, for an ENA, X, and its corresponding ion, X⁺. In the
 918 following, *I*, the intensity, *P*, the momentum transfer, \mathcal{R}^{CX} , the charge transfer, and,
 919 *Q*, the local production, depend upon (τ, E, μ). The transport of ENAs, denoted X, is
 920 as follows:

$$\mu \frac{\partial I_X}{\partial \tau} = -I_X + \frac{\mathcal{P}_X + \mathcal{Q}_X + \mathcal{R}_{X^+ \rightarrow X}^{\text{CX}}}{\sum_k \sigma_{k,\text{elas}}(E) n_k(z)} \quad (53)$$

$$\mu \frac{\partial I_{X^+}}{\partial \tau} = -I_{X^+} + \frac{\mathcal{P}_{X^+} + \mathcal{Q}_{X^+} + \mathcal{R}_{X \rightarrow X^+}^{\text{CX}}}{\sum_k \sigma_{k,\text{elas}}(E) n_k(z)} \quad (54)$$

921 Numerical solutions of this system have historically made use of continuous slowing-
 922 down approximations (Decker et al., 1996), DSMC techniques (Basu et al., 2001; She-
 923 matovich et al., 2011), and a semi-analytical exponential matrix solution (both with dis-
 924 sipative forces and angular redistributions Galand et al. (1997); Simon et al. (2007)).

925 Motivated by the Mars Express and MAVEN missions, there are an increasing num-
 926 ber of studies of proton precipitation at Mars. (Shematovich et al., 2011) have developed
 927 a DSMC model of the coupled (H⁺,H) system in a (CO₂, N₂, O) atmosphere and ap-
 928 plied it to Mars Express ASPERA data in solar minimum conditions. They concluded
 929 that about 20% (10%) of the incoming particle (energy) flux was backscattered by the
 930 atmosphere, and emphasized the role of the solar wind magnetic field pile-up region at
 931 altitudes above 100 km in increasing the backscattered flux by a factor up to 50%. (Shematovich,
 932 2017) recently studied the production of suprathermal O atoms in Mars' thermosphere
 933 via this process and concluded that a hot oxygen corona may form, creating an additional
 934 non-thermal escape flux of O that may become prevalent when extreme solar transient
 935 events, such as flares and Coronal Mass Ejections (CMEs), take place. Finally, Halekas
 936 (2017) derived the ENA flux originating from the solar wind interaction with the Mar-
 937 tian atmosphere from the observation of protons by MAVEN/SWIA. From there, it was
 938 possible to retrieve the exospheric temperature of Mars (as well as the solar wind veloc-
 939 ity).

940 At Jupiter, energetic precipitation involves protons (Bisikalo et al., 1996), but also
 941 singly or multiply-charged heavy ions such as Sⁿ⁺ and Oⁿ⁺ (with *n* the charge number)
 942 (Horanyi et al., 1988), colliding with H and H₂ (J. Waite & Lummerzheim, 2002). The
 943 high charged states of O at very high energies (above 200 keV/amu) are responsible for
 944 auroral X-ray emissions, as modelled in (Cravens et al., 1995) and compared to X-ray
 945 observations of Jupiter. Such ion precipitation creating fast energetic atoms is also ex-
 946 pected to play a role for satellites of Jupiter, and at Saturn, and its satellites.

947 **2.3.5 Charge exchange in the ionosphere**

948 This process is an hybrid between charge exchange and photochemical escape; it
 949 consists of having excess kinetic energy when a charge exchange is performed, such as
 950 $\text{He}^+ + \text{N}_2 \rightarrow \text{He}^*(+9\text{eV}) + \text{N}_2^+$ (Shizgal & Arkos, 1996). This process has been suggested
 951 to address the problem of the He budget in the Earth's thermosphere (Shizgal & Arkos,
 952 1996; Lie-Svendsen et al., 1992).

953 **2.3.6 Key parameters**

954 The important parameters in the computation of the pick-up / sputtering are the
 955 solar wind parameters, that can usually be found thanks to models of the interaction of
 956 the solar wind with the planet (Curry et al., 2013; C. O. Lee et al., 2017), and the cross
 957 sections for ionization and stopping power/elastic scattering. In addition, it is necessary
 958 to have good inelastic/interaction potential (Johnson, 1994) cross sections to be able to
 959 compute the α , β and p parameters in Equation 43. Finally, a particular attention should
 960 be given towards the nature of the model with respect to modifying the inputs of ion pickup
 961 models: for example, it is usually assumed that an exosphere is present in a MHD model,
 962 and mass loading will reduce the accuracy of the model. Hybrid modeling will better im-
 963 prove such models, as is done in a cometary environment (Simon Wedlund et al., 2017).
 964 A review of the comparative advantages/inconvenients of each type of solar wind mod-
 965 els can be found in Ledvina et al. (2008).

966 For the majority of the recent work in pick-up and sputtering, many cross sections
 967 are being used without being published, which is a major problem for the community.
 968 The state-of-the-art models for sputtering are now using a DSMC approach (Johnson
 969 et al., 2000).

970 For charge-exchange processes, in addition to the particle precipitation models and
 971 the solar wind models, it is important to have a good knowledge of the atmosphere com-
 972 position and temperature, including the ion temperature.

973 **2.3.7 Questions**

974 How much do these processes scale up with the solar wind density, speed, and ori-
 975 entation? How does the creation of an induced magnetic field influence these charge ex-
 976 changes processes?

977 **2.3.8 Observables**

978 **2.3.8.1 Composition change** The observation of the change in solar wind com-
 979 position is a proof of charge exchange, for example at comets (Simon Wedlund, Behar,
 980 Kallio, et al., 2019; Simon Wedlund, Bodewits, et al., 2019; Simon Wedlund, Behar, Nils-
 981 son, et al., 2019). At Mars, the charge exchange of solar wind protons at the bow shock
 982 leads to precipitation of H that can be observed by the effects on the chemistry and by
 983 the backscatter (Halekas, 2017), even if the H chemistry at Mars is complex (M. Chaf-
 984 fin et al., 2017) One more striking example of charge-exchange processes at Mars is the
 985 observation of heavier ions, such as O^+ , that later lead to sputtering (Leblanc et al., 2015,
 986 2018).

987 **2.3.8.2 Fractionation due to pickup/sputtering** The fractionation due to pickup
 988 and sputtering is efficient because of its tendency to make the species at the top of the
 989 thermosphere escape. Since isotopes have a gravitational fractionation at these altitudes,
 990 the overall effect is to increase the number of heavier species in the atmosphere. This
 991 is known as a Rayleigh distillation [see section 3.4.2.2].

992 2.4 Ionospheric outflow

993 Heating and energization of electrons and ions at a magnetized planet results in
 994 escape of ionospheric plasma, either onto open field lines where it joins the solar wind
 995 flow and is lost to interplanetary space, or onto closed or reconnecting magnetic field lines
 996 where it becomes trapped in the magnetosphere and becomes subject to magnetospheric
 997 dynamics and loss processes. The escape of ionospheric plasma is often considered in the
 998 context of magnetospheric dynamics and as a competing source of magnetospheric plasma
 999 together with the solar wind. However, it also has a vital role in the context of atmo-
 1000 spheric escape and evolution in that a charged particle has additional plasma physics pro-
 1001 cesses acting on it, as compared to a neutral particle which does not respond to the mag-
 1002 netic or electric field. These processes help reduce the gravitational potential barrier bind-
 1003 ing the charged particle to the planet.

1004 The escape of ionized particles to space has several names in the literature, ion out-
 1005 flow, polar wind, bulk ion escape, polar outflow, etc. This leads to some confusion as some-
 1006 times authors are generically referring to escaping plasma, but other times they are talk-
 1007 ing about outflow energized by particular processes that vary in space and time, as shown
 1008 in Figure 4. For instance, the “polar wind” typically refers to the supersonic outflow of
 1009 ions from the polar ionosphere accelerated by ambipolar electric fields (Axford, 1968; Banks
 1010 & Holzer, 1968). As the name implies, this polar wind is similar in concept to the so-
 1011 lar wind, the supersonic expansion of the solar corona into space, proposed by Parker
 1012 (1958) nearly a decade before. While outflows of polar wind were initially thought to con-
 1013 tain only light species such as protons, the first quantitative observations of O^+ in the
 1014 polar wind by the Retarding Ion Mass Spectrometer on-board the Dynamics Explorer
 1015 1 (DE-1) demonstrated that heavy ions can be present as well in quite significant num-
 1016 bers. O^+ accelerated by wave-particle interactions in the cusp is sometimes referred to
 1017 as the “cleft ion fountain” while the same process above the auroral region is occasion-
 1018 ally referred to as an “auroral wind”. The variability in location, composition, and en-
 1019 ergy of outflowing ions at Earth has led to the variety of names that describe escape along
 1020 magnetic field lines. In this section, we eschew these more specific terms instead will use
 1021 the term ionospheric outflow or ion outflow with the more broad meaning of any pop-
 1022 ulation of plasma upflowing from the planet at high altitude.

1023 When thinking about what drives ionospheric outflows, it is instructive to consider
 1024 the types of energy input. These break down into two broad categories as outlined in
 1025 (Strangeway et al., 2005) (see Figure 5): (1) particle and (2) electromagnetic energy in-
 1026 put from the magnetosphere. Both downward Poynting flux and soft electron precipi-
 1027 tation from the magnetosphere were shown to correlate very well with outflow of ions
 1028 observed by the Fast Auroral Snapshot (FAST) Explorer spacecraft. While correlation
 1029 is not the same as causation, it so happens that there are a number of causal mechanisms
 1030 associated with each type of energy input:

- 1031 1. Particle: Suprathermal electrons (Photoelectrons, auroral electrons, secondary elec-
 1032 trons,...) enhancing the ambipolar electric field and depositing energy to the ther-
 1033 mal electron population.
- 1034 2. Electrodynamic: Transverse heating of ions as a result of wave-particle interac-
 1035 tions, ponderomotive forcing from Alfvén waves, field-aligned currents driving E_{\parallel} ,
 1036 low altitude frictional heating driving upwelling, centrifugal force due to field line
 1037 convection and curvature change and/or magnetic field co-rotation with the planet.

1038 The varied timescales and spatial regions over which these processes act result in dynamic
 1039 outflow that varies spatially. At lower altitudes, the influence of different drivers sepa-
 1040 rates the upflowing plasma into what has been called Type 1 and Type 2 outflow (Wahlund
 1041 et al., 1992), where **Type 1 involves strong electric fields and Joule heating, and**
 1042 **Type 2 involves particle precipitation and enhanced electron temperatures.**

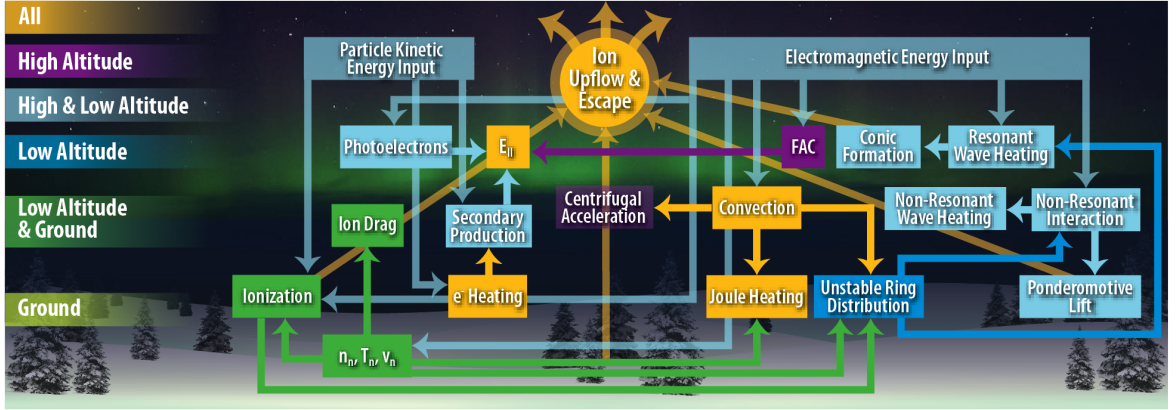


Figure 4. Processes leading to the creation of ion outflow/polar escape

1043 At high altitudes, the escaping plasma also exhibits temporal and spatial variability. The
 1044 polar region at Earth typically contains lower energy polar wind outflow, whereas ad-
 1045 dditional energization, particularly from wave particle interactions, results in an energetic
 1046 ion outflow and preferential acceleration of heavy ions in the auroral and cusp regions.
 1047 Figure 5 shows the different pathways to ion outflow and some of the unknown.

1048 **2.4.1 Suprathermal electron effect**

1049 Suprathermal electrons refer to electrons whose mean energy is much greater than
 1050 the thermal energy. The source of these electrons are either from XUV light shining on
 1051 the atmosphere creating photoelectrons, precipitating electrons of magnetospheric ori-
 1052 gin (auroral electrons), or secondary electrons formed by impact ionization of the neu-
 1053 tral atmosphere. This population is known to alter the ion outflow solution though two
 1054 main processes:

- 1055 1. Formation of the self-consistent ambipolar electric field.
- 1056 2. Coulomb collisions between the superthermal and thermal electrons raising T_e .

1057 Relative to ions, suprathermal electrons are unbound by gravity and in absence of any
 1058 other process would escape. However, this would lead to a net charge in the plasma vi-
 1059 olating the quasi-neutrality condition. Therefore, an electric field forms that retards the
 1060 electrons and accelerates the ions, reducing the gravitational potential barrier. Another
 1061 pathway through which these electrons influence the outflow is through the deposition
 1062 of energy to the thermal electrons raising the electron temperature and eventually the
 1063 ion temperature.

1064 Photoelectrons, formed from ionization of the atmosphere by solar/stellar radia-
 1065 tion, have been particularly well studied in the context of ionospheric outflows. There

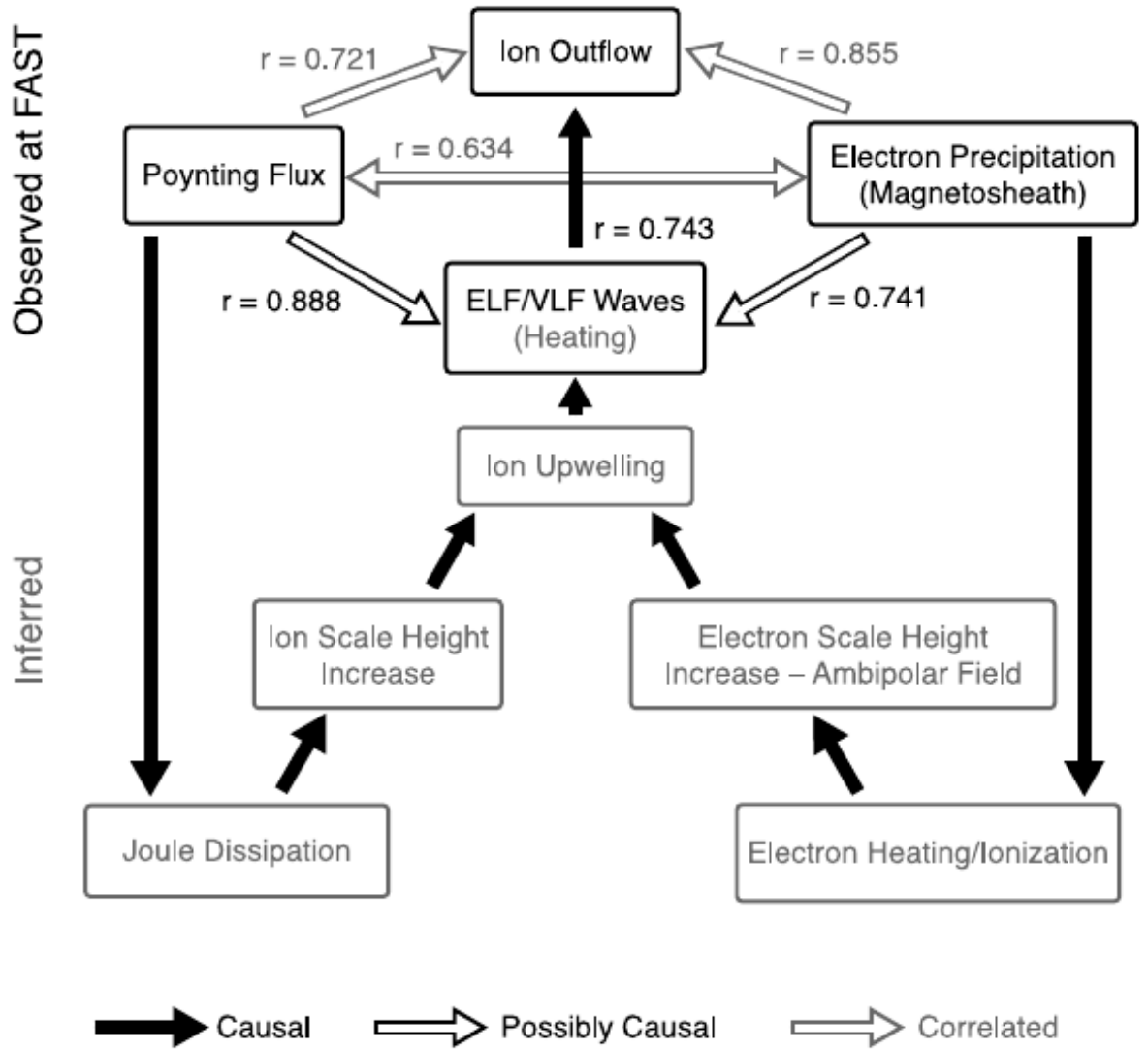


Figure 5. Correlation and causation in the ion outflow. The correlations are under current and proposed investigation to prove if they are actual causes or just coincidences/effect of similar causes. From Strangeway et al. (2005).

1066 have a large number of theoretical studies (Lemaire, 1972; Tam et al., 1995, 1998; Khaz-
 1067 anov et al., 1997; Wilson et al., 1997; Su et al., 1998) and observational studies (Lee et
 1068 al., 1980; Peterson et al., 2008; Kitamura et al., 2011) showing that this population is
 1069 critical to setting up the quiet time outflow solution.

1070 **2.4.2 Electrodynamic Energy Input**

1071 Waves also play an important role in the acceleration of plasma in the high-latitude,
 1072 high-altitude polar region. They do this primarily through two mechanisms: the pon-
 1073 deromotive forces of Alfvén waves (Li & Temerin, 1993; Guglielmi et al., 1996; Khazanov
 1074 et al., 1998; Khazanov et al., 2000, 2004) and wave heating (Retterer et al., 1987; Crew
 1075 et al., 1990; Barghouthi, 1997; Bouhram et al., 2003; Waara et al., 2011).

1076 Ponderomotive forcing due to low frequency electromagnetic waves allows electro-
 1077 magnetic energy from the magnetosphere to transfer energy to the ionospheric plasma.
 1078 It arises from a non-resonant interaction between the particle encountering different por-
 1079 tions of the wave during different parts of the particle gyration. The ponderomotive forc-
 1080 ing depends on the wave mode, propagation direction, frequency, and background fields.
 1081 While there are several types of ponderomotive force derived in the literature, a useful
 1082 description of the total field-aligned force F_{\parallel} from Alfvén waves as given by Lundin
 1083 and Guglielmi (2006) is:

$$F_{\parallel} = -\frac{mc^2}{2B^2} \left[\frac{E^2}{B} \frac{\partial B}{\partial z} - \frac{1}{2} \frac{\partial E^2}{\partial z} \pm \frac{1}{c_A} \left(\frac{\partial}{\partial t} + \nu \right) E^2 \right] \quad (55)$$

1084 Where m is the mass, c_A the Alfvén speed, and ν the collision frequency. E the electric
 1085 field and B the magnetic field.

1086 Although the upward ponderomotive acceleration of ions is not species-dependent,
 1087 it is countered by a downward force on electrons, resulting in a downward ambipolar field
 1088 and a resulting species-dependent reduction to the acceleration (Miller et al., 1995).

1089 In contrast, wave-heating arises from the resonant interaction of particles with the
 1090 portion of the turbulent wave spectrum that corresponds to the cyclotron motion of the
 1091 particle. This preferentially heats the ions perpendicularly to the magnetic field. The
 1092 mirror force converts this excess perpendicular energy into organized parallel motion.
 1093 When modeling this interaction, the wave-heating is often represented as a diffusion term
 1094 on the right hand side of the Boltzmann equation having a form like (Crew & Chang,
 1095 1985):

$$\frac{1}{v_{\perp}} \frac{\partial}{\partial v_{\perp}} \left(v_{\perp} D_{\perp} \frac{\partial f}{\partial v_{\perp}} \right) \quad (56)$$

1096 where f is the velocity space distribution function, v_{\perp} is the perpendicular velocity, and
 1097 D_{\perp} is a diffusion coefficient. The diffusion coefficient can be written approximately as
 1098 (Crew et al., 1990):

$$D_{\perp} = (\pi q^2 / 2m^2) |E_L|^2 \Omega(l) \quad (57)$$

1099 Where $|E_L|^2$ is the electric field spectral density of left hand polarized waves, and $\Omega(l)$
 1100 is the gyrofrequency of an ion of mass m and charge q at position ‘ l ’ along a field line.
 1101 Clearly this term acts to add energy to the ions transverse motion around the field in-
 1102 creasing the first adiabatic invariant and enhancing the mirror force which accelerates
 1103 the ion.

1104 Resonant wave-heating has a clear signature in the shape of the ion distribution
 1105 function. When the wave heating is active, the distribution function becomes increas-
 1106 ingly perpendicular and pancake shaped. The mirror force, which acts more strongly on
 1107 particles with higher perpendicular velocity, causes the distribution to “fold” upward into

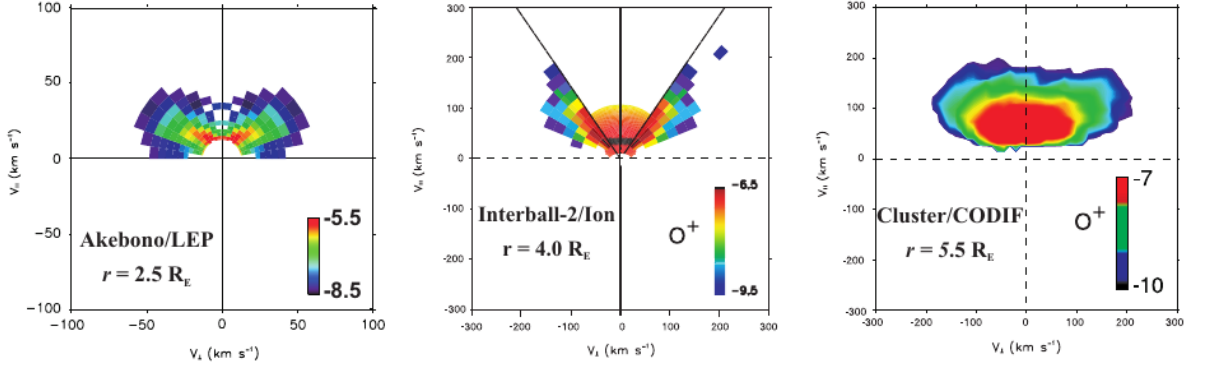


Fig. 2. From the left to the right, 3 examples of ion velocity distributions in $\text{cm}^{-3} \text{km}^{-3} \text{s}^3$ measured by Akebono/LEP at $r=2.5 R_E$, Interball-2/Ion at $r=4.0 R_E$, and Cluster/CODIF at $r=5.5 R_E$.

Figure 6. The conic distribution function of ions as observed by different satellites. These observations are a signature of wave excitation typical of polar outflow. From Bouhram et al. (2004), Creative Commons.

1108 a characteristic “V” shape. In three-dimensional velocity space this looks like a cone, and
 1109 hence the name “conic” distribution. The observation of a conic distribution is a clear
 1110 signature of the presence of resonant wave-particle interactions. Figure 6, from Bouhram
 1111 et al. (2004), shows three examples of this feature observed by different satellites.

1112 2.4.3 Field-Aligned Currents

1113 Field-aligned currents (FAC, also known as “Birkeland currents”), driven by a planet’s
 1114 magnetic interaction with the stellar wind, are another form of electromagnetic energy
 1115 input that contributes to ionospheric escape. This process was looked at by Gombosi and
 1116 Nagy (1989), who found that including a field aligned current causes the thermal elec-
 1117 trons to respond by possibly enhancing the ambipolar electric field. More generally, a
 1118 current conservation equation can be defined as follows (Glocer, 2016):

$$n_e u_e + n_{se} u_{se} - \sum_i n_i u_i = -\frac{j}{en} \quad (58)$$

1119 which states that the current density, j , must be equal to the difference between the flux
 1120 of electrons (thermal and suprathermal) and the flux of ions. If a large current is driven
 1121 into the ionosphere, then this condition requires other populations to react.

1122 2.4.4 Joule Heating

1123 Joule heating (see also Section 3.2.3) refers to the frictional heating caused by the
 1124 differential motion of ions being dragged through the neutral atmosphere. In this pro-
 1125 cess, the planet’s magnetic field interaction with the stellar wind generates a cross po-
 1126 lar cap potential which sets up magnetospheric convection as well as strong convective
 1127 flows in the E and F regions of the polar ionosphere. This convective flow is generated
 1128 by the ExB drift and is not felt directly by the neutral population. As a result there is
 1129 a differential motion between the ions and the electrons. There are several presentations
 1130 of Joule heating as described by R. J. Strangeway (2012), but fundamentally the most
 1131 direct way to model this process is as a frictional heating term. This term can be pre-

1132 sented based on Burger's fully linear approximation (Burgers, 1969) as:

$$\sum_j \frac{\rho_i \nu_{ij}}{m_i + m_j} \left[m_j (u_i - u_j)^2 \right] \quad (59)$$

1133 (Gombosi & Killeen, 1987) and (Cannata et al., 1988) examined the role of Joule heat-
1134 ing and found that transient upflows can result from this process.

1135 Centrifugal forces play a role both at Earth (Horwitz et al., 1994) and at Jupiter
1136 (Nagy et al., 1986), but the origin of the centrifugal forcing is different for the two plan-
1137 ets. At Earth, the solar-wind connected field lines convect across the high altitude pol-
1138 ar cap region, resulting in changes to the field line curvature that centrifugally accel-
1139 erate the particles outward along the magnetic field. At Jupiter, solar wind-driven con-
1140 vection plays a less important role, but the rapid rotation of the planet results in out-
1141 ward acceleration at lower latitudes.

1142 2.4.5 Escape equations

1143 There are several types of methods for modeling ionospheric outflows, but they can
1144 generally be divided into two categories: hydrodynamic models and kinetic models. In
1145 the case of hydrodynamic models usually a multimoment expansion of the Boltzmann
1146 equation for each ion species is undertaken. For magnetized planets, this is taken in the
1147 low β limit where the magnetic field is strong. In this case the gyrotropic 5 moment equa-
1148 tions with heat flux along an expanding magnetic field are given by (Gombosi & Nagy,
1149 1989):

$$\frac{\partial}{\partial t} (A\rho_i) + \frac{\partial}{\partial r} (A\rho_i u_i) = AS_i \quad (60)$$

1150

$$\begin{aligned} \frac{\partial}{\partial t} (A\rho_i u_i) + \frac{\partial}{\partial r} (A\rho_i u_i^2) + A \frac{\partial p_i}{\partial r} = \\ A\rho_i \left(\frac{e}{m_i} E_{\parallel} - g \right) + A \frac{\delta M_i}{\delta t} + Au_i S_i \end{aligned} \quad (61)$$

1151

$$\begin{aligned} \frac{\partial}{\partial t} \left(\frac{1}{2} A\rho_i u_i^2 + \frac{1}{\gamma_i - 1} A p_i \right) + \frac{\partial}{\partial r} \left(\frac{1}{2} A\rho_i u_i^3 + \frac{\gamma_i}{\gamma_i - 1} A u_i p_i \right) \\ = A\rho_i u_i \left(\frac{e}{m_i} E_{\parallel} - g \right) + \frac{\partial}{\partial r} \left(A\kappa_i \frac{\partial T_i}{\partial r} \right) + A \frac{\delta E_i}{\delta t} \\ + Au_i \frac{\delta M_i}{\delta t} + \frac{1}{2} A u_i^2 S_i \end{aligned} \quad (62)$$

1152 In this case m refers to mass, ρ is the mass density, u refers to the velocity, T to the tem-
1153 perature, p to the pressure, r to the distance along the field line, and e is the charge of
1154 an electron. The subscriptions denote ion species or electron. Other terms include the
1155 expanding cross-sectional area of the flux tube (A), the heat conductivity (κ), the spe-
1156 cific heat ratio γ , and Boltzmann's constant (k). The electric field (E_{\parallel}) is derived as an
1157 Ohm's law from a the steady state electron momentum equation as:

$$\begin{aligned} E_{\parallel} = -\frac{1}{en_e} \left[\frac{\partial}{\partial r} (p_e + \rho_e u_e^2) + \frac{A'}{A} \rho_e u_e^2 \right] + \\ \frac{1}{en_e} \frac{\partial}{\partial r} \left(\sum_i \frac{m_e}{m_i} \left[(u_e - u_i) S_i - \frac{\delta M_i}{\delta t} \right] + \frac{\delta M_e}{\delta t} \right) \end{aligned} \quad (63)$$

1158 The source on the right hand side of equations 60-62 represent the source due to ion pro-
1159 duction and loss (S_i), the source due to momentum transfer ($\frac{\delta M_i}{\delta t}$), and the source due

1160 to energy transfer ($\frac{\delta E_i}{\delta t}$), which includes Joule heating effects. There are several deriva-
 1161 tions of the collision based source terms for momentum and energy transfer, but a com-
 1162 mon choice are determined by using Burgers' fully linear approximation (Burgers, 1969).
 1163 Specific expressions for these terms can be found in the textbook by (Schunk & Nagy,
 1164 2004). The equations outlined above are used in the Polar Wind Outflow Model (Glocer
 1165 et al., 2013, 2009). However, other codes use different hydrodynamics expansions includ-
 1166 ing higher moment approximations. For example, the model presented by Varney et al.
 1167 (2014) uses the 8 moment approximation, while Barakat and Schunk (1982) uses the 16
 1168 moment approximation. We do not elaborate further on these approach here but refer
 1169 the interested reader to those papers.

1170 Kinetic solutions to ionospheric outflow typically solve the Boltzmann equation in
 1171 some approximation. In the steady state this equation is given by Khazanov et al. (1997);
 1172 Khazanov (2010):

$$\begin{aligned}
 & \mu \frac{\partial f_\alpha}{\partial t} + \mu v \frac{\partial f_\alpha}{\partial r} - \frac{1 - \mu^2}{2B} \frac{\partial B}{\partial r} v \frac{\partial f_\alpha}{\partial \mu} = \\
 & - \left(\frac{e}{m_e} E_{\parallel} - g \right) \left(\mu \frac{\partial f_\alpha}{\partial v} + \frac{1 - \mu^2}{v} \frac{\partial f_\alpha}{\partial \mu} \right)
 \end{aligned} \tag{64}$$

1174 Solving this equation usually takes one of two forms. Khazanov et al. (1997) use
 1175 a direct solution of the Vlasov equation along a field line, whereas Barakat and Schunk
 1176 (2006) use a 3D macroscopic particle-in-cell Monte Carlo technique. (Depending on the
 1177 study, the time dependent or the static case are solved).

1178 **2.4.6 Questions**

1179 The PWOM model (Glocer et al., 2009) was applied to exoplanets (Airapetian et
 1180 al., 2017) with the study of the atmospheric escape of a Earth-like planet at Proxima-
 1181 b (Garcia-Sage et al., 2017). These studies were able to show that large escape rates hap-
 1182 pen even in the presence of magnetic fields. This model has the advantage of taking into
 1183 account the diffusion of ions, assuring that this escape is not limited by ionospheric mod-
 1184 eling. The questions remaining for this process is how it evolves in the absence of a per-
 1185 manent magnetic field, i.e. when there is only an induced magnetic field. Studies by Collinson
 1186 et al. (2019) tends to indicate that ambipolar diffusion helps the ion escape at Venus,
 1187 but it remains to be modeled exhaustively. The long-lived doubly charged ions, observed/predicted
 1188 in several ionospheres (Simon et al., 2005; Lilensten et al., 2005; Gronoff et al., 2007; Thissen
 1189 et al., 2011), are easier to lift and therefore to escape through these processes. Are the
 1190 O^{2+} observed by ISEE (Horwitz, 1981) due to these processes, and are they a signifi-
 1191 cant source of escape? The dependence upon the EUV flux in certain situations (D. T. Young
 1192 et al., 1982) is consistent with such an hypothesis.

1193 **2.4.7 Observables**

1194 As explained, the polar wind is directly observed by plasma instruments. The de-
 1195 pendence of the escape efficiency upon the q/m ratio means that lighter isotopes are eas-
 1196 ier to lift, therefore enhancing the gravitational distillation of the ions (which can be af-
 1197 fected by the self-shielding effect Section 2.2.6).

1198 **2.5 Other ion escape**

1199 While the main sources of losses could be linked to the previously cited ones, other
 1200 ion escape mechanisms, have been reported in the literature. They mainly come from
 1201 the observation of “bulk” ion escape at Mars or Venus, during specific solar conditions
 1202 (Halekas et al., 2016). This general denomination groups together escape that could come

1203 from very different processes while leading to loss of ions in an organized way. Overall,
 1204 it is transfer of momentum from the solar wind to the ionosphere that makes these plasma
 1205 escape, and it could be considered as ion pickup in a first approximation, but with more
 1206 complex MHD effects. As explained in Terada et al. (2002), the main problem is that
 1207 the production of ions above the ionopause is less than the escaping flux, which means
 1208 that different processes have to diffuse these ions from the ionosphere to above the ionopause
 1209 where they would be picked up.

1210 This is this second class of processes, that comes from complex interactions between
 1211 the ionosphere and the interplanetary magnetic field to help transfer ions to the top of
 1212 the thermosphere, that are studied here. These ions are usually not energetic enough to
 1213 escape, but their presence makes it easier for pickup and “bulk” escape. It is to be noted
 1214 that, when conditions are extreme, it is possible to reach levels where the production/diffusion
 1215 of ions is limiting the escape. Numerous models of ion pickup do not take that situation
 1216 into account, leading up to unrealistic ion escape fluxes (Egan et al., 2019).

1217 In magnetospheres, similar problems arise: the different ion energizing processes
 1218 lead to the creation of a plasmasphere, i.e. ions trapped inside the magnetosphere, and
 1219 these ions are removed either by falling back to the planet or leaving through different
 1220 processes (Seki et al., 2015; Jackman et al., 2014).

1221 ***2.5.1 Fluid processes: Kelvin-Helmholtz and other instabilities***

1222 Kelvin-Helmholtz instabilities (KHI) (J. R. Johnson et al., 2014) have been observed
 1223 at Mercury (Sundberg et al., 2010), Venus (S. A. Pope et al. (2009); Lammer et al. (2006);
 1224 Terada et al. (2002) and references therein: the observations of flux rope and detached
 1225 plasma clouds are linked to KHI through modeling), Earth (J. R. Johnson et al., 2014)
 1226 and Mars (Ruhunusiri et al., 2016). They occur at the interface between two fluids or
 1227 plasmas having a velocity shear and lead to upward pressure gradients and the forma-
 1228 tion of a vortex. KHI have effects in a variety of planetary processes. In the case that
 1229 interest us, i.e. the development of KHI at the interface between an ionosphere and the
 1230 solar wind, it leads to the transfer of solar wind momentum to the ion and, ultimately,
 1231 to their acceleration into space. Penz et al. (2004) computed, for Mars, O^+ escape val-
 1232 ues of the order of $2 \cdot 10^{23} - 3 \cdot 10^{24}$ ions/s. Rayleigh-Taylor instabilities, ion-ion instabil-
 1233 ities, electron-ion instabilities, have also been proposed as mean of momentum exchange
 1234 leading to escape (Dubinin et al., 2011).

1235 ***2.5.2 Pick-up processes: the ion plume***

1236 The ion plume of Mars was inferred from Mars Express observations, and fully char-
 1237 acterized by MAVEN (Liemohn et al., 2014; Dong et al., 2015). It originates from the
 1238 interaction between the solar wind and the ionosphere of Mars, which creates an upward
 1239 electric fields through $\vec{E} = -\vec{U}_{SW} \times \vec{B}$. This process can be looked as a special case
 1240 of ion-pickup since it is observed in such-models. At Mars, this plume escape for O^+ is
 1241 estimated to be 30% of the tailward escape, equivalent to 23% of the total ion escape
 1242 (Dong et al., 2015).

1243 ***2.5.3 Ambipolar fluxes / outflow anomalies / snowplow***

1244 The “cold” ions, i.e. ions not energized at suprathermal temperature and coming
 1245 from the ionosphere, are prominent in the plasmasphere (Kun et al., 2017). Several pro-
 1246 cesses leads to the filling of that plasmasphere. Ion upwelling (Strangeway et al., 2005),
 1247 which can be linked to the ambipolar electric field, but at levels that do not lead to es-
 1248 cape, is one of these processes at Earth. For unmagnetized planets, ions are transported
 1249 in the upper layers of the ionosphere by ambipolar electric field (Collinson et al., 2019;
 1250 Akbari et al., 2019). The draping of the interplanetary magnetic field (IMF) could lead

1251 to additional induced field with respect to the processes described in Section 2.4, this
 1252 process is called the “snowplow” (Halekas et al., 2016). From there, the transfer of mo-
 1253 mentum from the solar wind to the ionosphere creates detached plasma clouds that are
 1254 escaping. It is important to note that the $\vec{E} \times \vec{B}$ drift can help these ions escape as ob-
 1255 served at Mars, where different escape rates are observed in the +E and -E hemispheres
 1256 (Inui et al., 2019).

1257 **2.5.4 Plasmaspheric ion losses / substorm losses / plasmoids / flux ropes**

1258 As previously shown, the charge exchange is a major ion loss process in magneto-
 1259 spheres. A fraction of ions can be lost from escape from the tail, but, as shown from the
 1260 observations at Jupiter, this is a low percentage of the escape (Jackman et al., 2014) (At
 1261 Jupiter, other processes have to be taken into account to balance the input of plasma
 1262 from Io.). This escape from the tail works through the creation of a plasmoid: the pres-
 1263 sure of the IMF elongates the planetary magnetic field, leading to the reconnection of
 1264 that magnetic field. This reconnection means that a part of the initial magnetosphere is
 1265 no more linked to the magnetic field of the planet and is ejected into space, along with
 1266 the plasma it contains. Ejection of plasmoids is also associated to a return of plasma to-
 1267 wards the planet. (This is different for situations when magnetic fields are weaker, such
 1268 as Mars). The equivalent of these plasmoids have been observed at Mars near the mag-
 1269 netospheres created by the crustal magnetic field, they are usually named “flux ropes”
 1270 (Hara, Brain, et al., 2017), are linked with coronal mass ejection disturbances and other
 1271 processes (Hara, Harada, et al., 2017). They could be responsible for up to 10% of the
 1272 present day ion escape at Mars (D. A. Brain et al., 2010). Finally, plasmoid escape has
 1273 also been observed at Venus, in the induced magnetic field, and looks like the Earth’s
 1274 or Jupiter’s plasmoids (Zhang et al., 2012).

1275 **2.5.5 Questions**

1276 These ion escape processes are actively studied with missions such as MEX, VEX,
 1277 MAVEN, etc., as well as numerical models. Most of the questions are linked to the ac-
 1278 tual amount of ions escaping due to these processes and how these evolve with the so-
 1279 lar/stellar activity. From an observation point of view, it may be difficult to distinguish
 1280 between processes from the a single point observation of the amount and location of plasma
 1281 escaping (Inui et al., 2019). In addition, some processes can be seen as generalization
 1282 of other processes (e.g. the “snowplowing” is a generalization of the ion outflow observed
 1283 in magnetospheres). These points led to the above definitions and organization of these
 1284 ion escape processes.

1285 **2.6 Ion Return and Net Escape Rates**

1286 While the ionospheric outflow processes detailed above determine the escape of plasma
 1287 from the ionosphere, a significant fraction of this plasma becomes trapped in Earth’s mag-
 1288 netosphere. Magnetospheric ions mostly consist in a mixture of H^+ and O^+ ions. Con-
 1289 trary to H^+ ions, which can either originate from the solar wind or the ionosphere, O^+
 1290 ions almost exclusively originate from the ionosphere and are used as tracers of ionospheric
 1291 material in the magnetosphere. They have been observed by several spacecraft, includ-
 1292 ing GOES 1 and 2 (D. T. Young et al., 1982), ISEE (Lennartsson & Shelley, 1986; Lennarts-
 1293 son, 1989), Van Allen Probes (Fernandes et al., 2017), GEOTAIL (Nosé et al., 2009; Ohtani
 1294 et al., 2011), and Cluster (Maggiolo & Kistler, 2014; Kistler & Mouikis, 2016). All these
 1295 observations show an increase the amount of O^+ ions in the magnetosphere, and thus
 1296 of ionospheric material, with increasing solar EUV/UV flux and geomagnetic activity,
 1297 i.e. with the amount of energy deposited in the ionosphere. Once in the magnetosphere,
 1298 ionospheric material enters magnetospheric circulation patterns, which may ultimately
 1299 result in loss to interplanetary space or return to the ionosphere. Seki et al. (2001) es-

1300 timate the fraction of Earth’s oxygen lost to interplanetary space at about 1/10 of the
 1301 ionospheric oxygen outflow during periods of low solar activity, based on the estimate
 1302 of the O^+ loss due to the main four escape routes for terrestrial ions: the escape of cold
 1303 detached plasmaspheric particles through the magnetopause, of high-energy ring current/dayside
 1304 plasma sheet particles through the magnetopause, of plasmasheet ions through antisun-
 1305 ward flow in the nightside plasma sheet, and of terrestrial ion beams through the lobe/mantle.
 1306 Note that the charge exchange loss of ring current ions was not considered by Seki et al.
 1307 (2001). The outflow and loss rates are enhanced during high solar and geomagnetic ac-
 1308 tivity but may not account for all magnetospheric loss mechanisms, particularly for low
 1309 energy ions that are difficult to observe. This estimate, then, should be considered a lower
 1310 bound on escape, but the important point here is that not all outflowing ions escape from
 1311 the magnetosphere-ionosphere system.

1312 However, recent observations above the polar ionosphere in the magnetospheric lobes
 1313 by the Cluster spacecraft, provide evidence for a higher loss rate for ionospheric ions flow-
 1314 ing through the lobe and mantle region. Slapak et al. (2017) showed that energetic ions
 1315 (in the range of a few hundred to several thousand of eV) escaping from the cusp region
 1316 through the magnetospheric lobes/mantle have a high probability of being lost to inter-
 1317 planetary space rather than being returned to the ionosphere. They even claim that over
 1318 geological times a quantity of oxygen lost by the Earth’s atmosphere could be roughly
 1319 equal to the amount of the present atmospheric oxygen content if the young Sun was ac-
 1320 tually more active than nowadays. Furthermore, the flux of precipitating ions as esti-
 1321 mated by the the DMSP satellites is only of the order of 10^{24} (Newell et al., 2010): 1 to
 1322 2 orders of magnitude lower than the estimated flux of outflowing ionospheric ions. These
 1323 new observations provide strong evidence against a high return rate of ionospheric ions
 1324 and rather suggest that a significant fraction of ionospheric ions escaping from the iono-
 1325 sphere may actually be definitively lost into the interplanetary space.

1326 **3 Major Parameters and Concepts**

1327 In order to address the escape rate of an atmosphere and to retrieve its evolution
 1328 with time, it has been demonstrated that several processes are in action. To evaluate whether
 1329 or not they are negligible at a certain period in time, or to approximate the calculations,
 1330 several concepts have been proposed, such as the energy limited escape or the critical
 1331 heating rate for hydrodynamic escape. The two major parameters in the different mod-
 1332 els are the energetic inputs, from the EUV-XUV fluxes to the electron precipitations,
 1333 and the atmospheric structure and composition. Finally, it is very important to take into
 1334 account the evolution with time, from the time dependence on small scales (typically sen-
 1335 sitive to the solar/stellar activity) to the evolution of the atmospheric escape through
 1336 eons, leading to isotopic fractionation, which is the main probe for the history of our So-
 1337 lar system’s atmospheres (in the absence of better in-situ measurements, e.g. trapped
 1338 gases in rocks (Jakosky, 1991)).

1339 **3.1 Limiting parameters**

1340 **3.1.1 Critical Heating Rate**

1341 Present theory (Section 2.1.1.2) incompletely describes transition from Jeans es-
 1342 cape to hydrodynamic escape. Transonic models (Murray-Clay et al., 2009) have been
 1343 used to describe rapid escape from exoplanets and from Pluto (D. F. Strobel, 2008a).
 1344 However, Johnson et al. (2013b, 2013a) have recently discovered that this model for Pluto
 1345 gave an incorrect upper atmospheric structure (Tucker et al., 2012). This erroneous pre-
 1346 diction of the upper atmospheric structure results from applying the Jeans expressions
 1347 at the exobase (Chamberlain & Hunten, 1987) for uncertain boundary conditions at in-
 1348 finity (Tian et al., 2008) when simulating rapid escape using continuum gas dynamics.
 1349 In this context, a sonic point is assumed to occur at an altitude r_* , above which the den-

1350 sity and temperature dependence can be simply characterized (Parker, 1964b, 1964a).
 1351 The hydrodynamic, energy-limited (see Section 3.1.2) escape rate, applied to exoplanet
 1352 atmospheres (Lammer et al., 2009), is often assumed to imply that sonic boundary con-
 1353 ditions are applicable (Erkaev et al., 2013). Johnson et al. (2013b, 2013a) used molec-
 1354 ular kinetic simulations to show that this is not the case. Ignoring viscosity, (Parker, 1964b,
 1355 1964a) used the momentum and energy equations to describe escape when the dominant
 1356 heat source is internal. This same model was applied to planetary atmospheres primar-
 1357 ily heated at an altitude r_a . For a Jeans parameters at r_0 (the lower altitude considered)
 1358 as large as $\lambda_0 \sim 40$, such models were assumed to produce a transonic expansion, which
 1359 is often referred to as a slow hydrodynamic escape (D. F. Strobel, 2008a). However, rapid
 1360 escape can occur for large Jeans parameters only when the Knudsen number is low, i.e.
 1361 when the collisional approximation cannot be assumed. Therefore, the gas does not go
 1362 sonic in the collision-dominated region and the escape rate computed in the “slow hy-
 1363 drodynamic escape” paradigm is a few times larger than the Jeans rate (Volkov, Tucker,
 1364 et al., 2011; Volkov, Johnson, et al., 2011). As we explained in Section 2.1.3.1, the ob-
 1365 servations that led to the “slow hydrodynamic escape” hypothesis could be explained
 1366 by alternative processes based on chemistry.

1367 From there Johnson et al. (2013b, 2013a) have developed a criterion to check if a
 1368 transonic solution will exists, i.e. if we can approximate the escape by a hydrodynamic
 1369 model. Assuming that $r_0 < r_* < r_x$, which should be the case in hydrodynamic es-
 1370 cape, it was found that the net heating rate Q_{net} should follow equation 65:

$$Q_{net} > Q_c \approx 4\pi r_* \frac{\gamma}{c_c \sigma_c Kn_m} \sqrt{\frac{2U(r_*)}{m}} U(r_0) \quad (65)$$

$$U(r) = \frac{GmM}{r} \quad (66)$$

1371 K is the Knudsen number and c_c is determined by the energy dependence of the
 1372 total collision cross section, σ_c .

1373 If heat is primarily absorbed over a broad range of r below r_x , we can use $Kn_m \sim 1$
 1374 as an approximation. Here, it can be seen that Q_c does not explicitly depend on T_0 , but
 1375 on the sonic point only where a lower bound can be obtained by replacing r_* with r_a ,
 1376 the mean absorption depth. This mean absorption depth is estimated from σ_a , the ab-
 1377 sorption cross section. At threshold, the sonic point will approach r_x , such that $r_* \sim$
 1378 $r_a [1 + (\frac{\sigma_a}{c_c \sigma_c}) \lambda_{ave}]$ where $\lambda_{ave} \sim (\lambda_a + 2\gamma)/2$ which slightly increases Q_c . Using Pluto
 1379 as an example, UV/EUV absorption at $r_a \sim 1.5$ times Pluto’s radius, $Kn_m \sim 10^{-3}$, and
 1380 $r_* \sim r_a \sim r_0$, Equation (65) gives $Q_c \sim 4.5 \times 10^{10}$ W for Pluto, which is well above the
 1381 largest heating rate, and shows that hydrodynamic escape should not be applied for the
 1382 dwarf planet. We compiled the values of Q_c in Table 2.

1383 **3.1.2 Energy limited escape – Radiation / Recombination - limited es-** 1384 **cape**

1385 The estimation of mass loss rate of exoplanets often assume an energy-limited es-
 1386 cape (Section 2.1.1.4). The basis of that assumption is that an exoplanet thermosphere
 1387 is mainly composed of H, heated by ionization of H. From there, it is supposed that a
 1388 large quantity of that heat is transformed into hydrodynamic escape. Therefore, one uses
 1389 an efficiency coefficient ϵ (sometimes η) for transforming EUV-XUV energy into escape.
 1390 This led to equation 14, with the standard efficiency coefficients found in the literature.
 1391 Erkaev et al. (2007) shows that this equation can be slightly modified to account for stel-
 1392 lar gravity effects that affect close-in planets.

1393 For giant planets close to very active stars, the radiation-recombination limited es-
 1394 cape is often used as a harsher limit to the energy limited escape, because the H^+ can
 1395 recombine, reducing some of the energy in the system (Luger, 2017; Linsky, 2019), this

1396 leads to an escape proportional to $\sqrt{F_{XUV}}$ instead of F_{XUV} . In the case of H atmospheres
 1397 where the heating is only supposed to come from ionization, there is also a case where
 1398 the escape is limited by the number of ionizing photons.

1399 This approach has been developed to study close-in giant planets (Salz et al., 2016),
 1400 and led to energy diagrams (Ehrenreich & Désert, 2011) to evaluate the mass loss from
 1401 giant exoplanets. Unfortunately, it notably neglects the radiative cooling processes in
 1402 the upper atmosphere of the planet, i.e. it neglects the problem of the upper atmosphere
 1403 temperature (Note: Lopez (2017) includes radiative cooling in an energy-limited diffu-
 1404 sion approach). The main problem of the energy limited escape approximation is that
 1405 it is too often applied for rocky exoplanets while concealing these major limitations:

- 1406 1. **The escape regime is not evaluated:** if the exoplanet is not in hydrodynamic
 1407 escape, the energy-limited escape equation will give an overestimate of the escape.
- 1408 2. **The atmospheric profile is not evaluated:** what is exactly the profile of the
 1409 atmosphere, and therefore the efficiency of the escape if it is truly in hydrodynamic
 1410 regime?
- 1411 3. **The atmospheric composition is not taken into account, H is assumed**
 1412 **to be the only species:** this is related to the other problems; the presence of
 1413 cooling species such as CO₂ may totally change the escape regime; diffusion-limited
 1414 processes may prevent H to be present in large quantities in the thermosphere, etc.
- 1415 4. **Only photo-ionization heating is taken into account:** Joule heating or par-
 1416 ticle precipitations can be large sources of heating for close-in exoplanets.
- 1417 5. **Non-thermal processes are not addressed:** those can dramatically change
 1418 the profile of the escaping species.

1419 Energy-limited escape models can be interesting for studying H-rich rocky planets early
 1420 in their histories, for which the escape of H may not have been diffusion-limited but energy-
 1421 limited (Tian et al., 2005), however energy-limited escape is less relevant to more com-
 1422 prehensive habitability studies.

1423 *3.1.3 The diffusion-limited escape*

1424 Some escape processes can be very efficient, and limited by the amount of parti-
 1425 cle available for the escape, the bottleneck for the escape of these particles will then be
 1426 the diffusion from the lower layers of the atmosphere to the upper atmosphere. Typi-
 1427 cally, the escape of H at Earth is diffusion limited. It follows the Equation 15. At Ti-
 1428 tan, like Earth, H₂ escape is determined by the limiting flux through the homopause deep
 1429 in the lower thermosphere (Cui et al., 2008; D. F. Strobel, 2012; J. M. Bell et al., 2014).
 1430 However, there is currently a discrepancy between the densities of H₂ measured in-situ
 1431 by INMS and those produced by modeling studies (Magee et al., 2009; Cui et al., 2008;
 1432 D. Strobel, 2002; J. M. Bell et al., 2014). Despite this discrepancy, all modeling stud-
 1433 ies to date have indicated that the H₂ upwelling into the lower thermosphere, combined
 1434 with additional H₂ produced in the thermosphere, sets the eventual planetary escape flux
 1435 of H₂. A more complete theory of diffusion-limited escape, including the cases where the
 1436 diffusing species has a non-negligible mass with respect to the main species can be found
 1437 in Hunten (1973).

1438 **3.2 Energetic inputs**

1439 *3.2.1 The EUV/XUV flux*

1440 The EUV-XUV flux modifies the temperature of the exosphere and the exobase
 1441 altitude. It therefore changes the concentration of particles above the exobase. It is also
 1442 responsible for the creation of hot atoms through photochemical processes. At the Earth,
 1443 the EUV-XUV flux varies substantially as a function of solar activity. When the vari-

1444 ability of the solar irradiance is rather low for the visible and the IR, with less than 0.1%
1445 and 1% from minimum to maximum respectively, the solar irradiance variability in the
1446 XUV /EUV can be more than doubled with a direct impact on the upper atmosphere
1447 (Haigh, 2007). This variability is of two different origins: one depends on sporadic ex-
1448 plosive events such as flares with time scales from minutes to hours, while the second one
1449 is linked to the full Sun disk activity with longer cycles, from days to years. The latter
1450 one is then related to the appearance and disappearance of active regions on the solar
1451 disk, which causes then the variability on a 27-day solar rotation scale, associated with
1452 a 13.5-day modulation from the center-to-limb variation. The long-term monitoring of
1453 the solar EUV flux, however, is a difficult task, mainly because of the heavy degrada-
1454 tion experienced by the solar instruments that are in orbit (BenMoussa et al., 2013). Be-
1455 fore 2002 with the launch of the TIMED satellite (Woods et al., 2005), measurements
1456 of the solar EUV flux variability were rather scarce. This has led to the development of
1457 several empirical approaches for reconstructing the solar XUV/EUV part of the spec-
1458 trum.

1459 A common approach lies with using solar proxies such as the radio measurements
1460 at 10.7 cm (F10.7) (Tapping & Detracey, 1990) and the MgII core-to-wing index (Heath
1461 & Schlesinger, 1986). Many models are then using a linear combinations involving these
1462 proxies and their 81-days running means, or even non linear combinations (Hinteregger,
1463 1981; Lean et al., 2003; Richards et al., 2006). However, no single index can properly re-
1464 construct the solar XUV/EUV irradiance at all time scales (Dudok de Wit et al., 2009).
1465 Moreover, some widely used proxies, such as F10.7, are not really suited for the XUV/EUV
1466 lines reconstruction, whose originated from the solar corona. The F10.7 index is, how-
1467 ever, used as the solely index to estimate the solar variability within thermospheric and
1468 ionospheric models. For the solar minimum in 2008, when the thermospheric density dropped
1469 by 28%, the F10.7 only decreased by 4% (Emmert et al., 2010), outlying then the lim-
1470 itations of the F10.7 index for ionospheric studies (Solomon et al., 2010). More appro-
1471 priate solar proxies has been recently suggested such as the radio measurements at 3 cm
1472 and 30 cm which are directly linked to chromospheric and corona emissions (Dudok de
1473 Wit & Bruinsma, 2017).

1474 A different approach considers that the solar spectrum is a linear combination of
1475 reference spectra that coming from different regions of the solar disk. Those regions are
1476 attributed to the quiet Sun, coronal holes and active regions and can be disentangled us-
1477 ing solar images or solar magnetograms. Their respective contrast can be obtained by
1478 an empirical approach (Worden et al., 1998) or using the differential emission measure
1479 (Kretzschmar et al., 2004). A few terms is normally needed to reconstruct the solar ir-
1480 radiance in the XUV/EUV spectral range (Amblard et al., 2008). This strongly outlines
1481 that the spectral variability is highly coherent through the spectrum, but this only for
1482 time scales that exceed the dynamic time of solar flares, since the solar atmosphere is
1483 strongly structured by the magnetic field. The solar spectrum in the XUV/EUV can then
1484 be reconstructed from measurements of a few correctly chosen passbands (Cessateur et
1485 al., 2011, 2012). For the short term spectral variability, a specific model has been devel-
1486 oped, the Flare Irradiance Spectrum Model (FISM) (Chamberlin et al., 2008), based on
1487 TIMED/SEE and SDO data.

1488 The effects of the solar XUV/EUV variability on Earth's upper atmosphere have
1489 been quantified with empirical models (Bowman et al., 2008), that specify the exospheric
1490 temperatures as a function of indices of EUV radiation at different wavelengths (Tobiska
1491 et al., 2008). At Mars, J. G. Luhmann et al. (1992) computed the influence of the EUV
1492 flux on the escape processes. It is complicated by the fact that the solar wind pressure
1493 is also included in the calculations: the EUV flux increases, therefore the density of hot
1494 oxygen above the exobase increases (and the altitude of the exobase increases). There-
1495 fore the escape of hot oxygen increases, the density of pickup ions increases as well, and
1496 so the sputtering and the sputtered atoms. These non-linear effects lead to the large vari-

1497 ations in the escape rates as computed in Figure 3. More recent modeling and data shows
 1498 that the actual increase is less important than that previous simulations (Lillis et al., 2015).
 1499 The correlation of Mars Express’ observations of ion escape at Mars with the EUV flux
 1500 show that it is difficult to draw a direct relation between the two (Ramstad et al., 2015)
 1501 in the 7 year span these observations took place. However, the non-linearity of the de-
 1502 pendence, and the fact that negligible escape processes can become very important for
 1503 extreme EUV-XUV flux, such as in the conditions in the beginning of the solar system,
 1504 is still valid.

1505 **3.2.2 The electron flux**

1506 *3.2.2.1 The auroral-like electron flux* The energetic electron flux at high latitudes
 1507 is produced as a result of the interaction of the solar wind and interplanetary magnetic
 1508 field with the magnetic field and magnetosphere of the planet, which in turn drives iono-
 1509 spheric electric fields and currents. Upward currents may contain a significant, down-
 1510 ward energy flux from electrons (Fuller-Rowell & Evans, 1987). The energy flux at the
 1511 Earth typically ranges from under 1 GW up to 20 GW (Newell et al., 2010).

1512 As Mars only has a limited magnetosphere, there is no significant energy deposited
 1513 by the aurora as discovered by Mars Express in 2005 (Bertaux et al., 2005). This con-
 1514 clusion can be challenged by the observations of global aurora during solar events (Schneider
 1515 et al., 2018). Diffuse electron (Clancy et al., 2017) and proton aurora (Deighan et al.,
 1516 2018) observed by MAVEN may carry significant amounts of energy, but the total flux
 1517 still needs to be estimated.

1518 On the other hand, both Jupiter and Saturn do have large internal magnetic fields
 1519 and correspondingly large magnetospheres, so there is considerable power in their au-
 1520 rorae. As there are no direct measurements available, much of what is known about the
 1521 outer planets’ aurorae has been obtained from UV measurements, at first on the Voy-
 1522 ager flyby of Jupiter (Broadfoot et al., 1979). Most recent UV observations are from the
 1523 Hubble Space Telescope (HST). In a review of such observations, Grodent (2014) indi-
 1524 cated that the auroral emissions at Jupiter and Saturn are on the order of 1 TW and
 1525 0.1 TW respectively. Uranus and Neptune are much weaker, at 1 GW or less, and ob-
 1526 servations are sparse. Of course, the power of the emissions is less than the kinetic en-
 1527 ergy that is deposited. The Voyager UV measurements at Jupiter has implied a power
 1528 injection on the level of 12 TW (Broadfoot et al., 1981), and Gérard et al. (2014) stated
 1529 that the auroral precipitation at Jupiter has a power on the order of 10 to 50 TW. As
 1530 this level of heating is much greater than that from solar radiation, the aurora has a sig-
 1531 nificant contribution to the thermal properties of the upper atmosphere.

1532 *3.2.2.2 The supra-thermal electrons* Supra-thermal electrons are electrons with
 1533 energy higher than the typical electron in an ionosphere: when looking at the flux of elec-
 1534 trons in function of energy, the supra-thermal electrons are responsible for the depart-
 1535 ure of the curve from a Maxwellian at high energy. These electrons come mainly from
 1536 the precipitation of electrons from outside of the ionosphere, from local creation (typ-
 1537 ically photoionization -hence the name of photoelectrons-), but also from other ioniza-
 1538 tion, including from suprathemal electron impact). Electric potential drops can accel-
 1539 erate electrons to suprathemal energies, but they occur outside the ionosphere and are
 1540 responsible for some magnetospheric precipitation at Earth. To understand the effect
 1541 of the suprathemal electrons, it is necessary to compute their transport in an atmosphere.
 1542 Codes such as Aeroplanets and PWOM do that.

1543 The basis of these codes is to compute the flux of electrons by solving their trans-
 1544 port equation. The existence of codes not based on a Monte-Carlo scheme, such as Aero-
 1545 planets, allow to fastly compute large quantities of conditions and to perform sensitiv-
 1546 ity analysis (Gronoff, Simon Wedlund, Mertens, & Lillis, 2012; Gronoff, Simon Wedlund,

1547 Mertens, Barthélemy, et al., 2012). We refer to these papers for the equations to solve
1548 in the ionosphere/thermosphere, and for the uncertainties encountered.

1549 *3.2.3 The electromagnetic energy*

1550 The Joule heating is the heating created by the resistance of the thermosphere to
1551 the electric current due the ionospheric plasma (Vasyliunas & Song, 2005). It is com-
1552 puted by evaluating the electric field and the conductivities.

1553 Joule heating in the polar ionosphere has a significant effect on the exospheric tem-
1554 peratures, and hence the amount of outflow (Section 2.4.4). At the Earth the total Joule
1555 heating is normally in the range of a few hundred GW, but in extreme events can range
1556 from 1 TW (Lu et al., 1998) up to 5 TW, while increasing the mean temperature of ther-
1557 mosphere by up to 500°K (Weimer et al., 2011). At the same time, the additional heat-
1558 ing tends to increase the amount of nitric oxide in the thermosphere, which acts to ac-
1559 celerate the rate at which it cools down to the equilibrium temperature set by the so-
1560 lar EUV radiation (Weimer et al., 2015). Wilson et al. (2006) had found that Joule heat-
1561 ing is most typically about 3 times the energy from precipitating particles, with the ra-
1562 tio varying from 2 to 7 in the different events that were studied.

1563 At other planets there are no direct measurements of the electromagnetic energy
1564 input into their ionosphere and thermosphere, so at present it can only be estimated. At
1565 Jupiter, D. Strobel (2002) estimated the Joule and auroral particle heating to be about
1566 1000 times larger than at the Earth for typical conditions, which would be on the order
1567 of 500 TW.

1568 The generation of currents and electromagnetic energy at Jupiter may be domi-
1569 nated by processes much different from at the Earth, as the interaction of the solar wind
1570 and interplanetary magnetic field are weaker. It is thought that the planet’s rotation and
1571 magnetic field provide a significant contribution to the energy sources of the heating pro-
1572 cesses (Eviatar & Barbosa, 1984; J. Waite & Lummerzheim, 2002).

1573 Due to the lack of observations of the electromagnetic fields at other planets, most
1574 of what is known is derived from computer simulations, such as the Jupiter Thermospheric
1575 General Circulation Model (JTGCM), that addresses global temperatures, three-component
1576 neutral winds, and neutral-ion species distributions (Bougher et al., 2005). In a case study
1577 with auroral forcing plus ion drag, Bougher et al. (2005) calculated exospheric temper-
1578 atures at auroral latitudes ranging from 1200 to 1300 K, which match available multi-
1579 spectral observations. The levels of Joule heating are in the range of 70 to 140 mW/m²
1580 in the auroral ovals, while the auroral particles produce 2 to 8 mW/m². With different
1581 model parameters higher levels of the Joule heating can be produced and exospheric tem-
1582 peratures above 3000 K may be achieved. Other numerical studies have been done, too
1583 numerous to mention here. The main point is that Joule heating can significantly mod-
1584 ify the heat budget of the thermosphere in the Jovian gas giant, and similar processes
1585 would be expected at similar exoplanets. As there are many assumptions and approx-
1586 imations made in the modeling process, more work needs to be done to more accurately
1587 calculate the contribution of Joule heating to the exospheric temperatures and the re-
1588 sulting effects on the outflow, particularly the contributions from the solar wind dynamo.

1589 *3.2.4 The Cross Sections and the computation of ionization*

1590 Elastic and inelastic cross sections are at the core of the computation of the energy
1591 transfer from particle precipitation to the atmosphere. To that extent cross sections for
1592 ionization, excitation, and dissociation are necessary tools for all the computations. Sev-
1593 eral efforts have been made to gather cross sections. The most comprehensive one has
1594 been recently developed with the study of upper atmospheres in mind, called AtMoCIAD.
1595 Its advantage is the inclusion of error bars, that allows the computation of the propa-

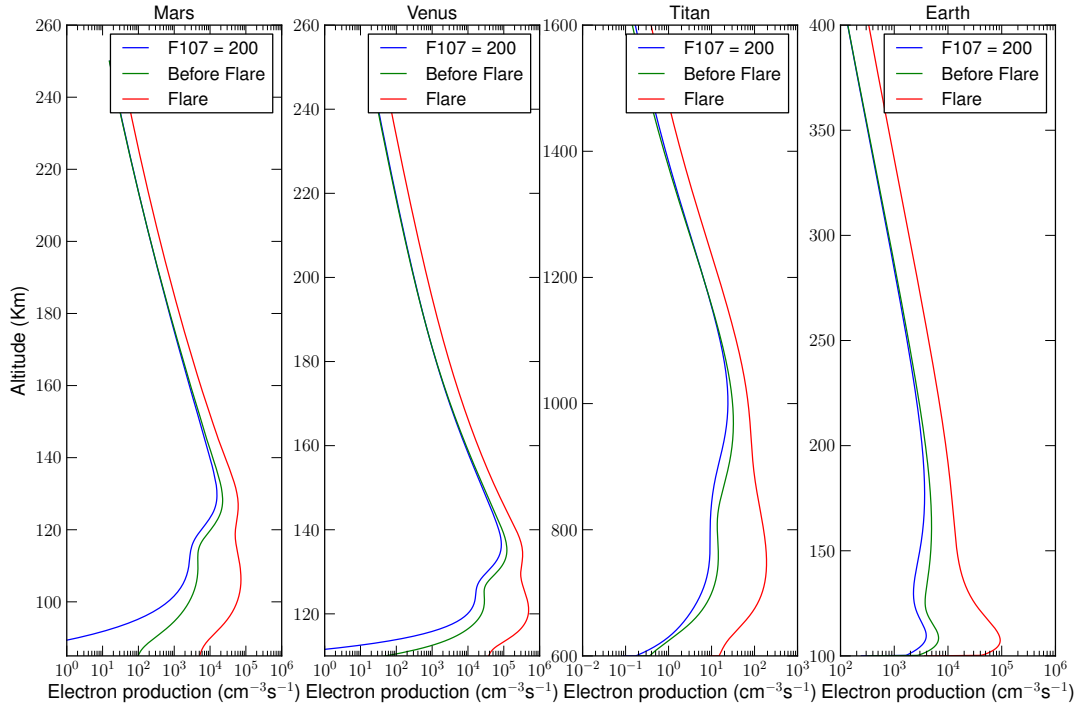


Figure 7. The ionization at Mars, Venus, and Titan for similar solar conditions, including a solar flare. The neutral atmosphere is of importance in deciding at which altitude the peak is. The extent of the atmosphere, roughly determined by the scale height (since it can be function of the altitude) of the atmosphere, is the main parameter to explain the height of the peak. These ionizations were computed using the Aeroplanets model (Gronoff, Simon Wedlund, Mertens, & Lillis, 2012); including both direct photoionization and secondary electron ionization.

1596 gation of the experimental or theoretical uncertainties (Gronoff, Simon Wedlund, Mertens,
 1597 & Lillis, 2012; Gronoff, Simon Wedlund, Mertens, Barthélemy, et al., 2012), but also the
 1598 inclusion of all kinds of particles (photons, electrons, protons, hydrogen, ...) colliding
 1599 with atoms or molecules.

1600 The precise knowledge of all types of cross section can improve the computation
 1601 of the different conditions at different planets. A consistent set of cross sections allows
 1602 to perform comparative planetology studies. An example of such a computation can be
 1603 seen in Figure 7.

1604 Other cross sections such as charge-exchange cross sections are of importance for
 1605 escape studies. The database maintained by the Atomic and Molecular Collisions Group
 1606 of the Department of Physics and Astronomy at Rice University (Houston, USA, <http://www.ruf.rice.edu/~atmol>)
 1607 is among the most populated with species of interest for space science studies (Lindsay
 1608 & Stebbings, 2005).

1609 3.3 Atmospheric structure

1610 Addressing the atmosphere structure is one of the more complex part of the study
 1611 of upper atmosphere. Model should address both ionospheric problems, such as the pre-

1612 precipitation of particles and Joule heating, as well as fluid problems like the heat trans-
 1613 port, winds, or radiative problems such as the CO₂ 15μm cooling (Johnstone et al., 2018,
 1614 and references therein).

1615 3.3.1 Vertical Mixing and Photochemical Modeling of Atmospheres

1616 Most of the planets in our Solar system have a substantial atmosphere, with the
 1617 exception of Mercury which has a very tenuous atmosphere. Several moons in the So-
 1618 lar system also have atmospheres. An atmospheric gas can be made up of a variety of
 1619 chemical species that were distributed unevenly at the time of the formation of the So-
 1620 lar system. A basic relationship between fundamental quantities governing the gas dis-
 1621 tribution of chemical species is the ideal gas law, $p = n(z)kT$, which becomes increas-
 1622 ingly less valid for pressures greater than 1 bar, after which Van der Waals equation of
 1623 state should be used (Parkinson, 2002).

1624 Knowledge of the photochemical and chemical processes governing the transforma-
 1625 tion of a particular atmospheric species into another can be used to calculate the dis-
 1626 tribution of each species considered throughout the atmosphere. Since a particular at-
 1627 mospheric constituent might be the source of one or more other constituents, this cal-
 1628 culation requires the simultaneous solution of a series of coupled continuity equations,
 1629 one for each atmospheric species considered, viz.,

$$\frac{\partial n_i}{\partial t} + \nabla \cdot \phi_i = P_i - L_i n_i \quad (67)$$

1630 where ϕ_i is the flux of a particular species, and t is time. The species number density
 1631 is given by n_i , P_i is the chemical production rate and L_i is the loss frequency at altitude
 1632 z and time t (Chamberlain & Hunten, 1987, see).

1633 The solution of Equation 67 yields the distribution of the species that are being
 1634 studied. This solution is obtained by considering the various photochemical and chem-
 1635 ical production and loss terms in addition to the effects of composition, eddy diffusion,
 1636 temperature, mixing ratio and the solar flux on the various constituents distribution. This
 1637 method of solution is described for one dimension in the sections that follow.

1638 *3.3.1.1 1-D General Method of Solution* The vertical distribution of a minor con-
 1639 stituent in a planetary atmosphere is governed by the 1-dimensional continuity equation
 1640 for each species, i ,

$$\frac{\partial n_i}{\partial t} + \frac{\partial \phi_i}{\partial z} = P_i - L_i n_i \quad (68)$$

1641 where the vertical flux, ϕ_i , can be approximated by

$$\phi_i = \phi_i^K + \phi_i^D. \quad (69)$$

1642 The eddy flux, ϕ_i^K ,

$$\phi_i^K = -K \left(\frac{\partial n_i}{\partial z} + \left(\frac{1}{H_{av}} + \frac{1}{T} \frac{\partial T}{\partial z} \right) n_i \right) \quad (70)$$

1643 represents the vertical flux that parameterizes macroscopic motions, such as the large
 1644 scale circulation and gravity waves, and ϕ_i^D

$$\phi_i^D = -D_i \left(\frac{\partial n_i}{\partial z} + \frac{(1 + \alpha_i)}{T} \frac{\partial T}{\partial z} + \frac{n_i}{H_i} \right) \quad (71)$$

1645 is the vertical flux carried by molecular diffusion. The species number density is given
 1646 by n_i , P_i is the chemical production rate ($\text{cm}^{-3} \text{s}^{-1}$) and L_i is the loss frequency (s^{-1})
 1647 at altitude z and time t (e.g. Chamberlain and Hunten (1987)). D_i and $K = K(z)$ are,

1648 respectively, the molecular and vertical eddy diffusion coefficients. The molecular dif-
 1649 fusion coefficients, D_i , are taken from Mason and Marrero (1970); Cravens (1987) where
 1650 applicable using the formula $D_i = \frac{b_i}{n_{bg}} = \frac{AT^s}{n_{bg}}$ where b is the binary collision param-
 1651 eter (expressed in terms of the coefficients A and s) and the subscript ‘ bg ’ denotes back-
 1652 ground. H_i and H_{av} are respectively the constituent and background atmospheric pres-
 1653 sure scale heights, i.e., $H_i = \frac{kT}{M_i g}$ and $H_{av} = \frac{kT}{M_{av} g}$ where M_i and M_{av} are respectively
 1654 the molecular weights of the constituent and the atmosphere. In these calculations we
 1655 have neglected the effects of the thermal diffusion factor, α_i , as its inclusion contributed
 1656 less than 1% to a given species column in test runs.

1657 Eddy mixing tends to homogenize the atmosphere such that, where there are no
 1658 effects due to chemistry, all species would be distributed according to the mean atmo-
 1659 spheric pressure scale height. Molecular diffusion tends to separate constituents by their
 1660 individual molecular weights. The atmospheric level at which the molecular diffusion coef-
 1661 ficient is equal to the eddy diffusion coefficient is defined as the homopause for the i^{th}
 1662 constituent. Above this altitude, molecular diffusion dominates and the time constant
 1663 for reaching diffusive equilibrium is given by $\tau_D = \frac{H_{av}^2}{D_i}$ (Chapman et al., 1990; Cole-
 1664 grove et al., 1966). Below the homopause, eddy diffusion dominates and the long lived
 1665 species are “mixed”, and the mixing time constant is analogously expressed as $\tau_K = \frac{H_{av}^2}{K}$.

1666 Equation (68) is solved using a finite central difference approximation for the ver-
 1667 tical derivatives and the species densities are solved semi-implicitly in time using a sim-
 1668 ple tridiagonal solver. For these applications we have assumed a steady state exists and
 1669 so have driven the solution so that $\frac{1}{P} \frac{\partial n_i}{\partial t} \rightarrow 0$. Examples of such models and details
 1670 are given in (Parkinson, 2002; Yung & DeMore, 1982)

1671 *3.3.1.2 Eddy Diffusion Coefficient, $K(z)$* One of the fundamental properties of
 1672 a planetary atmosphere is the amount of mechanical mixing forced by large scale circula-
 1673 tion, gravity waves and other processes. In a one-dimensional model, this mixing is of-
 1674 ten characterized by the eddy diffusion coefficient, which we will denote by K , K_z or $K(z)$.
 1675 The value of $K(z)$ in the vicinity of the homopause, K_h , is critical in determining the
 1676 onset of the importance of molecular diffusion. Estimates of K_h for the outer planets have
 1677 been obtained by various means: e.g., analyses of the H Lyman- α albedo (Wallace and
 1678 Hunten, 1973; Atreya, 1982; Ben Jaffel et al., 1993; Ben Jaffel et al., 1994), the fall-off
 1679 in hydrocarbon profiles, as measured against an H_2 background, using solar and stellar
 1680 occultation data (Atreya et al., 1981; Festou & Atreya, 1982; Romani et al., 1993), the
 1681 He 584 Å albedo (McConnell et al., 1981; Sandel et al., 1982; Vervack et al., 1995; Parkin-
 1682 son et al., 1998) and the CH_4 fluorescence (Drossart et al., 1999).

1683 *3.3.1.3 Thermospheric-ionospheric simulations* The modeling of a thermosphere-
 1684 ionosphere is slightly different than the deeper layers of the atmosphere: a density pro-
 1685 file has to be taken into account for each different neutral species, since they follow their
 1686 own scale height. Supra-thermal species can exist, such O in the upper atmosphere of
 1687 Mars, resulting from O_2^+ dissociation. For the ionized species, a different temperature
 1688 has to be computed (and it changes with the species in the most complicated simula-
 1689 tions). Finally electron temperatures have to be addressed. The full description of these
 1690 models is outside the scope of this paper. We refer the reader to the following studies
 1691 and their included references Johnstone et al. (2018); Bougher et al. (2005).

1692 *3.3.1.4 Importance of the 3-D modeling* Three dimensional models (3-D) mod-
 1693 els provide a broad characterization of the whole atmosphere that couple chemistry, dy-
 1694 namics, and energy balance. These numerical tools, while not capable of including the
 1695 details of their one-dimensional (1-D) counterparts, can capture the effects of global dy-
 1696 namics, diurnal chemistry, and the resulting energy balance. It has been shown that the
 1697 approximations made with 1-D modeling are not able to fully reflect the reality of a plan-
 1698 etary climate. For example, the presence of clouds, ice sheets, oceans, etc. have large ef-

1699 fect able to change a non-habitable planet into one (Way et al., 2016, 2018). For thermospheres-
 1700 ionospheres, the 3-D effects of transport and cooling lead to different results as well, which
 1701 may change our view of an exoplanet.

1702 **3.3.2 Exospheric temperature**

1703 The exospheric temperature, T_{exo} is one of the most important parameters in the
 1704 study of non-hydrodynamic atmospheric escape. It is the temperature at the base of the
 1705 exosphere. Its effects on atmospheric escape are numerous. First, a higher T_{exo} means
 1706 a higher thermal escape. Secondly, with a warmer thermosphere, the exobase increases
 1707 with altitude thereby increasing the exobase surface. This in turn implies a higher to-
 1708 tal escape from the planet and a greater cross section to non-thermal escape. Thirdly,
 1709 a high T_{exo} means that non-thermal processes can be more efficient.

1710 The exospheric temperature depends upon (a) the UV flux (photon heating), (b)
 1711 the chemical heating, (c) the electromagnetic energy (Joule heating), and (d) precipi-
 1712 tation (auroral heating) in the atmosphere. The rate of cooling, primarily by infrared
 1713 radiation, depends upon the composition and the adiabatic expansion. The equilibrium
 1714 between the heating and cooling factors gives the temperature. Since wind and UV heat-
 1715 ing are important factors, major dayside-nightside exospheric temperature differences
 1716 can occur. Full 3-D models such as the Global Ionosphere-Thermosphere Model (GITM)
 1717 (Ridley et al., 2006) are therefore necessary to obtain a correct value for the exospheric
 1718 temperature. A 1-D approximation of the temperature can be made, but, in the case of
 1719 the study of non-thermal escape, it may become a major problem. This is because the
 1720 day-night asymmetry from the escape processes is correlated with the asymmetry from
 1721 the exospheric temperature, which could lead to severe errors in the determination of
 1722 the magnitude of the escape.

1723 The exospheric temperature is determined by the equilibrium between heating and
 1724 cooling. Since these processes are altitude dependent, it is often necessary to determine
 1725 the structure of the thermosphere and compute the exospheric temperature from the ba-
 1726 sic equations. Empirical models exist, for example, for Earth (Weimer et al., 2011). In
 1727 the planets of the Solar system, heating is dominated by (1) photoexcitation and cool-
 1728 ing by (2) thermal conduction (González-Galindo et al., 2009). The photoexcitation/photodissociation
 1729 heating is due to the kinetic energy left in these processes: the difference between the
 1730 threshold $E_{t,k}$ of the k^{th} reaction on a species, s , and the energy, E , of the photon is trans-
 1731 formed into heat. When the flux of photon per unit energy is $\Phi(E)$ we have:

$$1732 \quad Q_{UV,k} = \int_{E_{t,k}}^{\infty} (E - E_{t,k}) n_k \sigma_k(E) \Phi(E) dE \quad (72)$$

1733 The thermal conduction is solved through the following equation (González-Galindo et
 al., 2009):

$$\frac{\partial T}{\partial t} = \frac{1}{\rho c_p} \frac{\partial (k \frac{\partial T}{\partial z})}{\partial z} \quad (73)$$

$$k = AT^{0.69} \quad (74)$$

1734 With ρ being the density (kg/m^3), c_p the heat capacity, and A the weighted average of
 1735 the thermal conductivities.

1736 Two major parameters are to be carefully determined when estimating the exospheric
 1737 temperature, and are the most complicated to address to date: (3) the chemical heat-
 1738 ing/cooling, (4) the radiative cooling.

1739 The chemical heating, due to the exothermic reactions, and cooling, due to the en-
 1740 dothermic reactions, follow the ionization and dissociation by precipitating particles (in-
 1741 cluding photons). Evaluating this contribution requires to carefully evaluate the chem-

1742 ical reactions chains and their energies. Those are atmospheric-composition dependent
1743 and can be quite complex and not well understood (e.g. Titan).

1744 The radiative cooling is mainly due to the de-excitation of molecular species in a
1745 rotational or vibrational state. Simple approximations of that cooling can be made if the
1746 cooling species is in low quantity in the atmosphere and if it is excited only by thermal
1747 processes; i.e. if it is in a local thermodynamic equilibrium (LTE) and if the emission
1748 line (or band) is optically thin. More complex cases exist in the atmospheres (such as
1749 non-LTE processes that are known to happen in auroral regions and optically thick cases),
1750 that require precise radiative transfer calculations (Mertens et al., 2008, 2009). In ad-
1751 dition, very complex cases such as state inversion and MASER can be obtained, such
1752 as those occurring at Mars and Venus at 10 μm (Mumma, 1993) and probably at some
1753 exoplanets (Cosmovici & Pogrebenko, 2018). Finally, some of the radiative species can
1754 be obtained by chemical reactions when the system is out of equilibrium, e.g. NO cool-
1755 ing at Earth (Weimer et al., 2015). For the extrapolation of Solar system planets' sit-
1756 uation to other stellar systems, it is important to validate such approximations .

1757 Other important parameters have to be considered depending on the cases stud-
1758 ies: (5) NIR heating, important in the case of CO_2 -rich planets, (6) dynamic cooling -
1759 from winds or expansion-, and (7) heating from gravity waves dissipation (Hargreaves,
1760 1992).

1761 **3.3.3 The exobase altitude**

1762 The exobase is the altitude at which the scale height is equal to the mean free path
1763 of a thermalized particle (at T_{exo}). Above this altitude, the mean free path is greater
1764 than the scale height, and a particle with sufficient energy is likely to escape without any
1765 collision.

1766 One can approximate the density in the thermosphere by $n(z) = n_o \times e^{(-\frac{z-z_o}{H})}$
1767 (nb: this is valid for a thermosphere with one constituent; if multi-constituent a H will
1768 have to be defined for each of those, but the exobase is usually defined for the main con-
1769 stituent). At the exobase, we have $n_{exo} = \frac{H}{\sigma}$ with σ being the collision cross section
1770 between the main molecules. If we suppose an isothermal thermosphere, i.e. H does not
1771 vary with altitude, it is possible to easily retrieve the exobase altitude: $z_{exo} = z_o - H \ln(\frac{n_{exo}}{n_o})$.
1772 For multi-component atmospheres and varying temperature, the evaluation becomes more
1773 complex since H and σ (and therefore n_{exo}) vary with altitude.

1774 **3.4 Time dependence and creation of observable markers**

1775 Once the main processes leading to atmospheric escape are known, the study of their
1776 influence in time requires evaluating the evolution of the stellar forcing parameters. If
1777 possible, the study of the isotopic ratio in the planetary atmosphere will be a major in-
1778 put for validating the calculations and estimating the influence of other processes such
1779 as outgassing, etc.

1780 **3.4.1 Evolution in time of the stellar forcing parameters**

1781 Stellar rotation drives the magnetic activity responsible for UV to X-ray emission
1782 from Sun-like stars through a dynamo mechanism thought to be seated near the bottom
1783 of the stellar convection zone. In turn, this magnetic activity influences rotation itself
1784 through angular momentum loss to a magnetized wind that leads to a gradual slow down
1785 of the rate of spin.

1786 Stars are born with a natural spread in their rotation periods and these initially
1787 evolve quite rapidly with time due to changes in moment of inertia as stars contract on
1788 to the main sequence. This initial rotational evolution then involves *spin up*, rather than

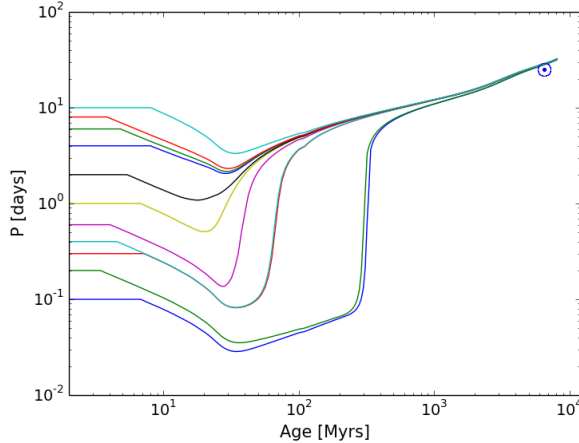


Figure 8. Evolution of the rotation period of a $1 M_{\odot}$ star as a function of age for different initial periods during the disk-locked T Tauri phase based on the rotation evolution model of Garraffo et al. (2018).

1789 spin down. All newly-formed Sun-like stars are thought to possess a residual disk of gas,
 1790 called a protoplanetary disk, within which planets form. In the early, so called “T Tauri”,
 1791 phase of evolution (named after the representative prototype) lasting a few million years,
 1792 the protoplanetary disk is expected to prevent them from spin up through a mechanism
 1793 known as disk-locking (Rebull et al., 2002, 2004). While the detailed physics behind this
 1794 is still poorly understood, the underpinning of the idea is that there is angular momen-
 1795 tum exchange between the star and the disk modulated by magnetic fields that connect
 1796 them—in essence, the disk applies a magnetic brake. After anything from a few Myr up
 1797 to 10 Myr, the disk gets dispersed and stars then freely spin-up as a consequence of con-
 1798 traction. Once on the main-sequence, contraction has stopped and magnetic braking through
 1799 the stellar wind results in an efficient spin-down process.

1800 Magnetic braking is determined by the magnetic fields on their surfaces (Weber &
 1801 Davis, 1967; Kawaler, 1988). This self-regulating mechanism results in the rotation peri-
 1802 od evolving with time following the Skumanich law for spin-down $P_{rot} \propto t^{1/2}$ (Skumanich,
 1803 1972). This is the foundation of Gyrochronology (Meibom et al., 2015), a very power-
 1804 ful tool that enables the conversion of rotation periods into stellar ages. Studies of the
 1805 rotation periods of stars in young open clusters have revealed a bimodal distribution, re-
 1806 cently attributed to different magnetic evolutionary paths of stars with different initial
 1807 rotation periods (Garraffo et al., 2018). Stars that start off spinning faster will have smaller
 1808 Rossby numbers, and this is expected to result in a more complex geometry of the sur-
 1809 face magnetic fields. This, in turn, has the effect of closing otherwise open field lines, pre-
 1810 venting the stellar wind to escape removing angular momentum. As a consequence, stars
 1811 with short initial rotation periods will remain rotating fast for longer than their initial
 1812 slow rotators counterparts (see Figure 8 for an illustration of the effect of different ini-
 1813 tial periods in the spin evolution of a $1 M_{\odot}$ star). The period of time for which the ini-
 1814 tially fast rotators will remain rotating fast is larger the lower the stellar mass is. Even-
 1815 tually, at an age that depends on the stellar mass (~ 600 Myrs for solar mass stars),
 1816 initial conditions have been erased and all stars follow the Skumanich law, making Gy-
 1817 rochronology fairly reliable. However, the activity history of these stars can be quite dif-
 1818 ferent depending on their initial rotation history, and that can potentially make a dif-
 1819 ference in the survivability of their planets’ atmospheres and habitability.

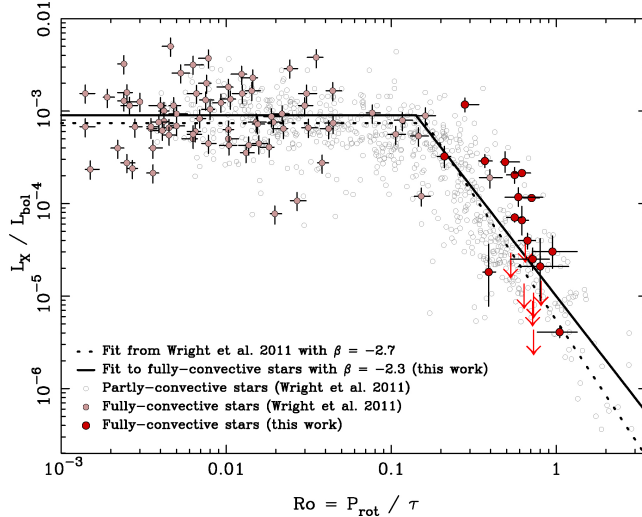


Figure 9. X-ray to bolometric luminosity ratio, L_X/L_{bol} , as a function of the Rossby number, $Ro = P_{rot}/\tau$, for both partly convective and fully convective stars. The best-fitting activity–rotation relations found for fully convective stars by N. J. Wright et al. (2018) ($\beta = -2.3$ and $Ro_{sat} = 0.14$, solid line) and from N. J. Wright et al. (2011) ($\beta = -2.7$ and $Ro_{sat} = 0.16$, dotted line) are shown. From N. J. Wright et al. (2018); see text for details.

1820 The establishment of rotation (or more correctly, differential rotation) as the driver
 1821 for the magnetic dynamo activity that gives rise to UV, EUV and X-ray emission that
 1822 drive planetary atmospheric ionization and loss processes can be traced back to the 1960s
 1823 when it was noticed that Ca II H & K emission fluxes of stars declined linearly with stel-
 1824 lar rotation velocity. The magnetic nature of stellar coronae was essentially established
 1825 a decade later by the *Einstein* observatory and the realization that X-ray luminosity was
 1826 highly correlated with stellar rotation (Vaiana, 1981; Pallavicini et al., 1981; Walter et
 1827 al., 1980). Some fraction of the magnetic energy created within the star by dynamo ac-
 1828 tion and subject to buoyant rise is dissipated at the stellar surface and converted into
 1829 particle acceleration and plasma heating. Although none of these processes are fully un-
 1830 derstood, the dependence of activity diagnostics and stellar UV and X-ray fluxes on ro-
 1831 tation shows a very simple empirical relation in terms of a magnetic “Rossby” num-
 1832 ber illustrated in Figure 9. The Rossby number in this case is the ratio of the rotation pe-
 1833 riod and convective turnover time near the base of the convection zone, $Ro = P_{rot}/\tau_{conv}$
 1834 (see also Noyes et al. (1984)).

1835 Figure 9 shows stellar X-ray luminosities normalized to the total stellar bolomet-
 1836 ric output, L_X/L_{bol} , as a function of the Rossby number for late-type stars ranging from
 1837 spectral type F down to mid-M, including fully-convective M dwarfs. At slower rotation
 1838 rates, $L_X/L_{bol} \propto Ro^\beta$, where N. J. Wright et al. (2018) find $\beta = -2.3$, up until a thresh-
 1839 old at which point X-ray emission saturates, $L_X/L_{bol} \sim 10^{-3}$, close to a Rossby num-
 1840 ber $Ro = 0.13$. This saturation behavior was already apparent from data obtained by
 1841 the *Einstein* observatory (Vilhu, 1984; Micela et al., 1985), although its origin is still de-
 1842 bated. It is likely that it represents saturation of the dynamo itself (see, e.g., the discus-
 1843 sion in N. J. Wright et al. (2011) and Blackman and Thomas (2014)). The rotation pe-
 1844 riod at which saturation sets in increases for decreasing stellar mass. For a solar mass
 1845 main-sequence star, X-ray emission saturates at a ~ 1.25 days period, while it can be
 1846 more than 100 days for an early M dwarf. (N. J. Wright et al., 2011). This means that
 1847 lower mass stars are expected to be saturated, and therefore comparatively more active
 1848 and UV and X-ray bright, than higher mass stars for much longer.

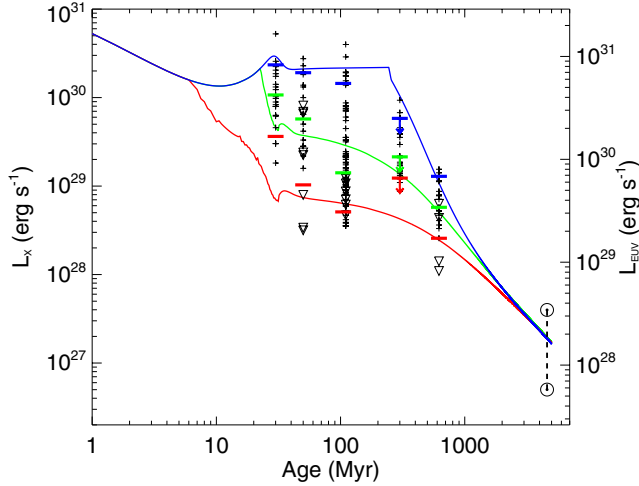


Figure 10. The X-ray and EUV luminosities, L_X and L_{EUV} , for a solar mass star as a function of time. Shown are the luminosity trajectories for three different rotation evolution tracks, together with observed X-ray luminosities for single stars in open clusters. Upper limits are indicated by inverted triangles. Solid horizontal lines indicate 10th, 50th, and 90th percentiles of the observed distributions of L_X at each age calculated by counting upper limits as detections. Two solar symbols at 4.5 Gyr show the range in L_X for the Sun over the solar cycle. From Tu et al. (2015).

1849 The X-ray luminosities and cumulative X-ray doses for a $1M_{\odot}$ star as a function
 1850 of age for the different rotation histories shown in Figure 8 based on the rotation-activity
 1851 relations of N. J. Wright et al. (2018) are illustrated in Figure 10.

1852 **3.4.2 Isotopic Fractionations and Retrieving the History of Planetary** 1853 **Atmospheres**

1854 The study of isotopes is the major tool to study the history of planetary systems.
 1855 In planetary atmospheres, it allows to create an history of the escape. Unfortunately,
 1856 it is usually a ill-posed problem, and hypothesis are required, such as an atmosphere with
 1857 basically the same composition over eons, and it allows to retrieve the fraction lost to
 1858 space, without any other data about the fraction lost to e.g. surface; which prevents one
 1859 to have a good idea of the surface pressure in the past as explained in D. Brain et al. (2016);
 1860 the situation is complicated once surface processes are able to perform isotopic fraction-
 1861 ation (Parai & Mukhopadhyay, 2018). Once productions/outgassing are taken into ac-
 1862 count, it is possible to reach a steady state for isotopic fractionations, which complicates
 1863 the interpretation (Mandt et al., 2009).

1864 **3.4.2.1 Theory for hydrodynamic fractionation** we have seen in Section 2.1.4 how
 1865 to retrieve the differential flux of a species n_b dragged by a species n_a in hydrodynamic
 1866 escape. Considering N_b , the total content of the species b in the atmosphere, it is pos-
 1867 sible to estimate the variation of N_b in function of the history of the hydrodynamic es-
 1868 cape of the atmospheric species a . Following Pepin (1992), we assume no replenishment
 1869 and that the escaping flux of a in function of time, $F_a(t)$, follows $F_a(t) = F_a^0 f(t)$, with
 1870 f being a decreasing function with time. In that case, we find that:

$$\frac{dN_b}{N_b} = -\frac{F_a^0}{N_a} \left[f(t) - \frac{m_b - m_a}{m_c - m_a} \right] dt \quad (75)$$

1871 Solving this equation allows to evaluate the total amount of b that escaped. The most
 1872 interesting conclusion that we can make from this equation, while having no knowledge
 1873 of $f(t)$, it that the escape of N_b stops at the time t_2 such that $f(t_2) = \frac{m_b - m_a}{m_a^0 - m_a}$.

1874 *3.4.2.2 Theory for Jeans/non-thermal fractionation* When discussing fractionation
 1875 with respect to an escaping atmosphere, the Rayleigh fractionation/distillation law
 1876 and its notation are often used (Jakosky, 1994; Johnson et al., 2000; Mandt et al., 2009).
 1877 In this nomenclature, R , the ratio of two species –often isotopes–, is the main param-
 1878 eter. First, it is important to not make a confusion between the observed ratio of species
 1879 b and a , $R(z) = n_b(z)/n_a(z)$, and the total ratio $R = N_b(z)/N_a(z) \approx N_b(z_i)/N_a(z_i)|_{z_i < z_{homopause}}$. The observed ratio is fractionated in altitude above the homopause. The main
 1880 hypothesis of the Rayleigh distillation law is that any species i is lost proportionally to
 1881 its total amount: $dN_i = k_i N_i$. Therefore we have:

$$\frac{dN_b}{dN_a} = \frac{k_b}{k_a} \frac{N_b}{N_a} = f \frac{N_b}{N_a} \quad (76)$$

$$\frac{dN_b}{N_b} = f \frac{dN_a}{N_a} \Rightarrow \ln \left(\frac{N_b}{N_b^0} \right) = f \ln \left(\frac{N_a}{N_a^0} \right) \quad (77)$$

$$\left(\frac{N_b/N_a}{N_b^0/N_a^0} \right) = \left(\frac{N_a^0}{N_a} \right)^{(1-f)} \quad (78)$$

$$\frac{N_a^0}{N_a} = \left(\frac{R}{R^0} \right)^{\frac{1}{(1-f)}} \quad (79)$$

1883 The Rayleigh distillation equation 79 allows to evaluate the total loss of a species
 1884 through escape provided the fractionation factor f and the initial isotopic ratio R^0 and
 1885 the current one R . If one considers an escape flux F proportional to N , it is easy to see
 1886 that $k = F/N$, and therefore that $f_e = \frac{F_b}{F_a} \times \frac{1}{R}$. Using equation 5, it appears that the
 1887 fractionation factor for Jeans escape is:

$$f_{Jeans} = \sqrt{\frac{m_a}{m_b} \frac{1 + \lambda_{ex,b}}{1 + \lambda_{ex,a}}} e^{\lambda_{ex,a} - \lambda_{ex,b}} \quad (80)$$

1888 *3.4.2.3 Outstanding problems related to fractionation* The observation and mod-
 1889 eling of fractionation highlighted major events in the evolution of planetary atmospheres.
 1890 The D/H ratio observed at Venus, $> \sim 1.6 \times 10^{-2}$ (Donahue et al., 1982; Marcq et al.,
 1891 2018), suggests that the loss of water at Venus may be consistent with the loss of a Earth’s
 1892 ocean (Shizgal & Arkos, 1996).

1893 The enrichment of ^{15}N over ^{14}N at Mars can be explained by non-thermal processes
 1894 (Shizgal & Arkos, 1996). Since Ar does not reacts chemically, Jakosky et al. (2017) used
 1895 the $^{38}\text{Ar}/^{36}\text{Ar}$ ratio to determine that Mars lost 66% of its atmosphere to space. It is
 1896 to be noted that the location and timing at which an isotopic ratio is measured can have
 1897 an effect: Livengood et al. (2020) has shown that surface adsorption at Mars performs
 1898 isotopic fractionation that can be highlighted by daily variations (temperature changes
 1899 the amount of gas adsorbed).

1900 At Earth, the fractionation of noble gases have been explained by hydrodynamic
 1901 escape processes (Shizgal & Arkos, 1996), except for xenon. Xenon is depleted by one
 1902 order of magnitude relative to other noble gases and other volatile elements when nor-
 1903 malized to the chondritic composition (e.g. Marty (2012)) and is largely enriched in its
 1904 heavy isotopes relatively to Solar or chondritic xenon. This peculiarity of xenon com-
 1905 pared to other noble gases is known as the “xenon paradox”. The specific electronic struc-
 1906 ture of xenon which makes it the most reactive element among noble gases with the low-
 1907 est ionization potential (12.13 eV or 102.23 nm) and an extended photoabsorption cross
 1908 section covering part of the VUV spectrum (up to about 150 nm). From this consider-
 1909 ation and because of the difficulty to explain Xe depletion and fractionation with other

1910 mechanisms, the escape of Xe^+ driven by H^+ ion escape is considered as a plausible ex-
 1911 planation of the xenon paradox (Zahnle et al., 2019). On the other hand, Hébrard and
 1912 Marty (2014) proposed a scenario combining the trapping of heavy xenon isotopes in haze
 1913 with an efficient escape of Xe^+ ions which is both consistent with the Xenon depletion
 1914 and fractionation. The time history of Xe isotope fractionation has been investigated in
 1915 detail by Avicé et al. (2018), and showed that it started evolving at least 3.5 Ga ago un-
 1916 til it reached the modern-like atmospheric Xe composition at around 2.1 Ga ago. They
 1917 concluded that termination of the isotopic fractionation of Xe may coincide with the end
 1918 of the hydrogen escape which has previously been suggested to explain the progressive
 1919 oxygenation of the Earth’s atmosphere (Zahnle et al., 2013). However, such significant
 1920 escape of Xe^+ ions with no associated loss of other noble gases is challenging due to the
 1921 large mass of Xe^+ and its associated large gravitational binding energy (~ 85 eV). The
 1922 work of Parai and Mukhopadhyay (2018) shows that xenon can be trapped in the crust
 1923 from the oceans, but is basing its atmospheric fractionation on the work of (Pepin, 1991)
 1924 who does not consider that xenon can be trapped back into the Earth. It may be that
 1925 the xenon paradox could be solved not by escape physics, but by crustal absorption. This
 1926 is in agreement with the organic haze scavenging of Xe hypothesis, investigated in Avicé
 1927 et al. (2018), that solves the paradox without requiring atmospheric escape. An inter-
 1928 esting point is the requirement for atmospheric hazes in that hypothesis: specific atmo-
 1929 spheric conditions, similar to the present Titan (McKay et al., 2001), are required to cre-
 1930 ate those, and therefore Xe isotopic fractionation may be an indicator of the atmospheric
 1931 conditions of the Archaean Earth. Such a solution has the potential to reconcile the con-
 1932 clusions of Parai and Mukhopadhyay (2018), i.e. no plate tectonics before 2.5 Gyr ago
 1933 or extremely dry tectonics, with the observation of ancient plate tectonics with excess
 1934 water before 3.3 Gyr by Sobolev et al. (2019).

1935 4 Escape at Solar System’s Planets and Bodies

1936 The atmospheric escape in the Solar system shaped most of the planets and dwarf
 1937 planets’ atmospheres, as well as those of some satellites. Mercury may have had a proto-
 1938 atmosphere above its magma ocean, like the Moon (Greenwood et al., 2018), but, un-
 1939 like the Moon, no sample from the surface are available and a detailed study of the his-
 1940 tory of Mercury’s atmosphere lacks too much experimental evidence. Mars, Venus, the
 1941 Earth, and Titan have on the contrary a large quantity of data showing an atmosphere
 1942 that has been transformed by escape. Currently H and He are the most important species
 1943 escaping for these objects. We are also observing other escape processes, such as O, and
 1944 we try to understand the pathways of escape of CO_2 at Mars, so we can understand the
 1945 evolution of its atmosphere in time. Non-thermal escape processes at Jupiter and Sat-
 1946 urn are known to fill a part of their plasmaspheres and leads to some minor escape. Over-
 1947 all, the giant planets are too big for efficient escape to take part and change drastically
 1948 their atmospheric evolution. Uranus and Neptune are similar in that their mass prevents
 1949 a lot of escape. In addition, the ice giants have only been visited by the Voyager probes
 1950 and have not had a Galileo or Cassini-like mission allowing study of their atmospheres
 1951 as comprehensively as Jupiter or Saturn. A recent work by DiBraccio and Gershman (2019)
 1952 has shown that, as for Jupiter and Saturn, plasmoids have been observed at Uranus. How-
 1953 ever, a large quantity of these plasmoids’ loss can come from the satellite of the giant
 1954 planets. Finally, relatively small loss are suspected to come from polar wind (Glocer et
 1955 al., 2007).

1956 Understanding the current escape processes allows to perform some interpolation
 1957 back in time, thanks to a better understanding of the conditions (especially the solar forc-
 1958 ing in time), and of the important parameters for each escape process. Such work nec-
 1959 essary to understand how the atmosphere could evolve into an habitable one. To have
 1960 a control point to these interpolations, it is necessary to know about the isotope ratio.
 1961 Unfortunately, surface processes (volcanism, adsorption) and other events such as comet

1962 falls or cosmic ray spallation processes [e.g. A. Pavlov et al. (2014)] can affect these re-
 1963 sults and possible concurrent models leads to the currently observed state.

1964 **4.1 The Solar forcing in time**

1965 The solar magnetic activity forcing changed substantially over the lifetime of the
 1966 Sun, as discussed in the general stellar context in Section 3.4.1. In its early stages, the
 1967 rotation of the young Sun was faster than its present rotation, with rotation periods of
 1968 only few days compared to its present 27 days period. During this time, the Sun's ra-
 1969 tio of X-ray to bolometric luminosity declined by a factor of about 1000. Thus, in gen-
 1970 eral, the most important aspect of the evolution of solar forcing is that the EUV and X-
 1971 ray fluxes were much higher during the early Solar system than today, with related con-
 1972 sequences for earlier planetary atmospheric escape rates. This time evolution is shown
 1973 in Figure 10.

1974 In addition to the solar radiation, the solar wind also plays a role in planetary at-
 1975 mospheric escape. However, the change of the solar wind in time is much less well-defined
 1976 than the solar radiation, since it is almost impossible to measure the signatures of weak
 1977 winds of solar analogs. In general, the magnetic activity paradigm suggests that a more
 1978 active Sun should produce a stronger solar wind. However, no clear evidence of that as-
 1979 sumption has been discovered so far. Scaling laws have been developed based on obser-
 1980 vations of the neutral Hydrogen absorption line generated at the edge of stellar astro-
 1981 spherics, where the stellar wind collides with the Inter Stellar Medium (ISM) (Wood, 2006;
 1982 Wood et al., 2014). Some modeling work was done to characterize the winds of Sun-like
 1983 stars (e.g., Cohen et al. (2010); Cohen and Drake (2014)). In both cases, the winds of
 1984 young stars were not found to be dramatically stronger than older stars, and many of
 1985 the observed systems were found to deviate from the scaling law and present weaker winds
 1986 than expected.

1987 Understanding the young Sun is important in the context of solving the Faint Young
 1988 Sun Paradox (Section 7.1.1). However, it is important to note that if the hypothesis on
 1989 the atmosphere composition and pressure is off, no conclusion can be made only from
 1990 the star parameters.

1991 **4.2 Coupling with the world below**

1992 The escaping region of an atmosphere does not exist in isolation. Once the primor-
 1993 dial atmosphere of a telluric planet has eroded, the hydrogen and other light elements
 1994 that escape ultimately come from the interior of the planet and pass through the lower/middle
 1995 atmosphere to reach the region of escape. Just to understand hydrogen escape, it is cru-
 1996 cial to understand the basic processes that control: (1) the flux of hydrogen-bearing species
 1997 (e.g. water, methane, H₂) from their source regions at the surface throughout the atmo-
 1998 sphere; and (2) the flux of hydrogen-bearing species to the atmosphere.

1999 Accurate modeling of hydrogen-bearing species are particularly important for un-
 2000 derstanding potentially habitable exoplanets. First, methane is a potential biosignature.
 2001 Second, the chemistry of these species is often connected with the chemistry of O₂, O₃,
 2002 CO₂, and CO through the HO_x reactions in the atmosphere and through analogous re-
 2003 actions in the interior (e.g., Kasting et al. (1993)). Third, sufficient hydrogen escape can
 2004 modify the redox state of the atmosphere, surface and interior (e.g. Kasting et al. (1993);
 2005 D. C. Catling and Claire (2005)).

2006 **4.2.1 The Present: A Focus on Hydrogen-Bearing Species**

2007 The vertical temperature structure of the atmosphere is a critical control on the
 2008 ability of condensible species to move upward from the warm troposphere to where it

2009 can escape. The stratospheric water trap on present-day Earth is the classical example
 2010 of such a control. Transport across such barriers may be accomplished diffusively or dy-
 2011 namically by means of atmospheric moist convection. The effectiveness of the cold trap
 2012 for water may depend on the presence of other hydrogen-bearing species, such as methane.

2013 *4.2.1.1 Earth* On present day Earth, the dominant sources of hydrogen-bearing
 2014 species are evaporation from the Earth’s oceans (H_2O) and anthropogenic sources of methane.
 2015 Non-anthropogenic, biogenic sources of methane remain significant and probably greatly
 2016 exceed geological sources (Dlugokencky et al., 2011), though (Etiope & Klusman, 2002)
 2017 argue that natural geological sources may be currently accounted to anthropogenic emis-
 2018 sions in error. Atmospheric water poorly mixes into the middle atmosphere. There is a
 2019 strong contrast between water vapor mixing ratios typical of the troposphere (≈ 1000
 2020 ppm) and water vapor mixing ratios near the Earth’s mesopause (≈ 5 ppm), where
 2021 the photodissociation of water by solar radiation at Lyman α wavelengths takes place
 2022 (Roell, 2012). A parallel contrast exists between water vapor concentrations near the sur-
 2023 face and in the upper troposphere (≈ 10000 ppm vs. ≈ 100 ppm in the tropics: (Sun
 2024 & Lindzen, 1993)). The region of rapid fall-off in water vapor mixing ratio is known as
 2025 the hygropause.

2026 The contrast in humidity between the troposphere and the mesosphere results from
 2027 the large-scale temperature structure of the atmosphere, in which the atmospheric tem-
 2028 perature minimum is at the tropopause and lower stratosphere. Any excess water be-
 2029 yond the point of saturation will condense to liquid and ice, which may precipitate. Thus,
 2030 moist air is freeze-dried to the equilibrium water vapor concentration at the ambient tem-
 2031 perature. At the temperature minimum of the tropopause and the lower stratosphere,
 2032 an “atmospheric cold trap” forms. The contrast in humidity between the surface and the
 2033 upper troposphere partly arises from the same mechanism. Therefore, relatively slow ver-
 2034 tical mixing of water vapor by large-scale processes such as the Hadley cell or synoptic-
 2035 scale systems will be set by the vertical thermal structure of the atmosphere, which radiative-
 2036 convective models can estimate approximately (A. A. Pavlov et al., 2000).

2037 Mesoscale processes also have some impact on water vapor transport. Strong ver-
 2038 tical motions in buoyant moist convection can transport ice to higher altitudes, evad-
 2039 ing “cold trap” effects. In some cases, moist convection can “overshoot” the tropopause,
 2040 injecting large amounts of water ice into the stratosphere over an areally limited region.
 2041 If this water ice sublimates in the stratosphere, the stratosphere is hydrated locally by
 2042 the same order as the background stratospheric water vapor concentration (Grosvenor
 2043 et al., 2007; Liu et al., 2010). If overshooting moist convection were more intense and/or
 2044 more efficient at transporting water ice to the stratosphere, the contrast between tro-
 2045 pospheric and mesospheric water vapor concentrations could be reduced. (We assume
 2046 that the increase in water vapor due to overshooting convection is greater than the de-
 2047 crease in water vapor due to mixing resulting from downdrafts of overshooting convec-
 2048 tion.)

2049 Methane does not condense at atmospheric temperatures, which reduces the surface–
 2050 mesosphere contrast considerably (1.8 ppm vs. 0.1 ppm) (Summers et al., 1997). It is
 2051 slowly dissociated in the stratosphere and mesosphere, so its composition in the upper
 2052 atmosphere will be controlled by the relative balance between chemistry and vertical trans-
 2053 port in the stratosphere and mesosphere as well as the intensity of stratospheric-tropospheric
 2054 exchange.

2055 *4.2.1.2 Mars* On present day Mars, the vertical structure of water vapor differs
 2056 greatly from that of the Earth. The main source and sink of water vapor is sublimation
 2057 from and condensation on the polar caps. A seasonally varying hygropause is apparent
 2058 at a characteristic height of 40 km above the surface in the tropics (Clancy et al., 2017;
 2059 Heavens et al., 2018). Yet detached water vapor layers are frequently observed as high
 2060 as 80–90 km above the surface (Maltagliati et al., 2013). This structure partly reflects

2061 differences in the atmospheric temperature structure. The tropical middle atmosphere
 2062 is not separated from the lower atmosphere by a strong thermal inversion analogous to
 2063 the stratosphere (except perhaps in global dust storms, when the entire atmosphere is
 2064 effectively inflated by the heating of dust). Thus, to first order, the depth of the Hadley
 2065 cell sets the hygropause height (Richardson & Wilson, 2002). Detached water vapor lay-
 2066 ers originate from mesoscale transport processes, such as injection within dust plumes
 2067 in Mars’s well-known dust storms (Heavens et al., 2011; Maltagliati et al., 2013; Spiga
 2068 et al., 2013; Heavens et al., 2015; Heavens et al., 2018; Fedorova et al., 2018) or associ-
 2069 ated with topographically-driven circulations, with or without dust storm activity (Rafkin
 2070 et al., 2002; Michaels et al., 2006; Heavens et al., 2015; Heavens et al., 2018). In regional
 2071 and global dust storms, convective transport of water to the middle atmosphere within
 2072 dusty air can be so strong that we cannot really speak of detached water vapor layers;
 2073 the mean hygropause of the planet can rise to 80 km (a change mostly caused by ascent
 2074 in the tropical hygropause) (Fedorova et al., 2018; Heavens et al., 2018).

2075 While a variety of observations suggest the presence of atmospheric methane, suf-
 2076 ficiently little is known about it to make discussion of its surface sources and transport
 2077 to the upper atmosphere entirely speculative (Formisano et al., 2004; Mumma et al., 2009;
 2078 Webster et al., 2015).

2079 *4.2.1.3 Venus* On present day Venus, the main sources of water to the atmo-
 2080 sphere are believed to be cometary and meteoritic impacts and volcanic outgassing in
 2081 uncertain proportions (F. Taylor & Grinspoon, 2009). The possibility of ongoing volcanic
 2082 outgassing has been bolstered by observations of temporal and spatial variability in at-
 2083 mospheric SO₂ and transient NIR emission from a prominent rift zone (Marcq et al., 2013;
 2084 Shalygin et al., 2015).

2085 Estimated lower atmospheric (5–45 km) water vapor concentrations from spectro-
 2086 scopic observations range from 25–50 ppmv with typical uncertainties at the 20% level
 2087 (S. Chamberlain et al., 2013). There is an outlier estimate of 200 ppmv in the 30–45 km
 2088 altitude range (J. F. Bell et al., 1991). While this value is consistent with some *in situ*
 2089 measurements by entry probes, the entry probe data is mutually inconsistent and gen-
 2090 erally mistrusted (Meadows & Crisp, 1996). Current observations are unable to probe
 2091 water vapor concentrations within 5 km of the surface, but it is speculated that water
 2092 vapor might be depleted near the surface because of reactions with surface rocks (Fegley,
 2093 2003; S. Chamberlain et al., 2013).

2094 Water vapor concentrations above the troposphere are 3–11 ppmv near the top of
 2095 the sulfuric acid cloud deck at 60–70 km altitude and likely decrease to 1 ppmv at 100
 2096 km (Fedorova et al., 2008, 2016). Water vapor at these altitudes would be vulnerable
 2097 to photochemical loss processes. Water vapor in the middle atmosphere is most abun-
 2098 dant near the Equator, a phenomenon that suggests convective transport of water va-
 2099 por from the lower atmosphere into the middle atmosphere (Fedorova et al., 2016). Oth-
 2100 erwise, the water vapor distribution in the middle atmosphere appears quite sensitive
 2101 to the altitude of the cloud deck, suggesting that the sulfuric acid cloud deck is an ef-
 2102 fective hygropause for Venus due to the formation of sulfuric acid from H₂O and SO₂.

2103 Venus’s atmosphere does not contain measurable amounts of methane at present
 2104 measurement sensitivities (F. Taylor & Grinspoon, 2009). Early *in situ* measurements
 2105 by Pioneer Venus suggested atmospheric methane concentrations were up to 6000 ppmv,
 2106 but these measurements likely were contaminated by reactions within the measurement
 2107 apparatus itself (Donahue & Hodges, 1993). Yet some methane input from meteoritic
 2108 and cometary sources is possible. If the mantle of Venus has remained sufficiently reduc-
 2109 ing, a source of methane from volcanic outgassing is possible as well.

2110 *4.2.1.4 Titan* The principal hydrogen-bearing species in the present day atmo-
 2111 sphere of Titan is CH₄. The total amount in the atmosphere as vapor exceeds the amount

2112 present on the surface as liquid by at least a factor of 2 (Lorenz et al., 2008). Most hydrogen-
 2113 bearing species in Titan’s atmosphere, such as H₂ and various organic compounds, are
 2114 likely derived from photochemical reactions involving CH₄ (Owen & Niemann, 2009; D. F. Stro-
 2115 bel, 2012; Krasnopolsky, 2014), though an H₂ source derived from serpentinization also
 2116 has been proposed (e.g. Atreya et al. (2006)). An exception is H₂O, which is likely sup-
 2117 plied to Titan by ablation of micrometeorites and/or plume material from Enceladus (Lara
 2118 et al., 1996; Coustenis et al., 1998; Dobrijevic et al., 2014). The ultimate source of methane
 2119 on Titan is believed to be episodic outgassing from Titan’s deep interior (Lorenz et al.,
 2120 1997; Tobie et al., 2009; Wong et al., 2015).

2121 CH₄ concentrations near the surface are \approx 50000 ppmv, decrease to \approx 15000 ppmv
 2122 in Titan’s stratosphere (above 32 km) (Niemann et al., 2005) and remains uniformly mixed
 2123 at that up to altitudes near the homopause region \approx 850 - 1000 km where diffusive sep-
 2124 aration causes the relative fraction of methane to increase with altitude up to the exobase
 2125 (Yelle et al., 2008; Johnson et al., 2010; J. M. Bell et al., 2014). The major barrier to
 2126 transport is an atmospheric cold trap occasionally broken by deep convective clouds of
 2127 CH₄ (Griffith, 2009).

2128 *4.2.2 The Past: Coupling, Unusual Escape Regimes, and Current Ev-* 2129 *idence for Atmospheric Mass and Upper Atmospheric Composi-* 2130 *tion*

2131 *4.2.2.1 Earth* In the course of the Earth’s early history, the upper mantle was
 2132 gradually oxidized by means of coupled pathways: (1) reductants in the upper mantle
 2133 were emitted into the atmosphere by volcanic processes, were transported into the up-
 2134 per atmosphere by processes at mesoscale to planetary scales, and escaped the Earth sys-
 2135 tem by a mixture of physical and chemical processes in the upper atmosphere, result-
 2136 ing in an unbalanced loss of reducing power from the upper mantle; and (2) weathered
 2137 (hydrated) or even oxidized crust was recycled into the mantle, where water reacted with
 2138 mantle material to form hydrogen, a light, readily escaping reductant (Holland, 1984).
 2139 This period of mantle oxidation closed when the mantle was sufficiently oxidized that
 2140 water-hydrogen conversion in the mantle ceased (Kasting et al., 1993).

2141 These processes are mediated by escape itself. Water that is vertically transported
 2142 into the upper atmosphere photodissociates, leading to the production of H₂ and O₂ abi-
 2143 otically (Lewis et al., 1983). The H₂ is highly vulnerable to escape, transporting reduc-
 2144 ing power out of the system, while the O₂ may mix down into the lower atmosphere and
 2145 oxidize the crust. Simultaneously, precipitation of atmospheric water to the surface hy-
 2146 drates the crust.

2147 Planets like present day Earth exchange water with the mantle in the course of plate
 2148 tectonic processes such as subduction, which are relatively efficient. If Venus’ surface were
 2149 wetter, some exchange would take place during putative resurfacing events (Strom et al.,
 2150 1994). Similar speculations on might be made about Mars’ volcanic activity. However,
 2151 crustal recycling on both Mars and Venus are thought to be much weaker than the Earth
 2152 and, on average, weaker in the past (S. R. Taylor & McLennan, 2009).

2153 However, there are signs from the extant record of early Earth history that plate
 2154 tectonics may not be the upper limit for crustal recycling rates on the Earth. Instead,
 2155 the Earth may have experienced a “heat-pipe” phase (W. B. Moore & Webb, 2013). In
 2156 this phase, persistent mafic to ultramafic volcanism regularly re-surfaced the Earth. Both
 2157 crustal material and surface water are cycled back into the mantle through repeated erup-
 2158 tion and burial of older flows. The heat pipes were associated with greater eruptive vol-
 2159 umes of volcanic material as well as faster crustal recycling than plate tectonics. Obser-
 2160 vations of the other terrestrial bodies in the Solar system are also consistent with heat
 2161 pipe operation in their early phases (Moore et al., 2017).

2162 Therefore, the upper mantle of the Earth began in a far more reduced state than
 2163 today and may have degassed far more intensely than today. An important consequence
 2164 of the reduced state of the Earth’s early mantle (without enhanced degassing) would have
 2165 been higher proportional degassing of carbon from the interior in the form of CH₄ as op-
 2166 posed to CO₂. In addition, formation of H₂ from H₂O in the mantle would have resulted
 2167 in significant emission of H₂ to the atmosphere (Kasting et al., 1993). High concentra-
 2168 tions of atmospheric H₂ would have interrupted the OH radical pathway for CH₄ oxi-
 2169 dation. Both gases have a demonstrable greenhouse effect (A. A. Pavlov et al., 2000; Wordsworth
 2170 & Pierrehumbert, 2013), which enhances near-surface water vapor abundance. And ab-
 2171 sorption of visible/near-infrared radiation by CH₄ strongly heats the lower stratosphere
 2172 (A. A. Pavlov et al., 2000). Based on radiative-convective simulations with variable CH₄
 2173 values, (A. A. Pavlov et al., 2000) argued that there would be a direct relationship be-
 2174 tween a more reduced mantle, a warmer “cold trap”, deeper vertical mixing of water va-
 2175 por, weaker contrast in water vapor concentrations across the hygropause, enhanced wa-
 2176 ter vapor photolysis, and oxygen production in the upper atmosphere.

2177 As in the present day, CH₄, unlike H₂O, would not condense at Earth atmosphere
 2178 temperatures. Therefore, under a variety of “cold trap” conditions, CH₄ from the pu-
 2179 tative reduced mantle source would diffuse or advect beyond the hygropause to altitudes
 2180 at which it will photolyze to produce H₂ (but not O₂).

2181 Speculations that H₂O and CH₄ would react to form an organic haze (e.g., C₄H₂
 2182 and C₅H₄), which would oppose any CH₄ or H₂ greenhouse effect, challenge this picture
 2183 (Pavlov et al., 2001; Haqq-Misra et al., 2008). However, recent simulations of this aerosol
 2184 suggest that it would be optically thin in the visible but optically thick in the ultravi-
 2185 olet. The haze would have little effect on greenhouse warming but shield the atmosphere
 2186 below it from photolysis (Wolf & Toon, 2010) (and may affect the Xenon isotopic ratio,
 2187 Section 3.4.2.3).

2188 At the same time, A. A. Pavlov et al. (2000)’s simulations greatly simplify quan-
 2189 titative treatment of chemistry, transport, and hydrogen escape. As is noted, “[a figure
 2190 which shows the relationship between CH₄ flux and atmospheric concentration] is some-
 2191 what deceptive in that it implies that atmospheric CH₄ concentrations can be calculated
 2192 by specifying the surface CH₄ flux.” One example of a complication is that higher wa-
 2193 ter vapor abundance in the atmosphere will reduce the atmospheric concentration of CH₄
 2194 by providing an abundant source of OH radical. The source of CH₄ of the Early Earth
 2195 has also been suggested as being biological of origin, and a possible biosignature (Arney
 2196 et al., 2016).

2197 Another distinct type of hydrogen escape regime might occur if the entire surface
 2198 were glaciated, as is speculated to have occurred during portions of Paleoproterozoic and
 2199 Neoproterozoic time on the Earth. This regime has been invoked to explain mysterious
 2200 rises in atmospheric p_{O₂} (O₂ partial pressure) during the deglaciation from Snowball events.

2201 p_{O₂} climbed to 10% or even close to present-level p_{O₂} in the aftermath of the Pa-
 2202 leoproterozoic Snowball (Barley et al., 2005). However, the connection between an in-
 2203 crease in atmospheric oxygen and the Paleoproterozoic glaciation is disputed (Hoffman,
 2204 2013). It is entirely possible that the glaciations preceded the rise in oxygen by ≈ 100
 2205 million years. p_{O₂} then dropped to 1-3% before rising again to 5-18% in the Neoprotero-
 2206 zoic, a time when the connection between deglaciation and the oxygen rise is better es-
 2207 tablished (Fike et al., 2006; Scott et al., 2008; Canfield et al., 2007, 2008; Halverson et
 2208 al., 2009; Sahoo et al., 2012). This higher level of p_{O₂} coincided with the first appear-
 2209 ance of metazoans in the rock record at around 600 Ma (Canfield et al., 2007), and with
 2210 the end of the Cryogenian era of Snowball Earth glaciations.

2211 Simple models of atmospheric chemistry suggest that the unusually cold conditions
 2212 of an entirely ice-covered Earth would favor the production of H₂O₂ in the atmosphere

2213 (Liang et al., 2006). As in present day Antarctica, this H_2O_2 would be incorporated into
 2214 ice. During deglaciation, this H_2O_2 would enter an ocean rich with Fe and Mn, poison-
 2215 ing existing anaerobic organisms while creating the selection pressure for the develop-
 2216 ment of oxygenic photosynthesis (Kopp et al., 2005; Liang et al., 2006). Oxygen limi-
 2217 tation thereafter then would be due to oxidation and precipitation of Fe and Mn out-
 2218 competing oxygen production by nitrogen-limited early photosynthetic autotrophs (Liang
 2219 et al., 2006). The dependence of this mechanism on the composition and emission rate
 2220 of mantle effluents (and thus geological activity/upper mantle oxidation state) is unknown.
 2221 And this question does figure in interpreting and extrapolating from the Snowballs, be-
 2222 cause the Earth’s mantle was likely more oxidized during Neoproterozoic time than Pa-
 2223 leoproterozoic time.

2224 An additional variable to consider for the past is the identity and abundance of the
 2225 principal atmospheric constituent (N_2 at present). Models consistent with abundant liq-
 2226 uid water that assume a Faint Young Sun either assume higher atmospheric pressure from
 2227 gases such as N_2 (e.g. Goldblatt et al. (2009)) or assume higher concentrations of green-
 2228 house gases such as CH_4 , H_2 , and CO_2 , whose ability to warm climate is strongly de-
 2229 pendent on pressure broadening (e.g. Kasting et al. (1984)). Higher atmospheric pres-
 2230 sure also can reduce surface temperature as a result of increased molecular scattering
 2231 of incoming solar radiation (Goldblatt et al., 2009; Poulsen et al., 2015). However, the
 2232 sign of the net effect is unclear. Radiative-convective model simulations suggest that in-
 2233 creased N_2 or O_2 will result in net positive radiative forcing even at p_{CO_2} much less than
 2234 at present (Goldblatt et al., 2009; Payne et al., 2016). Simulations with a GCM that in-
 2235 cluded clouds suggest that the net radiative forcing can be negative as a result of cloud
 2236 feedback effects at higher atmospheric pressure (Poulsen et al., 2015).

2237 Data from the geological record about past atmospheric pressure has wide uncer-
 2238 tainties but may argue against the Earth’s atmosphere being much thicker in the Archean.
 2239 A recent study of gas bubbles in an Archean (2.7 Ga) lava flow near paleo-sea level by
 2240 Som et al. (2016) suggests that the Earth’s atmospheric pressure was no more 50% of
 2241 present and most likely $\approx 25\%$ of present at that time. Raindrop-based reconstructions
 2242 also have been attempted. Som et al. (2012) suggested an upper bound for atmospheric
 2243 density of approximately twice present, but Kavanagh and Goldblatt (2015) argued that
 2244 raindrop size was more sensitive to rainfall rate than atmospheric pressure and suggested
 2245 an upper bound for atmospheric density of approximately 11 times present. It is to be
 2246 noted that the work of Airapetian et al. (2016) and its extension (Gronoff et al. in. prep.)
 2247 consider an alteration of the atmospheric chemistry by SEP events to create N_2O , which
 2248 increase the temperature of the Early Earth even for atmospheric pressure lower than
 2249 0.5 bars.

2250 Modeling suggests that if were possible to keep liquid water stable in a low pres-
 2251 sure N_2 atmosphere (200 hPa), water transport by moist convection to the middle and
 2252 upper atmosphere would be extremely efficient, resulting in high rates of water photol-
 2253 ysis (Kleinböhl et al., 2018). The resulting atmosphere evolves to a state in which abi-
 2254 otic oxygen dominates the atmosphere, unless there is a strong sink of oxygen at the sur-
 2255 face (Kleinböhl et al., 2018). Such a mechanism could explain bursts of oxygenation co-
 2256 incident with the formation of banded iron formations, but the model relies on a one-
 2257 dimensional parameterization of moist convective adjustment (Kasting, 1988) that re-
 2258 quires testing in a framework that more explicitly resolves the physical processes.

2259 *4.2.2.2 The Moon* The exosphere of the Moon is interesting in several ways: 1-
 2260 it is easier to experiment on it: we can study the decay of artificial gases released on it
 2261 by lunar lander in function of the solar activity (Vondrak, 1974; Vondrak et al., 1974;
 2262 Vondrak, 1992); 2- it has the same solar wind conditions as the one measured for space
 2263 weather at Earth, and therefore studies such as the impact of CME on it are easier (Killen
 2264 et al., 2012); 3- we have samples from the Moon, and we can study the possibilities of
 2265 ancient atmosphere from it.

2266 The hypothesis of a secondary atmosphere due to volcanic activity at the moon has
 2267 been proposed in (Needham & Kring, 2017) based on the analysis of samples from the
 2268 Apollo mission. It is possible that an an atmosphere with up to a few mb at the surface
 2269 was created and stable for 1000s of years. In Aleinov et al. (2019), a study of the ther-
 2270 mal escape was made, showing the limitations of the creation of such an atmosphere, as
 2271 well as the climatic conditions an atmosphere would have had. These conditions are in-
 2272 teresting since they show the transport of volatiles to the poles. it would be possible to
 2273 find some clues of that atmosphere in samples from the poles.

2274 *4.2.2.3 Mars* When Mars had an intrinsic magnetic field early in its history, its
 2275 hydrogen-bearing species fluxes to the upper atmosphere likely occupied a phase space
 2276 that could be described by the early Earth or even present day Earth phase spaces (Alho
 2277 et al., 2015). Transition to the regime observed today may have depended on the tim-
 2278 ing of magnetic field loss. This transition has so far been modeled as a primarily CO₂
 2279 atmosphere condensing to form at least one permanent ice cap (Soto et al. (2015) and
 2280 references therein). The principal unknown about the last billion years or so is how fluc-
 2281 tuations in Mars’ obliquity have changed the location of surface and sub-surface ice reser-
 2282 voirs, which could affect the water cycle, the total atmospheric mass, and the dust cy-
 2283 cle (Fastook et al., 2008; Madeleine et al., 2009). A lot of questions have also been asked
 2284 about the effect of the magnetic field in the loss of the atmosphere. Since observation
 2285 shows that similar amount of heavy ions are lost above magnetic fields at the current
 2286 Mars than above non-magnetized parts (Sakai et al., 2018), it may be that it influence
 2287 has been greatly exaggerated in previous studies.

2288 Like Earth, there are some constraints on past atmospheric mass for Mars. The
 2289 atmosphere filters the impact crater population by ablating the lower end of the bolide
 2290 size distribution (Jakosky et al., 2017). On this basis, (Kite et al., 2014) proposed that
 2291 Martian paleopressure was never higher than ≈ 3 bar (and likely much less). A higher
 2292 palopressure would have led to a collapse of the atmosphere. From meteoritic observa-
 2293 tion constraints, and considering that some isotopic reservoirs can be replenished by me-
 2294 teoritic/cometic falls Kurokawa et al. (2018) slightly modified the history presented in
 2295 Jakosky et al. (2017) and suggested a minimum paleopressure of 0.5 bar. Jakosky et al.
 2296 (2018) suggested that Mars lost more than 0.8 bar of CO₂ or the equivalent of 28 m of
 2297 water.

2298 An interesting point at Mars is the observation of solar-wind H deposition in the
 2299 thermosphere (Halekas et al., 2015), this deposition follows a charge-exchange process,
 2300 and could have led to changes in D/H ratio if large enough in the Early Solar system;
 2301 however, it is probable that this deposition would have been counteracted by hydrody-
 2302 namic escape.

2303 *4.2.2.4 Venus* Venus, at some point during its history, likely occupied an addi-
 2304 tional phase space with respect to coupling between the surface and the exosphere: that
 2305 of the runaway greenhouse (Ingersoll, 1969). However, this regime is somewhat analo-
 2306 gous to the elimination of the “cold trap” by absorption of visible/near-infrared radi-
 2307 ation by CH₄. The twist is that it is the infrared greenhouse effect of H₂O that breaks
 2308 the cold trap.

2309 The effect can be conceptualized semi-quantitatively. Consider a layer of the at-
 2310 mosphere at which vertical mixing from the surface is relatively efficient. Now raise the
 2311 surface temperature by some amount by introducing a higher amount of solar insolation.
 2312 To first order, the relationship between water vapor concentration and temperature should
 2313 be exponential, following the Clausius-Clapeyron relation that defines the saturation curve.
 2314 In the Earth’s atmosphere, however, it is observed that the effects of vertical mixing and
 2315 pseudo-adiabatic precipitation processes reduces the sensitivity of mean p_{H_2O} to surface
 2316 temperature in the lower troposphere (Held & Soden, 2006) but may enhance it in the
 2317 upper troposphere (Gettelman & Fu, 2008). Thus, water vapor concentration will increase

2318 exponentially in response to the increase in surface temperature. The layer’s tempera-
 2319 ture likely will increase as well in response to the increase in surface temperature. (This
 2320 is easiest to visualize at the surface itself.)

2321 At the same time, the increase in water vapor will increase the infrared opacity of
 2322 the layer, reducing outgoing longwave radiation from the layer (and below the layer). Yet
 2323 the increase in the layer’s temperature will result in increased outgoing longwave radi-
 2324 ation according to Stefan-Boltzmann’s Law. At low temperatures and water concentra-
 2325 tions, it is easy to see that the principal change in outgoing longwave radiation will be
 2326 due to the increase in layer temperature. However, as temperatures increase, the expo-
 2327 nential dependence of water vapor on temperature eventually will overcome the quar-
 2328 tic dependence of outgoing longwave radiation on temperature. Thus, for any sufficiently
 2329 abundant infrared absorber condensing and evaporating, there is some critical point at
 2330 which outgoing longwave radiation in the layer will decrease rather than increase with
 2331 surface temperature, initiating a runaway positive feedback loop. Warming of the tro-
 2332 posphere eventually results in its expansion and enhancement of vertical transport in the
 2333 middle and upper atmosphere. For water, this runaway loop is slowed by UV hydrolysis
 2334 of water in the middle and upper atmosphere and stopped by exhaustion of the sur-
 2335 face reservoir, a process that Ingersoll (1969) argued had occurred on Venus (rather than
 2336 Earth or Mars) as a result of the former’s higher insulation.

2337 This escape regime has been simulated by Kasting and Pollack (1983); Kumar et
 2338 al. (1983); Chassefière (1996a, 1996b). None of these simulations challenge the basic mech-
 2339 anism but emphasize: (1) that hydrolysis rates will be dependent on the oxidation state
 2340 of the atmosphere and buffering by chemical reactions in the crust and (2) that the EUV
 2341 flux of the Sun (a major unknown early in its lifetime) is the principal control on the rate
 2342 of escape. Another interesting conclusion is that the present D/H ratio in Venus’ atmo-
 2343 sphere must be a consequence of a period of reduced escape rates that closed the run-
 2344 away greenhouse phase. In the ideal runaway greenhouse escape regime for Venus, D would
 2345 have been stripped off as easily as H (Kasting & Pollack, 1983). The question of when
 2346 that runaway escape happened is difficult as it was suggested that Venus could have been
 2347 able to sustain liquid water up to a \approx Gyr ago (Way et al., 2016).

2348 *4.2.2.5 Titan* The large size of the atmospheric reservoir of methane in compar-
 2349 ison with the surface reservoir of methane and methane’s photochemical products (Lorenz
 2350 et al., 2008) strongly suggests that a methane-rich atmosphere for Titan has been a rel-
 2351 atively unusual condition during Titan’s history (Lorenz et al., 1997). Once a sufficient
 2352 amount of time has passed, photochemistry will refine methane to organic compounds
 2353 that will form surface deposits of liquid and solid higher order hydrocarbons. The re-
 2354 sulting atmosphere will lose the portion of its greenhouse effect driven by pressure broad-
 2355 ening of methane, and Titan will lose its stratosphere (Wong et al., 2015). Any hydro-
 2356 gen escape presumably will be restricted to photochemical loss of water derived from mi-
 2357 crometeorite ablation, etc.

2358 Yet the presence of CH₄ in Titan’s atmosphere likewise implies occasional, episodic
 2359 release of methane into the atmosphere by volcanism (Tobie et al., 2009). Depending on
 2360 the exact nature of this volcanism, Titan could have experienced a more intense hydro-
 2361 gen escape regime in the past.

2362 5 Escape at Exoplanets

2363 Since their first detections around stars in the mid-late 1990s (Mayor & Queloz,
 2364 1995), a particular interest has been set to the atmospheric escape of exoplanets. In par-
 2365 ticular, the intense heating and radiation at close-in orbit planets, such as the planets
 2366 orbiting M-dwarfs in the Habitable Zone (HZ), or the giants close to their host stars (the
 2367 so-called “hot-Jupiters” that we name close-in giant in the following since the nature of,

notably, their atmospheric escape cannot be considered as Jupiter-like), may lead to very high atmospheric mass-loss rate and potentially a complete evaporation of the planetary atmosphere (in addition to potential atmospheric stripping by the stellar wind) (e.g. Lammer, Selsis, et al. (2003); Cohen et al. (2015)).

5.1 Current observations and modeling

5.1.1 Close-in giants

Observations of the close-in giant planet HD 209458 have revealed absorption in the Lyman α line, which associated with the existence of neutral Hydrogen (H I) at or above the estimated Rosch lobe (Vidal-Madjar et al., 2003, 2004). The fractional difference of in- and out-of-transit flux was wavelength dependent, with much of the flux decrease occurring at wavelengths more than 100 km s^{-1} from line center. Though the atom-photon cross section is much larger at line center, and one would expect much larger transit depths there, interstellar absorption and geocoronal emission contaminate wavelengths $< 50 \text{ km s}^{-1}$ from line center, and only measurements further from line center may be trusted. Later observations have indicated the existence of heavier atoms, such as Ca II and O I at this altitude (Ehrenreich et al., 2008; Linsky et al., 2010). These observations suggest that the planet has an inflated atmosphere with a high mass-loss rate of the order of 10^7 kg s^{-1} , and an escape velocity of the order of 100 km s^{-1} .

The current paradigm assumes that close-in giants lose mass from their atmospheres due to hydrodynamic escape (Ben-Jaffel, 2007, 2008; Vidal-Madjar et al., 2008; Linsky et al., 2010). However, it is not obvious what is the mass-loss rate and the escape speed, what is the altitude of the observations, and what is the overall structure of the inflated atmosphere. It has also been suggested that due to the fast orbital motion, the extended atmosphere may have a comet-like tail (Linsky et al., 2010; Cohen et al., 2011).

A number of models have been developed to study atmospheric escape from close-in giants (Baraffe et al., 2004; Yelle, 2004; García Muñoz, 2007; Lecavelier Des Etangs, 2007; Schneiter et al., 2007; Penz et al., 2008; Murray-Clay et al., 2009; Tian, 2009; Stone & Proga, 2009; Adams, 2011; Trammell et al., 2011; Koskinen et al., 2014), where most of the models assumed that the intense hydrodynamic escape is due to photo-evaporation by the intense stellar radiation. The models listed above (partial list) vary in the equations they solve, their assumptions about the energy sources and distributions, their complexity, and the way they are solved. The mass-loss rate obtained by these models covers few orders of magnitude. Therefore, despite of the vast modeling effort, the nature of atmospheric escape from these close-in giants is not fully understood yet. The efforts by (Tanaka et al., 2014, 2015) to model atmospheric escape from close-in giants have to be noticed since the model is based on MHD wave heating leading to ionospheric outflow. This is a case of the more general ionospheric outflow described in section 2.4.

In the case of HD 209458b, this implies the existence of a large “corona” or “cloud” of atomic hydrogen. This cloud must be optically thick to Lyman- α at wavelengths $> 100 \text{ km s}^{-1}$ from line center out to several (optical continuum) planetary radii, approaching the planet’s Hill radius, beyond which stellar tides dominate over the planet’s gravity. There are two models to account for this large hydrogen density at such high altitudes.

The first model (Yelle, 2004) is that the absorption is due to thermal particles in the planet’s upper atmosphere. Photoelectric heating from hydrogen ionization, balanced by slow adiabatic expansion, raises the temperature to $T \sim 10^4 \text{ K}$. The resulting large scale height implies a slow outward decrease of the density and hence large density at high altitude. In this model, the thermal speed of the atoms is $v_{\text{th}} \sim 10 \text{ km s}^{-1}$ and absorption at $> 100 \text{ km s}^{-1}$ implies a large column of hydrogen is needed to overcome the small cross section at > 10 Doppler widths from line center.

2418 The second model (Holmström et al., 2008) relies on fast hydrogen atoms (ENA),
 2419 which must move at speeds comparable to the line width. The large atomic speeds im-
 2420 ply that vastly smaller columns are needed to attain optical depth unity. The thermal
 2421 hydrogen speeds, and bulk velocity in hydrodynamic escape, are expected to be only \sim
 2422 10 km s^{-1} . The production of fast hydrogen atoms is through charge exchange with $v_{\text{th}} \simeq$
 2423 $v_{\text{bulk}} \sim 100 \text{ km s}^{-1}$ stellar wind protons. There are variants of this model in which atoms
 2424 are ballistically fired outward from the planet and interact with the stellar wind (Holmström
 2425 et al., 2008) and also models in which the mean free paths of the atoms are small, and
 2426 the interaction occurs in a hydrodynamic mixing layer (Tremblin & Chiang, 2013).

2427 These models are in a sense not independent, but rather focus on two separate as-
 2428 pects of the same problem, since both thermal and non-thermal hydrogen may contribute
 2429 to the absorption. In particular, the density of hydrogen atoms which may interact with
 2430 the stellar wind (model 2) is set by the outer limit of the upper atmosphere (model 1).
 2431 It has to be noted that, even if the models are complementary, the conclusion drawn from
 2432 a peculiar aspect are not totally the same: the ENA model is consistent with a much smaller
 2433 escape than the thermal escape model.

2434 **5.1.2 Rocky planets**

2435 In the case of atmospheric escape from terrestrial/rocky planets, some modeling
 2436 work has been done (Tian, 2009; Wordsworth & Pierrehumbert, 2013; Kislyakova, John-
 2437 stone, et al., 2014; Cohen et al., 2015; Gao et al., 2015; Dong et al., 2017), but no reli-
 2438 able observations have been obtained so far, mainly due to the large size of the telescopes
 2439 needed for the measurements (Gronoff, Maggiolo, et al., 2014), except in the case of ex-
 2440 tremely close-in rocky planets such as the disintegrating planet KIC 12557548b (Rappaport
 2441 et al., 2012).

2442 Major efforts went to model the planets in the HZ of Proxima Centauri B and Trap-
 2443 pist 1. The work of Garcia-Sage et al. (2017) shows that a Earth-like planet at the lo-
 2444 cation of these planets would suffer an enhanced ion escape, leading to the loss of the
 2445 equivalent of the Earth’s oceans over a billion years; the location of many of the plan-
 2446 ets inside the Alfvén surface (section 5.2) further prevents the existence of a sustainable
 2447 atmosphere. It means that, to sustain habitability in the sense of liquid water existing
 2448 at the surface, such planets would require a large amount of volatiles in their initial in-
 2449 ventory, and that they should not lose them in the active young years of their host star.
 2450 To that extent, work has been done to look at the hydrodynamic escape of planets in
 2451 the habitable zone of their active stars showing that even N_2 would be hydrodynamic
 2452 (Johnstone et al., 2019). This theoretical work has been confirmed by the recent work
 2453 of Kreidberg et al. (2019) that was able to show, using NASA/Spitzer observations, that
 2454 the exoplanet LHS 3844b has no thick atmosphere: such an atmosphere would have been
 2455 able to reduce the temperature difference between the nightside and the dayside of the
 2456 planet compared to the observations. The conclusion of that problem is that, while their
 2457 are the easiest target for detecting habitable exo-atmospheres with instruments such as
 2458 the James Webb Space Telescope (JWST), planets in the HZ of red-dwarfs may not be
 2459 able to sustain them and therefore would be the worst target.

2460 **5.2 The Stellar Wind and the Alfvén Surface**

2461 The classical HZ of stars fainter than the Sun resides closer to the star. In partic-
 2462 ular, the HZ of M-dwarf stars is located at planetary orbits of less than 0.1 AU . While
 2463 the size of M-dwarf stars is about $0.1\text{--}0.3 R_{\odot}$, their magnetic fields seemed to be over-
 2464 all stronger than the field of K, and G stars (Reiners & Basri, 2007). As a result, their
 2465 Alfvén surface, at which the stellar wind exceeds the Alfvén speed and open the cor-
 2466 onal field lines into the interplanetary space, is more extended than that of the Sun.

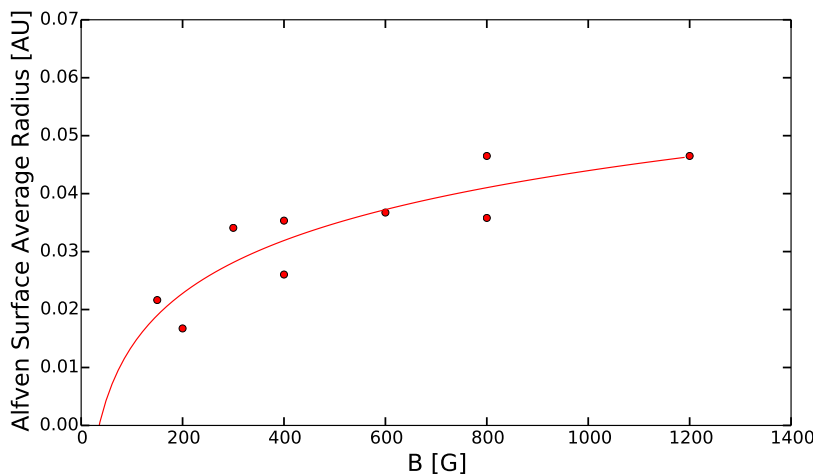


Figure 11. Dots represent the average Alfvén Surface size as a function of average magnetic field strength from MHD simulations. The line represents the trend derived from them.

2467

2468

2469

2470

2471

2472

2473

2474

2475

2476

2477

2478

2479

2480

2481

2482

2483

2484

2485

2486

2487

2488

Since the Alfvén surface can be a measure to the boundary between the stellar corona and the interplanetary space (filled with the fully developed stellar wind), planets residing within the Alfvén surface could be considered to be inside the corona. In addition to the extreme temperatures that can exceed a million degrees, planets in this regime will orbit in densities and magnetic fields that can reach 2-4 orders of magnitude higher than those at Earth (Garraffo et al., 2016b) and, as a result, experience extreme dynamic and magnetic pressures at the planetary orbit. Such space environment conditions (Garraffo et al., 2017) may lead to an Alfvén wings (Io-like) topology of the planetary magnetosphere, at which a significant fraction of the planetary field is open to the stellar wind. As a result, the planetary atmosphere may be exposed to intense heating due to the incoming stellar wind energy in the form direct particle precipitation, and Alfvén wave energy that is transmitted by the stellar wind. Additionally, since the planets reside in the sub-Alfvénic corona, some of the Alfvén wave heating that is deposited in the corona may be transferred to the planet. While essentially no work has been done on these processes in exoplanets, the scenario described above may suggest that it is unlikely that these planets are habitable. **Therefore, the Alfvén surface might serve as an inner limit at which the HZ can be placed for a given stellar system.** The result of the simulations of the distance of the Alfvén surface from its parent star as a function of the average magnetic field of that star is given in Figure 11. The spread in distance for a given magnetic field strength arises from possible differences in the geometric distribution of the magnetic field on the stellar surface. The Alfvén surface is smaller for complex field structures (i.e. higher order in the multipolar expansion) (Garraffo et al., 2016a).

2489

2490

6 Developments Needed in Measurements and Modeling of Atmospheric Escape

2491

2492

2493

2494

2495

2496

2497

In the context of astrobiology, developments are needed in modeling, observations, and laboratory measurements for being able to observe and characterize rocky exoplanets' atmospheres and for reconstructing the history of the atmospheres of the planets in the Solar system. We review here some of the planned and suggested improvements. For a more comprehensive list of suggestion, white papers submitted to the National Academy of Science (2019) have a comprehensive list. The JWST, being the astrophysics flagship of the 2020s, is shaping the direction of astrobiology research and therefore many currently pro-

2498 posed studies and developments are linked to its targets of choice, the exoplanets around
2499 M-dwarfs.

2500 6.1 Measurements/Observations

2501 The detection of a technosignature, currently searched in radio-waves, would be the
2502 ultimate proof of a life that developed outside Earth (J. T. Wright, 2019). The devel-
2503 opment of observatories for such endeavor is outside the scope of this study since a mere
2504 detection would not provide data on how life developed there, under which conditions,
2505 and how it started. To answer these questions, better measurements are needed to un-
2506 derstand the Sun and other Stars, laboratory measurements and sophisticated measure-
2507 ments are needed for better interpreting our planetary observations, and better instru-
2508 ments are needed for looking at exoplanets.

2509 Space missions such as CHEOPS (Broeg et al., 2014) and Transiting Exoplanet Sur-
2510 vey Satellite (TESS) (Ricker et al., 2015) are expected to find thousands of transiting
2511 planets with many terrestrial-like planets including hundreds of super-Earths over the
2512 next few years (Fridlund et al., 2016). With the ability to discover transiting exoplan-
2513 ets, efforts are being pursued for spectroscopic observations of exoplanetary atmospheres.
2514 The National Academy of Sciences (NAS) “Exoplanet Science Strategy” report mandated
2515 by the US Congress recommends a direct-imaging telescope as a follow-on to the Wide
2516 Field InfraRed Survey Telescope (WFIRST) mission scheduled to fly in the mid-2020’s
2517 after the launch of the James Webb Space Telescope (JWST). Large amounts of time
2518 are being dedicated on the Hubble and Spitzer space telescopes, as well as major ground-
2519 based telescopes (e.g. VLT, Keck, Gemini, Magellan, CFHT, etc.) (Madhusudhan et al.,
2520 2016). JWST and European-Extremely Large Telescope (E-ELT) will revolutionize ex-
2521 oplanetary spectroscopy. M dwarfs are prime targets for the detection and characteri-
2522 zation of terrestrial exoplanets by the JWST, as they are abundant in the solar neigh-
2523 borhood and their small radii allow for greater transit signals from Earth-sized exoplan-
2524 ets (e.g., (Quintana et al., 2014)). Future spectra with JWST would be of unprecedented
2525 precision and resolution which will enable us to derive precise chemical abundances for
2526 transiting exoplanets. Our modeling can help constrain future observations in making
2527 precise determinations of detectable key species abundances, distributions and under-
2528 standing of their processes. The NAS report also recommends that the US National Sci-
2529 ence Foundation (NSF) invest more in the future Giant Magellan telescope (GMT) and
2530 proposed Thirty Metre Telescope (TMT) now being built in Hawaii and Chile, respec-
2531 tively. These telescopes would provide more focused study of exoplanets by using spec-
2532 troscopy to seek out signs of free oxygen in their atmospheres. Such a study would be
2533 perfect suited for the goals of the astrobiology community.

2534 For F and G stars, much of the observing is likely to initially be in the IR so the
2535 lower bound to some of the observations are likely to be near the tropopause (outside
2536 of H₂O bands). For Venus-like exoplanets, this does not present a problem, but for Earth-
2537 like exoplanets it may be for F type stars. However, for all K and M type stars, processes
2538 of interest governing distribution of key species in atmospheres for these types of detec-
2539 tions may be directly observed in the mesosphere and thermosphere. Additionally, there
2540 are spectral regions in the UV (and possibly in the visible to IR) where O₂ and O₃ in
2541 the mesosphere/upper stratosphere would dominate remote measurements. Those spec-
2542 tral regions would be an ideal target for future observations.

2543 6.1.1 Solar and Stellar measurements

2544 The capabilities of the JWST mean that the search for biosignature with that ob-
2545 servatory is mainly limited to M dwarfs. The increased risk of atmospheric escape due
2546 to joule heating in the classical HZ around these stars (Garraffo et al., 2016b) means that
2547 it is extremely important to study the activity of these stars. The best way to perform

2548 this is with UV instruments such as STIS on the HST (France et al., 2013). The HST
 2549 being on its end of life, with no repair mission planned, a mission dedicated to the EUV-
 2550 XUV measurements on close stars (such measurements would be less affected by inter-
 2551 stellar H absorption) would be critical to support the modeling and observations of plan-
 2552 etary atmospheres that could harbor life.

2553 The recent observation of a CME around another star (Argiroffi et al., 2019) shows
 2554 the possibilities of such measurements. However, they should be improved to have a bet-
 2555 ter idea of the fluxes of particles at other stars and to validate the semi-empirical laws
 2556 linking flares and CME (Moschou et al., 2019). See also Section 3.4.1.

2557 **6.1.2 For planets**

2558 As already emphasized, the knowledge of accurate cross sections is of critical im-
 2559 portance for the precise evaluation of escape processes. For charge transfer, including
 2560 double charge exchange, electron capture and stripping, it has been customary to study
 2561 these processes in the laboratory in two main directions: (i) under the wide umbrella of
 2562 nuclear research, radiation dosimetry, and the effect of radiation on living tissues (Nikjoo
 2563 et al., 2012), especially in water and carbon, and (ii) in astrophysics and heliophysics stud-
 2564 ies, especially rather recently with respect to X-ray production (Wargelin et al., 2008;
 2565 Dennerl, 2010). In (i), one of the goals is to calculate the stopping power of particles in
 2566 matter using so-called track-structure Monte Carlo models. In (ii), the applications are
 2567 numerous, from interstellar medium to cometary X-ray emissions. This has resulted in
 2568 a rather well-understood behaviour of charge-transfer cross sections at energies typically
 2569 above 10 keV/amu impactor energy and peaking in the MeV range (Uehara & Nikjoo,
 2570 2002). At low energies, from a few tens of eV/amu to 10 keV/amu, which are the typ-
 2571 ical energies for solar wind charge exchange and in planetary ionospheres, the informa-
 2572 tion is usually fragmented and one is often forced to extrapolate, more or less arbitrar-
 2573 ily, the shape of the cross sections, leading to high uncertainties (Simon Wedlund, Be-
 2574 har, Kallio, et al., 2019).

2575 Over the two last decades, experimental physicists have punctually studied aspects
 2576 of solar wind charge exchange. Several international groups have specialised on differ-
 2577 ent aspects (Dennerl, 2010), for example the UV spectroscopy group at the University
 2578 of Groningen (Netherlands) for cometary environments (Juhász, 2004; Bodewits et al.,
 2579 2004; Bodewits, 2007), motivating studies of impacts of fast solar-wind like ions with sev-
 2580 eral neutral species of planetary atmosphere relevance. The examples of H₂O, CH₄, CO
 2581 and CO₂ are particularly relevant: (Greenwood et al., 2000, 2004) and (Bodewits et al.,
 2582 2006) have recently measured with good accuracy charge-transfer cross sections of pro-
 2583 tons and helium ions on H₂O, CH₄, CO and CO₂ for astrophysics applications. How-
 2584 ever, these cross sections were not measured in the very low-energy range (below 50 eV
 2585 for helium ions, below 1.5 keV for protons). Moreover, certain electron capture and strip-
 2586 ping reaction cross sections have yet to be altogether measured by any group. For ex-
 2587 ample, the stripping reaction involving hydrogen or helium fast atoms and H₂O ((H,He)
 2588 + H₂O → (H⁺,He⁺) + H₂O + e⁻) has never been measured below 20 keV/amu energy;
 2589 it may prove an important sink for the produced ENAs, and hence may play a role in
 2590 the escape of such particles into space.

2591 A few online databases exist for several charge transfer cross-sections. Despite on-
 2592 going work made to create online database and recommended sets of cross sections (e.g.
 2593 Lindsay and Stebbings (2005)), it is left for a supplementary critical review of charge-
 2594 transfer cross sections in planetary and cometary atmospheres to list all of the available
 2595 cross sections, their energy range, evaluate their uncertainties and the gaps in our present
 2596 knowledge and provide a final recommendation that can be used in models and data anal-
 2597 ysis. Such a specific review is outside the scope of the present article, and we will here

2598 only point out one direction that experimental physics teams are encouraged to further
2599 study, that is, the solar wind charge transfer with a neutral atmosphere.

2600 Further studies will have to choose colliding species, such as:

- 2601 • Neutrals of interest (non-exhaustive list by increasing atomic/molecular weight):
2602 H, H₂, He, C, N, O, CH₄, OH, H₂O, Ne, N₂, CO, O₂, S, Ar, CO₂.
- 2603 • Impactor of interest: H, H⁺, He, He⁺, He²⁺, and high ion states of O and Fe.

2604 and to consider the two following points:

- 2605 • Study more systematically all sources and sinks for the ion-ENA system: single
2606 and multiple electron capture, single and multiple electron stripping, impact ion-
2607 isation by fast atoms and ions.
- 2608 • Measure new energy-dependent cross sections, and uniformly extend current cross
2609 section measurements to energies ranging from threshold to 20 keV/amu energy,
2610 most relevant for solar wind studies.

2611 Other developments are needed for planets, such as Cassini-like missions to the Ice
2612 Giants, for a better understanding of the development of these atmosphere and their satel-
2613 lite. Such missions would give more insight into the evolution of our Solar system. Im-
2614 proved instrumentation could be of use around the Earth to better discriminate the es-
2615 caping species: it is currently extremely difficult to know if it is an O or a N that is leav-
2616 ing the atmosphere.

2617 From that point of view, both for planets and exoplanets, it is interesting to look
2618 at the X-Ray emission of the planets: the X-ray halo, created by charge exchange be-
2619 tween the exosphere and the incoming solar wind, gives some insight to the composition
2620 of escaping species (Krasnopolsky et al., 1997; Dennerl, 2007; Dennerl, 2010). This is of
2621 interest both for planets and exoplanets since detecting such an halo in another stellar
2622 system would give some direct insight in the composition of the exoplanetary exosphere.

2623 **6.1.3 For exoplanets**

2624 Atmospheric escape from exoplanets can be constrained by observations of com-
2625 ponents that affect the escape. This includes compositional observations (i.e., transmis-
2626 sion spectra), direct observations of escaping material. These observations will pose chal-
2627 lenges in the upcoming decades.

2628 It is also necessary to observe magnetic fields of exoplanets as they may play a key
2629 role in the atmospheric escape. One promising option is to obtain information about ex-
2630 oplanets magnetic fields via observed signature star-planet interaction. These signatures
2631 include induced chromospheric activity(e.g. Shkolnik et al. (2008); Cauley et al. (2019)),
2632 or modulation of coronal radio emissions (Cohen, Moschou, et al., 2018). The direct de-
2633 tection of exoplanets magnetic fields (via radio observations of auroral emissions Zarka
2634 (2007)) has recently been reported (Vedantham et al., 2020). This has only confirmed
2635 the existence of the magnetosphere: more work is needed to be able to estimate (e.g.)
2636 the magnetic moment from these observations. The modeling of the interaction of the
2637 stellar wind with the planetary magnetosphere of HD 209458b led to the estimation of
2638 its magnetic moment (Kislyakova, Holmström, et al., 2014) from the observation of Ly-
2639 α . Giant space UV-telescopes would be choice instruments to study the upper atmosphere
2640 of rocky exoplanets. Gronoff, Maggiolo, et al. (2014) proposed a technique to detect hy-
2641 drodynamic escape of CO₂ or O₂ rich planets using such laboratories. For the detection
2642 of biosignatures, a review of techniques and developments needed can be found in Fujii
2643 et al. (2018). The generalization of the detection technique used by Kreidberg et al. (2019)

2644 to detect the absence of an atmosphere around LHS 3844b is also needed to look at the
2645 best target for future telescopes.

2646 **6.2 Modeling**

2647 To get a comprehensive view of the escape of planetary atmospheres, models have
2648 to be developed to take into account all the energetic inputs and all the processes lead-
2649 ing to the escape. The outputs of such models have to be compared with observations.
2650 Problems lies with inputs parameters for the model (cross sections, observation of e.g.
2651 solar flux), the estimation of the uncertainties, but also with the neglected parameters.
2652 It is often the case that our instrumentation gives a very detailed view of the conditions
2653 on a planet; however, the uncertainties in the input parameters of the models make it
2654 challenging to interpret (Sánchez-Cano et al., 2018). The estimation of model uncertain-
2655 ties from the different input parameters can be an arduous task (Gronoff, Simon Wed-
2656 lund, Mertens, & Lillis, 2012; Gronoff, Simon Wedlund, Mertens, Barthélemy, et al., 2012)
2657 and becomes problematic once free parameters are needed, which is often the case in our
2658 models of atmospheres, stellar wind, stellar wind interactions, etc. It is possible to be-
2659 gin solving the problem by careful comparison with solar system observations, then with
2660 extrapolation. On the other hand, the instrumentation may not be sensitive enough to
2661 observe interesting phenomenon in exoplanetary atmospheres, or to provide significant
2662 model constrains.

2663 Future modeling should also include the dynamical response of the planet’s atmo-
2664 sphere to dynamic drivers, stellar evolution scale changes of atmospheric escape, as well
2665 as self-consistent coupling between the external drivers and the different regions of the
2666 atmosphere.

2667 **6.2.1 Modeling of Solar and Stellar Environments**

2668 Global models for the solar corona have been developed since the late 1960s by solv-
2669 ing the MHD equations. The models are driven by data of the photospheric radial mag-
2670 netic field in combination with the potential field method (Altschuler & Newkirk, 1969).
2671 In recent years, more self-consistent models have been developed for the solar corona and
2672 solar wind (e.g. Lionello et al. (2014); van der Holst et al. (2014); Downs et al. (2016)).
2673 These models incorporate coronal heating and wind acceleration in the form of large-
2674 scale heating and momentum terms. These large-scale terms are parameterized and tuned
2675 to match solar observations, and the models have been successful in reproducing the ob-
2676 served density and temperature structure of the solar corona, and the observed struc-
2677 ture of the solar wind.

2678 The limited availability of observations of photospheric magnetic field of selected
2679 stars using the Zeeman-Doppler Imaging technique (Semel, 1980) has led to a growing
2680 global modeling in stellar coronae and stellar winds of Sun-like stars (e.g. Cohen et al.
2681 (2010); Vidotto et al. (2011); Garraffo et al. (2016b)). However, since the stellar winds
2682 of solar analogs cannot be directly measured, the results of these studies are poorly con-
2683 straints. Therefore, A better modeling work is needed to constrain the magnitude of the
2684 stellar wind, and the coronal structure and temperature for different stars as these pa-
2685 rameters define the stellar environments at which exoplanets reside in. In particular, the
2686 scaling of the global heating and acceleration parameters needs further investigation and
2687 quantification to better understand how these processes scaled with stellar type.

2688 **6.2.2 Modeling Atmospheric Escape from Exoplanets**

2689 The current modeling tools for planetary atmospheric escape are built on and tune
2690 to known, measurable atmospheres within the Solar system. These tools have already
2691 been used to study escape from exoplanetary atmospheres with no significant constraints

of the results. A number of features, which are different from Solar system bodies, has already been identified to be crucial for exoplanetary atmospheric escape, especially in the case of close-orbit planets. However, these features need more self-consistent modeling in order to be better defined and quantified.

The first notable feature is that atmospheric escape from close-orbit planets may be extremely high, to the point that atmosphere could be completely lost. This is due to extremely high dynamic pressure of the stellar wind near these planets (e.g. Garraffo et al. (2016b); Garcia-Sage et al. (2017); Dong et al. (2017)), the strong orbital variations of the stellar wind conditions, and potential strong heating of the upper atmosphere (e.g. Cohen et al. (2014); Cohen, Glocer, et al. (2018)). A more detailed model is required to quantify the exact energy deposition between the wind and the planetary atmosphere, as current models focus on the stellar wind - magnetosphere interaction, without detailed modeling of the energy and mass transfer to and from the atmosphere itself.

The second notable feature is the impact on the planetary upper atmosphere and ionosphere. Current models provided estimation about the Joule Heating assuming specific, constant atmospheric conductance. Since the conductance is the key to determine the heating, further self-consistent modeling is needed to estimate the ionospheric conductance. In particular, these calculations are needed for the case where the EUV and X-ray stellar radiation are much higher than the Earth case, and for different atmospheric composition.

Finally, close-orbit exoplanets may reside within the Alfvénic point inside the stellar corona. Therefore, a direct star-planet interaction is expected to occur. In order to investigate the impact of such a direct interaction between the stellar corona and the planet, a self-consistent modeling that couples the corona and the planetary atmosphere domains is needed.

An example of a code in development to address some of these problems could be IAPIC, a particles-in-cell electromagnetic 3D global code, used (Baraka & Ben-Jaffel, 2010; Ben-Jaffel & Ballester, 2013, 2014; Baraka, 2016) to produce the magnetosphere (XZ plane) of an earth-like planet. Both plasma density and field lines are shown in Figure 12. It is interesting to see that the PIC simulations naturally recover the field aligned currents (streams of particles appearing between cusps and current sheet in the figure) that drive particles precipitation from the magnetosphere into the polar regions, producing auroral emissions. IAPIC can provide both the angular and energy distributions of the impinging magnetospheric particles into the ionosphere. Charge separation is obtained in the code so that kinetic effects could be obtained while conserving charge (Villasenor & Buneman, 1992). These electrons and ions enter the upper atmosphere to trigger ion-chemistry, heating, and winds. Their fluxes should be used as input in existing ionospheric models to evaluate new species produced and atmospheric inflation due to the extra heating deposit in the auroral region of any exoplanet. The simulation, shown in Figure 12, was carried out with these code parameters for a grid size of $0.1R_E$ and an ion-electron mass ratio of $\frac{m_i}{m_e} = 100$.

2733 ***6.2.3 Modeling Exoplanetary Magnetic Field Observations***

2734 Following the previous sections, it seems like exoplanetary Magnetic fields may play
2735 a crucial role in the evolution and sustainability of exoplanets atmospheres. However,
2736 these planetary field currently cannot be detected and observed.

2737 Modeling of star-planet interaction suggest that this interaction can potentially gen-
2738 erate observable signatures that can help to quantify the planetary magnetic field (e.g.
2739 the broadening of Ly- α in Kislyakova, Johnstone, et al. (2014) and the soft X-ray emis-
2740 sion in Kislyakova et al. (2015)). However, it is clear that a deep understanding of the
2741 stellar background field is need for this purpose (Shkolnik et al., 2008; Cohen et al., 2011;

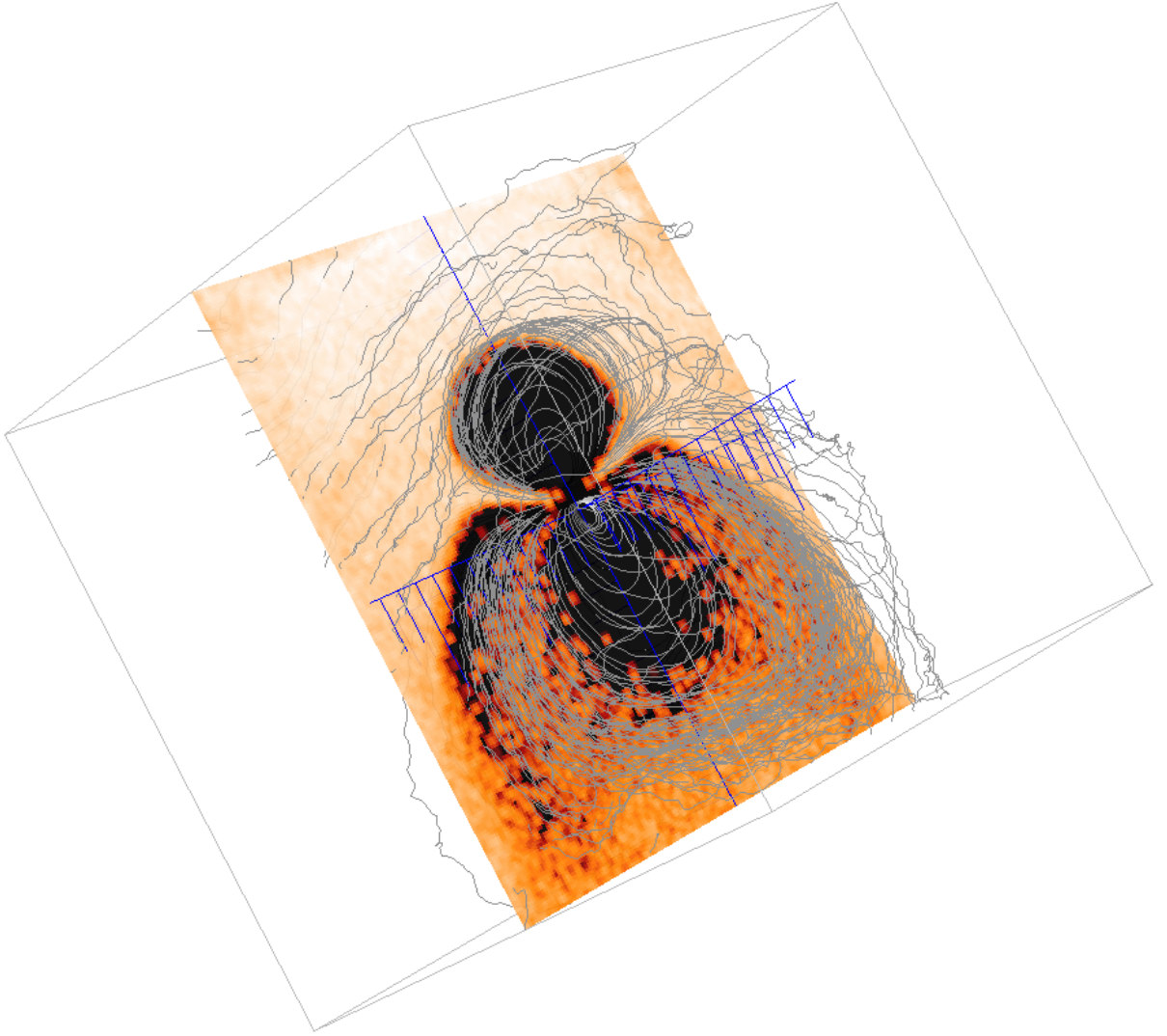


Figure 12. Field aligned current and prototype kinetic simulation of exoplanet. These simulations are leading to a better understanding of the dynamic within an exoplanetary magnetosphere, which is needed for computing both energetic inputs in the atmosphere and loss of plasma from the magnetosphere.

2742 Strugarek et al., 2014; Matsakos et al., 2015). In that context, more detailed modeling
 2743 work on the background stellar environment can support the interpretation of star-planet
 2744 interaction observations.

2745 A number of attempts were made to estimate auroral radio emissions from exoplanets
 2746 (Zarka, 2007; Lazio & Farrell, 2007; Grießmeier et al., 2007; Vidotto et al., 2015; See
 2747 et al., 2015; Nichols & Milan, 2016; Burkhart & Loeb, 2017; Turnpenney et al., 2018; Lynch
 2748 et al., 2018). Most of these studies have concluded that such auroral emissions are not
 2749 detectable with the current radio telescopes. An alternative approach has been recently
 2750 proposed by (Cohen, Moschou, et al., 2018), who proposed to look for planetary mod-
 2751 ulations of the ambient coronal radio emission (exoplanet radio transit), instead of look-
 2752 ing for the planet as a radio source. Using idealized models for the planetary and stel-
 2753 lar fields, (Cohen, Moschou, et al., 2018) have shown that observing the ambient coro-
 2754 nal radio intensity, as well as the planetary modulation are more feasible. To better quan-
 2755 tify and estimate the latter method, further, more detailed modeling work is needed, tar-
 2756 geting specific planetary systems.

2757 **7 Discussion and conclusion**

2758 The problem of atmosphere escape is more complex than just the estimation of Jeans’
 2759 escape or energy-limited escape. Several outstanding questions in planetary science can
 2760 be linked to atmosphere escape, from the problem of the faint young Sun to the ques-
 2761 tion of detection of astrobiological signatures. These problems are leading to a roadmap
 2762 of future investigations.

2763 **7.1 Problems still to be resolved**

2764 **7.1.1 *The faint young sun paradox***

2765 The Faint Young Sun paradox was introduced by (Sagan & Mullen, 1972). The para-
 2766 dox states that based on stellar evolution models, during its earlier stages, the Sun’s lu-
 2767 minosity was about 30% lower than its current luminosity. As a result, the surface equi-
 2768 librium temperature of the Earth would be below the freezing point of water. However,
 2769 many types of geological evidence for the existence of liquid water were found both at
 2770 Earth and Mars. Therefore, we need to introduce some heating process which increased
 2771 the average surface temperature of the Earth above zero degrees Celsius.

2772 The most prominent solution to the paradox is the existence of greenhouse gases
 2773 in the atmosphere, which lock the infrared radiation and lead to a global warming of the
 2774 Earth’s surface (see e.g. Kasting (1993)). An enormous amount of work has been done
 2775 on this topic in what came to be the science field of “Global Climate Change” (Feulner,
 2776 2012). It has been suggested tropical cirrus clouds could also enhance the greenhouse
 2777 effect, being either the main explanation to the FYS paradox or an complementary source
 2778 to a greenhouse gas (Rondanelli & Lindzen, 2010). Goldblatt and Zahnle (2011) further
 2779 develop the more general discussion on the effect of clouds on the climate, noting that
 2780 Rondanelli and Lindzen (2010) base the cirrus solution to the FYS on the “iris theory”
 2781 which stipulates that the cirrus coverage should increase if the surface temperatures de-
 2782 crease, which is quite controversial for the current Earth (see e.g. the comparison of the
 2783 theory with observations by Chambers et al. (2002)), but may be applicable on other at-
 2784 mospheres. Urata and Toon (2013) applied the theory to the Early Mars, but the work
 2785 of Ramirez and Kasting (2017) show that there is no room for error when considering
 2786 cirrus clouds for warming: a large cirrus cloud coverage, greater than 70%, should be present.
 2787 This explanation is therefore unlikely to be applicable to Mars since such a cloud cov-
 2788 erage is not realistic: cirrus cloud formation is limited by the parts of the atmosphere
 2789 that are under-saturated in water. Overall, cloud warming has not been proven to be
 2790 the solution to the FYS paradox, but it shows the importance of addressing the prob-

2791 lem of cloud formation and humidity transport, and therefore shows the importance of
 2792 looking at the climate using 3D GCMs. On the other hand, solutions to the FYS para-
 2793 dox that involve external factors, i.e. particle precipitations or a heavier Sun, are attrac-
 2794 tive since they could solve the problem both at Mars and the Earth. Some theories sug-
 2795 gested that cosmic-rays may affect the cloud condensation in the Earth’s atmosphere,
 2796 with an overall cooling effect when there is fewer GCR (i.e. when the solar activity is
 2797 higher) (Svensmark & Friis-Christensen, 1997; Shaviv, 2005). Thus, a significant reduc-
 2798 tion in the cosmic-ray flux may increase the surface temperature of the Earth. These mod-
 2799 els are controversial both in the cosmic-rays ability to affect the cloud condensation (Kirkby
 2800 et al., 2011) and the heating efficiency of the process. The results of the CLOUD exper-
 2801 iment at CERN tend to indicate that the present day cloud formation cannot be effec-
 2802 tively affected by GCR flux (Dunne et al., 2016; Pierce, 2017): the aerosols responsible
 2803 for cloud condensation come mainly from the ground, and setting the GCR flux at 0 would
 2804 only reduce the cloud coverage by $\approx 10\%$. It is to be noted that this experiment does in-
 2805 dicate that GCR can affect aerosol/particle formation (Kirkby et al., 2016; Tröstl et al.,
 2806 2016), which is something that is also observed on other atmospheres such as Titan (Dobrijevic
 2807 et al., 2016; Loison et al., 2015). The contentious point is whether or not GCR varia-
 2808 tion has an influence on the current climate or not. Studies such as Lanci et al. (2020)
 2809 do not find historical evidence of GCR control of climate while Svensmark et al. (2017)
 2810 advocates for a strong control of the climate by GCR in the past, with increased GCR
 2811 leading to aerosols that act as cloud condensation nuclei (CCN), that lead to the forma-
 2812 tion of clouds, and ultimately heating. It has to be noted that aerosols do not always
 2813 act as CCN, but can act as coolant (e.g. Trainer et al. (2006)). The work of Airapetian
 2814 et al. (2016) suggests, on the contrary, that the increased particle flux from the Solar En-
 2815 ergetic Particle events, more frequent for the Young Sun, led to the creation of green-
 2816 house gases, that could help resolve the paradox. This interaction between ionizing ra-
 2817 diation and climate is fundamentally different since it requires extreme radiation rates
 2818 (compared to present values) to get a significant increase in greenhouse gases. In addi-
 2819 tion, it does not suppose that CCN is the limiting factor in the creation of clouds: the
 2820 atmosphere can be under-saturated (Ramirez & Kasting, 2017).

2821 In the context of Astrophysics, a solution for the paradox can be found if one can
 2822 show that the solar mass was about 10% larger than its current mass. This requires the
 2823 young Sun’s mass loss rate to be very high, with the ability to keep this high mass loss
 2824 rate for rather long time. As mentioned in Section 4.1, it is unlikely that the mass loss
 2825 to the ambient solar wind can be sufficient. However, it is possible that due to high ac-
 2826 tivity levels at early stellar stages, the Sun lost large amount of its mass via CMEs, al-
 2827 though present estimates also indicate this mechanism is insufficient (Drake et al., 2013).

2828 ***7.1.2 Impact of planetary magnetic field***

2829 Whether a planet is magnetized or not impacts ionospheric ion outflow processes
 2830 and the return rate of ions outflowing from the ionosphere. It was believed that a plan-
 2831 etary magnetic field was shielding its atmosphere from escape, until observations, reported
 2832 by Barabash (2010), was showing that the escape rate at Earth is higher than the one
 2833 at Venus and Mars. This was further discussed by R. Strangeway et al. (2010), and ex-
 2834 plored more in Brain et al. (2013). This later work also discussed the influence of the
 2835 magnetic field on incoming gases that could also have an effect on climate. Tarduno et
 2836 al. (2014) and Ehlmann et al. (2016) looked at the effect of magnetospheric escape re-
 2837 spectively for the Early Earth and exoplanets.

2838 Gunell et al. (2018) compiled the effect of the planetary magnetic moment on iono-
 2839 spheric ions outflow rate in the current solar system, and compared it to other sources
 2840 of escape. Considering that the observed ionospheric ion outflow rate on Earth, Mars
 2841 and Venus is of the same order of magnitude (10^{25} s^{-1}) while only Earth has a strong
 2842 magnetic field, the authors made empirical models of ion outflow for three hypotheti-

2843 cal planets with atmospheric conditions similar to the Earth, Mars and Venus but with
 2844 a variable magnetic moment. They show that for each of those planets the mass escape
 2845 rate, including both oxygen and hydrogen is similar in the unmagnetized range and for
 2846 high magnetizations. In-between, they identify two maxima where outflow is enhanced
 2847 by a factor of 2-5, one corresponding to polar cap escape and dominant for hydrogen and
 2848 another corresponding to cusp escape. The presence of a large magnetosphere around
 2849 a planet actually diverts part of the stellar wind energy and protects the atmosphere from
 2850 sputtering and ion pickup. The induced magnetospheres of the unmagnetized planets
 2851 also provide protection from sputtering and ion pickup but to a lesser extent. However,
 2852 magnetospheres are much bigger objects than the planets themselves. The presence of
 2853 a magnetosphere increases the size of the interaction region between the stellar wind and
 2854 the planet and thus the amount of energy which can potentially be transferred into the
 2855 ionosphere. For instance the cross section of the Earth magnetosphere with the solar wind
 2856 is about 100 times higher than the cross section of the Earth itself with the solar wind.
 2857 Consequently, the amount of energy transferred from the stellar wind to the ionosphere
 2858 of magnetized planet is not necessarily lower than for unmagnetized planets (Brain et
 2859 al., 2013).

2860 Large-scale magnetospheres enable polar cap and cusp escape, which increases the
 2861 escape rate. Two outflow processes are enhanced by the presence of a magnetosphere.
 2862 The first is the polar wind which corresponds to a thermal ion outflow on the open mag-
 2863 netic field lines at high latitudes, above the polar caps. It maximizes for moderate mag-
 2864 netic moments when the size of the polar cap is maximum. The second corresponds to
 2865 outflow from the cusp region where a significant amount of the stellar wind energy is de-
 2866 posited. This energy deposition increases with the size of the magnetosphere (i.e. with
 2867 its cross section with the stellar wind) but is limited by the amount of ions available at
 2868 the ionospheric level.

2869 The effect of magnetospheres on the ion return rate is discussed in Section 2.5. In
 2870 that case the protective effect of the magnetosphere is not related to the outflow itself
 2871 but to the trapping of outflowing ionospheric ions, even those with high energies well above
 2872 the gravitational binding energy, which was thought to result in a significant return rate
 2873 into the atmosphere. However, recent observations in the Earth magnetosphere question
 2874 the validity of this protective effect. Indeed, that the measured flux of precipitating ions
 2875 in the ionosphere is well below the measured flux of outflowing ionospheric ions and the
 2876 escape route above the polar ionosphere, where polar cap and cusp outflows occur, seems
 2877 to preferentially lead to a direct ion loss to interplanetary space rather than to a return
 2878 in the atmosphere.

2879 On the other hand, the thermospheres of Mars and Venus are called cryospheres
 2880 because of the cooling effect of CO₂: their thermospheric temperature is extremely low,
 2881 effectively shielding the atmospheres from several escape processes: the Earth's atmo-
 2882 sphere without a magnetic field is believed to be escaping more efficiently. In addition,
 2883 the main species in the ionosphere of Venus is O₂⁺, while it is O⁺ at Earth (Mendillo,
 2884 2019), and this may affect the amount of ions able to escape via non-thermal processes
 2885 (Mars is a special case since above ≈200 km O⁺ is in majority while it is O₂⁺ below). A
 2886 recent study by Wei et al. (2014) shows that using an escape model developed for Mars,
 2887 but with Earth's upper atmosphere, increases greatly the O escape. This study also sug-
 2888 gests that there are some correlations between lower content of O₂ at Earth and mag-
 2889 netic field inversions. Such a study could be criticized on the basis that the magnetic field
 2890 does not seem to disappear during inversions (e.g. Nowaczyk et al. (2012)), or on the
 2891 basis that the fluxes of O₂ at Earth are dominated by the biosphere and the oxidation
 2892 of the crust. The fluxes of oxygen in Wei et al. (2014) are indeed of the same order of
 2893 magnitude as the current oxygen losses in the crust (D. Catling, 2014). A reduction of
 2894 carbon burial – which is a life-controlled process leading to net O₂ fluxes – could explain
 2895 the loss of oxygen without the need for a fast process. It is also in disagreement with the

2896 observation of higher ion escape near magnetic anomalies at Mars (Sakai et al., 2018; Inui
2897 et al., 2019).

2898 To summarize, while the presence of a magnetosphere has a clear impact on iono-
2899 spheric outflow, recent developments in the study of the coupling between stellar wind,
2900 magnetospheres and ionospheres challenge the idea of a protective effect of magnetospheres
2901 on atmospheric erosion. It could simply be that the question is poorly asked and that
2902 a better question is “what kind of atmospheres require a magnetic field to be sustain-
2903 able in a given set of solar/stellar activity conditions”. In any case, recent studies such
2904 as Brain et al. (2013); Gunell et al. (2018); Airapetian et al. (2017); Garcia-Sage et al.
2905 (2017), as well as the case of Mercury, show that an intrinsic magnetic field does not
2906 totally protect an atmosphere. A contrario, the case of Venus shows that a magnetic field
2907 absence does not prevent sustaining a dense atmosphere.

2908 *7.1.3 Impacts of stellar dynamics*

2909 In a large fraction of the studies of escape through time, the stellar parameters, i.e.
2910 the EUV-XUV fluxes and the stellar wind, are considered as slowly varying with the epoch.
2911 The impact of the frequency of intermittent stellar events such as flares, CMEs, and SEPs
2912 on the escape is seldom taken into account. This is a major problem for studies of close-
2913 in exoplanets since these events can extremely affect the atmosphere as the observations
2914 of the variations of escape rate at Mars due to a CME has shown (Jakosky et al., 2015).
2915 MAVEN is currently showing that extreme solar events have a very important role in
2916 the loss of atmosphere at Mars (Jakosky et al., 2018; Mayyasi et al., 2018). As an ex-
2917 ample, the increase in the exospheric temperature due to a flare has been observed (Elrod
2918 et al., 2018), along with change in the upper atmospheric ion and neutral composition
2919 (Thiemann et al., 2018), and an increase of $\approx 20\%$ of the escape (C. Lee et al., 2018).

2920 The work of Garcia-Sage et al. (2017) has shown that the EUV-XUV flux can lead
2921 to extreme absorption at rocky exoplanets around M dwarfs, however, it does not an-
2922 swer the question of how much active a G-star an Earth-like planet could survive.

2923 **7.2 The role of non-atmospheric/stellar processes**

2924 While it is not generally explicit in the discussion above, the mass of the planet that
2925 is experiencing escape is a critical factor. Closely related is its radius, and therefore its
2926 density. The planets of the Solar system are there to show that the mass is the first fac-
2927 tor to consider when estimating if a body will have an atmosphere or not; the energy re-
2928 ceived/distance to the Sun being the second factor. Mass is still challenging to retrieve,
2929 especially the mass of small planets, whose signal in radial velocities can be hidden by
2930 the natural variations of the star. Once mass and distances are considered, it may be
2931 possible that interesting effects come from close-in exoplanets, such as the roche-limit
2932 of the star reaching for the planet’s atmosphere. **Overall it should not be forgot-**
2933 **ten that the inventory of volatiles, which has be estimated from the density**
2934 **of the exoplanet, will define the lifetime of an habitable world with large es-**
2935 **cape rates.**

2936 **7.3 The future of research on escape processes**

2937 The study of planetary atmosphere habitability and evolution has, as shown here,
2938 three main directions.

- 2939 1. Escape modeling efforts. The approach of this review has been reductionist; we
2940 have sought to isolate the individual escape processes and identify simple ad hoc
2941 models that can determine whether or not a specific escape process is important.
2942 Yet a better approach to escape would be to create so-called “grand-ensemble mod-

2943 els” that are able to examine the interactions between the different processes with-
 2944 out a priori exclusion of processes. An already invoked example comes from Chassefière
 2945 (1997), in which comprehensive treatment of multiple types of charge exchange
 2946 predicted an increased exospheric temperature and therefore, indirectly, higher ther-
 2947 mal escape. Improved models will allow the evaluation of critical parameters to
 2948 help people work on the deeper parts of the atmosphere to estimate which species
 2949 are escaping and at which rate, in order to prevent poor estimates based on energy-
 2950 limited escape (that do not take diffusion limitation into account). An additional
 2951 consideration in modeling is to devise a standard procedure for asynchronously
 2952 coupling climate, chemistry, and escape models at exoplanets to study the evolu-
 2953 tion of climate and composition in tandem with stellar evolution.

- 2954 2. Laboratory work. A major limiting factor of escape models is the quality of the
 2955 input parameters, such as chemical reaction rates, cross sections, etc. Laboratory
 2956 experiments and model-laboratory data comparisons such as that of Simon Wed-
 2957 lund et al. (2011) are needed to refine the accuracy of the physico-chemistry pa-
 2958 rameters, and, in turn, may help identify the needs of the community for the study
 2959 of specific processes. Laboratory data are also crucial to retrieve parameters from
 2960 observational data.
- 2961 3. Observation work. Observations efforts are limited and currently concentrated to
 2962 what is believed to be the “best known targets” for habitability. Unfortunately,
 2963 our instrumentation is not optimized for detecting habitability signatures on these
 2964 targets. Future observations should be designed not just to characterize the bulk
 2965 properties of the atmosphere but also to consider known or potential observables
 2966 affecting atmospheric stability. One advantage of doing so is that processes like
 2967 thermal escape mostly take place above cloud and haze layers and so may not be
 2968 as challenging as observing lower in the atmosphere. These targets have broader
 2969 characteristics than current one, and could benefit from the whole range of exist-
 2970 ing instrumentation to answer questions leading to constrain the conditions re-
 2971 quired for habitability. Techniques should be improved to better understand the
 2972 stellar environment of exoplanets, such as the observation of the stellar winds po-
 2973 tentially impacting exoplanets as well as stellar variability in general, which has
 2974 a strong potential impact on transit observations of planetary atmospheres (Wakeford
 2975 et al., 2018). As characterizing the variability of a host star typically requires less
 2976 sensitive instrumentation than detecting a telluric planet orbiting it (particularly
 2977 for warmer stars), it may be worth prioritizing observations of variability of types
 2978 other than those around which telluric planets currently can be observed.

2979 Overall, the challenge is thus to couple a grand-ensemble escape model with a com-
 2980 plex planetary atmosphere model, itself coupled with a planetary interior model. From
 2981 there it would be possible to obtain the whole story of an empirical planetary atmosphere
 2982 in time. The uncertainties in each of these sub-models have to be correctly evaluated,
 2983 so that it is possible to address the overall model validity. This is why a validation strat-
 2984 egy is also of utmost importance for this kind of work.

2985 On the stellar part, the challenge will be to determine the activity history of a star,
 2986 both from the slowly evolving parameters, such as luminosity, and the discrete events
 2987 such as flares. From there, it would be possible to evaluate how a given star stresses an
 2988 atmosphere over time. Finally, it will be necessary to develop observation missions ded-
 2989 icated to study the UV flux of stars to validate the model of activity in time.

2990 **7.4 Effects of escape on biosignatures**

2991 The escape processes reviewed above have significant influence on the composition
 2992 of the upper atmosphere, and acting over geologic time can affect the bulk composition
 2993 of the atmosphere, surface and interior. The consequences of atmospheric escape for our
 2994 search for life via chemical biosignatures in the atmosphere and on the surface must there-

fore be considered (Des Marais et al., 2002; Domagal-Goldman et al., 2014; Airapetian et al., 2016). The alteration of planetary chemistry by escape can result in both false positive and false negative biosignature errors if it is not accounted for (Gao et al., 2015).

False positive biosignatures that can be produced by interactions at the top of the atmosphere include oxygen and oxidized species such as NO as well as organics such as the haze materials produced through UV photolysis at Titan and elsewhere. The preferential loss of hydrogen from water is one way for oxygen to arise from escape-related abiogenic processes. The processing of sufficient water to influence the bulk oxidation state of the surface materials is likely the cause of high oxidation in the Martian surface (Lammer, Lichtenegger, et al., 2003). False negative biosignatures would result from the masking of true biogenic molecules by escape processes, either through rapid modification by particle or photon radiation or through chemical interaction with, for example, photolysis-produced oxygen.

Biosignatures related to disequilibrium chemistry (Krissansen-Totton et al., 2018) must contend with non-LTE behavior in the upper atmosphere and the potential for disequilibrium signatures to be transferred from the upper to the lower atmosphere. Even biosignatures that are based on time variations (Olson et al., 2018) need to contend with seasonal variations in star-planet interaction caused by a tilted magnetic field axis which could produce either false positive or false negative results.

This discussion is not intended to be exhaustive or definitive, but instead we seek to highlight the importance of understanding the impact of the stellar environment on the production, destruction, or masking of putative chemical biosignatures. In general, although space weather processes involve small fractions of the planetary mass they can, like biological reactions, be quite selective in their reactants and products and over time can yield significant signals that must be differentiated from biological ones.

7.5 Final thoughts

We have reviewed the different escape processes considered so far in the literature, and summarized in Figure 13. Understanding these processes, and also ones that are still to be discovered, makes it possible to understand how a planetary atmosphere evolves. This is however not enough to understand the whole history of an atmosphere: change in the atmosphere composition, change in the stellar activity, and change of the outgassing from the planetary interior are examples of processes that affect the development of an atmosphere, and can lead to very different pathways. To that extent, life is one of the major modifiers of Earth’s atmosphere. It would be easy to consider an atmosphere that is out of equilibrium, or that is very difficult to model/undertand by our current means, as harboring life; this is the idea behind the concept of biosignatures. However, the detection of a Titan-like atmosphere outside our Solar system may lead to life detection claims that are not (at least to date) consistent with Titan’s observations. On the other hand, the atmosphere of an Early Earth may be detected, but considered as sterile.

Since this paper has been showing that habitability is a dynamic process, and that the habitability of a planet is the result of its history, and not just of its location with respect to its star, it is important to extend that notion to biosignatures. In this respect, it would be preferable to announce the detection of molecules relevant to pre-biotic chemistry instead of directly announce biosignatures, so that no extraordinary claim is made without extraordinary evidence.

Acronyms

CME Coronal Mass Ejection

DSMC Direct Simulation Monte Carlo

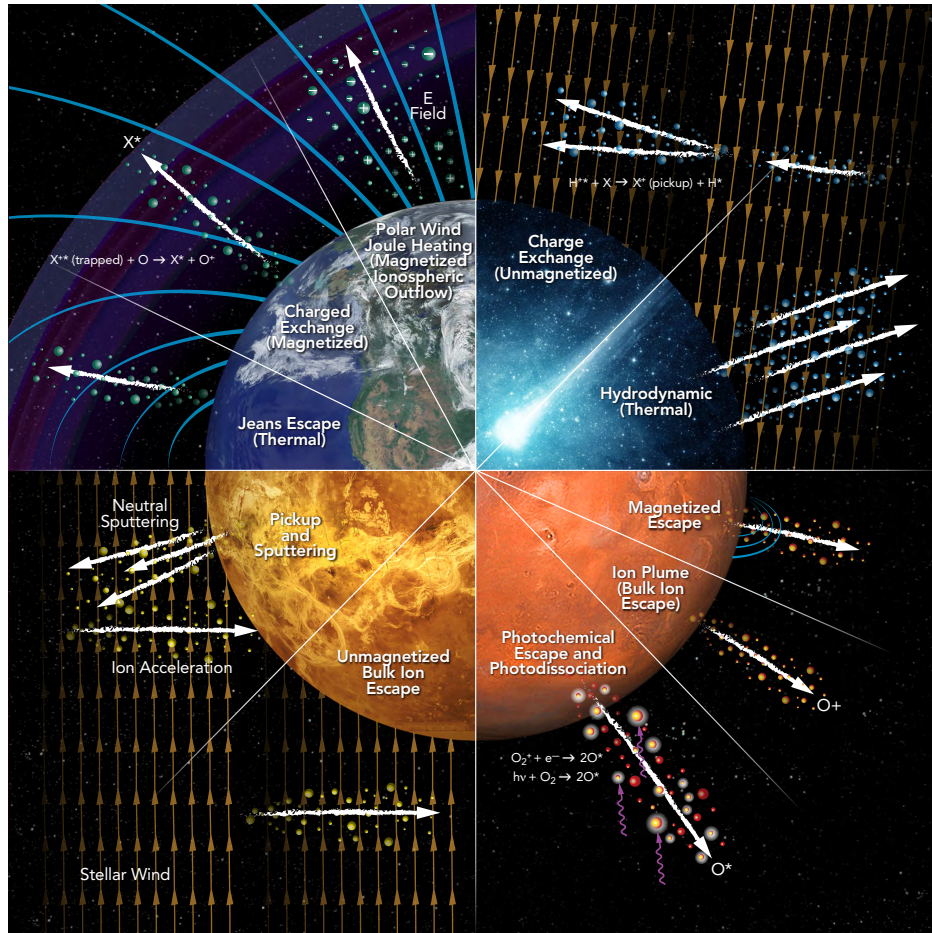


Figure 13. Overview of the escape processes, along with an example of a planet where they are major/important. The Earth’s main escape processes are Jeans’, charge-exchange, and polar wind. At Venus, interaction with the solar wind; at Mars, photochemical escape and ion escape; at some exoplanets/comets hydrodynamic escape.

3043 **ENA** Energetic Neutral Atom
 3044 **ESA** European Space Agency
 3045 **EUV** Extreme Ultraviolet
 3046 **FAC** Field Aligned Currents
 3047 **FYS** Faint Young Sun (typically for speaking about the Faint Young Sun paradox)
 3048 **GCM** Global Circulation Model
 3049 **HZ** Habitable Zone
 3050 **KHI** Kelvin-Helmholtz instability
 3051 **MAVEN** NASA / Mars Atmosphere and Volatile and Evolution mission
 3052 **MEX** ESA / Mars Express
 3053 **MHD** Magneto-Hydro Dynamic
 3054 **NASA** National Aeronautics and Space Administration
 3055 **SEP** Solar Energetic Particle
 3056 **UV** Ultraviolet
 3057 **VEX** ESA / Venus Express
 3058 **XUV** X-Ultraviolet

3059 **Notation**

3060 **k** the Boltzman constant
 3061 **m** the average molecular mass
 3062 **g** the gravitational acceleration (typically dependent upon the altitude)
 3063 **z** the altitude
 3064 **\vec{x}** the location in space
 3065 **Θ, Φ** angles in spherical coordinates
 3066 **T** the temperature (of neutral constituents, the subscript can show if it is of electrons
 3067 or ions, and it is generally dependent upon the altitude)
 3068 **T_{exo}** the exospheric temperature
 3069 **n** the density of the considered species or of the gas (typically dependent upon the al-
 3070 titude). n_a is usually used to note the total density. A typical unit is species.cm^{-3} .
 3071 **$X_i = \frac{n_i}{n_a}$** mole fraction of the gas i .
 3072 **$H = \frac{kT}{mg}$** The scale height.
 3073 **H_{exo}** is the scale height at the exosphere, so when $T = T_{exo}$
 3074 **R** radius of the planet. Sometimes the radius of the exosphere $R_{exo} = R + z_{exo}$
 3075 **λ** photon wavelength
 3076 **$l = \frac{1}{\sqrt{2n\sigma}}$** the characteristic length between collisions.
 3077 **$v_{esc} = \sqrt{2GM/R}$** the escape speed.
 3078 **$K_n = l/H$** the Knudsen number: characteristic parameter for the transition between
 3079 collisionless and fluid regimes. If $K_n \rightarrow 0$, the collisions are dominant, we are in
 3080 a fluid regime. If $K_n > 1$, we are in a collisionless regime.
 3081 **$\lambda_{ex} = R_{exo}/H_{exo}$** is the characteristic number for the thermal escape. In other work,
 3082 such as Selsis (2006), this parameter is designed by χ .
 3083 **$\gamma = \frac{C_p}{C_v}$** heat capacity ratio, or adiabatic index. directly linked to the degree of free-
 3084 dom f of the molecule/atom by the equation $\gamma = 1 + \frac{2}{f}$.

3085 **Acknowledgments**

3086 The Living Breathing Planet team is funded by the NASA Nexus for Exoplanet System
 3087 Science under grant NNX15AE05G. Work at the Royal Belgian Institute for Space Aeron-
 3088 omy was supported by PRODEX/Cluster contract 13127/98/NL/VJ(IC)-PEA90316. The

work of C.S.W. has been partially funded by the Austrian Science Fund under project number P 32035-N36. We thank Mary Pat Hrybyk-Keith at NASA/GSFC for her graphics work on the summary figures. We would like to thank N. Wright (Keele University) for his assistance in providing additional figures. The authors would like to thank the Institut d’Astrophysique de Paris (IAP), France and Ben Jaffel for the IAPIC continuous development.

References

- Adams, F. C. (2011, March). Magnetically Controlled Outflows from Hot Jupiters. *Astrophys. J.*, *730*, 27. doi: 10.1088/0004-637X/730/1/27
- Airapetian, V. S., Barnes, R., Cohen, O., Collinson, G. A., Danchi, W. C., Dong, C. F., . . . Yamashiki, Y. (2019, july). Impact of space weather on climate and habitability of terrestrial-type exoplanets. *International Journal of Astrobiology*, 1–59. doi: 10.1017/S1473550419000132
- Airapetian, V. S., Glocer, A., Gronoff, G., Hébrard, E., & Danchi, W. (2016, June). Prebiotic chemistry and atmospheric warming of early Earth by an active young Sun. *Nature Geoscience*, *9*, 452-455. doi: 10.1038/ngeo2719
- Airapetian, V. S., Glocer, A., Khazanov, G. V., Loyd, R. O. P., France, K., Sojka, J., . . . Liemohn, M. W. (2017). How hospitable are space weather affected habitable zones? the role of ion escape. *The Astrophysical Journal Letters*, *836*(1), L3.
- Akbari, H., Andersson, L., Peterson, W. K., Espley, J., Benna, M., & Ergun, R. (2019). Ambipolar electric field in the martian ionosphere: MAVEN measurements. *Journal of Geophysical Research: Space Physics*. Retrieved from <https://agupubs.onlinelibrary.wiley.com/doi/abs/10.1029/2018JA026325> doi: 10.1029/2018JA026325
- Aleinov, I., Way, M. J., Harman, C., Tsigaridis, K., Wolf, E. T., & Gronoff, G. (2019). Modeling a transient secondary paleolunar atmosphere: 3-D simulations and analysis. *Geophysical Research Letters*. Retrieved from <https://agupubs.onlinelibrary.wiley.com/doi/abs/10.1029/2019GL082494> doi: 10.1029/2019GL082494
- Alho, M., McKenna-Lawlor, S., & Kallio, E. (2015). Paleo Mars energetic particle precipitation. *Planetary and Space Science*, *119*, 103–110.
- Altschuler, M. D., & Newkirk, G. (1969, September). Magnetic Fields and the Structure of the Solar Corona. I: Methods of Calculating Coronal Fields. *Sol. Phys.*, *9*, 131-149. doi: 10.1007/BF00145734
- Amblard, P., Moussaoui, S., Dudok de Wit, T., Abouadarham, J., Kretzschmar, M., Liliensten, J., & Auchère, F. (2008, August). The EUV Sun as the superposition of elementary Suns. *Astronomy and Astrophysics*, *487*, L13-L16. doi: 10.1051/0004-6361:200809588
- Anglada-Escudé, G., Amado, P. J., Barnes, J., Berdiñas, Z. M., Butler, R. P., Coleman, G. A. L., . . . Zechmeister, M. (2016, August). A terrestrial planet candidate in a temperate orbit around Proxima Centauri. *Nature*, *536*, 437-440. doi: 10.1038/nature19106
- Argiroffi, C., Reale, F., Drake, J., Ciaravella, A., Testa, P., Bonito, R., . . . Peres, G. (2019). A stellar flare- coronal mass ejection event revealed by X-ray plasma motions. *Nature Astronomy*, *1*.
- Arney, G., Domagal-Goldman, S. D., Meadows, V. S., Wolf, E. T., Schwieterman, E., Charnay, B., . . . Trainer, M. G. (2016). The Pale Orange Dot: The Spectrum and Habitability of Hazy Archean Earth. *Astrobiology*, *16*(11), 873-899. Retrieved from <https://doi.org/10.1089/ast.2015.1422> (PMID: 27792417) doi: 10.1089/ast.2015.1422
- Arney, G., & Kane, S. (2018, April). Venus as an Analog for Hot Earths. *ArXiv e-prints*.

- 3142 Atreya, S. K., Adams, E. Y., Niemann, H. B., Demick-Montelara, J. E., Owen,
3143 T. C., Fulchignoni, M., . . . Wilson, E. H. (2006, October). Titan's methane
3144 cycle. *Plan. Space Sci.*, *54*, 1177-1187. doi: 10.1016/j.pss.2006.05.028
- 3145 Atreya, S. K., Donahue, T. M., & Festou, M. (1981, July). Jupiter - Structure and
3146 composition of the upper atmosphere. *Astrophys. J. Let.*, *247*, L43-L47. doi:
3147 10.1086/183586
- 3148 Avice, G., Marty, B., Burgess, R., Hofmann, A., Philippot, P., Zahnle, K., & Za-
3149 kharov, D. (2018, July). Evolution of atmospheric xenon and other noble gases
3150 inferred from Archean to Paleoproterozoic rocks. *Geochim. Cosmochim. Acta*,
3151 *232*, 82-100. doi: 10.1016/j.gca.2018.04.018
- 3152 Axford, W. I. (1968). The polar wind and the terrestrial helium budget. *Journal of*
3153 *Geophysical Research*, *73*, 68,55.
- 3154 Baliukin, I. I., Bertaux, J.-L., Quémerais, E., Izmodenov, V. V., & Schmidt, W.
3155 (2019). SWAN/SOHO Lyman- α mapping: The hydrogen geocorona extends
3156 well beyond the Moon. *Journal of Geophysical Research: Space Physics*.
3157 Retrieved from [https://agupubs.onlinelibrary.wiley.com/doi/abs/](https://agupubs.onlinelibrary.wiley.com/doi/abs/10.1029/2018JA026136)
3158 [10.1029/2018JA026136](https://doi.org/10.1029/2018JA026136) doi: 10.1029/2018JA026136
- 3159 Banks, P. M., & Holzer, T. E. (1968). The Polar Wind. *Journal of Geophysical Re-*
3160 *search*, *73*, 6846-6854. doi: 10.1029/JA073i021p06846
- 3161 Barabash, S. (2010). Venus, earth, mars: comparative ion escape rates. In *Egu gen-*
3162 *eral assembly conference abstracts* (Vol. 12, p. 5308).
- 3163 Baraffe, I., Selsis, F., Chabrier, G., Barman, T. S., Allard, F., Hauschildt, P. H.,
3164 & Lammer, H. (2004, May). The effect of evaporation on the evolution of
3165 close-in giant planets. *Astronomy and Astrophysics*, *419*, L13-L16. doi:
3166 10.1051/0004-6361:20040129
- 3167 Baraka, S. (2016). Large Scale Earth's Bow Shock with Northern IMF as Simu-
3168 lated by PIC Code in Parallel with MHD Model. *Journal of Astrophysics and*
3169 *Astronomy*, *37*(2), 1-16. doi: 10.1007/s12036-016-9389-6
- 3170 Baraka, S., & Ben-Jaffel, L. (2010). Impact of solar wind depression on the dayside
3171 magnetosphere under northward interplanetary magnetic field. *arXiv preprint*
3172 *arXiv:1012.5722*. Retrieved from <http://arxiv.org/abs/1012.5722>
- 3173 Barakat, A. R., & Schunk, R. W. (1982). Comparison of transport equations
3174 based on Maxwellian and bi-Maxwellian distributions for anisotropic plas-
3175 mas. *Journal of Physics D: Applied Physics*, *15*(7), 1195. Retrieved from
3176 <http://stacks.iop.org/0022-3727/15/i=7/a=014>
- 3177 Barakat, A. R., & Schunk, R. W. (2006). A three-dimensional model of the gener-
3178 alized polar wind. *Journal of Geophysical Research: Space Physics*, *111*(A12),
3179 n/a-n/a. Retrieved from <http://dx.doi.org/10.1029/2006JA011662>
3180 (A12314) doi: 10.1029/2006JA011662
- 3181 Barghouthi, I. A. (1997, September). Effects of wave-particle interactions on H^+
3182 and O^+ outflow at high latitude: A comparative study. *Journal of Geophysical*
3183 *Research*, *102*, 22065-22076. doi: 10.1029/96JA03293
- 3184 Barley, M. E., Bekker, A., & Krapež, B. (2005, September). Late Archean to Early
3185 Paleoproterozoic global tectonics, environmental change and the rise of atmo-
3186 spheric oxygen [rapid communication]. *Earth and Planetary Science Letters*,
3187 *238*, 156-171. doi: 10.1016/j.epsl.2005.06.062
- 3188 Basu, B., Decker, D. T., & Jasperse, J. R. (2001, January). Proton trans-
3189 port model: A review. *Journal of Geophysics Research*, *106*, 93-106. doi:
3190 10.1029/2000JA002004
- 3191 Bell, J. F., Crisp, D., Lucey, P. G., Ozoroski, T. A., Sinton, W. M., Willis, S. C.,
3192 & Campbell, B. A. (1991). Spectroscopic observations of bright and dark
3193 emission features on the night side of Venus. *Science*, *252*(5010), 1293-1296.
3194 Retrieved from <http://science.sciencemag.org/content/252/5010/1293>
3195 doi: 10.1126/science.252.5010.1293
- 3196 Bell, J. M., Bougher, S. W., Waite, J. H., Ridley, A. J., Magee, B. A., Mandt,

- 3197 K. E., ... Fletcher, G. (2011). Simulating the one-dimensional structure of titan's upper atmosphere: 3. mechanisms determining methane escape. *Journal of Geophysical Research: Planets*, *116*(E11), n/a–n/a. Retrieved from <http://dx.doi.org/10.1029/2010JE003639> (E11002) doi: 10.1029/2010JE003639
- 3198
- 3199
- 3200
- 3201
- 3202 Bell, J. M., Hunter Waite, J., Westlake, J. H., Bougher, S. W., Ridley, A. J., Perryman, R., & Mandt, K. (2014). Developing a self-consistent description of titan's upper atmosphere without hydrodynamic escape. *Journal of Geophysical Research: Space Physics*, *119*(6), 4957–4972. Retrieved from <http://dx.doi.org/10.1002/2014JA019781> doi: 10.1002/2014JA019781
- 3203
- 3204
- 3205
- 3206
- 3207 Ben-Jaffel, L. (2007, December). Exoplanet HD 209458b: Inflated Hydrogen Atmosphere but No Sign of Evaporation. *Astrophys. J. Let.*, *671*, L61–L64. doi: 10.1086/524706
- 3208
- 3209
- 3210 Ben-Jaffel, L. (2008, December). Spectral, Spatial, and Time Properties of the Hydrogen Nebula around Exoplanet HD 209458b. *Astrophys. J.*, *688*, 1352–1360. doi: 10.1086/592101
- 3211
- 3212
- 3213 Ben-Jaffel, L., & Ballester, G. (2013). Hubble Space Telescope detection of oxygen in the atmosphere of exoplanet HD 189733b. *Astronomy & Astrophysics*, *553*, A52.
- 3214
- 3215
- 3216 Ben-Jaffel, L., & Ballester, G. E. (2014). Transit of exomoon plasma tori: new diagnosis. *The Astrophysical Journal Letters*, *785*(2), L30.
- 3217
- 3218 BenMoussa, A., Gissot, S., Schühle, U., Del Zanna, G., Auchère, F., Mekaoui, S., ... Woods, T. N. (2013, November). On-Orbit Degradation of Solar Instruments. *Solar Physics*, *288*, 389–434. doi: 10.1007/s11207-013-0290-z
- 3219
- 3220
- 3221 Bernard, D., Lilensten, J., Barthélemy, M., & Gronoff, G. (2014). Can hydrogen coronae be inferred around a CO₂-dominated exoplanetary atmosphere? *Icarus*, *239*, 23–31.
- 3222
- 3223
- 3224 Bertaux, J.-L., Leblanc, F., Witasse, O., Quemerais, E., Lilensten, J., Stern, S. A., ... Korablev, O. (2005, Jun). Discovery of an aurora on Mars. *Nature*, *435*(7043), 790–794. doi: 10.1038/nature03603
- 3225
- 3226
- 3227 Bisikalo, D. V., Shematovich, V. I., Gérard, J.-C., Gladstone, G. R., & Waite, J. H. (1996, September). The distribution of hot hydrogen atoms produced by electron and proton precipitation in the Jovian aurora. *Journal of Geophysical Research*, *101*, 21157–21168. doi: 10.1029/96JE01952
- 3228
- 3229
- 3230
- 3231 Blackman, E. G., & Thomas, J. H. (2014). Explaining the observed relation between stellar activity and rotation. *Monthly Notices of the Royal Astronomical Society: Letters*, *446*(1), L51–L55.
- 3232
- 3233
- 3234 Bodewits, D. (2007). *Cometary X-rays. Solar wind charge exchange in cometary atmospheres* (Unpublished doctoral dissertation). University of Groningen, P.O. Box 72, 9700 AB Groningen, The Netherlands.
- 3235
- 3236
- 3237 Bodewits, D., Hoekstra, R., Seredyuk, B., McCullough, R. W., Jones, G. H., & Tielens, A. G. G. M. (2006, May). Charge Exchange Emission from Solar Wind Helium Ions. *The Astrophysical Journal*, *642*, 593–605. doi: 10.1086/500731
- 3238
- 3239
- 3240 Bodewits, D., Kelley, M. S. P., Li, J.-Y., Farnham, T. L., & A'Hearn, M. F. (2015, March). The Pre-perihelion Activity of Dynamically New Comet C/2013 A1 (Siding Spring) and Its Close Encounter with Mars. *Astrophys. J. Let.*, *802*, L6. doi: 10.1088/2041-8205/802/1/L6
- 3241
- 3242
- 3243
- 3244 Bodewits, D., McCullough, R. W., Tielens, A. G. G. M., & Hoekstra, R. (2004, January). X-Ray and Far-Ultraviolet Emission from Comets: Relevant Charge Exchange Processes. *Physica Scripta*, *70*, C17–C20. doi: 10.1088/0031-8949/70/6/N01
- 3245
- 3246
- 3247
- 3248 Bougher, S. W., Waite, J. H., Majeed, T., & Gladstone, G. R. (2005). Jupiter thermospheric general circulation model (JTGCM): Global structure and dynamics driven by auroral and joule heating. *Journal of Geophysical Research: Planets*, *110*(E4). Retrieved from <http://dx.doi.org/10.1029/2003JE002230>
- 3249
- 3250
- 3251

- 3252 (E04008) doi: 10.1029/2003JE002230
- 3253 Bouhram, M., Klecker, B., Miyake, W., Reme, H., Sauvaud, J.-A., Malingre, M., ...
- 3254 Blăgău, A. (2004). On the altitude dependence of transversely heated O⁺
- 3255 distributions in the cusp/cleft. *Annales Geophysicae*, *22*(5), 1787–1798.
- 3256 Bouhram, M., Malingre, M., Jasperse, J. R., & Dubouloz, N. (2003, August). Mod-
- 3257 eling transverse heating and outflow of ionospheric ions from the dayside
- 3258 cusp/cleft. 1 A parametric study. *Annales Geophysicae*, *21*, 1753.
- 3259 Bowman, B. R., Tobiska, W. K., Marcos, F. A., Huang, C. Y., Lin, C. S., & Burke,
- 3260 W. J. (2008). A new empirical thermospheric density model JB2008 using new
- 3261 solar and geomagnetic indices. In *Aiaa 2008-6438*. Honolulu, HI.
- 3262 Brain, D., Bagenal, F., Ma, Y.-J., Nilsson, H., & Stenberg Wieser, G. (2016). At-
- 3263 mospheric escape from unmagnetized bodies. *Journal of Geophysical Research:*
- 3264 *Planets*, *121*(12), 2364–2385.
- 3265 Brain, D. A., Baker, A. H., Briggs, J., Eastwood, J. P., Halekas, J. S., & Phan, T.-
- 3266 D. (2010). Episodic detachment of Martian crustal magnetic fields leading
- 3267 to bulk atmospheric plasma escape. *Geophysical Research Letters*, *37*(14).
- 3268 Retrieved from [https://agupubs.onlinelibrary.wiley.com/doi/abs/](https://agupubs.onlinelibrary.wiley.com/doi/abs/10.1029/2010GL043916)
- 3269 [10.1029/2010GL043916](https://agupubs.onlinelibrary.wiley.com/doi/abs/10.1029/2010GL043916) doi: 10.1029/2010GL043916
- 3270 Brain, D. A., Leblanc, F., Luhmann, J. G., Moore, T. E., & Tian, F. (2013). Plane-
- 3271 tary Magnetic Fields and Climate Evolution. In S. J. Mackwell, A. A. Simon-
- 3272 Miller, J. W. Harder, & M. A. Bullock (Eds.), *Comparative climatology of*
- 3273 *terrestrial planets* (p. 487). doi: 10.2458/azu_uapress_9780816530595-ch20
- 3274 Broadfoot, A., Belton, M., Takacs, P., Sandel, B., Shemansky, D., Holberg, J., ...
- 3275 Mcelroy, M. (1979). Extreme ultraviolet observations from voyager-1 encounter
- 3276 with jupiter. *Science*, *204*(4396), 979-982. doi: 10.1126/science.204.4396.979
- 3277 Broadfoot, A., Sandel, B., Shemansky, D., McConnell, J., Smith, G., Holberg, J., ...
- 3278 Bertaux, J. (1981). Overview of the voyager ultraviolet spectrometry results
- 3279 through jupiter encounter. *J. Geophys. Res.-Sp.Phy.*, *86*(NA10), 8259-8284.
- 3280 doi: 10.1029/JA086iA10p08259
- 3281 Broeg, C., Benz, W., & Thomas, N. C. T. (2014). The cheops mission. *Contrib As-*
- 3282 *tron Obs Skaln Pleso*, *43*, 498.
- 3283 Burch, J. L., Cravens, T. E., Llera, K., Goldstein, R., Mokashi, P., Tzou, C.-Y., &
- 3284 Broiles, T. (2015, July). Charge exchange in cometary coma: Discovery of H⁻
- 3285 ions in the solar wind close to comet 67P/Churyumov-Gerasimenko. *Geophys.*
- 3286 *Res. Lett.*, *42*, 5125-5131. doi: 10.1002/2015GL064504
- 3287 Burgers, J. M. (1969). *Flow Equations for Composite Gases*. New York: Academic
- 3288 Press.
- 3289 Burkhart, B., & Loeb, A. (2017, November). The Detectability of Radio Auroral
- 3290 Emission from Proxima b. *Astrophys. J.*, *849*, L10. doi: 10.3847/2041-8213/
- 3291 aa9112
- 3292 Canfield, D. E., Poulton, S. W., Knoll, A. H., Narbonne, G. M., Ross, G., Gold-
- 3293 berg, T., & Strauss, H. (2008, August). Ferruginous Conditions Domi-
- 3294 nated Later Neoproterozoic Deep-Water Chemistry. *Science*, *321*, 949-. doi:
- 3295 10.1126/science.1154499
- 3296 Canfield, D. E., Poulton, S. W., & Narbonne, G. M. (2007, January). Late-
- 3297 Neoproterozoic Deep-Ocean Oxygenation and the Rise of Animal Life. *Science*,
- 3298 *315*, 92-. doi: 10.1126/science.1135013
- 3299 Cannata, R. W., Killeen, T. L., Gombosi, T. I., Burns, A. G., & Roble, R. G.
- 3300 (1988). Modelling of time-dependent ion outflows at high geomagnetic lati-
- 3301 tudes. *Advances in Space Research*, *8*, 89-92. doi: 10.1016/0273-1177(88)90267
- 3302 -0
- 3303 Catling, D. (2014). *The great oxidation event transition in treatise on geochemistry.*
- 3304 *turekian kk, editor; and holland hd, editor*. Amsterdam: Elsevier.
- 3305 Catling, D. C., & Claire, M. W. (2005). How earth's atmosphere evolved to an oxic
- 3306 state. *Earth Plan. Sci. Lett.*, *237*, 1–20.

- 3307 Cauley, P. W., Shkolnik, E. L., Llama, J., & Lanza, A. F. (2019, Jul). Magnetic
3308 field strengths of hot Jupiters from signals of star-planet interactions. *Nature*
3309 *Astronomy*, 408. doi: 10.1038/s41550-019-0840-x
- 3310 Cessateur, G., Dudok de Wit, T., Kretzschmar, M., Lilensten, J., Hochedez, J., &
3311 Snow, M. (2011, April). Monitoring the solar UV irradiance spectrum from the
3312 observation of a few passbands. *Astronomy and Astrophysics*, 528, A68. doi:
3313 10.1051/0004-6361/201015903
- 3314 Cessateur, G., Lilensten, J., Dudok de Wit, T., BenMoussa, A., & Kretzschmar,
3315 M. (2012). New observation strategies for the solar uv spectral irradiance.
3316 *J. Space Weather Space Clim.*, 2, A16. Retrieved from [http://dx.doi.org/
3317 10.1051/swsc/2012016](http://dx.doi.org/10.1051/swsc/2012016) doi: 10.1051/swsc/2012016
- 3318 Chaffin, M., Deighan, J., Schneider, N., & Stewart, A. (2017). Elevated atmospheric
3319 escape of atomic hydrogen from Mars induced by high-altitude water. *Nature*
3320 *Geoscience*, 10(3), 174.
- 3321 Chaffin, M. S., Chaufray, J.-Y., Stewart, I., Montmessin, F., Schneider, N. M.,
3322 & Bertaux, J.-L. (2014). Unexpected variability of Martian hydrogen
3323 escape. *Geophysical Research Letters*, 41(2), 314–320. Retrieved from
3324 <http://dx.doi.org/10.1002/2013GL058578> doi: 10.1002/2013GL058578
- 3325 Chamberlain, J. W., & Hunten, D. M. (1987). *Theory of planetary atmospheres. An*
3326 *introduction to their physics and chemistry*. Academic Press. Retrieved from
3327 <http://adsabs.harvard.edu/abs/1987tpaa.book.....C>
- 3328 Chamberlain, J. W., & Smith, G. R. (1971, July). Comments on the rate of evap-
3329 oration of a non-Maxwellian atmosphere. *Plan. Sp. Sci.*, 19, 675-684. doi: 10
3330 .1016/0032-0633(71)90025-0
- 3331 Chamberlain, S., Bailey, J., Crisp, D., & Meadows, V. (2013, January). Ground-
3332 based near-infrared observations of water vapour in the Venus troposphere.
3333 *Icarus*, 222, 364-378. doi: 10.1016/j.icarus.2012.11.014
- 3334 Chamberlin, P. C., Woods, T. N., & Eparvier, F. G. (2008, May). Flare Irradi-
3335 ance Spectral Model (FISM): Flare component algorithms and results. *Space*
3336 *Weather*, 6, 5001-+. doi: 10.1029/2007SW000372
- 3337 Chambers, L. H., Lin, B., & Young, D. F. (2002). Examination of new ceres data for
3338 evidence of tropical iris feedback. *Journal of climate*, 15(24), 3719–3726.
- 3339 Chapman, S., Cowling, T. G., & Burnett, D. (1990). *The mathematical theory*
3340 *of non-uniform gases: an account of the kinetic theory of viscosity, thermal*
3341 *conduction and diffusion in gases*. Cambridge university press.
- 3342 Chassefière, E. (1996a). Hydrodynamic escape of hydrogen from a hot water-rich
3343 atmosphere: The case of Venus. *Journal of Geophysical Research: Plan-*
3344 *ets*, 101(E11), 26039–26056. Retrieved from [http://dx.doi.org/10.1029/
3345 96JE01951](http://dx.doi.org/10.1029/96JE01951) doi: 10.1029/96JE01951
- 3346 Chassefière, E. (1996b). Hydrodynamic escape of oxygen from primitive atmo-
3347 spheres: Applications to the cases of Venus and Mars. *Icarus*, 124(2), 537 -
3348 552. Retrieved from [http://www.sciencedirect.com/science/article/pii/
3349 S0019103596902298](http://www.sciencedirect.com/science/article/pii/S0019103596902298) doi: <http://dx.doi.org/10.1006/icar.1996.0229>
- 3350 Chassefière, E. (1997). Loss of water on the young Venus: The effect of a
3351 strong primitive solar wind. *Icarus*, 126(1), 229 - 232. Retrieved from
3352 <http://www.sciencedirect.com/science/article/pii/S0019103597956773>
3353 doi: <http://dx.doi.org/10.1006/icar.1997.5677>
- 3354 Chassefière, E., & Leblanc, F. (2004, September). Mars atmospheric escape and evo-
3355 lution; interaction with the solar wind. *Plan. Sp. Sci.*, 52, 1039-1058. doi: 10
3356 .1016/j.pss.2004.07.002
- 3357 Chaufray, J. Y., Modolo, R., Leblanc, F., Chanteur, G., Johnson, R. E., & Luh-
3358 mann, J. G. (2007, September). Mars solar wind interaction: Formation of
3359 the Martian corona and atmospheric loss to space. *Journal of Geophysical*
3360 *Research (Planets)*, 112, E09009. doi: 10.1029/2007JE002915
- 3361 Cipriani, F., Leblanc, F., & Berthelier, J. J. (2007). Martian corona: Nonther-

- mal sources of hot heavy species. *Journal of Geophysical Research: Planets*, 112(E7). Retrieved 2018-06-15, from <https://agupubs.onlinelibrary.wiley.com/doi/abs/10.1029/2006JE002818> doi: 10.1029/2006JE002818
- Claire, M. W., Sheets, J., Cohen, M., Ribas, I., Meadows, V. S., & Catling, D. C. (2012, sep). The evolution of solar flux from 0.1 nm to 160 μm : Quantitative estimates for planetary studies. *The Astrophysical Journal*, 757(1), 95. Retrieved from <https://doi.org/10.1088/0004-637x/757/1/95> doi: 10.1088/0004-637x/757/1/95
- Clancy, R., Smith, M. D., Lefèvre, F., McConnochie, T. H., Sandor, B. J., Wolff, M. J., . . . Navarro, T. (2017, September). Vertical profiles of Mars 1.27 μm O₂ dayglow from MRO CRISM limb spectra: Seasonal/global behaviors, comparisons to LMDGCM simulations, and a global definition for Mars water vapor profiles. *Icarus*, 293, 132-156. doi: 10.1016/j.icarus.2017.04.011
- Coates, A. J. (2004, January). Ion pickup at comets. *Advances in Space Research*, 33(11), 1977-1988. Retrieved 2018-06-14, from <http://www.sciencedirect.com/science/article/pii/S0273117704000213> doi: 10.1016/j.asr.2003.06.029
- Cohen, O., & Drake, J. J. (2014, March). A Grid of MHD Models for Stellar Mass Loss and Spin-down Rates of Solar Analogs. *Astrophys. J.*, 783, 55. doi: 10.1088/0004-637X/783/1/55
- Cohen, O., Drake, J. J., Glocer, A., Garraffo, C., Poppenhaeger, K., Bell, J. M., . . . Gombosi, T. I. (2014, July). Magnetospheric Structure and Atmospheric Joule Heating of Habitable Planets Orbiting M-dwarf Stars. *Astrophys. J.*, 790, 57. doi: 10.1088/0004-637X/790/1/57
- Cohen, O., Drake, J. J., Kashyap, V. L., Hussain, G. A. J., & Gombosi, T. I. (2010, September). The Coronal Structure of AB Doradus. *Astrophys. J.*, 721, 80-89. doi: 10.1088/0004-637X/721/1/80
- Cohen, O., Glocer, A., Garraffo, C., Drake, J. J., & Bell, J. M. (2018, March). Energy Dissipation in the Upper Atmospheres of TRAPPIST-1 Planets. *Astrophys. J.*, 856, L11. doi: 10.3847/2041-8213/aab5b5
- Cohen, O., Kashyap, V. L., Drake, J. J., Sokolov, I. V., Garraffo, C., & Gombosi, T. I. (2011, May). The Dynamics of Stellar Coronae Harboring Hot Jupiters. I. A Time-dependent Magnetohydrodynamic Simulation of the Interplanetary Environment in the HD 189733 Planetary System. *Astrophys. J.*, 733, 67. doi: 10.1088/0004-637X/733/1/67
- Cohen, O., Ma, Y., Drake, J. J., Glocer, A., Garraffo, C., Bell, J. M., & Gombosi, T. I. (2015, June). The Interaction of Venus-like, M-dwarf Planets with the Stellar Wind of Their Host Star. *Astrophys. J.*, 806, 41. doi: 10.1088/0004-637X/806/1/41
- Cohen, O., Moschou, S.-P., Glocer, A., Sokolov, I. V., Mazeh, T., Drake, J. J., . . . Alvarado-Gómez, J. D. (2018, November). Exoplanet Modulation of Stellar Coronal Radio Emission. *Astrophys. J.*, 156, 202. doi: 10.3847/1538-3881/aae1f2
- Colegrove, F., Johnson, F., & Hanson, W. (1966). Atmospheric composition in the lower thermosphere. *Journal of Geophysical Research*, 71(9), 2227-2236.
- Collinson, G., Glocer, A., Xu, S., Mitchell, D., Frahm, R. A., Grebowsky, J., . . . Jakosky, B. (2019). Ionospheric ambipolar electric fields of Mars and Venus: Comparisons between theoretical predictions and direct observations of the electric potential drop. *Geophysical Research Letters*, 46(3), 1168-1176. Retrieved from <https://agupubs.onlinelibrary.wiley.com/doi/abs/10.1029/2018GL080597> doi: 10.1029/2018GL080597
- Cosmovici, C., & Pogrebenko, S. (2018). Water maser emission from exoplanetary systems. *International Journal of Astrobiology*, 17(1), 70-76.
- Coustenis, A., Salama, A., Lellouch, E., Encrenaz, T., Bjoraker, G. L., Samuelson, R. E., . . . Kessler, M. F. (1998, August). Evidence for water vapor in Titan's

- atmosphere from ISO/SWS data. *Astron. Astrophys.*, *336*, L85-L89.
- 3417 Cravens, T. E. (1987). Vibrationally excited molecular hydrogen in the upper atmo-
 3418 sphere of Jupiter. *Journal of Geophysical Research: Space Physics*, *92*(A10),
 3419 11083-11100. Retrieved from [https://agupubs.onlinelibrary.wiley.com/](https://agupubs.onlinelibrary.wiley.com/doi/abs/10.1029/JA092iA10p11083)
 3420 [doi/abs/10.1029/JA092iA10p11083](https://doi.org/10.1029/JA092iA10p11083) doi: 10.1029/JA092iA10p11083
 3421
- 3422 Cravens, T. E. (1997). Comet Hyakutake x-ray source: Charge transfer of solar wind
 3423 heavy ions. *Geophys. Res. Lett.*, *24*, 105-108. doi: 10.1029/96GL03780
- 3424 Cravens, T. E., Howell, E., Waite, J. H., & Gladstone, G. R. (1995, September). Au-
 3425 roral oxygen precipitation at Jupiter. *J. Geophys. Res.*, *100*, 17153-17162. doi:
 3426 10.1029/95JA00970
- 3427 Cravens, T. E., Rahmati, A., Fox, J. L., Lillis, R., Bougher, S., Luhmann, J., ...
 3428 Jakosky, B. (2017). Hot oxygen escape from Mars: Simple scaling with solar
 3429 EUV irradiance. *Journal of Geophysical Research: Space Physics*, *122*(1),
 3430 1102-1116. Retrieved from [https://agupubs.onlinelibrary.wiley.com/](https://agupubs.onlinelibrary.wiley.com/doi/abs/10.1002/2016JA023461)
 3431 [doi/abs/10.1002/2016JA023461](https://doi.org/10.1002/2016JA023461) doi: 10.1002/2016JA023461
- 3432 Crew, G. B., Chang, T., Retterer, J. M., Peterson, W. K., & Gurnett, D. A. (1990,
 3433 April). Ion cyclotron resonance heated conics - Theory and observations. *Jour-
 3434 nal of Geophysical Research*, *95*, 3959.
- 3435 Crew, G. B., & Chang, T. S. (1985). Asymptotic theory of ion conic distribu-
 3436 tions. *The Physics of Fluids*, *28*(8), 2382-2394. Retrieved from [http://](http://aip.scitation.org/doi/abs/10.1063/1.865244)
 3437 aip.scitation.org/doi/abs/10.1063/1.865244 doi: 10.1063/1.865244
- 3438 Cui, J., Yelle, R. V., & Volk, K. (2008). Distribution and escape of molecular hydro-
 3439 gen in Titan's thermosphere and exosphere. *Journal of Geophysical Research:
 3440 Planets*, *113*(E10), n/a-n/a. Retrieved from [http://dx.doi.org/10.1029/](http://dx.doi.org/10.1029/2007JE003032)
 3441 [2007JE003032](http://dx.doi.org/10.1029/2007JE003032) (E10004) doi: 10.1029/2007JE003032
- 3442 Curry, S. M., Liemohn, M., Fang, X., Ma, Y., & Espley, J. (2013, January). The in-
 3443 fluence of production mechanisms on pick-up ion loss at Mars. *Journal of Geo-
 3444 physical Research (Space Physics)*, *118*, 554-569. doi: 10.1029/2012JA017665
- 3445 Daglis, I. A., Thorne, R. M., Baumjohann, W., & Orsini, S. (1999). The terrestrial
 3446 ring current: Origin, formation, and decay. *Reviews of Geophysics*, *37*(4), 407-
 3447 438. Retrieved from [https://agupubs.onlinelibrary.wiley.com/doi/abs/](https://agupubs.onlinelibrary.wiley.com/doi/abs/10.1029/1999RG900009)
 3448 [10.1029/1999RG900009](https://doi.org/10.1029/1999RG900009) doi: 10.1029/1999RG900009
- 3449 Decker, D. T., Kozelov, B. V., Basu, B., Jasperse, J. R., & Ivanov, V. E. (1996,
 3450 December). Collisional degradation of the proton-H atom fluxes in the at-
 3451 mosphere: A comparison of theoretical techniques. *J. Geophys. Res.*, *101*,
 3452 26947-26960. doi: 10.1029/96JA02679
- 3453 Deighan, J., Chaffin, M. S., Chaufray, J.-Y., Stewart, A. I. F., Schneider, N. M.,
 3454 Jain, S. K., ... Jakosky, B. M. (2015). MAVEN IUVS observation of the
 3455 hot oxygen corona at Mars. *Geophysical Research Letters*, *42*(21), 9009-9014.
 3456 Retrieved from [https://agupubs.onlinelibrary.wiley.com/doi/abs/](https://agupubs.onlinelibrary.wiley.com/doi/abs/10.1002/2015GL065487)
 3457 [10.1002/2015GL065487](https://doi.org/10.1002/2015GL065487) doi: 10.1002/2015GL065487
- 3458 Deighan, J., Jain, S. K., Chaffin, M. S., Fang, X., Halekas, J. S., Clarke, J. T., ...
 3459 Evans, J. S. (2018, Jul). Discovery of a proton aurora at Mars. *Nature Astron-
 3460 omy*, *2*, 802-807. doi: 10.1038/s41550-018-0538-5
- 3461 Dennerl, K. (2007). X-rays from mars. In C. T. Russell (Ed.), *The mars plasma
 3462 environment* (pp. 403-433). New York, NY: Springer New York. Retrieved
 3463 from https://doi.org/10.1007/978-0-387-70943-7_17 doi: 10.1007/978-0-
 3464 -387-70943-7_17
- 3465 Dennerl, K. (2010, Dec 01). Charge transfer reactions. *Space Science Reviews*,
 3466 *157*(1), 57-91. Retrieved from [https://doi.org/10.1007/s11214-010-9720-](https://doi.org/10.1007/s11214-010-9720-5)
 3467 [5](https://doi.org/10.1007/s11214-010-9720-5) doi: 10.1007/s11214-010-9720-5
- 3468 Des Marais, D. J., Harwit, M. O., Jucks, K. W., Kasting, J. F., Lin, D. N. C., Lu-
 3469 nine, J. I., ... Wolf, N. J. (2002, June). Remote Sensing of Planetary Prop-
 3470 erties and Biosignatures on Extrasolar Terrestrial Planets. *Astrobiology*, *2*,
 3471 153-181. doi: 10.1089/15311070260192246

- 3472 DiBraccio, G. A., & Gershman, D. J. (2019). Voyager 2 constraints on plasmoid-
 3473 based transport at Uranus. *Geophysical Research Letters*, *0*(ja). Retrieved
 3474 from [https://agupubs.onlinelibrary.wiley.com/doi/abs/10.1029/](https://agupubs.onlinelibrary.wiley.com/doi/abs/10.1029/2019GL083909)
 3475 [2019GL083909](https://agupubs.onlinelibrary.wiley.com/doi/abs/10.1029/2019GL083909) doi: 10.1029/2019GL083909
- 3476 Dlugokencky, E. J., Nisbet, E. G., Fisher, R., & Lowry, D. (2011). Global at-
 3477 mospheric methane: budget, changes and dangers. *Philosophical Trans-*
 3478 *actions of the Royal Society of London A: Mathematical, Physical and*
 3479 *Engineering Sciences*, *369*(1943), 2058–2072. Retrieved from [http://](http://rsta.royalsocietypublishing.org/content/369/1943/2058)
 3480 rsta.royalsocietypublishing.org/content/369/1943/2058 doi:
 3481 10.1098/rsta.2010.0341
- 3482 Dobrijevic, M., Hébrard, E., Loison, J. C., & Hickson, K. M. (2014, January). Cou-
 3483 pling of oxygen, nitrogen, and hydrocarbon species in the photochemistry of
 3484 Titan’s atmosphere. *Icarus*, *228*, 324–346. doi: 10.1016/j.icarus.2013.10.015
- 3485 Dobrijevic, M., Loison, J., Hickson, K., & Gronoff, G. (2016). 1d-coupled pho-
 3486 tochemical model of neutrals, cations and anions in the atmosphere of titan.
 3487 *Icarus*, *268*, 313 - 339. Retrieved from [http://www.sciencedirect.com/](http://www.sciencedirect.com/science/article/pii/S0019103515006119)
 3488 [science/article/pii/S0019103515006119](http://www.sciencedirect.com/science/article/pii/S0019103515006119) doi: [https://doi.org/10.1016/](https://doi.org/10.1016/j.icarus.2015.12.045)
 3489 [j.icarus.2015.12.045](https://doi.org/10.1016/j.icarus.2015.12.045)
- 3490 Domagal-Goldman, S. D., Segura, A., Claire, M. W., Robinson, T. D., & Meadows,
 3491 V. S. (2014, September). Abiotic Ozone and Oxygen in Atmospheres Similar
 3492 to Prebiotic Earth. *Astrophys. J.*, *792*, 90. doi: 10.1088/0004-637X/792/2/90
- 3493 Donahue, T. M., & Hodges, R. R. (1993). Venus methane and water. *Geo-*
 3494 *physical Research Letters*, *20*(7), 591–594. Retrieved from [https://](https://agupubs.onlinelibrary.wiley.com/doi/abs/10.1029/93GL00513)
 3495 agupubs.onlinelibrary.wiley.com/doi/abs/10.1029/93GL00513 doi:
 3496 10.1029/93GL00513
- 3497 Donahue, T. M., Hoffman, J. H., Hodges, R. R., & Watson, A. J. (1982). Venus
 3498 was wet: A measurement of the ratio of deuterium to hydrogen. *Science*,
 3499 *216*(4546), 630–633. Retrieved from [https://science.sciencemag.org/](https://science.sciencemag.org/content/216/4546/630)
 3500 [content/216/4546/630](https://science.sciencemag.org/content/216/4546/630) doi: 10.1126/science.216.4546.630
- 3501 Dong, C., Lingam, M., Ma, Y., & Cohen, O. (2017, March). Is Proxima Centauri b
 3502 Habitable? A Study of Atmospheric Loss. *Astrophys. J. Let.*, *837*, L26. doi: 10
 3503 .3847/2041-8213/aa6438
- 3504 Dong, Y., Fang, X., Brain, D. A., McFadden, J. P., Halekas, J. S., Connerney,
 3505 J. E., ... Jakosky, B. M. (2015). Strong plume fluxes at Mars observed
 3506 by MAVEN: An important planetary ion escape channel. *Geophysical Re-*
 3507 *search Letters*, *42*(21), 8942–8950. Retrieved 2018-06-04, from [https://](https://agupubs.onlinelibrary.wiley.com/doi/abs/10.1002/2015GL065346)
 3508 agupubs.onlinelibrary.wiley.com/doi/abs/10.1002/2015GL065346 doi:
 3509 10.1002/2015GL065346
- 3510 Downs, C., Lionello, R., Mikić, Z., Linker, J. A., & Velli, M. (2016, December).
 3511 Closed-field Coronal Heating Driven by Wave Turbulence. *Astrophys. J.*, *832*,
 3512 180. doi: 10.3847/0004-637X/832/2/180
- 3513 Drake, J. J., Cohen, O., Yashiro, S., & Gopalswamy, N. (2013, February). Implica-
 3514 tions of Mass and Energy Loss due to Coronal Mass Ejections on Magnetically
 3515 Active Stars. *Astrophys. J.*, *764*, 170. doi: 10.1088/0004-637X/764/2/170
- 3516 Drossart, P., Fouchet, T., Crovisier, J., Lellouch, E., Encrenaz, T., Feuchtgruber,
 3517 H., & Champion, J. (1999). Fluorescence in the 3 μ m bands of methane on
 3518 Jupiter and Saturn from ISO/SWS observations. In *The universe as seen by*
 3519 *iso* (Vol. 427, p. 169).
- 3520 Dubinin, E., Fraenz, M., Fedorov, A., Lundin, R., Edberg, N., Duru, F., & Vais-
 3521 berg, O. (2011, October). Ion Energization and Escape on Mars and
 3522 Venus. *Space Science Reviews*, *162*(1-4), 173–211. Retrieved 2012-02-24,
 3523 from <http://www.springerlink.com/content/ft77461t07732t13/> doi:
 3524 10.1007/s11214-011-9831-7
- 3525 Dudok de Wit, T., & Bruinsma, S. (2017, March). The 30 cm radio flux as a so-
 3526 lar proxy for thermosphere density modelling. *Journal of Space Weather and*

- 3527 *Space Climate*, 7(27), A9. doi: 10.1051/swsc/2017008
- 3528 Dudok de Wit, T., Kretzschmar, M., Lilensten, J., & Woods, T. (2009, May). Find-
3529 ing the best proxies for the solar UV irradiance. *Geophys. Res. Lett.*, 36,
3530 10107-+. doi: 10.1029/2009GL037825
- 3531 Dunne, E. M., Gordon, H., Kürten, A., Almeida, J., Duplissy, J., Williamson, C.,
3532 ... Carslaw, K. S. (2016, December). Global atmospheric particle forma-
3533 tion from CERN CLOUD measurements. *Science*, 354, 1119-1124. doi:
3534 10.1126/science.aaf2649
- 3535 Editors of Nature Astronomy. (2017, February). Towers of Babel. *Nature As-*
3536 *tronomy*, 1(2), 0053. Retrieved 2017-02-06, from [http://www.nature.com/](http://www.nature.com/articles/s41550-017-0053)
3537 [articles/s41550-017-0053](http://www.nature.com/articles/s41550-017-0053) doi: 10.1038/s41550-017-0053
- 3538 Egan, H., Jarvinen, R., & Brain, D. (2019, 03). Stellar influence on heavy ion escape
3539 from unmagnetized exoplanets. *Monthly Notices of the Royal Astronomical So-*
3540 *ciety*, 486(1), 1283-1291. Retrieved from [https://doi.org/10.1093/mnras/](https://doi.org/10.1093/mnras/stz788)
3541 [stz788](https://doi.org/10.1093/mnras/stz788) doi: 10.1093/mnras/stz788
- 3542 Ehlmann, B. L., Anderson, F. S., Andrews-Hanna, J., Catling, D. C., Chris-
3543 tensen, P. R., Cohen, B. A., ... Zahnle, K. J. (2016). The sustainability
3544 of habitability on terrestrial planets: Insights, questions, and needed mea-
3545 surements from mars for understanding the evolution of earth-like worlds.
3546 *Journal of Geophysical Research: Planets*, 121(10), 1927-1961. Retrieved
3547 from <http://dx.doi.org/10.1002/2016JE005134> (2016JE005134) doi:
3548 10.1002/2016JE005134
- 3549 Ehrenreich, D., Bourrier, V., Wheatley, P. J., Des Etangs, A. L., Hébrard, G., Udry,
3550 S., ... others (2015). A giant comet-like cloud of hydrogen escaping the warm
3551 Neptune-mass exoplanet GJ 436b. *Nature*, 522(7557), 459.
- 3552 Ehrenreich, D., & Désert, J.-M. (2011). Mass-loss rates for transiting exoplanets.
3553 *Astronomy & Astrophysics*, 529, 10. doi: 10.1051/0004-6361/201016356
- 3554 Ehrenreich, D., Lecavelier Des Etangs, A., Hébrard, G., Désert, J.-M., Vidal-Madjar,
3555 A., McConnell, J. C., ... Ferlet, R. (2008, June). New observations of the
3556 extended hydrogen exosphere of the extrasolar planet HD 209458b. *Astronomy*
3557 *and Astrophysics*, 483, 933-937. doi: 10.1051/0004-6361:200809460
- 3558 Elrod, M., Curry, S., Thiemann, E., & Jain, S. (2018). September 2017 solar flare
3559 event: Rapid heating of the martian neutral upper atmosphere from the x-class
3560 flare as observed by maven. *Geophysical Research Letters*, 45(17), 8803-8810.
- 3561 Emmert, J. T., Lean, J. L., & Picone, J. M. (2010, June). Record-low thermospheric
3562 density during the 2008 solar minimum. *Geophys. Res. Lett.*, 37, 12102-+. doi:
3563 10.1029/2010GL043671
- 3564 Erkaev, N. V., Kulikov, Y. N., Lammer, H., Selsis, F., Langmayr, D., Jaritz, G. F.,
3565 & Biernat, H. K. (2007). Roche lobe effects on the atmospheric loss from
3566 Hot Jupiters. *A&A*, 472(1), 329-334. Retrieved from [http://dx.doi.org/](http://dx.doi.org/10.1051/0004-6361:20066929)
3567 [10.1051/0004-6361:20066929](http://dx.doi.org/10.1051/0004-6361:20066929) doi: 10.1051/0004-6361:20066929
- 3568 Erkaev, N. V., Lammer, H., Odert, P., Kulikov, Y. N., & Kislyakova, K. G. (2015,
3569 April). Extreme hydrodynamic atmospheric loss near the critical thermal es-
3570 cape regime. *Mon. Not. R. Astron. Soc.*, 448, 1916-1921. doi: 10.1093/mnras/
3571 stv130
- 3572 Erkaev, N. V., Lammer, H., Odert, P., Kulikov, Y. N., Kislyakova, K. G., Kho-
3573 dachenko, M. L., ... Biernat, H. (2013, November). XUV exposed non-
3574 hydrostatic hydrogen-rich upper atmospheres of terrestrial planets. Part I:
3575 Atmospheric expansion and thermal escape. *Astrobiology*, 13(11), 1011-1029.
3576 (arXiv: 1212.4982) doi: 10.1089/ast.2012.0957
- 3577 Erwin, J. T., Tucker, O. J., & Johnson, R. E. (2013, September). Hybrid
3578 fluid/kinetic modeling of Pluto's escaping atmosphere. *Icarus*, 226(1), 375-
3579 384.
- 3580 Etiope, G., & Klusman, R. W. (2002). Geologic emissions of methane to the
3581 atmosphere. *Chemosphere*, 49(8), 777 - 789. Retrieved from <http://>

- 3582 www.sciencedirect.com/science/article/pii/S0045653502003806 doi:
3583 [http://dx.doi.org/10.1016/S0045-6535\(02\)00380-6](http://dx.doi.org/10.1016/S0045-6535(02)00380-6)
- 3584 Eviatar, A., & Barbosa, D. D. (1984). Jovian magnetospheric neutral wind
3585 and auroral precipitation flux. *Journal of Geophysical Research: Space*
3586 *Physics*, *89*(A9), 7393–7398. Retrieved from [http://dx.doi.org/10.1029/
3587 JA089iA09p07393](http://dx.doi.org/10.1029/JA089iA09p07393) doi: 10.1029/JA089iA09p07393
- 3588 Fahr, H. J., & Shizgal, B. (1983, February). Modern exospheric theories and their
3589 observational relevance. *Reviews of Geophysics and Space Physics*, *21*, 75-124.
3590 doi: 10.1029/RG021i001p00075
- 3591 Fang, X., Liemohn, M. W., Nagy, A. F., Luhmann, J. G., & Ma, Y. (2010, April).
3592 Escape probability of Martian atmospheric ions: Controlling effects of the
3593 electromagnetic fields. *Journal of Geophysical Research (Space Physics)*, *115*,
3594 A04308. doi: 10.1029/2009JA014929
- 3595 Fastook, J. L., Head, J. W., Marchant, D. R., & Forget, F. (2008). Tropical moun-
3596 tain glaciers on Mars: Altitude-dependence of ice accumulation, accumulation
3597 conditions, formation times, glacier dynamics, and implications for plane-
3598 tary spin-axis/orbital history. *Icarus*, *198*(2), 305 - 317. Retrieved from
3599 <http://www.sciencedirect.com/science/article/pii/S0019103508003126>
3600 doi: <http://dx.doi.org/10.1016/j.icarus.2008.08.008>
- 3601 Fedorova, A., Bertaux, J.-L., Betsis, D., Montmessin, F., Korablev, O., Maltagliati,
3602 L., & Clarke, J. (2018, January). Water vapor in the middle atmosphere
3603 of Mars during the 2007 global dust storm. *Icarus*, *300*, 440-457. doi:
3604 10.1016/j.icarus.2017.09.025
- 3605 Fedorova, A., Korablev, O., Vandaele, A.-C., Bertaux, J.-L., Belyaev, D., Mahieux,
3606 A., ... Villard, E. (2008). HDO and H₂O vertical distributions and isotopic
3607 ratio in the Venus mesosphere by solar occultation at infrared spectrometer on
3608 board Venus Express. *Journal of Geophysical Research: Planets*, *113*(E5),
3609 n/a–n/a. Retrieved from <http://dx.doi.org/10.1029/2008JE003146>
3610 (E00B22) doi: 10.1029/2008JE003146
- 3611 Fedorova, A., Marcq, E., Luginin, M., Korablev, O., Bertaux, J.-L., & Montmessin,
3612 F. (2016). Variations of water vapor and cloud top altitude in the Venus'
3613 mesosphere from SPICAV/VEx observations. *Icarus*, *275*, 143 - 162. Re-
3614 trieved from [http://www.sciencedirect.com/science/article/pii/
3615 S0019103516300550](http://www.sciencedirect.com/science/article/pii/S0019103516300550) doi: <http://dx.doi.org/10.1016/j.icarus.2016.04.010>
- 3616 Fegley, J. B. (2003). 1.19 - Venus. In H. D. Holland & K. K. Turekian (Eds.),
3617 *Treatise on geochemistry* (p. 487 - 507). Oxford: Pergamon. Retrieved from
3618 <http://www.sciencedirect.com/science/article/pii/B0080437516011506>
3619 doi: <http://dx.doi.org/10.1016/B0-08-043751-6/01150-6>
- 3620 Fernandes, P. A., Larsen, B. A., Thomsen, M. F., Skoug, R. M., Reeves, G. D.,
3621 Denton, M. H., ... Olson, D. K. (2017, September). The plasma envi-
3622 ronment inside geostationary orbit: A Van Allen Probes HOPE survey.
3623 *Journal of Geophysical Research (Space Physics)*, *122*, 9207-9227. doi:
3624 10.1002/2017JA024160
- 3625 Festou, M. C., & Atreya, S. K. (1982). Voyager ultraviolet stellar occultation mea-
3626 surements of the composition and thermal profiles of the Saturnian upper
3627 atmosphere. *Geophysical Research Letters*, *9*(10), 1147-1150. Retrieved
3628 from [https://agupubs.onlinelibrary.wiley.com/doi/abs/10.1029/
3629 GL009i010p01147](https://agupubs.onlinelibrary.wiley.com/doi/abs/10.1029/GL009i010p01147) doi: 10.1029/GL009i010p01147
- 3630 Feulner, G. (2012, April). The faint young Sun problem. *arXiv:1204.4449*. Re-
3631 trieved 2012-10-30, from <http://arxiv.org/abs/1204.4449> (Rev.Geophys.
3632 *50* (2012), RG2006) doi: 10.1029/2011RG000375
- 3633 Fike, D. A., Grotzinger, J. P., Pratt, L. M., & Summons, R. E. (2006, Decem-
3634 ber). Oxidation of the Ediacaran Ocean. *Nature*, *444*, 744-747. doi:
3635 10.1038/nature05345
- 3636 Fitzpatrick, J. M., & Shizgal, B. (1975, July). Temperature relaxation in a binary

- 3637 gas. I. Steady state solution. *J. Chem. Phys.*, *63*, 131-137. doi: 10.1063/1
3638 .431065
- 3639 Formisano, V., Atreya, S., Encrenaz, T., Ignatiev, N., & Giuranna, M. (2004). De-
3640 tection of methane in the atmosphere of Mars. *Science*, *306*(5702), 1758–1761.
3641 Retrieved from <http://science.sciencemag.org/content/306/5702/1758>
3642 doi: 10.1126/science.1101732
- 3643 France, K., Froning, C. S., Linsky, J. L., Roberge, A., Stocke, J. T., Tian, F., ...
3644 Walkowicz, L. M. (2013). The ultraviolet radiation environment around M
3645 dwarf exoplanet host stars. *The Astrophysical Journal*, *763*(2), 149. Retrieved
3646 from <http://stacks.iop.org/0004-637X/763/i=2/a=149>
- 3647 Fridlund, M., Hatzes, A., & Liseau, R. (2016, Dec). The Way Forward. *Space Sci-*
3648 *ence Reviews*, *205*(1-4), 349-372. doi: 10.1007/s11214-016-0247-2
- 3649 Fujii, Y., Angerhausen, D., Deitrick, R., Domagal-Goldman, S., Grenfell, J. L.,
3650 Hori, Y., ... Stevenson, K. B. (2018). Exoplanet biosignatures: Ob-
3651 servational prospects. *Astrobiology*, *18*(6), 739-778. Retrieved from
3652 <https://doi.org/10.1089/ast.2017.1733> (PMID: 29938537) doi:
3653 10.1089/ast.2017.1733
- 3654 Fuller-Rowell, T. J., & Evans, D. S. (1987). Height-integrated Pedersen and Hall
3655 conductivity patterns inferred from the TIROS-NOAA satellite data. *J. Geo-*
3656 *phys. Res.*, *92*(A7), 7606-7618.
- 3657 Gacesa, M., Zhang, P., & Kharchenko, V. (2012). Non-thermal escape of molec-
3658 ular hydrogen from Mars. *Geophysical Research Letters*, *39*(10). Retrieved
3659 from [https://agupubs.onlinelibrary.wiley.com/doi/abs/10.1029/](https://agupubs.onlinelibrary.wiley.com/doi/abs/10.1029/2012GL050904)
3660 [2012GL050904](https://agupubs.onlinelibrary.wiley.com/doi/abs/10.1029/2012GL050904) doi: 10.1029/2012GL050904
- 3661 Galand, M., Lilensten, J., Kofman, W., & Lummerzheim, D. (1998, October). Pro-
3662 ton transport model in the ionosphere. 2. Influence of magnetic mirroring and
3663 collisions on the angular redistribution in a proton beam. *Annales Geophysi-*
3664 *caae*, *16*, 1308-1321. doi: 10.1007/s00585-998-1308-y
- 3665 Galand, M., Lilensten, J., Kofman, W., & Sidje, R. B. (1997, September). Pro-
3666 ton transport model in the ionosphere 1. Multistream approach of the trans-
3667 port equations. *Journal of Geophysics Research*, *102*, 22261-22272. doi:
3668 10.1029/97JA01903
- 3669 Gao, P., Hu, R., Robinson, T. D., Li, C., & Yung, Y. L. (2015). Stability of CO₂
3670 Atmospheres on Desiccated M Dwarf Exoplanets. *The Astrophysical Journal*,
3671 *806*(2), 249. Retrieved from [http://stacks.iop.org/0004-637X/806/i=2/a=](http://stacks.iop.org/0004-637X/806/i=2/a=249)
3672 [249](http://stacks.iop.org/0004-637X/806/i=2/a=249)
- 3673 Gao, P., Hu, R., Robinson, T. D., Li, C., & Yung, Y. L. (2015, June). Stability of
3674 CO₂ Atmospheres on Desiccated M Dwarf Exoplanets. *Astrophys. J.*, *806*, 249.
3675 doi: 10.1088/0004-637X/806/2/249
- 3676 García Muñoz, A. (2007, July). Physical and chemical aeronomy of HD 209458b.
3677 *Plan. Sp. Sci.*, *55*, 1426-1455. doi: 10.1016/j.pss.2007.03.007
- 3678 Garcia-Sage, K., Glocer, A., Drake, J. J., Gronoff, G., & Cohen, O. (2017, July). On
3679 the Magnetic Protection of the Atmosphere of Proxima Centauri b. *Astrophys.*
3680 *J. Let.*, *844*, L13. doi: 10.3847/2041-8213/aa7eca
- 3681 Garraffo, C., Drake, J. J., & Cohen, O. (2016a, November). The missing magnetic
3682 morphology term in stellar rotation evolution. *Astronomy and Astrophysics*,
3683 *595*, A110. doi: 10.1051/0004-6361/201628367
- 3684 Garraffo, C., Drake, J. J., & Cohen, O. (2016b, December). The Space Weather of
3685 Proxima Centauri b. *Astrophys. J. Let.*, *833*, L4. doi: 10.3847/2041-8205/833/
3686 1/L4
- 3687 Garraffo, C., Drake, J. J., Cohen, O., Alvarado-Gómez, J. D., & Moschou, S. P.
3688 (2017, July). The Threatening Magnetic and Plasma Environment of the
3689 TRAPPIST-1 Planets. *Astrophys. J. Let.*, *843*, L33. doi: 10.3847/2041-8213/
3690 aa79ed
- 3691 Garraffo, C., Drake, J. J., Dotter, A., Choi, J., Burke, D. J., Moschou, S. P., ...

- 3692 Cohen, O. (2018, April). The Revolution Revolution: magnetic morphology
3693 driven spin-down. *ArXiv e-prints*.
- 3694 Gérard, J.-C., Bonfond, B., Grodent, D., Radioti, A., Clarke, J. T., Gladstone,
3695 G. R., ... Schematovich, V. I. (2014). Mapping the electron energy in Jupiter's
3696 aurora: Hubble spectral observations. *Journal of Geophysical Research: Space
3697 Physics*, 119(11), 9072–9088. doi: 10.1002/2014JA020514
- 3698 Gettelman, A., & Fu, Q. (2008). Observed and simulated upper-tropospheric wa-
3699 ter vapor feedback. *Journal of Climate*, 21(13), 3282-3289. Retrieved from
3700 <http://dx.doi.org/10.1175/2007JCLI2142.1> doi: 10.1175/2007JCLI2142
3701 .1
- 3702 Gillon, M., Triaud, A. H. M. J., Demory, B.-O., Jehin, E., Agol, E., Deck, K. M.,
3703 ... Queloz, D. (2017, February). Seven temperate terrestrial planets around
3704 the nearby ultracool dwarf star TRAPPIST-1. *Nature*, 542, 456-460. doi:
3705 10.1038/nature21360
- 3706 Gladstone, G. R., Pryor, W. R., & Stern, S. A. (2015). Ly@pluto. *Icarus*, 246, 279 -
3707 284. Retrieved from [http://www.sciencedirect.com/science/article/pii/
3708 S0019103514002085](http://www.sciencedirect.com/science/article/pii/S0019103514002085) (Special Issue: The Pluto System) doi: [https://doi.org/
3709 10.1016/j.icarus.2014.04.016](https://doi.org/10.1016/j.icarus.2014.04.016)
- 3710 Gladstone, G. R., Stern, S. A., Ennico, K., Olkin, C. B., Weaver, H. A., Young,
3711 L. A., ... Team, t. N. H. S. (2016, March). The atmosphere of Pluto as ob-
3712 served by New Horizons. *Science*, 351(6279), aad8866. Retrieved 2018-04-05,
3713 from <http://science.sciencemag.org/content/351/6279/aad8866> doi:
3714 10.1126/science.aad8866
- 3715 Glocer, A. (2016). Coupling ionospheric outflow into magnetospheric models: Trans-
3716 verse heating from wave-particle interactions. *Magnetosphere-Ionosphere Cou-
3717 pling in the Solar System*, 222, 195.
- 3718 Glocer, A., Fok, M., Meng, X., Toth, G., Buzulukova, N., Chen, S., & Lin, K. (2013,
3719 April). CRCM + BATS-R-US two-way coupling. *Journal of Geophysical Re-
3720 search (Space Physics)*, 118, 1635-1650. doi: 10.1002/jgra.50221
- 3721 Glocer, A., Gombosi, T. I., Toth, G., Hansen, K. C., Ridley, A. J., & Nagy,
3722 A. (2007). Polar wind outflow model: Saturn results. *Journal of Geo-
3723 physical Research: Space Physics*, 112(A1). Retrieved from [https://
3724 agupubs.onlinelibrary.wiley.com/doi/abs/10.1029/2006JA011755](https://agupubs.onlinelibrary.wiley.com/doi/abs/10.1029/2006JA011755) doi:
3725 10.1029/2006JA011755
- 3726 Glocer, A., Tóth, G., Gombosi, T., & Welling, D. (2009, May). Modeling
3727 ionospheric outflows and their impact on the magnetosphere, initial re-
3728 sults. *Journal of Geophysical Research (Space Physics)*, 114, A05216. doi:
3729 10.1029/2009JA014053
- 3730 Goldblatt, C., Claire, M. W., Lenton, T. M., Matthews, A. J., Watson, A. J., &
3731 Zahnle, K. J. (2009, December). Nitrogen-enhanced greenhouse warming on
3732 early Earth. *Nature Geoscience*, 2, 891-896. doi: 10.1038/ngeo692
- 3733 Goldblatt, C., & Zahnle, K. J. (2011, March). Clouds and the Faint Young Sun
3734 Paradox. *Climate of the Past*, 7(1), 203-220. doi: 10.5194/cp-7-203-2011
- 3735 Gombosi, T. I., & Killeen, T. L. (1987). Effects of thermospheric motions on the po-
3736 lar wind: A time-dependent numerical study. *Journal of Geophysical Research*,
3737 92(A5), 4725-4729.
- 3738 Gombosi, T. I., & Nagy, A. (1989). Time-dependent modeling of field aligned
3739 current-generated ion transients in the polar wind. *Journal of Geophysical
3740 Research*, 94, 359-369.
- 3741 González-Galindo, F., Forget, F., López-Valverde, M. A., Angelats i Coll, M., &
3742 Millour, E. (2009). A ground-to-exosphere Martian general circulation model:
3743 1. seasonal, diurnal, and solar cycle variation of thermospheric temperatures.
3744 *Journal of Geophysical Research: Planets*, 114(E4). Retrieved from [https://
3745 agupubs.onlinelibrary.wiley.com/doi/abs/10.1029/2008JE003246](https://agupubs.onlinelibrary.wiley.com/doi/abs/10.1029/2008JE003246) doi:
3746 10.1029/2008JE003246

- 3747 Greenwood, J. B., Chutjian, A., & Smith, S. J. (2000, January). Measurements of
3748 Absolute, Single Charge-Exchange Cross Sections of H^+ , He^+ and He^{2+} with
3749 H_2O and CO_2 . *The Astrophysical Journal*, *529*, 605-609. doi: 10.1086/308254
- 3750 Greenwood, J. B., Mawhorter, R. J., Cadez, I., Lozano, J., Smith, S. J., &
3751 Chutjian, A. (2004). The Contribution of Charge Exchange to Ex-
3752 treme Ultra-Violet and X-ray Astronomy. *Physica Scripta*, *110*, 358. doi:
3753 10.1238/Physica.Topical.110a00358
- 3754 Greenwood, J. P., Karato, S.-i., Vander Kaaden, K. E., Pahlevan, K., & Usui, T.
3755 (2018). Water and Volatile Inventories of Mercury, Venus, the Moon, and
3756 Mars. *Space Science Reviews*, *214*(5), 92.
- 3757 Griebmeier, J.-M., Zarka, P., & Spreeuw, H. (2007, November). Predicting low-
3758 frequency radio fluxes of known extrasolar planets. *A&A*, *475*, 359-368. doi: 10
3759 .1051/0004-6361:20077397
- 3760 Griffith, C. A. (2009). Storms, polar deposits and the methane cycle in Titan's at-
3761 mosphere. *Phil. Trans. Roy. Soc. Lond. A*, *367*(1889), 713-728. Retrieved from
3762 <http://rsta.royalsocietypublishing.org/content/367/1889/713> doi: 10
3763 .1098/rsta.2008.0245
- 3764 Grodent, D. (2014). A brief review of ultraviolet auroral emissions on giant planets.
3765 *Space Science Reviews*, *187*(1), 23-50. Retrieved from [http://dx.doi.org/10](http://dx.doi.org/10.1007/s11214-014-0052-8)
3766 .1007/s11214-014-0052-8 doi: 10.1007/s11214-014-0052-8
- 3767 Gröller, H., Lichtenegger, H., Lammer, H., & Shematovich, V. I. (2014, Au-
3768 gust). Hot oxygen and carbon escape from the martian atmosphere.
3769 *Planetary and Space Science*, *98*, 93-105. Retrieved 2018-06-15, from
3770 <http://www.sciencedirect.com/science/article/pii/S0032063314000117>
3771 doi: 10.1016/j.pss.2014.01.007
- 3772 Gronoff, G., Lilensten, J., Simon, C., Witasse, O., Thissen, R., Dutuit, O., & Al-
3773 caraz, C. (2007, April). Modelling dications in the diurnal ionosphere of Venus.
3774 *Astronomy and Astrophysics*, *465*, 641-645. doi: 10.1051/0004-6361:20065991
- 3775 Gronoff, G., Maggiolo, R., Simon Wedlund, C., Mertens, C. J., Norman, R. B., Bell,
3776 J., ... Vidal-Madjar, A. (2014, June). Theoretical UV Absorption Spec-
3777 tra of Hydrodynamically Escaping O_2/CO_2 -Rich Exoplanetary Atmospheres.
3778 *Astrophys. J.*, *788*, 191. doi: 10.1088/0004-637X/788/2/191
- 3779 Gronoff, G., Rahmati, A., Simon Wedlund, C., Mertens, C. J., Cravens, T. E., &
3780 Kallio, E. (2014, July). The precipitation of keV energetic oxygen ions at Mars
3781 and their effects during the comet Siding Spring approach. *Geophys. Res. Lett.*,
3782 *41*, 4844-4850. doi: 10.1002/2014GL060902
- 3783 Gronoff, G., Simon Wedlund, C., Mertens, C. J., Barthélemy, M., Lillis, R. J., &
3784 Witasse, O. (2012, May). Computing uncertainties in ionosphere-airglow mod-
3785 els: II. The Martian airglow. *Journal of Geophysical Research (Space Physics)*,
3786 *117*, A05309. doi: 10.1029/2011JA017308
- 3787 Gronoff, G., Simon Wedlund, C., Mertens, C. J., & Lillis, R. J. (2012, April). Com-
3788 puting uncertainties in ionosphere-airglow models: I. Electron flux and species
3789 production uncertainties for Mars. *Journal of Geophysical Research (Space*
3790 *Physics)*, *117*, A04306. doi: 10.1029/2011JA016930
- 3791 Gross, S. H. (1972). On the exospheric temperature of hydrogen-dominated plan-
3792 etary atmospheres. *Journal of the Atmospheric Sciences*, *29*(1), 214-218.
3793 Retrieved from [http://dx.doi.org/10.1175/1520-0469\(1972\)029<0214:](http://dx.doi.org/10.1175/1520-0469(1972)029<0214:OTETOH>2.0.CO;2)
3794 [OTETOH>2.0.CO;2](http://dx.doi.org/10.1175/1520-0469(1972)029(0214:OTETOH)2.0.CO;2) doi: 10.1175/1520-0469(1972)029(0214:OTETOH)2.0.CO;
3795 2
- 3796 Grosvenor, D. P., Choullarton, T. W., Coe, H., & Held, G. (2007, September). A
3797 study of the effect of overshooting deep convection on the water content of
3798 the TTL and lower stratosphere from Cloud Resolving Model simulations.
3799 *Atmospheric Chemistry & Physics*, *7*, 4977-5002.
- 3800 Gruzinov, A. (2011, January). The rate of thermal atmospheric escape. *ArXiv*
3801 *e-prints*, *1101*, arXiv:1101.1103. Retrieved 2016-01-27, from <http://adsabs>

- 3802 .harvard.edu/abs/2011arXiv1101.1103G
- 3803 Guglielmi, A., Kangas, J., Mursula, K., Pikkarainen, T., Pokhotelov, O., & Potapov,
3804 A. (1996, October). Pc 1 induced electromagnetic lift of background plasma in
3805 the magnetosphere. *Journal of Geophysical Research*, *101*, 21493-21500. doi:
3806 10.1029/96JA01750
- 3807 Gunell, H., Maggiolo, R., Nilsson, H., Wieser, G. S., Slapak, R., Lindkvist, J., ...
3808 Keyser, J. D. (2018, May). Why an intrinsic magnetic field does not pro-
3809 tect a planet against atmospheric escape. *A&A*. Retrieved 2018-06-04,
3810 from <https://articles/aa/abs/forth/aa32934-18/aa32934-18.html> doi:
3811 10.1051/0004-6361/201832934
- 3812 Haigh, J. D. (2007, October). The Sun and the Earth's Climate. *Living Reviews in*
3813 *Solar Physics*, *4*, 2. doi: 10.12942/lrsp-2007-2
- 3814 Halekas, J. S. (2017). Seasonal variability of the hydrogen exosphere of Mars.
3815 *Journal of Geophysical Research: Planets*, *122*(5), 901-911. Retrieved
3816 from [https://agupubs.onlinelibrary.wiley.com/doi/abs/10.1002/](https://agupubs.onlinelibrary.wiley.com/doi/abs/10.1002/2017JE005306)
3817 [2017JE005306](https://agupubs.onlinelibrary.wiley.com/doi/abs/10.1002/2017JE005306) doi: 10.1002/2017JE005306
- 3818 Halekas, J. S., Brain, D. A., Ruhunusiri, S., McFadden, J. P., Mitchell, D. L.,
3819 Mazelle, C., ... Jakosky, B. M. (2016). Plasma clouds and snowplows: Bulk
3820 plasma escape from Mars observed by MAVEN. *Geophysical Research Letters*,
3821 *43*(4), 1426-1434. Retrieved from [https://agupubs.onlinelibrary.wiley](https://agupubs.onlinelibrary.wiley.com/doi/abs/10.1002/2016GL067752)
3822 [.com/doi/abs/10.1002/2016GL067752](https://agupubs.onlinelibrary.wiley.com/doi/abs/10.1002/2016GL067752) doi: 10.1002/2016GL067752
- 3823 Halekas, J. S., Lillis, R. J., Mitchell, D. L., Cravens, T. E., Mazelle, C., Conner-
3824 ney, J. E. P., ... Ruhunusiri, S. (2015, November). MAVEN observations
3825 of solar wind hydrogen deposition in the atmosphere of Mars. *Geophysi-*
3826 *cal Research Letters*, *42*(21), 2015GL064693. Retrieved 2017-03-20, from
3827 <http://onlinelibrary.wiley.com/doi/10.1002/2015GL064693/abstract>
3828 doi: 10.1002/2015GL064693
- 3829 Halverson, G. P., Hurtgen, M. T., Porter, S. M., & Collins, A. S. (2009). Chapter
3830 10 neoproterozoic-cambrian biogeochemical evolution. In H. E. F. Clau-
3831 dio Gaucher Alcides N. Sial & G. P. Halverson (Eds.), *Neoproterozoic-*
3832 *cambrian tectonics, global change and evolution: A focus on south west-*
3833 *ern gondwana* (Vol. 16, p. 351 - 365). Elsevier. Retrieved from [http://](http://www.sciencedirect.com/science/article/pii/S0166263509016259)
3834 www.sciencedirect.com/science/article/pii/S0166263509016259 doi:
3835 [http://dx.doi.org/10.1016/S0166-2635\(09\)01625-9](http://dx.doi.org/10.1016/S0166-2635(09)01625-9)
- 3836 Haqq-Misra, J. D., Domagal-Goldman, S. D., Kasting, P. J., & Kasting, J. F. (2008,
3837 December). A Revised, Hazy Methane Greenhouse for the Archean Earth. *As-*
3838 *trobiology*, *8*, 1127-1137. doi: 10.1089/ast.2007.0197
- 3839 Hara, T., Brain, D. A., Mitchell, D. L., Luhmann, J. G., Seki, K., Hasegawa, H.,
3840 ... others (2017). MAVEN observations of a giant ionospheric flux rope near
3841 Mars resulting from interaction between the crustal and interplanetary draped
3842 magnetic fields. *Journal of Geophysical Research: Space Physics*, *122*(1),
3843 828-842.
- 3844 Hara, T., Harada, Y., Mitchell, D. L., DiBraccio, G. A., Espley, J. R., Brain, D. A.,
3845 ... Jakosky, B. M. (2017). On the origins of magnetic flux ropes in near-Mars
3846 magnetotail current sheets. *Geophysical Research Letters*, *44*(15), 7653-7662.
3847 Retrieved from [https://agupubs.onlinelibrary.wiley.com/doi/abs/](https://agupubs.onlinelibrary.wiley.com/doi/abs/10.1002/2017GL073754)
3848 [10.1002/2017GL073754](https://agupubs.onlinelibrary.wiley.com/doi/abs/10.1002/2017GL073754) doi: 10.1002/2017GL073754
- 3849 Hargreaves, J. K. (1992). *The solar-terrestrial environment: an introduction to*
3850 *geospace-the science of the terrestrial upper atmosphere, ionosphere, and mag-*
3851 *netosphere*. Cambridge University Press.
- 3852 Hartle, R. E., Sarantos, M., & Sittler, E. C. (2011). Pickup ion distributions
3853 from three-dimensional neutral exospheres. *Journal of Geophysical Re-*
3854 *search: Space Physics*, *116*(A10). Retrieved 2018-06-14, from [https://](https://agupubs.onlinelibrary.wiley.com/doi/abs/10.1029/2011JA016859)
3855 agupubs.onlinelibrary.wiley.com/doi/abs/10.1029/2011JA016859 doi:
3856 10.1029/2011JA016859

- 3857 Heath, D. F., & Schlesinger, B. M. (1986, July). The Mg 280-nm doublet as a mon-
 3858 itor of changes in solar ultraviolet irradiance. *J. Geophys. Res.*, *91*, 8672-8682.
 3859 doi: 10.1029/JD091iD08p08672
- 3860 Heavens, N. G., Cantor, B. A., Hayne, P. O., Kass, D. M., Kleinböhl, A., McCleese,
 3861 D. J., ... Shirley, J. H. (2015). Extreme detached dust layers near Martian
 3862 volcanoes: Evidence for dust transport by mesoscale circulations forced by
 3863 high topography. *Geophysical Research Letters*, *42*(10), 3730-3738. Retrieved
 3864 from <http://dx.doi.org/10.1002/2015GL064004> (2015GL064004) doi:
 3865 10.1002/2015GL064004
- 3866 Heavens, N. G., Kleinböhl, A., Chaffin, M. S., Halekas, J. S., Kass, D. M., Hayne,
 3867 P. O., ... Schofield, J. T. (2018, February). Hydrogen escape from Mars en-
 3868 hanced by deep convection in dust storms. *Nature Astronomy*, *2*, 126-132. doi:
 3869 10.1038/s41550-017-0353-4
- 3870 Heavens, N. G., Richardson, M. I., Kleinböhl, A., Kass, D. M., McCleese, D. J., Ab-
 3871 dou, W., ... Wolkenberg, P. M. (2011, January). Vertical distribution of dust
 3872 in the Martian atmosphere during northern spring and summer: High-altitude
 3873 tropical dust maximum at northern summer solstice. *Journal of Geophysical*
 3874 *Research (Planets)*, *116*, 1007. doi: 10.1029/2010JE003692
- 3875 Hébrard, E., & Marty, B. (2014, January). Coupled noble gas-hydrocarbon evolution
 3876 of the early Earth atmosphere upon solar UV irradiation. *Earth and Planetary*
 3877 *Science Letters*, *385*, 40-48. doi: 10.1016/j.epsl.2013.10.022
- 3878 Held, I. M., & Soden, B. J. (2006). Robust responses of the hydrological cycle
 3879 to global warming. *Journal of Climate*, *19*(21), 5686-5699. Retrieved from
 3880 <http://dx.doi.org/10.1175/JCLI3990.1> doi: 10.1175/JCLI3990.1
- 3881 Hinson, D. P., Linscott, I. R., Young, L. A., Tyler, G. L., Stern, S. A., Beyer,
 3882 R. A., ... Woods, W. W. (2017, July). Radio occultation measurements of
 3883 Pluto's neutral atmosphere with New Horizons. *Icarus*, *290*, 96-111. doi:
 3884 10.1016/j.icarus.2017.02.031
- 3885 Hinteregger, H. E. (1981). Representations of solar EUV fluxes for aeronomical ap-
 3886 plications. *Advances in Space Research*, *1*, 39-52. doi: 10.1016/0273-1177(81)
 3887 90416-6
- 3888 Hoffman, P. F. (2013). The great oxidation and a siderian snowball earth:
 3889 Mif-s based correlation of paleoproterozoic glacial epochs. *Chemical Geol-*
 3890 *ogy*, *362*(0), 143 - 156. Retrieved from [http://www.sciencedirect.com/
 3891 science/article/pii/S0009254113001836](http://www.sciencedirect.com/science/article/pii/S0009254113001836) (Special Issue dedicated to
 3892 H.D. Holland: Evolution of the atmosphere and ocean through time) doi:
 3893 <http://dx.doi.org/10.1016/j.chemgeo.2013.04.018>
- 3894 Holland, H. D. (1984). *The chemical evolution of the atmosphere and oceans*.
 3895 H. D. Holland. Princeton University Press.
- 3896 Holmström, M., Ekenbäck, A., Selsis, F., Penz, T., Lammer, H., & Wurz, P. (2008,
 3897 February). Energetic neutral atoms as the explanation for the high-velocity hy-
 3898 drogen around HD 209458b. *Nature*, *451*, 970-972. doi: 10.1038/nature06600
- 3899 Horanyi, M., Cravens, T. E., & Waite, J. H., Jr. (1988, July). The precipitation
 3900 of energetic heavy ions into the upper atmosphere of Jupiter. *J. Geophys. Res.*,
 3901 *93*, 7251-7271. doi: 10.1029/JA093iA07p07251
- 3902 Horwitz, J. L. (1981, Oct). ISEE 1 observations of O⁺⁺ in the magnetosphere. *J.*
 3903 *Geophys. Res.*, *86*(A11), 9225-9229. doi: 10.1029/JA086iA11p09225
- 3904 Horwitz, J. L., Ho, C. W., Scarbro, H. D., Wilson, G. R., & Moore, T. E. (1994, Au-
 3905 gust). Centrifugal acceleration of the polar wind. *Journal of Geophysical Re-*
 3906 *search*, *99*, 15051-15064. doi: 10.1029/94JA00924
- 3907 Howard, W. S., Tilley, M. A., Corbett, H., Youngblood, A., Loyd, R. O. P., Rat-
 3908 zloff, J. K., ... Haislip, J. (2018, June). The First Naked-eye Super-
 3909 flare Detected from Proxima Centauri. *Astrophys. J. Let.*, *860*, L30. doi:
 3910 10.3847/2041-8213/aacaf3
- 3911 Hu, R., Kass, D. M., Ehlmann, B. L., & Yung, Y. L. (2015, November). Tracing

- 3912 the fate of carbon and the atmospheric evolution of Mars. *Nature Communica-*
 3913 *tions*, 6, 10003. Retrieved from <http://dx.doi.org/10.1038/ncomms10003>
- 3914 Hunten, D. M. (1973, November). The Escape of Light Gases from Planetary Atmo-
 3915 spheres. *Journal of Atmospheric Sciences*, 30, 1481-1494. doi: 10.1175/1520-
 3916 -0469(1973)030<1481:TEOLGF>2.0.CO;2
- 3917 Hunten, D. M. (1982, August). Thermal and nonthermal escape mechanisms for
 3918 terrestrial bodies. *Planetary and Space Science*, 30(8), 773-783. Retrieved
 3919 2016-01-27, from [http://www.sciencedirect.com/science/article/pii/](http://www.sciencedirect.com/science/article/pii/0032063382901106)
 3920 0032063382901106 doi: 10.1016/0032-0633(82)90110-6
- 3921 Hunten, D. M., Pepin, R. O., & Walker, J. C. (1987). Mass fractionation in hy-
 3922 drodynamic escape. *Icarus*, 69(3), 532 - 549. Retrieved from [http://www](http://www.sciencedirect.com/science/article/pii/0019103587900224)
 3923 [.sciencedirect.com/science/article/pii/0019103587900224](http://www.sciencedirect.com/science/article/pii/0019103587900224) doi: [http://](http://dx.doi.org/10.1016/0019-1035(87)90022-4)
 3924 [dx.doi.org/10.1016/0019-1035\(87\)90022-4](http://dx.doi.org/10.1016/0019-1035(87)90022-4)
- 3925 Hunten, D. M., & Watson, A. J. (1982, September). Stability of Pluto's at-
 3926 mosphere. *Icarus*, 51(3), 665-667. Retrieved 2016-01-27, from [http://](http://www.sciencedirect.com/science/article/pii/0019103582901555)
 3927 www.sciencedirect.com/science/article/pii/0019103582901555 doi:
 3928 10.1016/0019-1035(82)90155-5
- 3929 Ingersoll, A. P. (1969). The runaway greenhouse: A history of water on Venus.
 3930 *Journal of the Atmospheric Sciences*, 26(6), 1191-1198. Retrieved from
 3931 [http://dx.doi.org/10.1175/1520-0469\(1969\)026<1191:TRGAHO>2.0.CO;2](http://dx.doi.org/10.1175/1520-0469(1969)026<1191:TRGAHO>2.0.CO;2)
 3932 doi: 10.1175/1520-0469(1969)026(1191:TRGAHO)2.0.CO;2
- 3933 Inui, S., Seki, K., Sakai, S., Brain, D., Hara, T., McFadden, J., ... Jakosky, B.
 3934 (2019). Statistical study of heavy ion outflows from Mars observed in the Mar-
 3935 tian induced magnetotail by MAVEN. *Journal of Geophysical Research: Space*
 3936 *Physics*, 0(ja). Retrieved from [https://agupubs.onlinelibrary.wiley.com/](https://agupubs.onlinelibrary.wiley.com/doi/abs/10.1029/2018JA026452)
 3937 [doi/abs/10.1029/2018JA026452](https://agupubs.onlinelibrary.wiley.com/doi/abs/10.1029/2018JA026452) doi: 10.1029/2018JA026452
- 3938 Jackman, C., Arridge, C., André, N., Bagenal, F., Birn, J., Freeman, M., ... others
 3939 (2014). Large-scale structure and dynamics of the magnetotails of Mercury,
 3940 Earth, Jupiter and Saturn. *Space Science Reviews*, 182(1-4), 85-154.
- 3941 Jakosky, B. (1994, October). Mars Atmospheric Loss and Isotopic Fractionation by
 3942 Solar-Wind-Induced Sputtering and Photochemical Escape. *Icarus*, 111(2),
 3943 271-288. Retrieved 2018-06-15, from [http://linkinghub.elsevier.com/](http://linkinghub.elsevier.com/retrieve/doi/10.1006/icar.1994.1145)
 3944 [retrieve/doi/10.1006/icar.1994.1145](http://linkinghub.elsevier.com/retrieve/doi/10.1006/icar.1994.1145) doi: 10.1006/icar.1994.1145
- 3945 Jakosky, B. M. (1991, November). Mars volatile evolution: Evidence from stable iso-
 3946 topes. *Icarus*, 94(1), 14-31. doi: 10.1016/0019-1035(91)90138-J
- 3947 Jakosky, B. M., Brain, D., Chaffin, M., Curry, S., Deighan, J., Grebowsky, J., ...
 3948 others (2018). Loss of the Martian atmosphere to space: Present-day loss
 3949 rates determined from MAVEN observations and integrated loss through time.
 3950 *Icarus*, 315, 146-157.
- 3951 Jakosky, B. M., Grebowsky, J. M., Luhmann, J. G., Connerney, J., Eparvier, F.,
 3952 Ergun, R., ... Yelle, R. (2015). MAVEN observations of the response of Mars
 3953 to an interplanetary coronal mass ejection. *Science*, 350(6261). Retrieved
 3954 from <https://science.sciencemag.org/content/350/6261/aad0210> doi:
 3955 10.1126/science.aad0210
- 3956 Jakosky, B. M., & Phillips, R. J. (2001, July). Mars' volatile and climate history.
 3957 *Nature*, 412, 237-244.
- 3958 Jakosky, B. M., Slipski, M., Benna, M., Mahaffy, P., Elrod, M., Yelle, R., ... Al-
 3959 saeed, N. (2017). Mars' atmospheric history derived from upper-atmosphere
 3960 measurements of ³⁸Ar/³⁶Ar. *Science*, 355(6332), 1408-1410. Retrieved
 3961 from <http://science.sciencemag.org/content/355/6332/1408> doi:
 3962 10.1126/science.aai7721
- 3963 Jarvinen, R., & Kallio, E. (2014, January). Energization of planetary pickup ions in
 3964 the solar system. *Journal of Geophysical Research: Planets*, 119(1), 219-236.
 3965 Retrieved 2016-04-18, from [http://onlinelibrary.wiley.com/doi/10.1002/](http://onlinelibrary.wiley.com/doi/10.1002/2013JE004534/abstract)
 3966 [2013JE004534/abstract](http://onlinelibrary.wiley.com/doi/10.1002/2013JE004534/abstract) doi: 10.1002/2013JE004534

- 3967 Johnson, J. R., Wing, S., & Delamere, P. A. (2014, Nov 01). Kelvin Helmholtz
3968 instability in planetary magnetospheres. *Space Science Reviews*, 184(1), 1–
3969 31. Retrieved from <https://doi.org/10.1007/s11214-014-0085-z> doi:
3970 10.1007/s11214-014-0085-z
- 3971 Johnson, R., Tucker, O., & Volkov, A. (2016). Evolution of an early Ti-
3972 tan atmosphere. *Icarus*, 271, 202 - 206. Retrieved from [http://www](http://www.sciencedirect.com/science/article/pii/S001910351600018X)
3973 [.sciencedirect.com/science/article/pii/S001910351600018X](http://www.sciencedirect.com/science/article/pii/S001910351600018X) doi:
3974 <https://doi.org/10.1016/j.icarus.2016.01.014>
- 3975 Johnson, R. E. (1994, August). Plasma-Induced Sputtering of an Atmosphere. *Sp.*
3976 *Sci. Rev.*, 69, 215-253. doi: 10.1007/BF02101697
- 3977 Johnson, R. E., Combi, M. R., Fox, J. L., Ip, W.-H., Leblanc, F., McGrath,
3978 M. A., ... Waite, J. H. (2008, August). Exospheres and Atmospheric
3979 Escape. *Space Sci Rev*, 139(1-4), 355–397. Retrieved 2011-05-27, from
3980 <http://www.springerlink.com/content/2275q53871236pp2/> doi:
3981 10.1007/s11214-008-9415-3
- 3982 Johnson, R. E., Michael, M., Sittler, E. C., Smith, H. T., Young, D. T., & Waite,
3983 J. H. (2010). Mass loss processes in Titan’s upper atmosphere. In *Titan from*
3984 *cassini-huygens* (pp. 373–391). Dordrecht: Springer Netherlands.
- 3985 Johnson, R. E., Schnellenberger, D., & Wong, M. C. (2000, January). The sput-
3986 tering of an oxygen thermosphere by energetic O+. *Journal of Geophysical Re-*
3987 *search*, 105, 1659–1670. Retrieved 2018-06-15, from [http://adsabs.harvard](http://adsabs.harvard.edu/abs/2000JGR...105.1659J)
3988 [.edu/abs/2000JGR...105.1659J](http://adsabs.harvard.edu/abs/2000JGR...105.1659J) doi: 10.1029/1999JE001058
- 3989 Johnson, R. E., Volkov, A. N., & Erwin, J. T. (2013a, dec). Erratum: “Molecular-
3990 Kinetic Simulations of Escape from the Ex-planet and Exoplanets: Criterion
3991 for Transonic Flow” . *Astrophys. J. Let.*, 779, L30. doi: 10.1088/2041-8205/
3992 779/2/L30
- 3993 Johnson, R. E., Volkov, A. N., & Erwin, J. T. (2013b, May). Molecular-kinetic Sim-
3994 ulations of Escape from the Ex-planet and Exoplanets: Criterion for Transonic
3995 Flow. *Astrophys. J. Let.*, 768, L4. doi: 10.1088/2041-8205/768/1/L4
- 3996 Johnstone, C., Khodachenko, M., Lüftinger, T., Kislyakova, K., Lammer, H., &
3997 Güdel, M. (2019). Extreme hydrodynamic losses of Earth-like atmospheres in
3998 the habitable zones of very active stars. *Astronomy & Astrophysics*, 624, L10.
- 3999 Johnstone, C. P., Güdel, M., Lammer, H., & Kislyakova, K. G. (2018, September).
4000 Upper atmospheres of terrestrial planets: Carbon dioxide cooling and the
4001 Earth’s thermospheric evolution. *Astronomy and Astrophysics*, 617, A107. doi:
4002 10.1051/0004-6361/201832776
- 4003 Juhász, Z. (2004). *Charge exchange processes that make comets radiate* (Unpub-
4004 lished doctoral dissertation). University of Groningen, P.O. Box 72, 9700 AB
4005 Groningen, The Netherlands.
- 4006 Kasting, J. F. (1988, June). Runaway and moist greenhouse atmospheres and the
4007 evolution of Earth and Venus. *Icarus*, 74, 472-494. doi: 10.1016/0019-1035(88)
4008 90116-9
- 4009 Kasting, J. F. (1993, February). Earth’s early atmosphere. *Science*, 259, 920-926.
4010 doi: 10.1126/science.259.5097.920
- 4011 Kasting, J. F., & Catling, D. (2003). Evolution of a habitable planet. *Annual*
4012 *Review of Astronomy and Astrophysics*, 41(1), 429-463. Retrieved from
4013 <http://dx.doi.org/10.1146/annurev.astro.41.071601.170049> doi:
4014 10.1146/annurev.astro.41.071601.170049
- 4015 Kasting, J. F., Egger, D. H., & Raeburn, S. P. (1993). Mantle redox evolution and
4016 the oxidation state of the archean atmosphere. *J. Geol.*, 101, 245–257.
- 4017 Kasting, J. F., & Ono, S. (2006, June). Palaeoclimates: the first two billion years.
4018 *Philos. Trans. R. Soc. Lond. B Biol. Sci.*, 361(1470), 917–929. doi: 10.1098/
4019 rstb.2006.1839
- 4020 Kasting, J. F., & Pollack, J. B. (1983, March). Loss of water from Venus. I.
4021 Hydrodynamic escape of hydrogen. *Icarus*, 53(3), 479–508. Retrieved

- 2012-12-14, from <http://www.sciencedirect.com/science/article/pii/S0019103583902129> doi: 10.1016/0019-1035(83)90212-9
- 4022
4023
4024 Kasting, J. F., Pollack, J. B., & Ackerman, T. P. (1984). Response of Earth's atmo-
4025 sphere to increases in solar flux and implications for loss of water from Venus.
4026 *Icarus*, 57(3), 335 - 355. Retrieved from <http://www.sciencedirect.com/science/article/pii/S0019103584901222> doi: [http://dx.doi.org/10.1016/0019-1035\(84\)90122-2](http://dx.doi.org/10.1016/0019-1035(84)90122-2)
4027
4028
- 4029 Kasting, J. F., Toon, O. B., & Pollack, J. B. (1988). How climate evolved on the ter-
4030 restrial planets. *Scientific American*, 258(2), 90-97. Retrieved from <http://www.jstor.org/stable/24988983>
4031
- 4032 Kasting, J. F., Whitmire, D. P., & Reynolds, R. T. (1993, January). Habitable
4033 Zones around Main Sequence Stars. *Icarus*, 101, 108-128. doi: 10.1006/icar
4034 .1993.1010
- 4035 Kavanagh, L., & Goldblatt, C. (2015). Using raindrops to constrain past atmo-
4036 spheric density. *Earth and Planetary Science Letters*, 413, 51 - 58. Re-
4037 trieved from <http://www.sciencedirect.com/science/article/pii/S0012821X14007936> doi: <http://dx.doi.org/10.1016/j.epsl.2014.12.032>
4038
- 4039 Kawaler, S. D. (1988, October). Angular momentum loss in low-mass stars. *Astro-
4040 phys. J.*, 333, 236-247. doi: 10.1086/166740
- 4041 Khazanov, G. V. (2010). *Kinetic theory of the inner magnetospheric plasma*
4042 (Vol. 372). Springer Science & Business Media.
- 4043 Khazanov, G. V., Khabibrakhmanov, I. K., & Krivorutsky, E. N. (2000). Interac-
4044 tion between an Alfvén wave and a particle undergoing acceleration along a
4045 magnetic field. *Physics of Plasmas*, 7, 1.
- 4046 Khazanov, G. V., Krivorutsky, E. N., & Liemohn, M. W. (2004, August). Nonlinear
4047 drift-kinetic equation in the presence of a circularly polarized wave. *Planetary
4048 and Space Science*, 52, 945.
- 4049 Khazanov, G. V., Liemohn, M. W., Krivorutsky, E. N., & Moore, T. E. (1998,
4050 April). Generalized kinetic description of a plasma in an arbitrary field-aligned
4051 potential energy structure. *Journal of Geophysical Research*, 103, 6871-6890.
4052 doi: 10.1029/97JA03436
- 4053 Khazanov, G. V., Liemohn, M. W., & Moore, T. E. (1997, April). Photoelectron ef-
4054 fects on the self-consistent potential in the collisionless polar wind. *Journal of
4055 Geophysical Research*, 102, 7509-7522. doi: 10.1029/96JA03343
- 4056 Killen, R. M., Hurley, D. M., & Farrell, W. M. (2012). The effect on the lunar ex-
4057 osphere of a coronal mass ejection passage. *Journal of Geophysical Research:
4058 Planets*, 117(E10). Retrieved from <https://agupubs.onlinelibrary.wiley.com/doi/abs/10.1029/2011JE004011> doi: 10.1029/2011JE004011
4059
- 4060 Kirkby, J., Curtius, J., Almeida, J., Dunne, E., Duplissy, J., Ehrhart, S., ... Kul-
4061 mala, M. (2011, August). Role of sulphuric acid, ammonia and galactic
4062 cosmic rays in atmospheric aerosol nucleation. *Nature*, 476, 429-433. doi:
4063 10.1038/nature10343
- 4064 Kirkby, J., Duplissy, J., Sengupta, K., Frege, C., Gordon, H., Williamson, C., ...
4065 Curtius, J. (2016, May). Ion-induced nucleation of pure biogenic particles.
4066 *Nature*, 533(7604), 521-526. doi: 10.1038/nature17953
- 4067 Kislyakova, K. G., Fossati, L., Johnstone, C. P., Holmström, M., Zaitsev, V. V., &
4068 Lammer, H. (2015, Feb). Stellar Wind Induced Soft X-Ray Emission from
4069 Close-in Exoplanets. *Astro. J. Lett.*, 799(2), L15. doi: 10.1088/2041-8205/799/
4070 2/L15
- 4071 Kislyakova, K. G., Holmström, M., Lammer, H., Odert, P., & Khodachenko, M. L.
4072 (2014, Nov). Magnetic moment and plasma environment of HD 209458b
4073 as determined from Ly α observations. *Science*, 346(6212), 981-984. doi:
4074 10.1126/science.1257829
- 4075 Kislyakova, K. G., Johnstone, C. P., Odert, P., Erkaev, N. V., Lammer, H.,
4076 Lüftinger, T., ... Güdel, M. (2014, February). Stellar wind interaction and

- pick-up ion escape of the Kepler-11 "super-Earths". *Astronomy and Astrophysics*, 562, A116. doi: 10.1051/0004-6361/201322933
- Kistler, L. M., & Mouikis, C. G. (2016, March). The inner magnetosphere ion composition and local time distribution over a solar cycle. *Journal of Geophysical Research (Space Physics)*, 121, 2009-2032. doi: 10.1002/2015JA021883
- Kitamura, N., Ogawa, Y., Nishimura, Y., Terada, N., Ono, T., Shinbori, A., ... Smilauer, J. (2011). Solar zenith angle dependence of plasma density and temperature in the polar cap ionosphere and low-altitude magnetosphere during geomagnetically quiet periods at solar maximum. *Journal of Geophysical Research*, 116(AO8227). doi: 10.1029/2011JA016631
- Kite, E. S., Williams, J.-P., Lucas, A., & Aharonson, O. (2014, May). Low palaeopressure of the martian atmosphere estimated from the size distribution of ancient craters. *Nature Geoscience*, 7, 335-339. doi: 10.1038/ngeo2137
- Kleinböhl, A., Willacy, K., Friedson, A. J., Chen, P., & Swain, M. R. (2018). Buildup of abiotic oxygen and ozone in moist atmospheres of temperate terrestrial exoplanets and its impact on the spectral fingerprint in transit observations. *Astrophys. J.*, 862(2), 92. Retrieved from <http://stacks.iop.org/0004-637X/862/i=2/a=92>
- Knauth, L. P., & Lowe, D. R. (2003). High Archean climatic temperature inferred from oxygen isotope geochemistry of cherts in the 3.5 Ga Swaziland Supergroup, South Africa. *Geological Society of America Bulletin*, 115(5), 566-580.
- Kopp, R. E., Kirschvink, J. L., Hilburn, I. A., & Nash, C. Z. (2005, August). The Paleoproterozoic snowball Earth: A climate disaster triggered by the evolution of oxygenic photosynthesis. *Proceedings of the National Academy of Science*, 102, 11131-11136. doi: 10.1073/pnas.0504878102
- Koskinen, T. T., Lavvas, P., Harris, M. J., & Yelle, R. V. (2014, March). Thermal escape from extrasolar giant planets. *Philosophical Transactions of the Royal Society of London Series A*, 372, 20130089-20130089. doi: 10.1098/rsta.2013.0089
- Kozelov, B. V., Ivanov, V. E., & Sergienko, T. I. (1994, October). Simplified algorithm for precise calculation of spatial distributions in combined electron-proton-hydrogen atom aurora. *Geomagnetism and Aeronomy*, 34, 81-85.
- Krasnopolsky, V. A. (2014, July). Chemical composition of Titan's atmosphere and ionosphere: Observations and the photochemical model. *Icarus*, 236, 83-91. doi: 10.1016/j.icarus.2014.03.041
- Krasnopolsky, V. A., Mumma, M. J., Abbott, M., Flynn, B. C., Meech, K. J., Yeomans, D. K., ... Cosmovici, C. B. (1997, September). Detection of Soft X-rays and a Sensitive Search for Noble Gases in Comet Hale-Bopp (C/1995 O1). *Science*, 277, 1488-1491. doi: 10.1126/science.277.5331.1488
- Krauss, S., Fichtinger, B., Lammer, H., Hausleitner, W., Kulikov, Y. N., Ribas, I., ... Hanslmeier, A. (2012). Solar flares as proxy for the young Sun: satellite observed thermosphere response to an X17.2 flare of Earth's upper atmosphere. *Annales Geophysicae*, 30(8), 1129-1141. Retrieved from <http://www.ann-geophys.net/30/1129/2012/> doi: 10.5194/angeo-30-1129-2012
- Kreidberg, L., Koll, D. D. B., Morley, C., Hu, R., Schaefer, L., Deming, D., ... Vanderspek, R. (2019, August). Absence of a thick atmosphere on the terrestrial exoplanet LHS 3844b. *Nature*, 1-4. Retrieved 2019-08-27, from <https://www.nature.com/articles/s41586-019-1497-4> doi: 10.1038/s41586-019-1497-4
- Kretzschmar, M., Lilensten, J., & Aboudarham, J. (2004, May). Variability of the EUV quiet Sun emission and reference spectrum using SUMER. *Astronomy and Astrophysics*, 419, 345-356. doi: 10.1051/0004-6361:20040068
- Krissansen-Totton, J., Olson, S., & Catling, D. C. (2018, January). Disequilibrium biosignatures over Earth history and implications for detecting exoplanet life. *Science Advances*, 4, eaao5747. doi: 10.1126/sciadv.aao5747

- 4132 Kuhn, W. R., & Atreya, S. K. (1979). Ammonia photolysis and the greenhouse ef-
4133 fect in the primordial atmosphere of the earth. *Icarus*, *37*, 207–213.
- 4134 Kumar, S., Hunten, D., & Pollack, J. (1983). Nonthermal escape of hydrogen and
4135 deuterium from Venus and implications for loss of water. *Icarus*, *55*(3), 369 -
4136 389. Retrieved from [http://www.sciencedirect.com/science/article/pii/](http://www.sciencedirect.com/science/article/pii/S0019103583901094)
4137 [0019103583901094](http://www.sciencedirect.com/science/article/pii/S0019103583901094) doi: [http://dx.doi.org/10.1016/0019-1035\(83\)90109-4](http://dx.doi.org/10.1016/0019-1035(83)90109-4)
- 4138 Kun, L., Y., W., M., A., A., E., S., H., A., K. E., ... X., W. W. (2017). Cold ion
4139 outflow modulated by the solar wind energy input and tilt of the geomagnetic
4140 dipole. *Journal of Geophysical Research: Space Physics*, *122*(10), 10,658-
4141 10,668. Retrieved from [https://agupubs.onlinelibrary.wiley.com/doi/](https://agupubs.onlinelibrary.wiley.com/doi/abs/10.1002/2017JA024642)
4142 [abs/10.1002/2017JA024642](https://agupubs.onlinelibrary.wiley.com/doi/abs/10.1002/2017JA024642) doi: 10.1002/2017JA024642
- 4143 Kurokawa, H., Kurosawa, K., & Usui, T. (2018). A lower limit of atmospheric pres-
4144 sure on early Mars inferred from nitrogen and argon isotopic compositions.
4145 *Icarus*, *299*, 443–459.
- 4146 Lammer, H., Bredehöft, J. H., Coustenis, A., Khodachenko, M. L., Kaltene-
4147 ger, L., Grasset, O., ... Rauer, H. (2009, Jun 01). What makes a planet
4148 habitable? *The Astronomy and Astrophysics Review*, *17*(2), 181–249.
4149 Retrieved from <https://doi.org/10.1007/s00159-009-0019-z> doi:
4150 10.1007/s00159-009-0019-z
- 4151 Lammer, H., Kasting, J. F., Chassefière, E., Johnson, R. E., Kulikov, Y. N., & Tian,
4152 F. (2008, August). Atmospheric Escape and Evolution of Terrestrial Plan-
4153 ets and Satellites. *Space Sci Rev*, *139*(1-4), 399–436. Retrieved 2011-05-27,
4154 from <http://www.springerlink.com/content/a7n32493705m0021/> doi:
4155 10.1007/s11214-008-9413-5
- 4156 Lammer, H., Lichtenegger, H., Biernat, H., Erkaev, N., Arshukova, I., Kolb, C.,
4157 ... Baumjohann, W. (2006). Loss of hydrogen and oxygen from the up-
4158 per atmosphere of venus. *Planetary and Space Science*, *54*(13), 1445 - 1456.
4159 Retrieved from [http://www.sciencedirect.com/science/article/pii/](http://www.sciencedirect.com/science/article/pii/S003206330600170X)
4160 [S003206330600170X](http://www.sciencedirect.com/science/article/pii/S003206330600170X) (The Planet Venus and the Venus Express Mission) doi:
4161 <https://doi.org/10.1016/j.pss.2006.04.022>
- 4162 Lammer, H., Lichtenegger, H. I. M., Kolb, C., Ribas, I., Guinan, E. F., Abart, R., &
4163 Bauer, S. J. (2003, September). Loss of water from Mars: Implications for the
4164 oxidation of the soil. *Icarus*, *165*, 9-25. doi: 10.1016/S0019-1035(03)00170-2
- 4165 Lammer, H., Selsis, F., Ribas, I., Guinan, E. F., Bauer, S. J., & Weiss, W. W. (2003,
4166 December). Atmospheric Loss of Exoplanets Resulting from Stellar X-Ray and
4167 Extreme-Ultraviolet Heating. *Astrophys. J. Let.*, *598*, L121-L124. doi: 10
4168 .1086/380815
- 4169 Lanci, L., Galeotti, S., Grimani, C., & Huber, M. (2020). Evidence against a long-
4170 term control on earth climate by galactic cosmic ray flux. *Global and Planetary*
4171 *Change*, *185*, 103095. Retrieved from [http://www.sciencedirect.com/](http://www.sciencedirect.com/science/article/pii/S0921818119305806)
4172 [science/article/pii/S0921818119305806](http://www.sciencedirect.com/science/article/pii/S0921818119305806) doi: [https://doi.org/10.1016/](https://doi.org/10.1016/j.gloplacha.2019.103095)
4173 [j.gloplacha.2019.103095](https://doi.org/10.1016/j.gloplacha.2019.103095)
- 4174 Laneuville, M., Kameya, M., & Cleaves, H. J. (2018). Earth without life: A sys-
4175 tems model of a global abiotic nitrogen cycle. *Astrobiology*, *18*(7), 897-914. Re-
4176 trieved from <https://doi.org/10.1089/ast.2017.1700> (PMID: 29634320)
4177 doi: 10.1089/ast.2017.1700
- 4178 Lara, L. M., Lellouch, E., López-Moreno, J. J., & Rodrigo, R. (1996, October). Ver-
4179 tical distribution of Titan's atmospheric neutral constituents. *J. Geophys. Res.*,
4180 *101*, 23261-23283. doi: 10.1029/96JE02036
- 4181 Lazio, T. J. W., & Farrell, W. M. (2007, October). Magnetospheric Emissions from
4182 the Planet Orbiting τ Bootis: A Multiepoch Search. *Astrophys. J.*, *668*, 1182-
4183 1188. doi: 10.1086/519730
- 4184 Lean, J. L., Warren, H. P., Mariska, J. T., & Bishop, J. (2003, February). A new
4185 model of solar EUV irradiance variability 2. Comparisons with empirical mod-
4186 els and observations and implications for space weather. *Journal of Geophysi-*

- 4187 *cal Research (Space Physics)*, 108, 1059-+. doi: 10.1029/2001JA009238
- 4188 Leblanc, F., & Johnson, R. E. (2001, May). Sputtering of the Martian atmosphere
- 4189 by solar wind pick-up ions. *Planetary and Space Science*, 49(6), 645–656. Re-
- 4190 trieved 2016-01-27, from [http://www.sciencedirect.com/science/article/](http://www.sciencedirect.com/science/article/pii/S0032063301000034)
- 4191 [pii/S0032063301000034](http://www.sciencedirect.com/science/article/pii/S0032063301000034) doi: 10.1016/S0032-0633(01)00003-4
- 4192 Leblanc, F., & Johnson, R. E. (2002, February). Role of molecular species in pickup
- 4193 ion sputtering of the Martian atmosphere. *J. Geophys. Res.*, 107(E2), 5–1.
- 4194 Retrieved 2016-01-27, from [http://onlinelibrary.wiley.com/doi/10.1029/](http://onlinelibrary.wiley.com/doi/10.1029/2000JE001473/abstract)
- 4195 [2000JE001473/abstract](http://onlinelibrary.wiley.com/doi/10.1029/2000JE001473/abstract) doi: 10.1029/2000JE001473
- 4196 Leblanc, F., Martinez, A., Chaufray, J. Y., Modolo, R., Hara, T., Luhmann, J., ...
- 4197 Jakosky, B. (2018). On Mars’s atmospheric sputtering after MAVEN’s first
- 4198 martian year of measurements. *Geophysical Research Letters*, 45(10), 4685-
- 4199 4691. Retrieved from [https://agupubs.onlinelibrary.wiley.com/doi/abs/](https://agupubs.onlinelibrary.wiley.com/doi/abs/10.1002/2018GL077199)
- 4200 [10.1002/2018GL077199](https://agupubs.onlinelibrary.wiley.com/doi/abs/10.1002/2018GL077199) doi: 10.1002/2018GL077199
- 4201 Leblanc, F., Modolo, R., Curry, S., Luhmann, J., Lillis, R., Chaufray, J. Y., ...
- 4202 Jakosky, B. (2015). Mars heavy ion precipitating flux as measured by Mars
- 4203 Atmosphere and Volatile Evolution. *Geophysical Research Letters*, 42(21),
- 4204 9135-9141. Retrieved from [https://agupubs.onlinelibrary.wiley.com/](https://agupubs.onlinelibrary.wiley.com/doi/abs/10.1002/2015GL066170)
- 4205 [doi/abs/10.1002/2015GL066170](https://agupubs.onlinelibrary.wiley.com/doi/abs/10.1002/2015GL066170) doi: 10.1002/2015GL066170
- 4206 Lecavelier Des Etangs, A. (2007, January). A diagram to determine the evaporation
- 4207 status of extrasolar planets. *Astronomy and Astrophysics*, 461, 1185-1193. doi:
- 4208 10.1051/0004-6361:20065014
- 4209 Ledvina, S. A., Ma, Y. J., & Kallio, E. (2008, Aug). Modeling and Simulating Flow-
- 4210 ing Plasmas and Related Phenomena. *Space. Sci. Rev.*, 139(1-4), 143-189. doi:
- 4211 10.1007/s11214-008-9384-6
- 4212 Lee, C., Jakosky, B., Luhmann, J., Brain, D., Mays, M., Hassler, D., ... others
- 4213 (2018). Observations and impacts of the 10 September 2017 solar events at
- 4214 Mars: An overview and synthesis of the initial results. *Geophysical Research*
- 4215 *Letters*, 45(17), 8871–8885.
- 4216 Lee, C. O., Hara, T., Halekas, J. S., Thiemann, E., Chamberlin, P., Eparvier, F.,
- 4217 ... Jakosky, B. M. (2017). MAVEN observations of the solar cycle 24 space
- 4218 weather conditions at Mars. *Journal of Geophysical Research: Space Physics*,
- 4219 122(3), 2768-2794. Retrieved from [https://agupubs.onlinelibrary.wiley](https://agupubs.onlinelibrary.wiley.com/doi/abs/10.1002/2016JA023495)
- 4220 [.com/doi/abs/10.1002/2016JA023495](https://agupubs.onlinelibrary.wiley.com/doi/abs/10.1002/2016JA023495) doi: 10.1002/2016JA023495
- 4221 Lee, J. S., Doering, J. P., Potemra, T. A., & Brace, L. H. (1980, October). Mea-
- 4222 surements of the ambient photoelectron spectrum from atmosphere explorer:
- 4223 II. AE-E measurements from 300 to 1000 km during solar minimum conditions.
- 4224 *Plan. Sp. Sc.*, 28, 973-996. doi: 10.1016/0032-0633(80)90059-8
- 4225 Lee, Y., Combi, M. R., Tennishev, V., Bougher, S. W., Deighan, J., Schneider,
- 4226 N. M., ... Jakosky, B. M. (2015, January). A comparison of 3-D model
- 4227 predictions of Mars’ oxygen corona with early MAVEN IUVS observations.
- 4228 *Geophysical Research Letters*, 2015GL065291. Retrieved 2015-11-06, from
- 4229 <http://onlinelibrary.wiley.com/doi/10.1002/2015GL065291/abstract>
- 4230 doi: 10.1002/2015GL065291
- 4231 Lemaire, J. (1972). Effect of escaping photoelectrons in a polar exospheric model.
- 4232 *Space Research*, 12, 1413-1416.
- 4233 Lennartsson, W. (1989, April). Energetic (0.1- to 16-keV/e) magnetospheric ion
- 4234 composition at different levels of solar F10.7. *J. Geophys. Res.*, 94, 3600-3610.
- 4235 doi: 10.1029/JA094iA04p03600
- 4236 Lennartsson, W., & Shelley, E. G. (1986, March). Survey of 0.1- to 16-keV/e
- 4237 plasma sheet ion composition. *J. Geophys. Res.*, 91, 3061-3076. doi:
- 4238 10.1029/JA091iA03p03061
- 4239 Lewis, B. R., Vardavas, I. M., & Carver, J. H. (1983, June). The aeronomic dissoci-
- 4240 ation of water vapor by solar H Lyman-alpha radiation. *J. Geophys. Res.*, 88,
- 4241 4935-4940. doi: 10.1029/JA088iA06p04935

- 4242 Lewkow, N. R., & Kharchenko, V. (2014, August). Precipitation of Energetic
4243 Neutral Atoms and Induced Non-thermal Escape Fluxes from the Martian
4244 Atmosphere. *Astrophys. J.*, *790*, 98. doi: 10.1088/0004-637X/790/2/98
- 4245 Li, X., & Temerin, M. (1993, January). Ponderomotive effects on ion acceleration in
4246 the auroral zone. *Geoph. Res. Let.*, *20*, 13-16. doi: 10.1029/92GL03011
- 4247 Liang, M.-C., Hartman, H., Kopp, R. E., Kirschvink, J. L., & Yung, Y. L. (2006,
4248 December). Production of hydrogen peroxide in the atmosphere of a Snowball
4249 Earth and the origin of oxygenic photosynthesis. *Proceedings of the National
4250 Academy of Science*, *103*, 18896-18899. doi: 10.1073/pnas.0608839103
- 4251 Liang, M.-C., Heays, A. N., Lewis, B. R., Gibson, S. T., & Yung, Y. L. (2007, Aug).
4252 Source of Nitrogen Isotope Anomaly in HCN in the Atmosphere of Titan. *As-
4253 trophys. J.*, *664*, L115-L118. doi: 10.1086/520881
- 4254 Lie-Svendsen, O., Rees, M. H., & Stamnes, K. (1992, December). Helium escape
4255 from the Earth's atmosphere - The charge exchange mechanism revisited.
4256 *Plan. Sp. Sci.*, *40*, 1639-1662. doi: 10.1016/0032-0633(92)90123-6
- 4257 Liemohn, M. W., Johnson, B. C., Fränz, M., & Barabash, S. (2014). Mars Ex-
4258 press observations of high altitude planetary ion beams and their relation
4259 to the "energetic plume" loss channel. *Journal of Geophysical Research:
4260 Space Physics*, *119*(12), 9702–9713. Retrieved 2018-06-04, from [https://
4261 agupubs.onlinelibrary.wiley.com/doi/abs/10.1002/2014JA019994](https://agupubs.onlinelibrary.wiley.com/doi/abs/10.1002/2014JA019994) doi:
4262 10.1002/2014JA019994
- 4263 Lilensten, J., Simon Wedlund, C., Barthélémy, M., Thissen, R., Ehrenreich,
4264 D., Gronoff, G., & Witasse, O. (2013, January). Dications and ther-
4265 mal ions in planetary atmospheric escape. *Icarus*, *222*, 169-187. doi:
4266 10.1016/j.icarus.2012.09.034
- 4267 Lilensten, J., Witasse, O., Simon, C., Soldi-Lose, H., Dutuit, O., Thissen, R., & Al-
4268 caraz, C. (2005). Prediction of a N_2^{++} layer in the upper atmosphere of Titan.
4269 *Geophysical research letters*, *32*(3).
- 4270 Lillis, R. J., Brain, D. A., Bougher, S. W., Leblanc, F., Luhmann, J. G., Jakosky,
4271 B. M., ... Lin, R. P. (2015, September). Characterizing Atmospheric Escape
4272 from Mars Today and Through Time, with MAVEN. *Space Sci Rev*, *195*(1-4),
4273 357–422. Retrieved 2016-01-27, from [http://link.springer.com/article/
4274 10.1007/s11214-015-0165-8](http://link.springer.com/article/10.1007/s11214-015-0165-8) doi: 10.1007/s11214-015-0165-8
- 4275 Lillis, R. J., Deighan, J., Fox, J. L., Bougher, S. W., Lee, Y., Combi, M. R., ...
4276 Chaufray, J.-Y. (2017). Photochemical escape of oxygen from Mars: First
4277 results from MAVEN in situ data. *Journal of Geophysical Research: Space
4278 Physics*, *122*(3), 3815-3836. Retrieved from [https://agupubs.onlinelibrary
4279 .wiley.com/doi/abs/10.1002/2016JA023525](https://agupubs.onlinelibrary.wiley.com/doi/abs/10.1002/2016JA023525) doi: 10.1002/2016JA023525
- 4280 Lindsay, B., & Stebbings, R. (2005). Charge transfer cross sections for energetic
4281 neutral atom data analysis. *Journal of Geophysical Research: Space Physics*,
4282 *110*(A12).
- 4283 Linsky, J. (2019). *Host Stars and their Effects on Exoplanet Atmospheres : An In-
4284 troduutory Overview*. Springer International Publishing. Retrieved 2019-08-01,
4285 from <https://www.springer.com/us/book/9783030114510>
- 4286 Linsky, J. L., Yang, H., France, K., Froning, C. S., Green, J. C., Stocke, J. T.,
4287 & Osterman, S. N. (2010, July). Observations of Mass Loss from the
4288 Transiting Exoplanet HD 209458b. *Astrophys. J.*, *717*, 1291-1299. doi:
4289 10.1088/0004-637X/717/2/1291
- 4290 Lionello, R., Velli, M., Downs, C., Linker, J. A., & Mikić, Z. (2014, Decem-
4291 ber). Application of a Solar Wind Model Driven by Turbulence Dissipa-
4292 tion to a 2D Magnetic Field Configuration. *Astrophys. J.*, *796*, 111. doi:
4293 10.1088/0004-637X/796/2/111
- 4294 Liu, X. M., Rivière, E. D., Marécal, V., Durrý, G., Hamdouni, A., Arteta, J., &
4295 Khaykin, S. (2010, September). Stratospheric water vapour budget and
4296 convection overshooting the tropopause: modelling study from SCOUT-

- 4297 AMMA. *Atmospheric Chemistry & Physics*, 10, 8267-8286. doi:
4298 10.5194/acp-10-8267-2010
- 4299 Livengood, T. A., Kostiuk, T., Hewagama, T., Smith, R. L., Fast, K. E., Annen,
4300 J. N., & Delgado, J. D. (2020). Evidence for diurnally varying enrichment
4301 of heavy oxygen in Mars atmosphere. *Icarus*, 335, 113387. Retrieved from
4302 <http://www.sciencedirect.com/science/article/pii/S0019103518307097>
4303 doi: <https://doi.org/10.1016/j.icarus.2019.113387>
- 4304 Loison, J., Hébrard, E., Dobrijevic, M., Hickson, K., Caralp, F., Hue, V., ...
4305 Bénilan, Y. (2015). The neutral photochemistry of nitriles, amines and
4306 imines in the atmosphere of titan. *Icarus*, 247, 218 - 247. Retrieved from
4307 <http://www.sciencedirect.com/science/article/pii/S0019103514005144>
4308 doi: <https://doi.org/10.1016/j.icarus.2014.09.039>
- 4309 Lopez, E. D. (2017, November). Born dry in the photoevaporation desert: Kepler's
4310 ultra-short-period planets formed water-poor. *Mon. Not. R. Astron. Soc.*, 472,
4311 245-253. doi: 10.1093/mnras/stx1558
- 4312 Lorenz, R. D., McKay, C. P., & Lunine, J. I. (1997). Photochemically driven
4313 collapse of Titan's atmosphere. *Science*, 275(5300), 642-644. Retrieved
4314 from <http://science.sciencemag.org/content/275/5300/642> doi:
4315 10.1126/science.275.5300.642
- 4316 Lorenz, R. D., Mitchell, K. L., Kirk, R. L., Hayes, A. G., Aharonson, O., Zebker,
4317 H. A., ... Stofan, E. R. (2008). Titan's inventory of organic surface materials.
4318 *Geophys. Res. Lett.*, 35(2), n/a-n/a. Retrieved from [http://dx.doi.org/](http://dx.doi.org/10.1029/2007GL032118)
4319 [10.1029/2007GL032118](http://dx.doi.org/10.1029/2007GL032118) (L02206) doi: 10.1029/2007GL032118
- 4320 Lu, G., Baker, D. N., McPherron, R. L., Farrugia, C. J., Lummerzheim, D., Ruo-
4321 honiemi, J. M., ... Greenwald, R. (1998). Global energy deposition during the
4322 January 1997 magnetic cloud event. *J. Geophys. Res.*, 103(A6), 11685.
- 4323 Luger, R. (2017). *On the evolution, detection, and characterization of small planets*
4324 *in the habitable zones of M dwarfs* (Unpublished doctoral dissertation). Uni-
4325 versity of Washington.
- 4326 Luhmann, J., Fedorov, A., Barabash, S., Carlsson, E., Futaana, Y., Zhang, T., ...
4327 Brain, D. (2008). Venus Express observations of atmospheric oxygen escape
4328 during the passage of several coronal mass ejections. *Journal of Geophysical*
4329 *Research: Planets*, 113(E9).
- 4330 Luhmann, J. G., Johnson, R. E., & Zhang, M. H. G. (1992, November). Evo-
4331 lutionary impact of sputtering of the Martian atmosphere by O⁺ pickup
4332 ions. *Geophys. Res. Lett.*, 19(21), 2151-2154. Retrieved 2016-01-27, from
4333 <http://onlinelibrary.wiley.com/doi/10.1029/92GL02485/abstract> doi:
4334 10.1029/92GL02485
- 4335 Lundin, R., & Guglielmi, A. (2006, December). Ponderomotive Forces in Cosmos.
4336 *Space Sci. Rev.*, 127, 1-116. doi: 10.1007/s11214-006-8314-8
- 4337 Lynch, C. R., Murphy, T., Lenc, E., & Kaplan, D. L. (2018, May). The detectability
4338 of radio emission from exoplanets. *MNRAS*. doi: 10.1093/mnras/sty1138
- 4339 Madeleine, J.-B., Forget, F., Head, J. W., Levrard, B., Montmessin, F., & Mil-
4340 lhour, E. (2009). Amazonian northern mid-latitude glaciation on Mars:
4341 A proposed climate scenario. *Icarus*, 203(2), 390 - 405. Retrieved from
4342 <http://www.sciencedirect.com/science/article/pii/S0019103509001936>
4343 doi: <http://dx.doi.org/10.1016/j.icarus.2009.04.037>
- 4344 Madhusudhan, N., Agundez, M., Moses, J., & Hu, Y. (2016). Exoplanetary at-
4345 mospheres – chemistry, formation, conditions, and habitability. *Space Sci Rev.*,
4346 205(1), 285-348. doi: 10.1007/s11214-016-0254-3
- 4347 Magee, B. A., Waite, J. H., Mandt, K. E., Westlake, J., Bell, J., & Gell, D. A.
4348 (2009). INMS-derived composition of Titan's upper atmosphere: Analysis
4349 methods and model comparison. *Planetary and Space Science*, 57(14-15),
4350 1895-1916. doi: 10.1016/j.pss.2009.06.016
- 4351 Maggiolo, R., & Kistler, L. M. (2014, April). Spatial variation in the plasma

- 4352 sheet composition: Dependence on geomagnetic and solar activity. *Jour-*
 4353 *nal of Geophysical Research (Space Physics)*, 119, 2836-2857. doi: 10.1002/
 4354 2013JA019517
- 4355 Maltagliati, L., Montmessin, F., Korablev, O., Fedorova, A., Forget, F., Määttänen,
 4356 A., ... Bertaux, J.-L. (2013, April). Annual survey of water vapor verti-
 4357 cal distribution and water-aerosol coupling in the martian atmosphere ob-
 4358 served by SPICAM/MEX solar occultations. *Icarus*, 223, 942-962. doi:
 4359 10.1016/j.icarus.2012.12.012
- 4360 Mandt, K., Mousis, O., & Chassefière, E. (2015, Jul). Comparative planetology of
 4361 the history of nitrogen isotopes in the atmospheres of Titan and Mars. *Icarus*,
 4362 254, 259-261. doi: 10.1016/j.icarus.2015.03.025
- 4363 Mandt, K. E., Waite Jr., J. H., Lewis, W., Magee, B., Bell, J., Lunine, J., ...
 4364 Cordier, D. (2009, December). Isotopic evolution of the major con-
 4365 stituents of Titan's atmosphere based on Cassini data. *Planetary and*
 4366 *Space Science*, 57(14-15), 1917-1930. Retrieved 2012-02-24, from [http://](http://www.sciencedirect.com/science/article/pii/S0032063309001640)
 4367 www.sciencedirect.com/science/article/pii/S0032063309001640 doi:
 4368 10.1016/j.pss.2009.06.005
- 4369 Mansfield, M., Kite, E. S., & Mischna, M. A. (2017). Effect of Mars Atmospheric
 4370 Loss on Snow Melt Potential in a 3.5 Gyr Mars Climate Evolution Model.
 4371 *Journal of Geophysical Research: Planets*, 123(4), 794-806. Retrieved 2018-
 4372 06-12, from [https://agupubs.onlinelibrary.wiley.com/doi/abs/10.1002/](https://agupubs.onlinelibrary.wiley.com/doi/abs/10.1002/2017JE005422)
 4373 [2017JE005422](https://agupubs.onlinelibrary.wiley.com/doi/abs/10.1002/2017JE005422) doi: 10.1002/2017JE005422
- 4374 Marcq, E., Bertaux, J.-L., Montmessin, F., & Belyaev, D. (2013, Jan). Variations
 4375 of sulphur dioxide at the cloud top of Venus's dynamic atmosphere. *Nature*
 4376 *Geosci*, 6(1), 25-28. Retrieved from <http://dx.doi.org/10.1038/ngeo1650>
 4377 doi: 10.1038/ngeo1650
- 4378 Marcq, E., Mills, F. P., Parkinson, C. D., & Vandaele, A. C. (2018, February). Com-
 4379 position and Chemistry of the Neutral Atmosphere of Venus. *Space Sci. Rev.*,
 4380 214, 10. doi: 10.1007/s11214-017-0438-5
- 4381 Marty, B. (2012, January). The origins and concentrations of water, carbon, nitro-
 4382 gen and noble gases on Earth. *Earth and Planetary Science Letters*, 313, 56-
 4383 66. doi: 10.1016/j.epsl.2011.10.040
- 4384 Mason, E., & Marrero, T. (1970). The diffusion of atoms and molecules. In *Advances*
 4385 *in atomic and molecular physics* (Vol. 6, pp. 155-232). Elsevier.
- 4386 Matsakos, T., Uribe, A., & Königl, A. (2015, June). Classification of magnetized
 4387 star-planet interactions: bow shocks, tails, and inspiraling flows. *A&A*, 578,
 4388 A6. doi: 10.1051/0004-6361/201425593
- 4389 Mayor, M., & Queloz, D. (1995). A Jupiter-mass companion to a solar-type star.
 4390 *Nature*, 378(6555), 355.
- 4391 Mayyasi, M., Bhattacharyya, D., Clarke, J., Catalano, A., Benna, M., Mahaffy,
 4392 P., ... Jakosky, B. (2018). Significant space weather impact on the escape
 4393 of hydrogen from Mars. *Geophysical Research Letters*, 45(17), 8844-8852.
 4394 Retrieved from [https://agupubs.onlinelibrary.wiley.com/doi/abs/](https://agupubs.onlinelibrary.wiley.com/doi/abs/10.1029/2018GL077727)
 4395 [10.1029/2018GL077727](https://agupubs.onlinelibrary.wiley.com/doi/abs/10.1029/2018GL077727) doi: 10.1029/2018GL077727
- 4396 McConnell, J. C., Sandel, B. R., & Broadfoot, A. L. (1981). Voyager UV spectrom-
 4397 eter observations of He 584 Å dayglow at Jupiter. *Planetary and Space Science*,
 4398 29(3), 283-292.
- 4399 McKay, C., Coustenis, A., Samuelson, R., Lemmon, M., Lorenz, R., Cabane, M.,
 4400 ... Drossart, P. (2001). Physical properties of the organic aerosols and
 4401 clouds on Titan. *Planetary and Space Science*, 49(1), 79 - 99. Retrieved from
 4402 <http://www.sciencedirect.com/science/article/pii/S0032063300000519>
 4403 doi: [https://doi.org/10.1016/S0032-0633\(00\)00051-9](https://doi.org/10.1016/S0032-0633(00)00051-9)
- 4404 Meadows, V. S., & Crisp, D. (1996). Ground-based near-infrared observations of the
 4405 Venus nightside: The thermal structure and water abundance near the surface.
 4406 *Journal of Geophysical Research: Planets*, 101(E2), 4595-4622. Retrieved from

- 4407 <http://dx.doi.org/10.1029/95JE03567> doi: 10.1029/95JE03567
- 4408 Meibom, S., Barnes, S. A., Platais, I., Gilliland, R. L., Latham, D. W., & Mathieu,
4409 R. D. (2015, January). A spin-down clock for cool stars from observations of a
4410 2.5-billion-year-old cluster. *Nature*, *517*, 589-591. doi: 10.1038/nature14118
- 4411 Mendillo, M. (2019, 02). The ionospheres of planets and exoplanets. *Astronomy &*
4412 *Geophysics*, *60*(1), 1.25-1.30. Retrieved from [https://dx.doi.org/10.1093/](https://dx.doi.org/10.1093/astrogeo/atz047)
4413 [astrogeo/atz047](https://dx.doi.org/10.1093/astrogeo/atz047) doi: 10.1093/astrogeo/atz047
- 4414 Merryfield, W. J., & Shizgal, B. D. (1994, May). Discrete velocity model for an
4415 escaping single-component atmosphere. *Plan. Sp. Sci.*, *42*, 409-419. doi: 10
4416 .1016/0032-0633(94)90130-9
- 4417 Mertens, C. J., Fernandez, J. R., Xu, X., Evans, D. S., Mlynczak, M. G., & Russell,
4418 J. M. (2008, September). A new source of auroral infrared emission observed
4419 by TIMED/SABER. *Geophysical Research Letters*, *35*, 17106. Retrieved
4420 2011-12-30, from <http://adsabs.harvard.edu/abs/2008GeoRL..3517106M>
- 4421 Mertens, C. J., Russell, J. M., Mlynczak, M. G., She, C.-Y., Schmidlin, F. J.,
4422 Goldberg, R. A., ... Xu, X. (2009). Kinetic temperature and carbon diox-
4423 ide from broadband infrared limb emission measurements taken from the
4424 TIMED/SABER instrument. *Advances in Space Research, Volume 43, Issue 1,*
4425 *p. 15-27., 43.* doi: 10.1016/j.asr.2008.04.017
- 4426 Micela, G., Sciortino, S., Serio, S., Vaiana, G. S., Bookbinder, J., Golub, L., ...
4427 Rosner, R. (1985, May). Einstein X-ray survey of the Pleiades : the depen-
4428 dence of X-ray emission on stellar age. *Astrophys. J.*, *292*, 172-180. doi:
4429 10.1086/163143
- 4430 Michaels, T. I., Colaprete, A., & Rafkin, S. C. R. (2006, August). Significant ver-
4431 tical water transport by mountain-induced circulations on Mars. *Geophys. Res.*
4432 *Lett.*, *33*, 16201. doi: 10.1029/2006GL026562
- 4433 Mihalas, D., & Mihalas, B. W. (1984). *Foundations of radiation hydrodynamics.*
4434 New York, Oxford University Press, 1984, 731 p.
- 4435 Miller, R. H., Rasmussen, C. E., Combi, M. R., Gombosi, T. I., & Winske, D.
4436 (1995). Ponderomotive acceleration in the auroral region: A kinetic simu-
4437 lation. *Journal of Geophysical Research: Space Physics*, *100*(A12), 23901-
4438 23916. Retrieved from <http://dx.doi.org/10.1029/95JA01908> doi:
4439 10.1029/95JA01908
- 4440 Mojzsis, S. J., Harrison, T. M., & Pidgeon, R. T. (2001, January). Oxygen-isotope
4441 evidence from ancient zircons for liquid water at the earth's surface 4,300 myr
4442 ago. *Nature*, *409*, 178-181. doi: 110.1038/35051557
- 4443 Moore, T. E., Chappell, C. R., Chandler, M. O., Craven, P. D., Giles, B. L., Pollock,
4444 C. J., ... Mozer, F. S. (1997, July). High-altitude observations of the polar
4445 wind. *Science*, *277*, 349-351. doi: 10.1126/science.277.5324.349
- 4446 Moore, W. B., Lenardic, A., Jellinek, A. M., Johnson, C. L., Goldblatt, C.,
4447 & Lorenz, R. D. (2017, February). How habitable zones and super-
4448 Earths lead us astray. *Nature Astronomy*, *1*(2), 0043. Retrieved 2017-
4449 02-06, from <http://www.nature.com/articles/s41550-017-0043> doi:
4450 10.1038/s41550-017-0043
- 4451 Moore, W. B., Simon, J. I., & Webb, A. A. G. (2017, September). Heat-pipe plan-
4452 ets. *Earth and Planetary Science Letters*, *474*, 13-19. doi: 10.1016/j.epsl.2017
4453 .06.015
- 4454 Moore, W. B., & Webb, A. A. G. (2013, September). Heat-pipe Earth. *Nature*, *501*,
4455 501-505. doi: 10.1038/nature12473
- 4456 Moschou, S.-P., Drake, J. J., Cohen, O., Alvarado-Gómez, J. D., Garraffo, C., &
4457 Frascetti, F. (2019, may). The stellar CME-flare relation: What do his-
4458 toric observations reveal? *The Astrophysical Journal*, *877*(2), 105. Re-
4459 trieved from <https://doi.org/10.3847/2F1538-4357/2Fab1b37> doi:
4460 10.3847/1538-4357/ab1b37
- 4461 Mumma, M. J. (1993). Natural lasers and masers in the solar system. In

- 4462 A. W. Clegg & G. E. Nedoluha (Eds.), *Astrophysical masers* (pp. 455–467).
 4463 Berlin, Heidelberg: Springer Berlin Heidelberg.
- 4464 Mumma, M. J., Villanueva, G. L., Novak, R. E., Hewagama, T., Bonev, B. P.,
 4465 DiSanti, M. A., ... Smith, M. D. (2009). Strong release of methane on
 4466 Mars in northern summer 2003. *Science*, *323*(5917), 1041–1045. Retrieved
 4467 from <http://science.sciencemag.org/content/323/5917/1041> doi:
 4468 10.1126/science.1165243
- 4469 Murray-Clay, R. A., Chiang, E. I., & Murray, N. (2009, March). Atmospheric Es-
 4470 cape From Hot Jupiters. *Astrophys. J.*, *693*, 23-42. doi: 10.1088/0004-637X/
 4471 693/1/23
- 4472 Nagy, A. F., Barakat, A. R., & Schunk, R. W. (1986, January). Is Jupiter’s iono-
 4473 sphere a significant plasma source for its magnetosphere? *J. Geophys. Res.*,
 4474 *91*, 351-354. doi: 10.1029/JA091iA01p00351
- 4475 National Academy of Science. (2019). *State of Science of Astrobiology*,
 4476 http://sites.nationalacademies.org/ssb/currentprojects/ssb_180812. Re-
 4477 trieved 2019-08-15, from [http://sites.nationalacademies.org/SSB/
 4478 CurrentProjects/SSB_180812](http://sites.nationalacademies.org/SSB/CurrentProjects/SSB_180812)
- 4479 Needham, D. H., & Kring, D. A. (2017, November). Lunar volcanism produced a
 4480 transient atmosphere around the ancient Moon. *Earth and Planetary Science
 4481 Letters*, *478*, 175-178. doi: 10.1016/j.epsl.2017.09.002
- 4482 Newell, P. T., Sotirelis, T., & Wing, S. (2010). Seasonal variations in diffuse,
 4483 monoenergetic, and broadband aurora. *Journal of Geophysical Research*,
 4484 *115*(A03216). doi: 10.1029/2009JA014805
- 4485 Nichols, J. D., & Milan, S. E. (2016, September). Stellar wind-magnetosphere in-
 4486 teraction at exoplanets: computations of auroral radio powers. *MNRAS*, *461*,
 4487 2353-2366. doi: 10.1093/mnras/stw1430
- 4488 Niemann, H. B., Atreya, S. K., Bauer, S. J., Carignan, G. R., Demick, J. E., Frost,
 4489 R. L., ... Way, S. H. (2005, December). The abundances of constituents of Ti-
 4490 tan’s atmosphere from the GCMS instrument on the Huygens probe. *Nature*,
 4491 *438*, 779-784. doi: 10.1038/nature04122
- 4492 Nikjoo, H., Uehara, S., & Emfietzoglou, D. (2012). *Interaction of radiation with
 4493 matter*. Taylor & Francis. Retrieved from [https://books.google.no/books
 4494 ?id=YJ1ZuwNvpmIC](https://books.google.no/books?id=YJ1ZuwNvpmIC)
- 4495 Nilsson, H., Stenberg Wieser, G., Behar, E., Simon Wedlund, C., Gunell, H.,
 4496 Yamauchi, M., ... Rubin, M. (2015, January). Birth of a comet mag-
 4497 netosphere: A spring of water ions. *Science*, *347*(1), aaa0571. doi:
 4498 10.1126/science.aaa0571
- 4499 Nosé, M., Ieda, A., & Christon, S. P. (2009, July). Geotail observations of plasma
 4500 sheet ion composition over 16 years: On variations of average plasma ion mass
 4501 and O⁺ triggering substorm model. *Journal of Geophysical Research (Space
 4502 Physics)*, *114*, A07223. doi: 10.1029/2009JA014203
- 4503 Nowaczyk, N., Arz, H., Frank, U., Kind, J., & Plessen, B. (2012). Dynam-
 4504 ics of the Laschamp geomagnetic excursion from Black Sea sediments.
 4505 *Earth and Planetary Science Letters*, *351-352*, 54 - 69. Retrieved from
 4506 <http://www.sciencedirect.com/science/article/pii/S0012821X12003421>
 4507 doi: <https://doi.org/10.1016/j.epsl.2012.06.050>
- 4508 Noyes, R. W., Weiss, N. O., & Vaughan, A. H. (1984, Dec). The relation between
 4509 stellar rotation rate and activity cycle periods. *Astrophys. J.*, *287*, 769-773.
 4510 doi: 10.1086/162735
- 4511 Ohtani, S., Nosé, M., Christon, S. P., & Lui, A. T. Y. (2011, October). Energetic
 4512 O⁺ and H⁺ ions in the plasma sheet: Implications for the transport of iono-
 4513 spheric ions. *Journal of Geophysical Research (Space Physics)*, *116*(A15),
 4514 A10211. doi: 10.1029/2011JA016532
- 4515 Olson, S. L., Schwieterman, E. W., Reinhard, C. T., Ridgwell, A., Kane, S. R.,
 4516 Meadows, V. S., & Lyons, T. W. (2018, May). Atmospheric Seasonality as

- 4517 an Exoplanet Biosignature. *Astrophys. J.*, *858*, L14. doi: 10.3847/2041-8213/
4518 aac171
- 4519 Owen, T., & Niemann, H. (2009). The origin of Titan’s atmosphere: some recent ad-
4520 vances. *Phil. Trans. Roy. Soc. Lond. A*, *367*(1889), 607–615. Retrieved from
4521 <http://rsta.royalsocietypublishing.org/content/367/1889/607> doi: 10
4522 .1098/rsta.2008.0247
- 4523 Pallavicini, R., Golub, L., Rosner, R., Vaiana, G., Ayres, T., & Linsky, J. (1981).
4524 Relations among stellar X-ray emission observed from Einstein, stellar rotation
4525 and bolometric luminosity. *The Astrophysical Journal*, *248*, 279–290.
- 4526 Parai, R., & Mukhopadhyay, S. (2018). Xenon isotopic constraints on the history of
4527 volatile recycling into the mantle. *Nature*, *560*(7717), 223.
- 4528 Parker, E. N. (1958, November). Dynamics of the Interplanetary Gas and Magnetic
4529 Fields. *Astrophys. J.*, *128*, 664. doi: 10.1086/146579
- 4530 Parker, E. N. (1964a, January). Dynamical Properties of Stellar Coronas and Stel-
4531 lar Winds. II. Integration of the Heat-Flow Equation. *The Astrophysical Jour-
4532 nal*, *139*, 93. doi: 10.1086/147741
- 4533 Parker, E. N. (1964b, January). Dynamical Properties of Stellar Coronas and Stel-
4534 lar Winds. I. Integration of the Momentum Equation. *The Astrophysical Jour-
4535 nal*, *139*, 72. doi: 10.1086/147740
- 4536 Parkinson, C. D. (2002). Photochemistry and radiative transfer studies in the atmo-
4537 sphere of jupiter and saturn. *Published Ph. D. thesis, York University, North
4538 York, Ontario, Canada.*
- 4539 Parkinson, C. D., Griffioen, E., McConnell, J. C., Gladstone, G. R., & Sandel, B. R.
4540 (1998). He 584 Å Dayglow at Saturn: A Reassessment. *Icarus*, *133*(2), 210 -
4541 220. Retrieved from [http://www.sciencedirect.com/science/article/pii/
4542 S0019103598959267](http://www.sciencedirect.com/science/article/pii/S0019103598959267) doi: <https://doi.org/10.1006/icar.1998.5926>
- 4543 Pavlov, A., Pavlov, A., Ostryakov, V., Vasilyev, G., Mahaffy, P., & Steele, A. (2014).
4544 Alteration of the carbon and nitrogen isotopic composition in the Martian
4545 surface rocks due to cosmic ray exposure. *Journal of Geophysical Research:
4546 Planets*, *119*(6), 1390–1402.
- 4547 Pavlov, A. A., Kasting, J. F., Brown, L. L., Rages, K. A., & Freedman, R. (2000).
4548 Greenhouse warming by ch4 in the atmosphere of early earth. *Journal of Geo-
4549 physical Research: Planets*, *105*(E5), 11981–11990. Retrieved from [http://dx
4550 .doi.org/10.1029/1999JE001134](http://dx) doi: 10.1029/1999JE001134
- 4551 Pavlov, A. A., Kasting, J. F., Eigenbrode, J. L., & Freeman, K. H. (2001, Novem-
4552 ber). Organic haze in Earth’s early atmosphere: Source of low-¹³C Late
4553 Archean kerogens? *Geology*, *29*, 1003. doi: 10.1130/0091-7613(2001)029<1003:
4554 OHIESE>2.0.CO;2
- 4555 Payne, R. C., Britt, A. V., Chen, H., Kasting, J. F., & Catling, D. C. (2016). The
4556 response of phanerozoic surface temperature to variations in atmospheric oxy-
4557 gen concentration. *Journal of Geophysical Research: Atmospheres*, n/a–n/a.
4558 Retrieved from <http://dx.doi.org/10.1002/2016JD025459> (2016JD025459)
4559 doi: 10.1002/2016JD025459
- 4560 Penz, T., Erkaev, N., Biernat, H., Lammer, H., Amerstorfer, U., Gunell, H., ...
4561 Baumjohann, W. (2004). Ion loss on Mars caused by the Kelvin–Helmholtz
4562 instability. *Planetary and Space Science*, *52*(13), 1157 - 1167. Retrieved from
4563 <http://www.sciencedirect.com/science/article/pii/S0032063304001023>
4564 doi: <https://doi.org/10.1016/j.pss.2004.06.001>
- 4565 Penz, T., Micela, G., & Lammer, H. (2008, January). Influence of the evolving stel-
4566 lar X-ray luminosity distribution on exoplanetary mass loss. *Astronomy and
4567 Astrophysics*, *477*, 309–314. doi: 10.1051/0004-6361:20078364
- 4568 Pepin, R. O. (1991, July). On the origin and early evolution of terrestrial planet
4569 atmospheres and meteoritic volatiles. *Icarus*, *92*(1), 2–79. Retrieved 2016-
4570 04-18, from [http://www.sciencedirect.com/science/article/pii/
4571 001910359190036S](http://www.sciencedirect.com/science/article/pii/S001910359190036S) doi: 10.1016/0019-1035(91)90036-S

- 4572 Pepin, R. O. (1992). Origin of noble gases in the terrestrial planets. *Annual Review*
4573 *of Earth and Planetary Sciences*, *20*(1), 389–430.
- 4574 Pepin, R. O. (2006, November). Atmospheres on the terrestrial planets: Clues to
4575 origin and evolution. *Earth and Planetary Science Letters*, *252*(1), 1–14. Re-
4576 trieved 2018-06-08, from [http://www.sciencedirect.com/science/article/](http://www.sciencedirect.com/science/article/pii/S0012821X06006522)
4577 [pii/S0012821X06006522](http://www.sciencedirect.com/science/article/pii/S0012821X06006522) doi: 10.1016/j.epsl.2006.09.014
- 4578 Peterson, W. K., Woods, T. N., Chamberlin, P. C., & Richards, P. G. (2008,
4579 September). Photoelectron flux variations observed from the FAST satellite.
4580 *Advances in Space Research*, *42*, 947–956. doi: 10.1016/j.asr.2007.08.038
- 4581 Pierce, J. R. (2017). Cosmic rays, aerosols, clouds, and climate: Recent find-
4582 ings from the cloud experiment. *Journal of Geophysical Research: Atmo-*
4583 *spheres*, *122*(15), 8051–8055. Retrieved from [http://dx.doi.org/10.1002/](http://dx.doi.org/10.1002/2017JD027475)
4584 [2017JD027475](http://dx.doi.org/10.1002/2017JD027475) (2017JD027475) doi: 10.1002/2017JD027475
- 4585 Pierrehumbert, R. T. (2010). *Principles of planetary climate*. Cambridge, UK: Cam-
4586 bridge University Press.
- 4587 Pope, E. C., Bird, D. K., & Rosing, M. T. (2012). Isotope composition and vol-
4588 ume of earth’s early oceans. *Proceedings of the National Academy of Sci-*
4589 *ences*. Retrieved from [http://www.pnas.org/content/early/2012/03/02/](http://www.pnas.org/content/early/2012/03/02/1115705109.abstract)
4590 [1115705109.abstract](http://www.pnas.org/content/early/2012/03/02/1115705109.abstract) doi: 10.1073/pnas.1115705109
- 4591 Pope, S. A., Balikhin, M. A., Zhang, T. L., Fedorov, A. O., Gedalin, M., &
4592 Barabash, S. (2009). Giant vortices lead to ion escape from venus and re-
4593 distribution of plasma in the ionosphere. *Geophysical Research Letters*, *36*(7).
4594 Retrieved from [https://agupubs.onlinelibrary.wiley.com/doi/abs/](https://agupubs.onlinelibrary.wiley.com/doi/abs/10.1029/2008GL036977)
4595 [10.1029/2008GL036977](https://agupubs.onlinelibrary.wiley.com/doi/abs/10.1029/2008GL036977) doi: 10.1029/2008GL036977
- 4596 Poulsen, C. J., Tabor, C., & White, J. D. (2015). Long-term climate forcing by
4597 atmospheric oxygen concentrations. *Science*, *348*(6240), 1238–1241. Re-
4598 trieved from <http://science.sciencemag.org/content/348/6240/1238> doi:
4599 [10.1126/science.1260670](http://science.sciencemag.org/content/348/6240/1238)
- 4600 Quintana, E. V., Barclay, T., Raymond, S. N., Rowe, J. F., Bolmont, E., Caldwell,
4601 D. A., ... others (2014). An Earth-sized planet in the habitable zone of a cool
4602 star. *Science*, *344*(6181), 277–280.
- 4603 Rafkin, S. C. R., Sta. Maria, M. R. V., & Michaels, T. I. (2002, October). Sim-
4604 ulation of the atmospheric thermal circulation of a martian volcano using a
4605 mesoscale numerical model. *Nature*, *419*, 697–699.
- 4606 Rahmati, A., Larson, D. E., Cravens, T. E., Lillis, R. J., Dunn, P. A., Halekas, J. S.,
4607 ... Jakosky, B. M. (2015, January). MAVEN insights into oxygen pickup
4608 ions at Mars. *Geophysical Research Letters*. Retrieved 2015-11-06, from
4609 <http://onlinelibrary.wiley.com/doi/10.1002/2015GL065262/abstract>
4610 doi: 10.1002/2015GL065262
- 4611 Rahmati, A., Larson, D. E., Cravens, T. E., Lillis, R. J., Halekas, J. S., McFadden,
4612 J. P., ... Jakosky, B. M. (2017, March). MAVEN measured oxygen and hydro-
4613 gen pickup ions: Probing the Martian exosphere and neutral escape. *Journal*
4614 *of Geophysical Research: Space Physics*, *122*(3). Retrieved 2017-05-04, from
4615 <http://onlinelibrary.wiley.com/doi/10.1002/2016JA023371/abstract>
4616 doi: 10.1002/2016JA023371
- 4617 Rahmati, A., Larson, D. E., Cravens, T. E., Lillis, R. J., Halekas, J. S., McFad-
4618 den, J. P., ... Jakosky, B. M. (2018). Seasonal Variability of Neutral Es-
4619 cape from Mars as Derived From MAVEN Pickup Ion Observations. *Journal*
4620 *of Geophysical Research: Planets*, *123*(5), 1192–1202. Retrieved 2018-06-
4621 27, from [https://agupubs.onlinelibrary.wiley.com/doi/abs/10.1029/](https://agupubs.onlinelibrary.wiley.com/doi/abs/10.1029/2018JE005560)
4622 [2018JE005560](https://agupubs.onlinelibrary.wiley.com/doi/abs/10.1029/2018JE005560) doi: 10.1029/2018JE005560
- 4623 Ramirez, R. (2018). A more comprehensive habitable zone for finding life on other
4624 planets. *Geosciences*, *8*(8), 280.
- 4625 Ramirez, R. M., & Kasting, J. F. (2017, January). Could cirrus clouds have warmed
4626 early Mars? *Icarus*, *281*, 248–261. doi: 10.1016/j.icarus.2016.08.016

- 4627 Ramstad, R., Barabash, S., Futaana, Y., Nilsson, H., Wang, X.-D., & Holmström,
4628 M. (2015). The martian atmospheric ion escape rate dependence on solar wind
4629 and solar evf conditions: 1. seven years of mars express observations. *Journal*
4630 *of Geophysical Research: Planets*, *120*(7), 1298-1309. Retrieved from [https://](https://agupubs.onlinelibrary.wiley.com/doi/abs/10.1002/2015JE004816)
4631 agupubs.onlinelibrary.wiley.com/doi/abs/10.1002/2015JE004816 doi:
4632 10.1002/2015JE004816
- 4633 Rappaport, S., Levine, A., Chiang, E., El Mellah, I., Jenkins, J., Kalomeni, B., ...
4634 Tran, K. (2012, June). Possible Disintegrating Short-period Super-Mercury Or-
4635 biting KIC 12557548. *Astrophys. J.*, *752*, 1. doi: 10.1088/0004-637X/752/1/1
- 4636 Rebull, L. M., Wolff, S. C., & Strom, S. E. (2004, Feb). Stellar Rotation in Young
4637 Clusters: The First 4 Million Years. *Astrophys. J.*, *127*(2), 1029-1051. doi: 10
4638 .1086/380931
- 4639 Rebull, L. M., Wolff, S. C., Strom, S. E., & Makidon, R. B. (2002, Jul). The Early
4640 Angular Momentum History of Low-Mass Stars: Evidence for a Regulation
4641 Mechanism. *Astroph. J.*, *124*(1), 546-559. doi: 10.1086/340806
- 4642 Rees, M. H. (1989). *Physics and chemistry of the upper atmosphere*. Cambridge and
4643 New York, Cambridge University Press.
- 4644 Reiners, A., & Basri, G. (2007, February). The First Direct Measurements of Surface
4645 Magnetic Fields on Very Low Mass Stars. *Astrophys. J.*, *656*, 1121-1135. doi:
4646 10.1086/510304
- 4647 Retterer, J. M., Chang, T., Crew, G. B., Jasperse, J. R., & Winningham, J. D.
4648 (1987, July). Monte Carlo modeling of ionospheric oxygen acceleration by
4649 cyclotron resonance with broad-band electromagnetic turbulence. *Physical*
4650 *Review Letters*, *59*, 148-151. doi: 10.1103/PhysRevLett.59.148
- 4651 Richards, P. G., Woods, T. N., & Peterson, W. K. (2006). HEUVAC: A new high
4652 resolution solar EUV proxy model. *Advances in Space Research*, *37*, 315-322.
4653 doi: 10.1016/j.asr.2005.06.031
- 4654 Richardson, M. I., & Wilson, R. J. (2002, March). A topographically forced asym-
4655 metry in the martian circulation and climate. *Nature*, *416*, 298-301.
- 4656 Ricker, G. R., Winn, J. N., Vanderspek, R., Latham, G., D. W. and Bakos, Bean,
4657 J. L., Berta-Thompson, Z. K., ... R. P., e. a. (2015). Transiting exoplanet
4658 survey satellite (tess). *J Astron Telesc Instrum Syst.*, *1*(1), 014003. doi:
4659 10.1117/1.JATIS.1.1.014003
- 4660 Ridley, A. J., Deng, Y., & Toth, G. (2006). The global ionosphere-thermosphere
4661 model. *J. Atmo. Terr. Phys.*, *68*(8), 839-864. doi: 10.1016/j.jastp.2006.01.008
- 4662 Roell, M. M. (2012). *Observed decadal variations of the zonal mean hygropause*
4663 *and its relationship to changes in the transport barrier* (Unpublished doctoral
4664 dissertation). Georgia Institute of Technology.
- 4665 Romani, P. N., Bishop, J., Bézard, B., & Atreya, S. (1993). Methane photochem-
4666 istry on Neptune: Ethane and acetylene mixing ratios and haze production.
4667 *Icarus*, *106*(2), 442 - 463. Retrieved from [http://www.sciencedirect.com/](http://www.sciencedirect.com/science/article/pii/S001910358371184X)
4668 [science/article/pii/S001910358371184X](http://www.sciencedirect.com/science/article/pii/S001910358371184X) doi: [https://doi.org/10.1006/](https://doi.org/10.1006/icar.1993.1184)
4669 [icar.1993.1184](https://doi.org/10.1006/icar.1993.1184)
- 4670 Rondanelli, R., & Lindzen, R. S. (2010). Can thin cirrus clouds in the trop-
4671 ics provide a solution to the faint young sun paradox? *Journal of Geo-*
4672 *physical Research: Atmospheres*, *115*(D2). Retrieved from [https://](https://agupubs.onlinelibrary.wiley.com/doi/abs/10.1029/2009JD012050)
4673 agupubs.onlinelibrary.wiley.com/doi/abs/10.1029/2009JD012050 doi:
4674 10.1029/2009JD012050
- 4675 Ruhunusiri, S., Halekas, J. S., McFadden, J. P., Connerney, J. E. P., Espley, J. R.,
4676 Harada, Y., ... Hasegawa, H. (2016). MAVEN observations of partially devel-
4677 oped Kelvin-Helmholtz vortices at Mars. *Geophysical Research Letters*, *43*(10),
4678 4763-4773. Retrieved from [https://agupubs.onlinelibrary.wiley.com/](https://agupubs.onlinelibrary.wiley.com/doi/abs/10.1002/2016GL068926)
4679 [doi/abs/10.1002/2016GL068926](https://agupubs.onlinelibrary.wiley.com/doi/abs/10.1002/2016GL068926) doi: 10.1002/2016GL068926
- 4680 Sagan, C., & Mullen, G. (1972, July). Earth and Mars: Evolution of Atmospheres
4681 and Surface Temperatures. *Science*, *177*, 52-56. doi: 10.1126/science.177.4043

- Sahoo, S. K., Planavsky, N. J., Kendall, B., Wang, X., Shi, X., Scott, C., ... Jiang, G. (2012, September). Ocean oxygenation in the wake of the Marinoan glaciation. *Nature*, *489*, 546-549. doi: 10.1038/nature11445
- Sakai, S., Andersson, L., Cravens, T. E., Mitchell, D. L., Mazelle, C., Rahmati, A., ... Jakosky, B. M. (2016, July). Electron energetics in the Martian dayside ionosphere: Model comparisons with MAVEN data. *Journal of Geophysical Research (Space Physics)*, *121*, 7049-7066. doi: 10.1002/2016JA022782
- Sakai, S., Seki, K., Terada, N., Shinagawa, H., Tanaka, T., & Ebihara, Y. (2018). Effects of a weak intrinsic magnetic field on atmospheric escape from Mars. *Geophysical Research Letters*, *45*(18), 9336-9343. Retrieved from <https://agupubs.onlinelibrary.wiley.com/doi/abs/10.1029/2018GL079972> doi: 10.1029/2018GL079972
- Salz, M., Schneider, P., Czesla, S., & Schmitt, J. (2016). Energy-limited escape revised—the transition from strong planetary winds to stable thermospheres. *Astronomy & Astrophysics*, *585*, L2.
- Sánchez-Cano, B., Witasse, O., Lester, M., Rahmati, A., Ambrosi, R., Lillis, R., ... Larson, D. (2018, Oct). Energetic Particle Showers Over Mars from Comet C/2013 A1 Siding Spring. *Journal of Geophysical Research (Space Physics)*, *123*, 8778-8796. doi: 10.1029/2018JA025454
- Sandel, B., McConnell, J., & Strobel, D. (1982). Eddy diffusion at Saturn's homopause. *Geophysical Research Letters*, *9*(9), 1077-1080.
- Schneider, N. M., Jain, S. K., Deighan, J., Nasr, C. R., Brain, D. A., Larson, D., ... Lee, C. O. (2018, Aug). Global Aurora on Mars During the September 2017 Space Weather Event. *Geophys. Res. Lett.*, *45*(15), 7391-7398. doi: 10.1029/2018GL077772
- Schneiter, E. M., Velázquez, P. F., Esquivel, A., Raga, A. C., & Blanco-Cano, X. (2007, December). Three-dimensional Hydrodynamical Simulation of the Exoplanet HD 209458b. *Astrophys. J. Let.*, *671*, L57-L60. doi: 10.1086/524945
- Schunk, R. W., & Nagy, A. F. (2004). *Ionospheres*. Cambridge university press.
- Scott, C., Lyons, T. W., Bekker, A., Shen, Y., Poulton, S. W., Chu, X., & Anbar, A. D. (2008, March). Tracing the stepwise oxygenation of the Proterozoic ocean. *Nature*, *452*, 456-459. doi: 10.1038/nature06811
- See, V., Jardine, M., Fares, R., Donati, J.-F., & Moutou, C. (2015, July). Time-scales of close-in exoplanet radio emission variability. *MNRAS*, *450*, 4323-4332. doi: 10.1093/mnras/stv896
- Seki, K., Elphic, R. C., Hirahara, M., Terasawa, T., & Mukai, T. (2001, March). On Atmospheric Loss of Oxygen Ions from Earth Through Magnetospheric Processes. *Science*, *291*, 1939-1941. doi: 10.1126/science.1058913
- Seki, K., Nagy, A., Jackman, C. M., Crary, F., Fontaine, D., Zarka, P., ... Schunk, R. W. (2015, Oct). A Review of General Physical and Chemical Processes Related to Plasma Sources and Losses for Solar System Magnetospheres. *Sp. Sci. Rev.*, *192*, 27-89. doi: 10.1007/s11214-015-0170-y
- Selsis, F. (2006, March). Evaporation planétaire. *Ecole de Goutelas*, *28*, 271-306.
- Semel, M. (1980, November). A precise optical polarization analyzer. *Astronomy and Astrophysics*, *91*, 369-371.
- Shalygin, E. V., Markiewicz, W. J., Basilevsky, A. T., Titov, D. V., Ignatiev, N. I., & Head, J. W. (2015). Active volcanism on Venus in the Ganiki Chasma rift zone. *Geophysical Research Letters*, *42*(12), 4762-4769. Retrieved from <http://dx.doi.org/10.1002/2015GL064088> (2015GL064088) doi: 10.1002/2015GL064088
- Shaviv, N. J. (2005, August). On climate response to changes in the cosmic ray flux and radiative budget. *Journal of Geophysical Research (Space Physics)*, *110*, A08105. doi: 10.1029/2004JA010866
- Shematovich, V., Bisikalo, D., & Gérard, J.-C. (2006). Energetic oxygen atoms

- 4737 in the polar geocorona. *Journal of Geophysical Research: Space Physics*,
4738 111(A10).
- 4739 Shematovich, V. I. (2017, July). Suprathermal oxygen atoms in the Martian upper
4740 atmosphere: Contribution of the proton and hydrogen atom precipitation. *Solar
4741 System Research*, 51, 249-257. doi: 10.1134/S0038094617040050
- 4742 Shematovich, V. I., Bisikalo, D. V., Diéval, C., Barabash, S., Stenberg, G., Nils-
4743 son, H., ... Gérard, J.-C. (2011, nov). Proton and hydrogen atom trans-
4744 port in the Martian upper atmosphere with an induced magnetic field.
4745 *Journal of Geophysical Research (Space Physics)*, 116(A15), A11320. doi:
4746 10.1029/2011JA017007
- 4747 Shematovich, V. I., Bisikalo, D. V., & Gérard, J. C. (1994, December). A kinetic
4748 model of the formation of the hot oxygen geocorona: 1. Quiet geomagnetic
4749 conditions. *Journal of Geophysical Research: Space Physics*, 99(A12), 23217–
4750 23228. Retrieved 2015-09-21, from [http://onlinelibrary.wiley.com/doi/
4751 10.1029/94JA01769/abstract](http://onlinelibrary.wiley.com/doi/10.1029/94JA01769/abstract) doi: 10.1029/94JA01769
- 4752 Shizgal, B., & Lindenfeld, M. J. (1982, February). A simple kinetic theory calcula-
4753 tion of terrestrial atomic hydrogen escape fluxes induced by charge exchange
4754 collisions. *J. Geophys. Res.*, 87, 853-858. doi: 10.1029/JA087iA02p00853
- 4755 Shizgal, B. D. (1999, July). Escape of H and D from Mars and Venus by
4756 energization with hot oxygen. *Journal of Geophysical Research: Space
4757 Physics*, 104(A7), 14833-14846. Retrieved 2016-04-18, from [http://
4758 onlinelibrary.wiley.com/doi/10.1029/1999JA900157/abstract](http://onlinelibrary.wiley.com/doi/10.1029/1999JA900157/abstract) doi:
4759 10.1029/1999JA900157
- 4760 Shizgal, B. D., & Arkos, G. G. (1996). Nonthermal escape of the atmospheres of
4761 Venus, Earth, and Mars. *Reviews of Geophysics*, 34, 483-505. doi: 10.1029/
4762 96RG02213
- 4763 Shkolnik, E., Bohlender, D. A., Walker, G. A. H., & Collier Cameron, A. (2008,
4764 March). The On/Off Nature of Star-Planet Interactions. *Astroph. J.*, 676,
4765 628-638. doi: 10.1086/527351
- 4766 Simon, C., Lilensten, J., Dutuit, O., Thissen, R., Witasse, O., Alcaraz, C., & Soldi-
4767 Lose, H. (2005, March). Prediction and modelling of doubly-charged ions
4768 in the Earth's upper atmosphere. *Annales Geophysicae*, 23, 781-797. doi:
4769 10.5194/angeo-23-781-2005
- 4770 Simon, C., Lilensten, J., Moen, J., Holmes, J. M., Ogawa, Y., Oksavik, K., &
4771 Denig, W. F. (2007, March). TRANS4: a new coupled electron/proton
4772 transport code - comparison to observations above Svalbard using ESR,
4773 DMSP and optical measurements. *Annales Geophysicae*, 25, 661-673. doi:
4774 10.5194/angeo-25-661-2007
- 4775 Simon Wedlund, C., Behar, E., Kallio, E., Nilsson, H., Alho, M., Gunell, H., ...
4776 Hoekstra, R. (2019, January). Solar wind charge exchange in cometary
4777 atmospheres. II. Analytical model. *Astronomy & Astrophysics*. Retrieved 2019-
4778 01-29, from <https://articles/aa/abs/forth/aa34874-18/aa34874-18.html>
4779 doi: 10.1051/0004-6361/201834874
- 4780 Simon Wedlund, C., Behar, E., Nilsson, H., Alho, M., Kallio, E., Gunell, H., ...
4781 Hoekstra, R. (2019, February). Solar wind charge exchange in cometary
4782 atmospheres. III. Results from the Rosetta mission to comet 67p/Churyumov-
4783 Gerasimenko. *Astronomy & Astrophysics*. Retrieved 2019-02-18, from
4784 <https://articles/aa/abs/forth/aa34881-18/aa34881-18.html> doi:
4785 10.1051/0004-6361/201834881
- 4786 Simon Wedlund, C., Bodewits, D., Alho, M., Hoekstra, R., Behar, E., Gronoff, G.,
4787 ... Beth, A. (2019, February). Solar wind charge exchange in cometary
4788 atmospheres: I. Charge-changing and ionisation cross sections for He and H
4789 particles in H₂o. *Astronomy & Astrophysics*. Retrieved 2019-02-22, from
4790 <https://articles/aa/abs/forth/aa34848-18/aa34848-18.html> doi:
4791 10.1051/0004-6361/201834848

- 4792 Simon Wedlund, C., Gronoff, G., Lilensten, J., Ménager, H., & Barthélemy, M.
4793 (2011, January). Comprehensive calculation of the energy per ion pair or W
4794 values for five major planetary upper atmospheres. *Annales Geophysicae*, *29*,
4795 187-195. doi: 10.5194/angeo-29-187-2011
- 4796 Simon Wedlund, C., Kallio, E., Alho, M., Nilsson, H., Stenberg Wieser, G., Gunell,
4797 H., ... Gronoff, G. (2016, March). The atmosphere of comet 67P/Churyumov-
4798 Gerasimenko diagnosed by charge-exchanged solar wind alpha particles. *A&A*,
4799 *587*, A154. doi: 10.1051/0004-6361/201527532
- 4800 Simon Wedlund, C., Alho, M., Gronoff, G., Kallio, E., Gunell, H., Nilsson, H., ...
4801 Miloch, W. J. (2017). Hybrid modelling of cometary plasma environments-I.
4802 Impact of photoionisation, charge exchange, and electron ionisation on bow
4803 shock and cometopause at 67P/Churyumov-Gerasimenko. *Astronomy & Astro-*
4804 *physics*, *604*, A73.
- 4805 Skumanich, A. (1972, February). Time Scales for CA II Emission Decay, Rota-
4806 tional Braking, and Lithium Depletion. *Astrophys. J.*, *171*, 565. doi: 10.1086/
4807 151310
- 4808 Slapak, R., Schillings, A., Nilsson, H., Yamauchi, M., Westerberg, L.-G., & Dan-
4809 douras, I. (2017, June). Atmospheric loss from the dayside open polar region
4810 and its dependence on geomagnetic activity: implications for atmospheric
4811 escape on evolutionary timescales. *Annales Geophysicae*, *35*, 721-731. doi:
4812 10.5194/angeo-35-721-2017
- 4813 Sobolev, A. V., Asafov, E. V., Gurenko, A. A., Arndt, N. T., Batanova, V. G.,
4814 Portnyagin, M. V., ... Byerly, G. R. (2019). Deep hydrous mantle reservoir
4815 provides evidence for crustal recycling before 3.3 billion years ago. *Nature*, *1*.
- 4816 Solomon, S. C., Woods, T. N., Didkovsky, L. V., Emmert, J. T., & Qian, L. (2010,
4817 August). Anomalously low solar extreme-ultraviolet irradiance and thermo-
4818 spheric density during solar minimum. *Geophys. Res. Lett.*, *37*, L16103. doi:
4819 10.1029/2010GL044468
- 4820 Som, S. M., Buick, R., Hagadorn, J. W., Blake, T. S., Perreault, J. M., Harnmeijer,
4821 J. P., & Catling, D. C. (2016, June). Earth's air pressure 2.7 billion years ago
4822 constrained to less than half of modern levels. *Nature Geoscience*, *9*, 448-451.
4823 doi: 10.1038/ngeo2713
- 4824 Som, S. M., Catling, D. C., Harnmeijer, J. P., Polivka, P. M., & Buick, R. (2012).
4825 Air density 2.7 billion years ago limited to less than twice modern levels by
4826 fossil raindrop imprints. *Nature*, *484*, 359-362. doi: 10.1038/nature10890
- 4827 Soto, A., Mischna, M., Schneider, T., Lee, C., & Richardson, M. (2015). Mar-
4828 tian atmospheric collapse: Idealized GCM studies. *Icarus*, *250*, 553 - 569.
4829 Retrieved from [http://www.sciencedirect.com/science/article/pii/](http://www.sciencedirect.com/science/article/pii/S0019103514006575)
4830 [S0019103514006575](http://www.sciencedirect.com/science/article/pii/S0019103514006575) doi: <http://dx.doi.org/10.1016/j.icarus.2014.11.028>
- 4831 Spiga, A., Faure, J., Madeleine, J.-B., Määttänen, A., & Forget, F. (2013, April).
4832 Rocket dust storms and detached dust layers in the Martian atmosphere. *Jour-*
4833 *nal of Geophysical Research (Planets)*, *118*, 746-767. doi: 10.1002/jgre.20046
- 4834 Stone, J. M., & Proga, D. (2009, March). Anisotropic Winds from Close-In Extrasol-
4835 ar Planets. *Astrophys. J.*, *694*, 205-213. doi: 10.1088/0004-637X/694/1/205
- 4836 Strangeway, R., Russell, C., Luhmann, J., Moore, T., Foster, J., Barabash, S., &
4837 Nilsson, H. (2010). Does a planetary-scale magnetic field enhance or inhibit
4838 ionospheric plasma outflows? In *Agu fall meeting abstracts*.
- 4839 Strangeway, R. J. (2012). The equivalence of Joule dissipation and frictional heat-
4840 ing in the collisional ionosphere. *Journal of Geophysical Research: Space*
4841 *Physics*, *117*(A2), n/a-n/a. Retrieved from [http://dx.doi.org/10.1029/](http://dx.doi.org/10.1029/2011JA017302)
4842 [2011JA017302](http://dx.doi.org/10.1029/2011JA017302) (A02310) doi: 10.1029/2011JA017302
- 4843 Strangeway, R. J., Ergun, R. E., Su, Y.-J., Carlson, C. W., & Elphic, R. C. (2005,
4844 March). Factors controlling ionospheric outflows as observed at intermediate
4845 altitudes. *Journal of Geophysical Research (Space Physics)*, *110*(A9), 3221.
4846 doi: 10.1029/2004JA010829

- 4847 Strangeway, R. J., Russell, C. T., Carlson, C. W., McFadden, J. P., Ergun, R. E.,
4848 Temerin, M., ... Moore, T. E. (2000, September). Cusp field-aligned currents
4849 and ion outflows. *J. Geophys. Res.*, *105*, 21. doi: 10.1029/2000JA900032
- 4850 Strobel, D. (2002). Aeronomic systems on planets, moons, and comets. In
4851 M. Mendillo, A. Nagy, & J. Waite (Eds.), *Atmospheres in the solar system:
4852 Comparative aeronomy* (Vol. 130, p. 7-22). (Yosemite Conference on Compar-
4853 ative Aeronomy in the Solar System, YOSEMITE, CA, FEB 08-11, 2000) doi:
4854 10.1029/130GM02
- 4855 Strobel, D. F. (2008a, February). N₂ escape rates from Pluto's atmosphere. *Icarus*,
4856 *193*(2), 612–619. doi: 10.1016/j.icarus.2007.08.021
- 4857 Strobel, D. F. (2008b, February). Titan's hydrodynamically escaping atmo-
4858 sphere. *Icarus*, *193*(2), 588–594. Retrieved 2016-01-27, from [http://](http://www.sciencedirect.com/science/article/pii/S0019103507003636)
4859 www.sciencedirect.com/science/article/pii/S0019103507003636 doi:
4860 10.1016/j.icarus.2007.08.014
- 4861 Strobel, D. F. (2012). Hydrogen and methane in Titan's atmosphere: chemistry,
4862 diffusion, escape, and the hunten limiting flux principle. *Canadian Journal
4863 of Physics*, *90*(8), 795-805. Retrieved from [http://dx.doi.org/10.1139/](http://dx.doi.org/10.1139/p11-131)
4864 [p11-131](http://dx.doi.org/10.1139/p11-131) doi: 10.1139/p11-131
- 4865 Strom, R. G., Schaber, G. G., & Dawson, D. D. (1994). The global resurfac-
4866 ing of venus. *Journal of Geophysical Research: Planets*, *99*(E5), 10899–
4867 10926. Retrieved from <http://dx.doi.org/10.1029/94JE00388> doi:
4868 10.1029/94JE00388
- 4869 Strugarek, A., Brun, A. S., Matt, S. P., & Réville, V. (2014, November). On the Di-
4870 versity of Magnetic Interactions in Close-in Star-Planet Systems. *Astrophys. J.*,
4871 *795*, 86. doi: 10.1088/0004-637X/795/1/86
- 4872 Su, Y.-J., Horwitz, J. L., Wilson, G. R., Richards, P. G., Brown, D. G., & Ho,
4873 C. W. (1998, February). Self-consistent simulation of the photoelectron-driven
4874 polar wind from 120 km to 9 Re altitude. *Journal of Geophysical Research*,
4875 *103*, 2279-2296. doi: 10.1029/97JA03085
- 4876 Summers, M. E., Siskind, D. E., Bacmeister, J. T., Conway, R. R., Zasadil,
4877 S. E., & Strobel, D. F. (1997). Seasonal variation of middle atmospheric
4878 CH₄ and H₂O with a new chemical-dynamical model. *Journal of Geo-
4879 physical Research: Atmospheres*, *102*(D3), 3503–3526. Retrieved from
4880 <http://dx.doi.org/10.1029/96JD02971> doi: 10.1029/96JD02971
- 4881 Sun, D.-Z., & Lindzen, R. S. (1993, June). Distribution of Tropical Tropospheric
4882 Water Vapor. *Journal of Atmospheric Sciences*, *50*, 1643-1660. doi: 10.1175/
4883 1520-0469(1993)050<1643:DOTTWV>2.0.CO;2
- 4884 Sundberg, T., Boardsen, S., Slavin, J., Blomberg, L., & Korth, H. (2010).
4885 The Kelvin–Helmholtz instability at Mercury: An assessment. *Plane-
4886 tary and Space Science*, *58*(11), 1434 - 1441. Retrieved from [http://](http://www.sciencedirect.com/science/article/pii/S0032063310001819)
4887 www.sciencedirect.com/science/article/pii/S0032063310001819 doi:
4888 <https://doi.org/10.1016/j.pss.2010.06.008>
- 4889 Svensmark, H., Enghoff, M. B., Shaviv, N. J., & Svensmark, J. (2017, December).
4890 Increased ionization supports growth of aerosols into cloud condensation nu-
4891 clei. *Nature Communications*, *8*, 2199. doi: 10.1038/s41467-017-02082-2
- 4892 Svensmark, H., & Friis-Christensen, E. (1997, July). Variation of cosmic ray flux
4893 and global cloud coverage—a missing link in solar-climate relationships. *Jour-
4894 nal of Atmospheric and Solar-Terrestrial Physics*, *59*, 1225-1232. doi: 10.1016/
4895 S1364-6826(97)00001-1
- 4896 Takasumi, N., & Eiichi, T. (2002). Climate change of mars-like planets due to
4897 obliquity variations: implications for mars. *Geophysical Research Letters*,
4898 *30*(13). Retrieved from [https://agupubs.onlinelibrary.wiley.com/doi/](https://agupubs.onlinelibrary.wiley.com/doi/abs/10.1029/2002GL016725)
4899 [abs/10.1029/2002GL016725](https://agupubs.onlinelibrary.wiley.com/doi/abs/10.1029/2002GL016725) doi: 10.1029/2002GL016725
- 4900 Tam, S. W. Y., Yasseen, F., & Chang, T. (1998, August). Further development
4901 in theory/data closure of the photoelectron-driven polar wind and day-

- 4902 night transition of the outflow. *Annales Geophysicae*, *16*, 948-968. doi:
4903 10.1007/s00585-998-0948-2
- 4904 Tam, S. W. Y., Yasseen, F., Chang, T., & Ganguli, S. B. (1995). Self-consistent ki-
4905 netic photoelectron effects on the polar wind. *Geoph. Res. Let.*, *22*, 2107-2110.
4906 doi: 10.1029/95GL01846
- 4907 Tanaka, Y. A., Suzuki, T. K., & Inutsuka, S.-i. (2014). Atmospheric Escape by Mag-
4908 netically Driven Wind from Gaseous Planets. *ApJ*, *792*(1), 18. Retrieved
4909 2016-01-27, from <http://stacks.iop.org/0004-637X/792/i=1/a=18> doi: 10
4910 .1088/0004-637X/792/1/18
- 4911 Tanaka, Y. A., Suzuki, T. K., & Inutsuka, S.-i. (2015). Atmospheric Escape by
4912 Magnetically Driven Wind from Gaseous Planets. II. Effects of Magnetic Diffu-
4913 sion. *ApJ*, *809*(2), 125. Retrieved 2016-01-27, from [http://stacks.iop.org/](http://stacks.iop.org/0004-637X/809/i=2/a=125)
4914 [0004-637X/809/i=2/a=125](http://stacks.iop.org/0004-637X/809/i=2/a=125) doi: 10.1088/0004-637X/809/2/125
- 4915 Tapping, K. F., & Detracey, B. (1990, June). The origin of the 10.7 CM flux. *Solar*
4916 *Physics*, *127*, 321-332. doi: 10.1007/BF00152171
- 4917 Tarduno, J. A., Blackman, E. G., & Mamajek, E. E. (2014, Aug). Detecting the
4918 oldest geodynamo and attendant shielding from the solar wind: Implications
4919 for habitability. *Physics of the Earth and Planetary Interiors*, *233*, 68-87. doi:
4920 10.1016/j.pepi.2014.05.007
- 4921 Tasker, E., Tan, J., Heng, K., Kane, S., Spiegel, D., Brasser, R., ... Wicks, J. (2017,
4922 February). The language of exoplanet ranking metrics needs to change. *Nature*
4923 *Astronomy*, *1*(2), 0042. Retrieved 2017-02-06, from [http://www.nature.com/](http://www.nature.com/articles/s41550-017-0042)
4924 [articles/s41550-017-0042](http://www.nature.com/articles/s41550-017-0042) doi: 10.1038/s41550-017-0042
- 4925 Taylor, F., & Grinspoon, D. (2009). Climate evolution of Venus. *Journal of Geo-*
4926 *physical Research: Planets*, *114*(E9), n/a-n/a. Retrieved from [http://dx.doi](http://dx.doi.org/10.1029/2008JE003316)
4927 [.org/10.1029/2008JE003316](http://dx.doi.org/10.1029/2008JE003316) (E00B40) doi: 10.1029/2008JE003316
- 4928 Taylor, S. R., & McLennan, S. M. (2009). *Planetary crusts: Their composition, ori-*
4929 *gin, and evolution*. Cambridge, UK: Cambridge University Press.
- 4930 Terada, N., Machida, S., & Shinagawa, H. (2002). Global hybrid simulation of the
4931 Kelvin-Helmholtz instability at the Venus ionopause. *Journal of Geophys-*
4932 *ical Research: Space Physics*, *107*(A12), SMP 30-1-SMP 30-20. Retrieved
4933 from [https://agupubs.onlinelibrary.wiley.com/doi/abs/10.1029/](https://agupubs.onlinelibrary.wiley.com/doi/abs/10.1029/2001JA009224)
4934 [2001JA009224](https://agupubs.onlinelibrary.wiley.com/doi/abs/10.1029/2001JA009224) doi: 10.1029/2001JA009224
- 4935 Thiemann, E., Andersson, L., Lillis, R., Withers, P., Xu, S., Elrod, M., ... others
4936 (2018). The Mars topside ionosphere response to the X8. 2 solar flare of 10
4937 September 2017. *Geophysical Research Letters*, *45*(16), 8005-8013.
- 4938 Thissen, R., Witasse, O., Dutuit, O., Simon Wedlund, C., Gronoff, G., & Lilensten,
4939 J. (2011). Doubly-charged ions in the planetary ionospheres: a review. *Physical*
4940 *Chemistry Chemical Physics*, *13*(41), 18264-18287.
- 4941 Tian, F. (2009, September). Thermal Escape from Super Earth Atmospheres in the
4942 Habitable Zones of M Stars. *Astrophys. J.*, *703*, 905-909. doi: 10.1088/0004
4943 -637X/703/1/905
- 4944 Tian, F., Chassefière, E., Leblanc, F., & Brain, D. (2013). Atmospheric Escape and
4945 Climate Evolution of Terrestrial Planets. In *Comparative Climatology of Ter-*
4946 *restrial Planets* (pp. 567-581). University of Arizona Press. Retrieved 2016-01-
4947 29, from <http://adsabs.harvard.edu/abs/2013cctp.book..567T>
- 4948 Tian, F., Kasting, J. F., Liu, H.-L., & Roble, R. G. (2008, May). Hydrodynamic
4949 planetary thermosphere model: 1. Response of the Earth's thermosphere to ex-
4950 treme solar EUV conditions and the significance of adiabatic cooling. *Journal*
4951 *of Geophysical Research (Planets)*, *113*, E05008. doi: 10.1029/2007JE002946
- 4952 Tian, F., Solomon, S. C., Qian, L., Lei, J., & Roble, R. G. (2008, July). Hy-
4953 drodynamic planetary thermosphere model: 2. Coupling of an electron
4954 transport/energy deposition model. *Journal of Geophysical Research*
4955 *(Planets)*, *113*, 07005. Retrieved 2012-04-02, from [http://adsabs.org/](http://adsabs.org/2008JGRE.11307005T)
4956 [2008JGRE.11307005T](http://adsabs.org/2008JGRE.11307005T)

- 4957 Tian, F., & Toon, O. B. (2005, September). Hydrodynamic escape of nitrogen from
4958 Pluto. *Geophys. Res. Lett.*, *32*, 4 PP. Retrieved 2012-03-07, from [http://](http://www.agu.org/pubs/crossref/2005/2005GL023510.shtml)
4959 www.agu.org/pubs/crossref/2005/2005GL023510.shtml doi: 200510.1029/
4960 2005GL023510
- 4961 Tian, F., Toon, O. B., Pavlov, A. A., & De Sterck, H. (2005). A hydrogen-rich early
4962 Earth atmosphere. *Science*, *308*(5724), 1014–1017.
- 4963 Tobie, G., Choukroun, M., Grasset, O., Le Mouélic, S., Lunine, J., Sotin, C., ...
4964 Le Corre, L. (2009). Evolution of Titan and implications for its hydrocarbon
4965 cycle. *Phil. Trans. Roy. Soc. Lond. A*, *367*(1889), 617–631. Retrieved from
4966 <http://rsta.royalsocietypublishing.org/content/367/1889/617> doi:
4967 10.1098/rsta.2008.0246
- 4968 Tobiska, W. K., Bouwer, S. D., & Bowman, B. R. (2008). The development of new
4969 solar indices for use in thermospheric density modeling. *J. Atmo. Terr. Phys.*,
4970 *70*, 803.
- 4971 Trainer, M. G., Pavlov, A. A., Dewitt, H. L., Jimenez, J. L., McKay, C. P., Toon,
4972 O. B., & Tolbert, M. A. (2006, November). Inaugural Article: Organic haze
4973 on Titan and the early Earth. *Proceedings of the National Academy of Science*,
4974 *103*(48), 18035–18042. doi: 10.1073/pnas.0608561103
- 4975 Trainer, M. G., Pavlov, A. A., DeWitt, H. L., Jimenez, J. L., McKay, C. P., Toon,
4976 O. B., & Tolbert, M. A. (2006). Organic haze on titan and the early earth.
4977 *Proceedings of the National Academy of Sciences*, *103*(48), 18035–18042. Re-
4978 trieved from <http://www.pnas.org/content/103/48/18035.abstract> doi:
4979 10.1073/pnas.0608561103
- 4980 Trammell, G. B., Arras, P., & Li, Z.-Y. (2011, February). Hot Jupiter Magneto-
4981 spheres. *Astrophys. J.*, *728*, 152. doi: 10.1088/0004-637X/728/2/152
- 4982 Tremblin, P., & Chiang, E. (2013, January). Colliding planetary and stellar winds:
4983 charge exchange and transit spectroscopy in neutral hydrogen. *Monthly No-*
4984 *tices of the Royal Astronomical Society*, *428*, 2565–2576. Retrieved 2015-
4985 09-16, from <http://adsabs.harvard.edu/abs/2013MNRAS.428.2565T> doi:
4986 10.1093/mnras/sts212
- 4987 Tröstl, J., Chuang, W. K., Gordon, H., Heinritzi, M., Yan, C., Molteni, U., ... Bal-
4988 tensperger, U. (2016, May). The role of low-volatility organic compounds in
4989 initial particle growth in the atmosphere. *Nature*, *533*(7604), 527–531. doi:
4990 10.1038/nature18271
- 4991 Tu, L., Johnstone, C. P., Güdel, M., & Lammer, H. (2015). The extreme ultraviolet
4992 and x-ray sun in time: High-energy evolutionary tracks of a solar-like star. *As-*
4993 *tronomy & Astrophysics*, *577*, L3.
- 4994 Tucker, O. J., Erwin, J. T., Deighan, J. I., Volkov, A. N., & Johnson, R. E. (2012,
4995 January). Thermally driven escape from Pluto’s atmosphere: A combined
4996 fluid/kinetic model. *Icarus*, *217*, 408–415. doi: 10.1016/j.icarus.2011.11.017
- 4997 Tucker, O. J., & Johnson, R. (2009, December). Thermally driven atmo-
4998 spheric escape: Monte Carlo simulations for Titan’s atmosphere. *Plane-*
4999 *tary and Space Science*, *57*(14–15), 1889–1894. Retrieved 2012-02-24, from
5000 <http://www.sciencedirect.com/science/article/pii/S0032063309001597>
5001 doi: 10.1016/j.pss.2009.06.003
- 5002 Turnpenney, S., Nichols, J. D., Wynn, G. A., & Burleigh, M. R. (2018, February).
5003 Exoplanet-induced Radio Emission from M Dwarfs. *Astrophys. J.*, *854*, 72.
5004 doi: 10.3847/1538-4357/aaa59c
- 5005 Uehara, S., & Nijkoo, H. (2002). Track structure for low energy ions including
5006 charge exchange processes. *Radiation Protection Dosimetry*, *99*(1-4), 53–55.
5007 Retrieved from <http://dx.doi.org/10.1093/oxfordjournals.rpd.a006838>
5008 doi: 10.1093/oxfordjournals.rpd.a006838
- 5009 Urata, R. A., & Toon, O. B. (2013, September). Simulations of the martian hy-
5010 drologic cycle with a general circulation model: Implications for the ancient
5011 martian climate. *Icarus*, *226*(1), 229–250. doi: 10.1016/j.icarus.2013.05.014

- 5012 Vaiana, G. (1981). Low luminosity galactic X-ray sources. *Space Science Reviews*,
5013 *30*(1-4), 151–179.
- 5014 Valeille, A., Bougher, S. W., Tennishev, V., Combi, M. R., & Nagy, A. F. (2010,
5015 March). Water loss and evolution of the upper atmosphere and exosphere
5016 over martian history. *Icarus*, *206*(1), 28–39. Retrieved 2012-02-24, from
5017 <http://www.sciencedirect.com/science/article/pii/S0019103509002358>
5018 doi: 10.1016/j.icarus.2009.04.036
- 5019 van der Holst, B., Sokolov, I. V., Meng, X., Jin, M., Manchester, I. W. B., Tóth,
5020 G., & Gombosi, T. I. (2014, February). Alfvén Wave Solar Model (AWSoM):
5021 Coronal Heating. *Astrophys. J.*, *782*, 81. doi: 10.1088/0004-637X/782/2/81
- 5022 Varney, R. H., Solomon, S. C., & Nicolls, M. J. (2014). Heating of the sun-
5023 lit polar cap ionosphere by reflected photoelectrons. *Journal of Geo-*
5024 *physical Research: Space Physics*, *119*(10), 8660–8684. Retrieved from
5025 <http://dx.doi.org/10.1002/2013JA019378> doi: 10.1002/2013JA019378
- 5026 Vasyliunas, V. M., & Song, P. (2005). Meaning of ionospheric Joule heating. *Journal*
5027 *of Geophysical Research: Space Physics*, *110*(A2). Retrieved from [https://](https://agupubs.onlinelibrary.wiley.com/doi/abs/10.1029/2004JA010615)
5028 agupubs.onlinelibrary.wiley.com/doi/abs/10.1029/2004JA010615 doi:
5029 10.1029/2004JA010615
- 5030 Vedantham, H. K., Callingham, J. R., Shimwell, T. W., Tasse, C., Pope, B. J. S.,
5031 Bedell, M., ... White, G. J. (2020, February). Coherent radio emission from
5032 a quiescent red dwarf indicative of star-planet interaction. *Nature Astronomy*.
5033 doi: 10.1038/s41550-020-1011-9
- 5034 Vervack, R. J., Sandel, B. R., Gladstone, G., McConnell, J. C., & Parkinson, C. D.
5035 (1995). Jupiter’s He 584 Å Dayglow: New Results. *Icarus*, *114*(1), 163 - 173.
5036 Retrieved from [http://www.sciencedirect.com/science/article/pii/](http://www.sciencedirect.com/science/article/pii/S0019103585710512)
5037 [S0019103585710512](http://www.sciencedirect.com/science/article/pii/S0019103585710512) doi: <https://doi.org/10.1006/icar.1995.1051>
- 5038 Vidal-Madjar, A., Désert, J.-M., Lecavelier des Etangs, A., Hébrard, G., Ballester,
5039 G. E., Ehrenreich, D., ... Parkinson, C. D. (2004, March). Detection of
5040 Oxygen and Carbon in the Hydrodynamically Escaping Atmosphere of the
5041 Extrasolar Planet HD 209458b. *Astrophys. J. Let.*, *604*, L69-L72. doi:
5042 10.1086/383347
- 5043 Vidal-Madjar, A., Lecavelier des Etangs, A., Désert, J.-M., Ballester, G. E., Ferlet,
5044 R., Hébrard, G., & Mayor, M. (2003, March). An extended upper atmo-
5045 sphere around the extrasolar planet HD209458b. *Nature*, *422*, 143-146. doi:
5046 10.1038/nature01448
- 5047 Vidal-Madjar, A., Lecavelier des Etangs, A., Désert, J.-M., Ballester, G. E., Ferlet,
5048 R., Hébrard, G., & Mayor, M. (2008, March). Exoplanet HD 209458b (Osiris):
5049 Evaporation Strengthened. *Astrophys. J. Let.*, *676*, L57. doi: 10.1086/587036
- 5050 Vidotto, A. A., Fares, R., Jardine, M., Moutou, C., & Donati, J.-F. (2015, June).
5051 On the environment surrounding close-in exoplanets. *MNRAS*, *449*, 4117-4130.
5052 doi: 10.1093/mnras/stv618
- 5053 Vidotto, A. A., Jardine, M., Opher, M., Donati, J. F., & Gombosi, T. I. (2011,
5054 March). Powerful winds from low-mass stars: V374 Peg. *Mon. Not. R. Astron.*
5055 *Soc.*, *412*, 351-362. doi: 10.1111/j.1365-2966.2010.17908.x
- 5056 Vilhu, O. (1984, Apr). The nature of magnetic activity in lower main sequence stars.
5057 *Astronomy and Astrophysics*, *133*, 117-126.
- 5058 Villasenor, J., & Buneman, O. (1992, March). Rigorous charge conservation for lo-
5059 cal electromagnetic field solvers. *Computer Physics Communications*, *69*(2-3),
5060 306-316. doi: 10.1016/0010-4655(92)90169-Y
- 5061 Volkov, A. N. (2015). A criterion for the validity of Parker’s model in thermal es-
5062 cape problems for planetary atmospheres. *The Astrophysical Journal Letters*,
5063 *812*(1), L1. Retrieved from [http://stacks.iop.org/2041-8205/812/i=1/a=](http://stacks.iop.org/2041-8205/812/i=1/a=L1)
5064 [L1](http://stacks.iop.org/2041-8205/812/i=1/a=L1)
- 5065 Volkov, A. N., Johnson, R. E., Tucker, O. J., & Erwin, J. T. (2011, March). Ther-
5066 mally driven atmospheric escape: Transition from hydrodynamic to Jeans

- 5067 escape. *ApJ*, 729(2), L24. Retrieved 2011-05-27, from <http://iopscience>
5068 [.iop.org/2041-8205/729/2/L24/](http://iopscience.iop.org/2041-8205/729/2/L24/) doi: 10.1088/2041-8205/729/2/L24
- 5069 Volkov, A. N., Tucker, O. J., Erwin, J. T., & Johnson, R. E. (2011, June). Kinetic
5070 simulations of thermal escape from a single component atmosphere. *Physics of*
5071 *Fluids*, 23, 066601–066601–16. doi: 10.1063/1.3592253
- 5072 Vondrak, R. R. (1974). Creation of an artificial lunar atmosphere. *Nature*,
5073 248(5450), 657.
- 5074 Vondrak, R. R. (1992, September). Lunar base activities and the lunar environ-
5075 ment. In W. W. Mendell et al. (Eds.), *Lunar bases and space activities of the*
5076 *21st century*.
- 5077 Vondrak, R. R., Freeman, J. W., & Lindeman, R. A. (1974). Measurements of lu-
5078 nar atmospheric loss rate. In *Lunar and planetary science conference proceed-*
5079 *ings* (Vol. 5, p. 2945-2954).
- 5080 Waara, M., Slapak, R., Nilsson, H., Stenberg, G., André, M., & Barghouthi, I. A.
5081 (2011, May). Statistical evidence for O⁺ energization and outflow caused
5082 by wave-particle interaction in the high altitude cusp and mantle. *Annales*
5083 *Geophysicae*, 29, 945-954. doi: 10.5194/angeo-29-945-2011
- 5084 Wahlund, J.-E., Opgenoorth, H. J., Haggstrom, I., Winser, K. J., & Jones, G. O. L.
5085 (1992, March). EISCAT observations of topside ionospheric ion outflows
5086 during auroral activity - Revisited. *J. Geophys. Res.*, 97, 3019-3037. doi:
5087 10.1029/91JA02438
- 5088 Waite, J., & Lummerzheim, D. (2002). Comparison of auroral processes: Earth and
5089 jupiter. In M. Mendillo, A. Nagy, & J. Waite (Eds.), *Atmospheres in the solar*
5090 *system: Comparative aeronomy* (Vol. 30, p. 115-139). (Yosemite Conference
5091 on Comparative Aeronomy in the Solar System, YOSEMITE, CA, FEB 08-11,
5092 2000) doi: 10.1029/130GM08
- 5093 Waite, J. H., Lewis, W. S., Kasprzak, W. T., Anicich, V. G., Block, B. P., Cravens,
5094 T. E., ... Yelle, R. V. (2004). The cassini ion and neutral mass spec-
5095 trometer (inms) investigation. *Space Science Reviews*, 114(1), 113–231.
5096 Retrieved from <http://dx.doi.org/10.1007/s11214-004-1408-2> doi:
5097 10.1007/s11214-004-1408-2
- 5098 Wakeford, H. R., Lewis, N. K., Fowler, J., Bruno, G., Wilson, T. J., Moran, S. E.,
5099 ... de Wit, J. (2018, dec). Disentangling the planet from the star in late-type
5100 m dwarfs: A case study of TRAPPIST-1g. *The Astronomical Journal*, 157(1),
5101 11. Retrieved from <https://doi.org/10.3847/2F1538-3881%2Faaf04d> doi:
5102 10.3847/1538-3881/aaf04d
- 5103 Walker, J. C. G., Hays, P. B., & Kasting, J. F. (1981). A negative feedback mech-
5104 anism for the long-term stabilization of earth's surface temperature. *Journal of*
5105 *Geophysical Research: Oceans*, 86(C10), 9776–9782. Retrieved from <http://dx>
5106 [.doi.org/10.1029/JC086iC10p09776](http://dx.doi.org/10.1029/JC086iC10p09776) doi: 10.1029/JC086iC10p09776
- 5107 Walter, F. M., Linsky, J. L., Bowyer, S., & Garmire, G. (1980, Mar). HEAO 1 ob-
5108 servations of active coronae in main-sequence and subgiant stars. *Astrophys. J.*
5109 *Let.*, 236, L137-L141. doi: 10.1086/183214
- 5110 Wang, Y.-C., Luhmann, J. G., Leblanc, F., Fang, X., Johnson, R. E., Ma, Y., ...
5111 Li, L. (2014, January). Modeling of the O⁺ pickup ion sputtering efficiency
5112 dependence on solar wind conditions for the Martian atmosphere. *Journal of*
5113 *Geophysical Research (Planets)*, 119, 93-108. doi: 10.1002/2013JE004413
- 5114 Wang, Y.-C., Luhmann, J. G., Rahmati, A., Leblanc, F., Johnson, R. E., Cravens,
5115 T. E., & Ip, W.-H. (2016, July). Cometary sputtering of the Martian at-
5116 mosphere during the Siding Spring encounter. *Icarus*, 272, 301-308. doi:
5117 10.1016/j.icarus.2016.02.040
- 5118 Wargelin, B., Beiersdorfer, P., & Brown, G. (2008). Ebit charge-exchange mea-
5119 surements and astrophysical applications. *Canadian Journal of Physics*, 86(1),
5120 151-169. Retrieved from <https://doi.org/10.1139/p07-125> doi: 10.1139/
5121 p07-125

- 5122 Watson, A. J., Donahue, T. M., & Walker, J. C. (1981, November). The dy-
5123 namics of a rapidly escaping atmosphere: Applications to the evolution
5124 of Earth and Venus. *Icarus*, *48*(2), 150–166. Retrieved 2012-02-24, from
5125 <http://www.sciencedirect.com/science/article/pii/0019103581901019>
5126 doi: 10.1016/0019-1035(81)90101-9
- 5127 Way, M. J., Del Genio, A. D., Aleinov, I., Clune, T. L., Kelley, M., & Kiang, N. Y.
5128 (2018). Climates of warm Earth-like planets. I. 3D model simulations. *The*
5129 *Astrophysical Journal Supplement Series*, *239*(2), 24.
- 5130 Way, M. J., Del Genio, A. D., Kiang, N. Y., Sohl, L. E., Grinspoon, D. H., Aleinov,
5131 I., ... Clune, T. (2016). Was Venus the first habitable world of our solar
5132 system? *Geophysical research letters*, *43*(16), 8376–8383.
- 5133 Weber, E. J., & Davis, L., Jr. (1967, April). The Angular Momentum of the Solar
5134 Wind. *Astrophys. J.*, *148*, 217–227. doi: 10.1086/149138
- 5135 Webster, C. R., Mahaffy, P. R., Atreya, S. K., Flesch, G. J., Mischna, M. A.,
5136 Meslin, P.-Y., ... Lemmon, M. T. (2015). Mars methane detection
5137 and variability at Gale crater. *Science*, *347*(6220), 415–417. Retrieved
5138 from <http://science.sciencemag.org/content/347/6220/415> doi:
5139 10.1126/science.1261713
- 5140 Wei, Y., Pu, Z., Zong, Q., Wan, W., Ren, Z., Fraenz, M., ... Hong, M. (2014). Oxy-
5141 gen escape from the Earth during geomagnetic reversals: Implications to mass
5142 extinction. *Earth and Planetary Science Letters*, *394*, 94 - 98. Retrieved from
5143 <http://www.sciencedirect.com/science/article/pii/S0012821X14001629>
5144 doi: <https://doi.org/10.1016/j.epsl.2014.03.018>
- 5145 Weimer, D. R., Bowman, B. R., Sutton, E. K., & Tobiska, W. K. (2011). Predict-
5146 ing global average thermospheric temperature changes resulting from auroral
5147 heating. *J. Geophys. Res.*, *116*. doi: 10.1029/2010JA015685
- 5148 Weimer, D. R., Mlynczak, M. G., Hunt, L. A., & Tobiska, W. K. (2015). High corre-
5149 lations between temperature and nitric oxide in the thermosphere. *J. Geophys.*
5150 *Res.*, *120*. doi: 10.1002/2015JA021461
- 5151 Wilson, G. R., Khazanov, G., & Horwitz, J. L. (1997). Achieving zero current for
5152 polar wind outflow on open flux tubes subjected to large photoelectron fluxes.
5153 *Geoph. Res. Let.*, *24*, 1183–1186. doi: 10.1029/97GL00923
- 5154 Wilson, G. R., Weimer, D. R., Wise, J. O., & Marcos, F. A. (2006). Response of
5155 the thermosphere to Joule heating and particle precipitation. *J. Geophys. Res.*,
5156 *111*. doi: 10.1029/2005JA011274
- 5157 Wolf, E. T., & Toon, O. B. (2010, June). Fractal Organic Hazes Provided an Ul-
5158 traviolet Shield for Early Earth. *Science*, *328*, 1266-. doi: 10.1126/science
5159 .1183260
- 5160 Wong, M. L., Yung, Y. L., & Gladstone, G. R. (2015). Pluto’s implications for
5161 a Snowball Titan. *Icarus*, *246*, 192 - 196. Retrieved from [http://www](http://www.sciencedirect.com/science/article/pii/S0019103514002723)
5162 [.sciencedirect.com/science/article/pii/S0019103514002723](http://www.sciencedirect.com/science/article/pii/S0019103514002723) (Special
5163 Issue: The Pluto System) doi: <http://dx.doi.org/10.1016/j.icarus.2014.05.019>
- 5164 Wood, B. E. (2006, October). The Solar Wind and the Sun in the Past. *Sp. Sci.*
5165 *Rev.*, *126*, 3–14. doi: 10.1007/s11214-006-9006-0
- 5166 Wood, B. E., Müller, H.-R., Redfield, S., & Edelman, E. (2014, February). Evidence
5167 for a Weak Wind from the Young Sun. *Astrophys. J. Let.*, *781*, L33. doi: 10
5168 .1088/2041-8205/781/2/L33
- 5169 Woods, T. N., Eparvier, F. G., Bailey, S. M., Chamberlin, P. C., Lean, J., Rottman,
5170 G. J., ... Woodraska, D. L. (2005, January). Solar EUV Experiment (SEE):
5171 Mission overview and first results. *Journal of Geophysical Research (Space*
5172 *Physics)*, *110*, 1312-+. doi: 10.1029/2004JA010765
- 5173 Worden, J. R., White, O. R., & Woods, T. N. (1998, March). Evolution of Chro-
5174 mospheric Structures Derived from Ca II K Spectroheliograms: Implications
5175 for Solar Ultraviolet Irradiance Variability. *Astrophys. J.*, *496*, 998-+. doi:
5176 10.1086/305392

- 5177 Wordsworth, R., & Pierrehumbert, R. (2013, January). Hydrogen-Nitrogen Green-
5178 house Warming in Earth's Early Atmosphere. *Science*, *339*(6115), 64–67. Re-
5179 trieved 2013-01-07, from <http://www.sciencemag.org/content/339/6115/64>
5180 doi: 10.1126/science.1225759
- 5181 Wordsworth, R. D., & Pierrehumbert, R. T. (2013, December). Water Loss from
5182 Terrestrial Planets with CO₂-rich Atmospheres. *Astrophys. J.*, *778*, 154. doi:
5183 10.1088/0004-637X/778/2/154
- 5184 Wright, J. T. (2019, Jul). Searches for Technosignatures in Astronomy and Astro-
5185 physics. *arXiv e-prints*, arXiv:1907.07831.
- 5186 Wright, N. J., Drake, J. J., Mamajek, E. E., & Henry, G. W. (2011, December). The
5187 Stellar-activity-Rotation Relationship and the Evolution of Stellar Dynamos.
5188 *Astrophys. J.*, *743*, 48. doi: 10.1088/0004-637X/743/1/48
- 5189 Wright, N. J., Newton, E. R., Williams, P. K. G., Drake, J. J., & Yadav, R. K.
5190 (2018, Sep). The stellar rotation-activity relationship in fully convective M dwarfs.
5191 *Mon. Not. R. Astron. Soc.*, *479*(2), 2351-2360. doi:
5192 10.1093/mnras/sty1670
- 5193 Yagi, M., Leblanc, F., Chaufray, J. Y., Gonzalez-Galindo, F., Hess, S., & Modolo, R.
5194 (2012, nov). Mars exospheric thermal and non-thermal components: Seasonal
5195 and local variations. *Icarus*, *221*(2), 682–693. Retrieved 2018-06-15, from
5196 <http://www.sciencedirect.com/science/article/pii/S0019103512002989>
5197 doi: 10.1016/j.icarus.2012.07.022
- 5198 Yelle, R. V. (2004, July). Aeronomy of extra-solar giant planets at small orbital dis-
5199 tances. *Icarus*, *170*, 167-179. doi: 10.1016/j.icarus.2004.02.008
- 5200 Yelle, R. V., Cui, J., & Müller-Wodarg, I. C. F. (2008, October). Methane escape
5201 from Titan's atmosphere. *J. Geophys. Res. Planets*, *113*(12), E10003. doi: 10
5202 .1029/2007JE003031
- 5203 Young, D. T., Balsiger, H., & Geiss, J. (1982, November). Correlations of magneto-
5204 spheric ion composition with geomagnetic and solar activity. *J. Geophys. Res.*,
5205 *87*, 9077-9096. doi: 10.1029/JA087iA11p09077
- 5206 Young, L. A., Kammer, J. A., Steffl, A. J., Gladstone, G. R., Summers, M. E., Stro-
5207 bel, D. F., ... Versteeg, M. (2018, January). Structure and composition
5208 of Pluto's atmosphere from the New Horizons solar ultraviolet occultation.
5209 *Icarus*, *300*, 174-199. doi: 10.1016/j.icarus.2017.09.006
- 5210 Yung, Y. L., & DeMore, W. (1982). Photochemistry of the stratosphere of Venus:
5211 Implications for atmospheric evolution. *Icarus*, *51*(2), 199–247.
- 5212 Yung, Y. L., Wen, J.-S., Moses, J. I., Landry, B. M., Allen, M., & Hsu, K.-J. (1989,
5213 October). Hydrogen and deuterium loss from the terrestrial atmosphere - A
5214 quantitative assessment of nonthermal escape fluxes. *J. Geophys. Res.*, *94*,
5215 14971-14989. doi: 10.1029/JD094iD12p14971
- 5216 Zahnle, K. J., Catling, D. C., & Claire, M. W. (2013, December). The rise of oxy-
5217 gen and the hydrogen hourglass. *Chemical Geology*, *362*, 26-34. doi: 10.1016/
5218 j.chemgeo.2013.08.004
- 5219 Zahnle, K. J., Gacesa, M., & Catling, D. C. (2019). Strange messenger: A new
5220 history of hydrogen on Earth, as told by Xenon. *Geochimica et Cosmochim-
5221 ica Acta*, *244*, 56 - 85. Retrieved from [http://www.sciencedirect.com/
5222 science/article/pii/S0016703718305349](http://www.sciencedirect.com/science/article/pii/S0016703718305349) doi: [https://doi.org/10.1016/
5223 j.gca.2018.09.017](https://doi.org/10.1016/j.gca.2018.09.017)
- 5224 Zahnle, K. J., & Kasting, J. F. (1986). Mass fractionation during transonic escape
5225 and implications for loss of water from Mars and Venus. *Icarus*, *68*(3), 462 -
5226 480. Retrieved from [http://www.sciencedirect.com/science/article/pii/
5227 0019103586900515](http://www.sciencedirect.com/science/article/pii/S0019103586900515) doi: [http://dx.doi.org/10.1016/0019-1035\(86\)90051-5](http://dx.doi.org/10.1016/0019-1035(86)90051-5)
- 5228 Zarka, P. (2007, April). Plasma interactions of exoplanets with their parent star and
5229 associated radio emissions. *Planetary and Space Science*, *55*, 598-617. doi: 10
5230 .1016/j.pss.2006.05.045
- 5231 Zechmeister, M., Dreizler, S., Ribas, I., Reiners, A., Caballero, J. A., Bauer, F. F.,

- 5232 ... Lalitha, S. (2019, Jun). The CARMENES search for exoplanets around M
5233 dwarfs. Two temperate Earth-mass planet candidates around Teegarden's Star.
5234 *arXiv e-prints*, arXiv:1906.07196.
- 5235 Zent, A. P., & Quinn, R. C. (1995, March). Simultaneous adsorption of CO₂ and
5236 H₂O under Mars-like conditions and application to the evolution of the Mar-
5237 tian climate. *J. Geophys. Res.*, *100*, 5341-5349. doi: 10.1029/94JE01899
- 5238 Zerkle, A. L., & Mikhail, S. (2017). The geobiological nitrogen cycle: From mi-
5239 crobes to the mantle. *Geobiology*, *15*(3), 343-352. Retrieved from [https://](https://onlinelibrary.wiley.com/doi/abs/10.1111/gbi.12228)
5240 onlinelibrary.wiley.com/doi/abs/10.1111/gbi.12228 doi: 10.1111/gbi
5241 .12228
- 5242 Zhang, T. L., Lu, Q. M., Baumjohann, W., Russell, C. T., Fedorov, A., Barabash,
5243 S., ... Balikhin, M. (2012). Magnetic Reconnection in the Near Venusian
5244 Magnetotail. *Science*, *336*(6081), 567-570. Retrieved from [https://science](https://science.sciencemag.org/content/336/6081/567)
5245 [.sciencemag.org/content/336/6081/567](https://science.sciencemag.org/content/336/6081/567) doi: 10.1126/science.1217013
- 5246 Zhao, J., & Tian, F. (2015, April). Photochemical escape of oxygen from early Mars.
5247 *Icarus*, *250*, 477-481. Retrieved 2017-05-04, from [http://www.sciencedirect](http://www.sciencedirect.com/science/article/pii/S0019103514007234)
5248 [.com/science/article/pii/S0019103514007234](http://www.sciencedirect.com/science/article/pii/S0019103514007234) doi: 10.1016/j.icarus.2014
5249 .12.032
- 5250 Zhu, X., Strobel, D. F., & Erwin, J. T. (2014). The density and thermal structure of
5251 Pluto's atmosphere and associated escape processes and rates. *Icarus*, *228*, 301
5252 - 314. Retrieved from [http://www.sciencedirect.com/science/article/](http://www.sciencedirect.com/science/article/pii/S0019103513004302)
5253 [pii/S0019103513004302](http://www.sciencedirect.com/science/article/pii/S0019103513004302) doi: <https://doi.org/10.1016/j.icarus.2013.10.011>